# Anthropocene in the Geomorphology

# of the Sonoran Desert

by

Ara Jeong

A Dissertation Presented in Partial Fulfillment
of the Requirements for the Degree
Doctor of Philosophy

Approved April 2019 by the
Graduate Supervisory Committee:

Ronald I. Dorn, Chair
Mark Schmeeckle
Ian J. Walker

ARIZONA STATE UNIVERSITY

May 2019

# ABSTRACT

Human endeavors move 7x more volume of earth than the world's rivers accelerating the removal of Earth's soil surface. Measuring anthropogenic acceleration of soil erosion requires knowledge of natural rates through the study of $^{10}$Be, but same-watershed comparisons between anthropogenically-accelerated and natural erosion rates do not exist for urbanizing watersheds. Here I show that urban sprawl from 1989 to 2013 accelerated soil erosion between 1.3x and 15x above natural rates for different urbanizing watersheds in the metropolitan Phoenix region, Sonoran Desert, USA, and that statistical modeling a century of urban sprawl indicates an acceleration of only 2.7x for the Phoenix region. Based on studies of urbanization's erosive effects, and studies comparing other land-use changes to natural erosion rates, we expected a greater degree of urban acceleration. Given that continued urban expansion will add a new city of a million every five days until 2050, given the potential importance of urban soils for absorbing anthropogenically-released carbon, and given the role of urban-sourced pollution, quantifying urbanization's acceleration of natural erosion in other urban settings could reveal important regional patterns. For example, a comparison of urban watersheds to nearby non-urban watersheds suggests that the Phoenix case study is on the low-end of the urban acceleration factor. This new insight into the urban acceleration of soil erosion in metropolitan Phoenix can help reduce the acute risk of flooding for many rapidly urbanizing desert cities around the globe. To reduce this risk, properly engineered Flood Control Structures must account for sediment accumulation as well as flood waters. While the Phoenix area used regional data from non-urban, non-desert watersheds to generate sediment yield rates, this research presents a new analysis of empirical data for

the Phoenix metropolitan region, where two regression models provide estimates of a more realistic sediment accumulation for arid regions and also urbanization of a desert cities. The new model can be used to predict the realistic sediment accumulation for helping provide data where few data exists in parts of arid Africa, southwest Asia, and India.

# DEDICATION

For my family

For my friends

For Ron

and for Hyerin

# ACKNOWLEDGMENTS

I would like to express the deepest appreciation to my advisor Dr. Ronald Dorn for the immeasurable support and encouragement. He used to say that you made my day. But actually, it is not too much to say that he made my every day in last four years in the United States. I would like to thank my committee members, Dr. Mark Schmeeckle and Dr. Ian Walker for all of the discussions that helped formulate the ideas presented within this work.

I would like to thank Dr. Ronald Dorn, Dr. Yeong Bae Seong, Dr. Arjun Heimsath, Sam Alter, Craig Turner and Suet Yi Cheung for their help with fieldwork. The laboratory work for this research would not have been possible without the generosity of Dr. Yeong Bae Seong at Korea University, Seoul, Korea. I would like to express the deepest gratitude to Dr. Yeong Bae Seong. I would like to thank Dr. Dong-Eun Kim, Hyun Hee Rhee, Cho Hee Lee, Purevmaa Khandsuren and Nansalmaa Radnaa for assisting laboratory work at Geochronology Laboratory at Korea University.

I would like to thank to JE Fuller Hydrology & Geomorphology, Inc. for their financial support granted through fellowship and for permission to access their consulting reports on sediment yield data in Phoenix metropolitan region.

I would also like to acknowledge my co-authors and coresearchers: Suet Yi Cheung, Dr. Ian Walker, Dr. Ronald Dorn (Chapter 2), Dr. Ronald Dorn (Chapter 3), Dr. Dylan Connor, Dr. Ronald Dorn, Dr. Yeong Bae Seong (Chapter 5).

TABLE OF CONTENTS

Page

CHAPTER Page

CHAPTER Page

APPENDIX Page

APPENDIX Page

LIST OF TABLES

LIST OF FIGURES

Figure Page

Figure Page

# CHAPTER 1

## INTRODUCTION

Since Greek and Roman times, western scholarship rarely focused on the negative aspects of human modification of Earth's surface; instead, much of western thought lauded the virtues of humans taming wilderness (Glacken, 1967). Then, George Perkins Marsh (Marsh, 1864), among others, initiated the sustainability movement, highlighting the role of humans on Earth's physical geography.

Humans have been an important driver of reconfiguring the terrestrial surface of the Earth by altering its morphology and processes. Human alterations in land use/cover influences the dynamics of hillslope hydrology, sediment production, sediment transport, and delivery of sediment to the upper reaches of streams. These changes can in turn effect river channel morphology, as water and sediment transport in hillslope-river systems are closely linked (Vanacker et al., 2005). Humans, thus, enhance 'the skinning of our planet' (Montgomery, 2007). As an agent of denudation, on a global basis, human move Earth materials up to seven times more than the world's river carry sediment into the ocean (Hooke 1994; Douglas and Lawson, 2001; Goudie and Viles, 2016). Furthermore, as technology continues to improve, so does the ability of humans to alter Earth's surface (Haff, 2010).

The effect of human activities on the physical landscape, however, show substantially uneven geographical patterns (Hooke, 1999). Activities in the USA, for example, has moved some 7.5 times the materials transported in the United Kingdom

(Hooke 1994; Douglas and Lawson, 2001; Goudie and Viles, 2016). This spatial variability in the impact of the Anthropocene effect largely depends on how long humans have been modifying a landscape, the intensity and frequency of human disturbances, and landscape sensitivity (i.e. the ability that landscape processes can mitigate impacts of human disturbances). Thus, approaching research at different scales, from local to regional, is essential for assessing anthropogenic impacts on landforms and the operation of geomorphological processes.

Most anthrogemorphoogical studies regarding human-induced denudation have focused on areas with a long history of human modifications, and it naturally follows that researchers will encounter substantial human impact on landscapes. However, soil erosion is a critical issue in locations with fairly recent human activity, such as rapidly growing cities in arid regions. Soil erosion can be particularly detrimental in deserts, because the loss of surface materials reduces available plant water and soil productivity by removing nutrient-rich surface horizons (Overby and Baker Jr., 1995). Reduced plant cover increases overland flow, that in turn strips these surface horizons, possibly leading to gully incision or mass wasting and eventually further destabilization of landscapes. Removed soil from hillslopes is conveyed into upper reaches of streams and these sediments can be a major water pollutant in the United States (National Research Council, 1998).

Prior to human settlements in Phoenix metropolitan region, extensive areas once hosted desert pavements, biological soil crusts (Allen, 2005, 2010), and interlocking colluvium on steeper slopes on steeper slopes that provided a net-armoring effect (Bowker et al., 2008; Granger et al., 2001; Seong et al., 2016a). Only patches of the

armored surfaces currently remain, providing glimpses into the original land surfaces due to the enhanced disturbance by anthropogenic impacts including periods of cattle grazing, periods of road building and home construction, and other influences, such as off-road vehicles (Jeong et al., 2018a).

Measuring human amplification of soil erosion requires an understanding of natural background erosion rates (Gellis et al., 2004), but it is challenging because traditional methods to measure sediment yield using sediment loads in the stream or reservoir do not always reflect background rates of erosion (Trimble, 1977). Furthermore, even contemporary data are unfortunately rare that can inform on long-term sediment yield reflecting land use/cover changes on arid and semiarid watersheds that can provide an integrated measure of soil erosion, sediment transport, and deposition (Nichols, 2006). Sediment yield data from the last two decades collected from stock ponds in north-central Sonoran Desert presents an opportunity to understand influences of anthropogenic variables on erosion rates in the last two decades, north-central Sonoran Desert. Concentrations of *in situ*-produced $^{10}$Be measured in fluvial sediments from the same watersheds, there exists an opportunity to compare anthropogenic soil erosion to catchment wide denudation rates (CWDR) over timescales of $10^3$ to $10^5$ years (von Blanckenburg, 2006).

This dissertation focuses on developing an understanding soil erosion in piedmont settings (e.g. pediment, alluvial fan) of what is now the Phoenix metropolitan region. I analyze three very different time periods for the same watersheds. First, catchment-wide denudation rates derived from cosmogenic $^{10}$Be provides insight into

natural erosion rates for 18 watersheds. Then, historic soil erosion measurements include a time of cattle grazing. The third time slice focuses on the period of urban sprawl exposing bare ground (Gober and Trapido-Lurie, 2005; Sheridan, 2007). Ultimately, this dissertation seeks to better understand anthropogenic impacts on landforms and the operation of geomorphological processes on the alluvial fan and pediment piedmonts of the Sonoran Desert.

This dissertation is structured into six chapters. This chapter 1 provides a basic overview of the larger research question, while the bookend chapter 6 is a conclusion presenting brief synopsis of the overall research findings. The four middle chapters are focused for publication in appropriate venues to distribute the research.

Chapter 2 is a book chapter published in a book *Urban geomorphology: Landforms and Processes in Cities*. Chapter 2 with collaborators Suet Yi Cheung, Dr. Ian Walker, and Dr. Ronald Dorn. This chapter provides the geomorphic setting of the dissertation study area and overviews the impact of the Anthropocene in the Phoenix metropolitan region. The proposed new geological Epoch called the Anthropocene has been minimally studied in warm desert settings. In the Phoenix area, much of the anthropogenic impacts derive from cattle crazing, wildfire that results from introduced grass species, and urbanization processes, such as road building and home construction.

Chapter 3 is a paper published in the peer-reviewed journal *Land degradation & development*. This paper was co-authored with Dr. Ronald Dorn and presents a two-decade long record of erosion dataset at the sprawling edge of the Phoenix metropolitan

region. These data reveal that anthropogenic activities led to an overall increase in erosion process intensity in the Phoenix metropolitan region.

Chapter 4 is a manuscript currently in review in *Environmental Research Letters*. This manuscript presents a model to forecast reliable sediment yield under the condition of urban sprawl. The idea is that rapidly urbanizing desert cities need to construct appropriately sized flood control structures (e.g. dams) to reduce the impact of flooding hazards. This chapter does not focus on the water aspect of these structures, but rather on the sediment accumulated, because the sediment volume is an important design parameter for flood control structure design. Unlike water volume, that can be drained off by spillways, sediment volume behind the flood control structure is continuously stored, and this storage reduces the life expectancy of the flood control structure. Flood risk reductions are a crucial goal for rapidly urbanizing desert cities to become economically, socially, and environmentally more resilient, and the proposed model in this chapter is cost-efficient and simple, so it will improve sustainable flood control structure construction in rapidly urbanizing desert cities in lesser developed settings in Africa, Middle East, India, and Asia where limited data on soil erosion exists.

Chapter 5 is a working draft for submission the peer-reviewed journal *Nature Geoscience*. This draft presents the first comparison of soil erosion from urbanization to natural background rates of erosion measured through cosmogenic $^{10}$Be catchment-wide denudation rates. This chapter also includes statistical modeling of the urban acceleration of erosion for the entire Phoenix metropolitan region, and then this urban acceleration is

compared to cities in non-arid settings. This chapter is written in collaboration with Dr. Dylan Connor, Dr. Ronald Dorn, and Dr. Yeong Bae Seong.

# CHAPTER 2

# URBAN GEOMORPHOLOGY OF AN ARID CITY:

# CASE STUDY OF PHOENIX, ARIZONA

# (PUBLISHED IN *URBAN GEOMORPHOLOGY: LANDFORMS AND PROCESSES IN CITIES*)

**Citation:** Jeong, A., Cheung, S. Y., Walker, I. J., & Dorn, R. I. (2018). Urban geomorphology of an arid city: case study of Phoenix, Arizona. In *Urban Geomorphology* (pp. 177-204). Elsevier. https://doi.org/10.1016/B978-0-12-811951-8.00010-2

## ABSTRACT

The urban metropolis of Phoenix, Arizona, USA rests on classic desert landforms, including extensive areas of pediments, alluvial fans, sand sheets, and former areas of desert pavement. The Phoenix area landforms exemplify classic desert geomorphic processes, such as rock varnish accretion, dirt cracking, desert pavement formation, rock fall, debris flows, high magnitude- low frequency flooding events, and pedimentation. Recent urban expansion has pushed housing up against the base of steep desert slopes that are capable of generating debris flows, rock falls, and rockslides. Other geomorphic hazards experienced by urbanism in the desert include dust storms and flash flooding. The Phoenix metropolitan region offers an opportunity to explore the impact of the Anthropocene, as the proposed new geological Epoch defined by the human imprint, in warm desert setting impacted by cattle crazing, wildfire that results from introduced grass species, and urbanization processes, such as road building and home construction.

## SONORAN DESERT SETTING OF THE PHOENIX METROPOLITAN AREA

The present day climate and vegetation of the Phoenix metropolitan region (Figure 2.1) resembles much of the rest of the Sonoran Desert in central Arizona, USA. Annual precipitation displays a bimodal distribution with summer and winter maxima. Summer convective thunderstorms occur during the July-September Mexican Monsoon. Winter frontal rainfall derives from Pacific cyclones. Mean annual precipitation tends to be evenly split between winter and summer, averaging about 200 mm. The arid climate is typified by a distinct biogeography typical of the Sonoran Desert. Trees include palo verde (*Parkinsonia microphylla*), ironwood (*Olneya tesota*), and elephant tree (*Bursera microphylla*). Common desert scrub vegetation includes creosote bush (*Larrea tridentata*), brittlebush (*Encelia farinosa*), triangle-leaf bursage (*Ambrosia deltoidea*), catclaw acacia (*Acacia greggii*), desert globe mallow (*Sphaeralcia ambigua*), ocotillo (*Fouquieria splendens*). Succulents occur in great variety notably the iconic saguaro (*Carnegiea gigantea*), barrel (*Ferocactus cylindraceus*) and hedgehog (*Echniocereus engelmannii*) cacti that are abundant throughout the natural landscape.

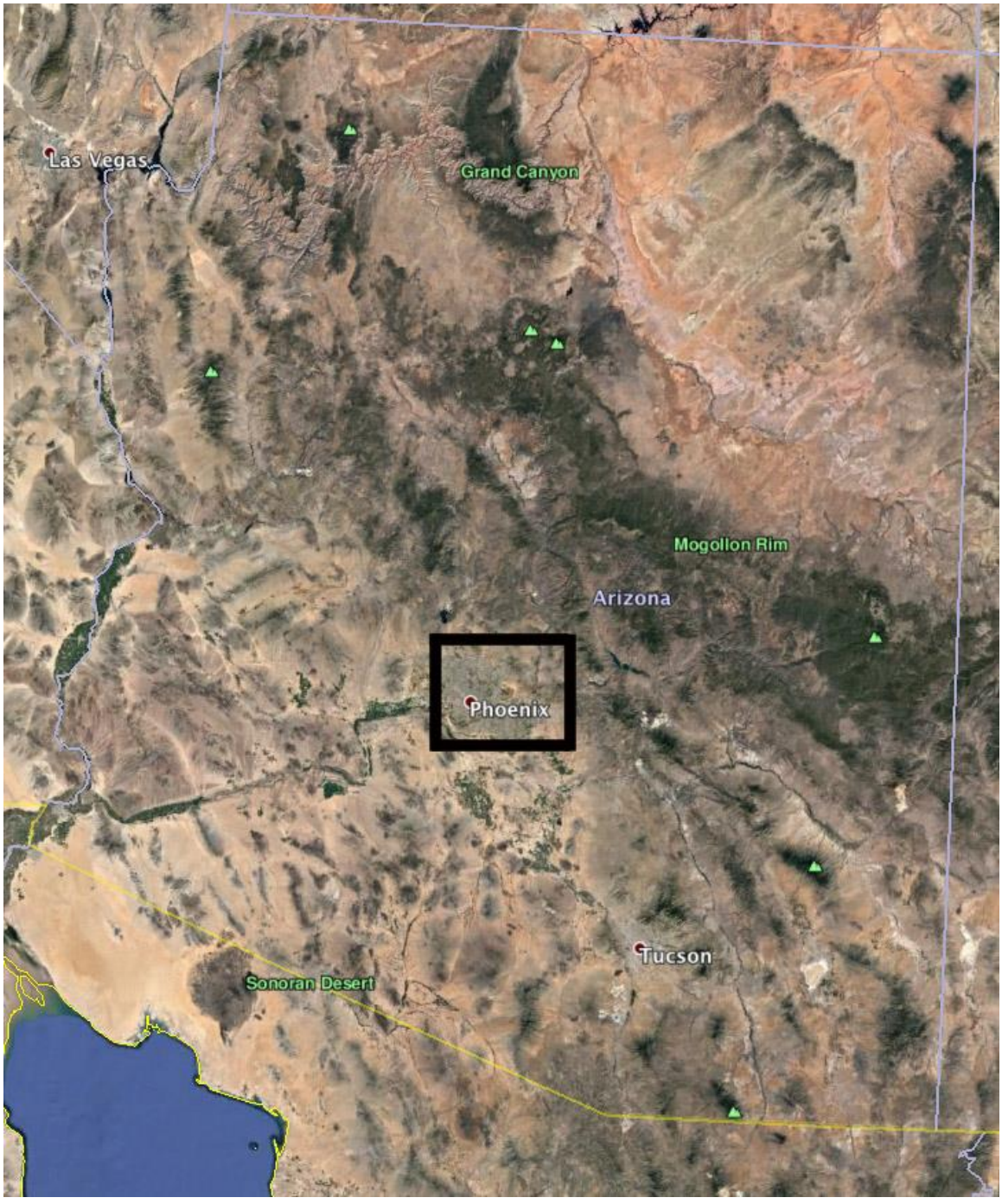


**Figure 2.1.** The state of Arizona as seen in Google Earth. The black box identifies the metropolitan Phoenix region as framed in Figure 2.2. Phoenix is situated in the northeastern corner of the Sonoran Desert. The forested highlands of the Mogollon Rim to the northeast provide much of the water for metropolitan Phoenix, funneled by the Verde and Salt River drainages.

Pollen and packrat midden studies in the Sonoran Desert and adjacent areas suggests the region did not become a desert until the Holocene, and it was not a desert in the latest Pleistocene. Pollen records in northern Baja California from 44 to 13 ka reveal the presence of pines, junipers, and sagebrush in that area indicating more humid and cooler conditions (Lozano-García et al., 2002). Packrat midden sequences in the Sonoran Desert indicate the presence of the dwarf conifers *Juniper osteosperma* and *Pinus monophylla* in the lower Sonoran Desert in this same late Pleistocene time range (Allen et al., 1998; McAuliffe and van Devender, 1998; van Devender, 1990). Thus, abundant evidence of a wetter and cooler time generated more extensive vegetation in the last glacial period and perhaps previous glacial cycles.

The geology of the Phoenix area underwent major crustal extension during the mid-Tertiary. This crustal extension resulted from the release of compressional stress after the Laramide mountain building period (Coney and Harms, 1984; Holt et al., 1986; Nations and Stump, 1981). This extension generated basin and range topography that developed between about 25 and 8 Ma. As a part of this extension, major rhyolite caldera eruptions started about 20 Ma, and metamorphic core complexes also domed up before most volcanic activity and extension finally ceased around 8 Ma (Reynolds, 1985; Spencer, 1984). The net result is a bedrock geology that mixes intrusive igneous granitic rocks, foliated metamorphic blocks, as well as extensive outcrops of rhyolitic welded tuff from major eruption episodes during extension (Figure 2.2).

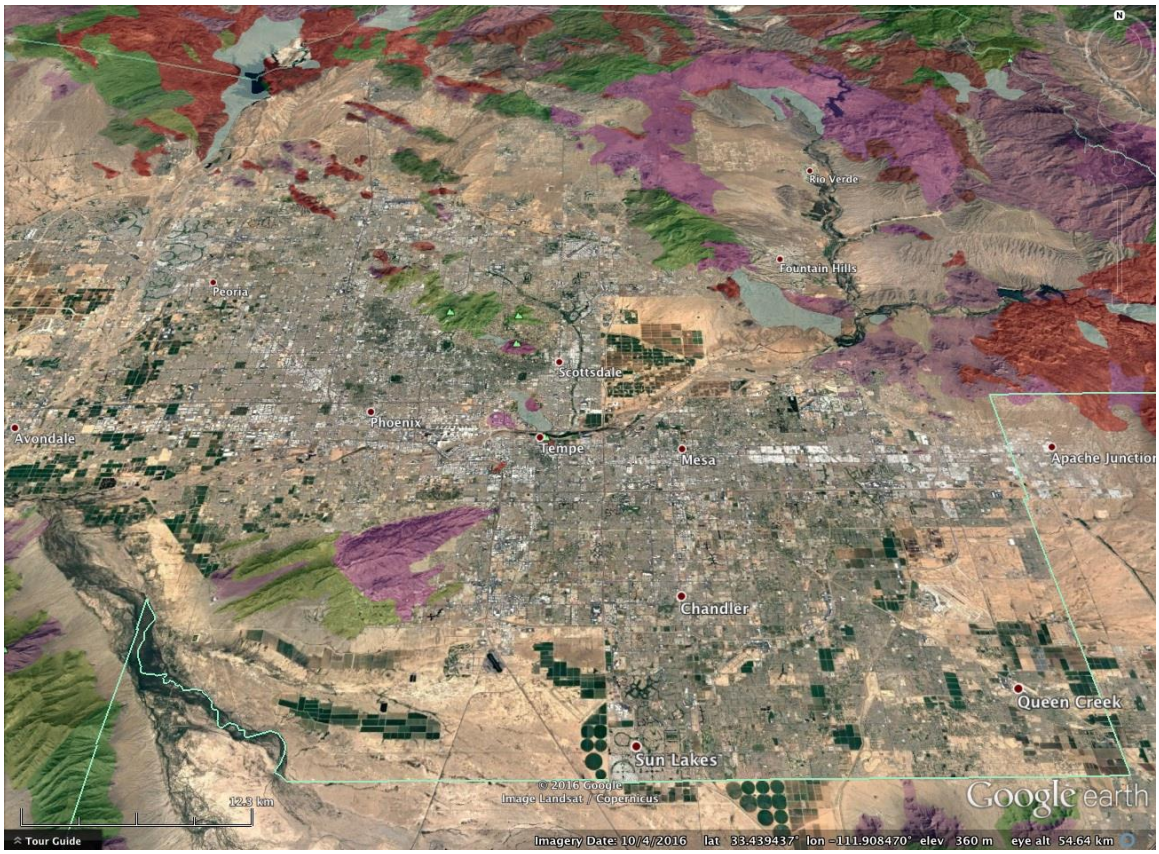


**Figure 2.2.** Geological map of bedrock ranges in the metropolitan Phoenix draped on a Google Earth oblique image. The mapping units derive from the Arizona Geological Survey (Richards et al., 2000), but are generalized here to help visualize isolated bedrock mountainous areas: intrusive igneous (pink), extrusive igneous (red), metamorphic (green), and mid-Tertiary sedimentary rocks (gray). Most urban space, thus, rests on Quaternary sediment ranging from Pliocene to Holocene in age.

The geomorphic landscapes of the Phoenix area contain a mixture of classic desert landforms. Bedrock landforms depend greatly upon the rock type. Granitic forms include classic domed inselbergs or bornhardts where jointing is far apart, but more complex landscapes where the jointing density increases and influences biotic communities (Seong et al., 2016b). Metamorphic slopes tend to host debris-flow chutes

and levees (Dorn, 2012). Rhyolitic welded tuff deposits of the Superstition volcanic field (Stuckless and Sheridan, 1971) develop more massive cliff faces.

The nature of piedmont slopes in front of the ranges depends on drainage area. Larger ranges have sufficient drainages to develop alluvial fans or alluvial slopes (Applegarth, 2004), whereas bedrock pediments form in front of smaller mountain masses (Kesel, 1977). The low relief areas now occupied by the urban scape of the Phoenix metropolitan area (Figure 2.2) consist of the distal ends of pediments, the distal end of alluvial fans, aeolian sand sheets, and alluvial deposits.

An individual walking on these landforms, before massive land-use change associated with cattle grazing and urban expansion, would have experienced very different surface conditions than found by the average hiker today. Extensive areas once hosted desert pavements, biological soil crusts (Nagy et al., 2005), and interlocking colluvium on steeper slopes, providing a net armoring effect (Bowker et al., 2008; Granger et al., 2001; Seong et al., 2016a). Today, only patches of such armored surfaces remain, providing glimpses into the original land surfaces. Thus, this chapter attempts to give the reader a sense of the geomorphology that once was (and still exists in a few places) and a desert geomorphology influenced by the Anthropocene (Waters et al., 2016) and its urban footprint.

## COMMON DESERT GEOMORPHIC PROCESSES IN THE PHOENIX METROPOLITAN AREA

This section presents some of the more important desert geomorphic processes that occur in the Phoenix area. The section starts with processes related to rock decay (weathering) rock coatings and soils. The second section explores how aeolian, fluvial, and human activities interact in the fringe of the Phoenix urban area. The third section overviews mass-wasting processes on the steep slopes of desert mountain ranges in the middle of Phoenix. Much of the Phoenix metropolitan region is built on pediments, and the fourth section explains that the Phoenix area is truly unique in terms of the occurrence of pediments in several different rock types.

### ROCK DECAY, ROCK COATINGS, AND SOILS

Dirt cracking is the dominant process of physical weathering in the Phoenix area. Any random rock fracture, when pried open, reveals evidence of the dirt-cracking process (Dorn, 2011; Ollier, 1965). A combination of laminar calcrete precipitation and the wetting and drying of dust accumulated in fractures gradually opens fissures to the point where spalling occurs. Unlike other forms of physical weathering, dirt cracking leaves behind visual evidence of the process. Laminar calcrete coats the walls along the narrowest parts of a fissure, which is a space wide enough for capillary water to penetrate that leads to calcium carbonate precipitation, but not dust infiltration. Eventually, the fracture widens enough to allow dust to infiltrate. Iron films coat the walls, where dust penetrated and remains in contact with rock surfaces. Iron from the dust and clays from

the dust result in iron films that are typically less than 10 μm thick. Black rock varnish forms a rim around the margins of the fracture, where rainwater has washed away the dust and the removal of this alkaline dust allows manganese-enhancing bacteria to develop and form a coating of rock varnish over the iron film.

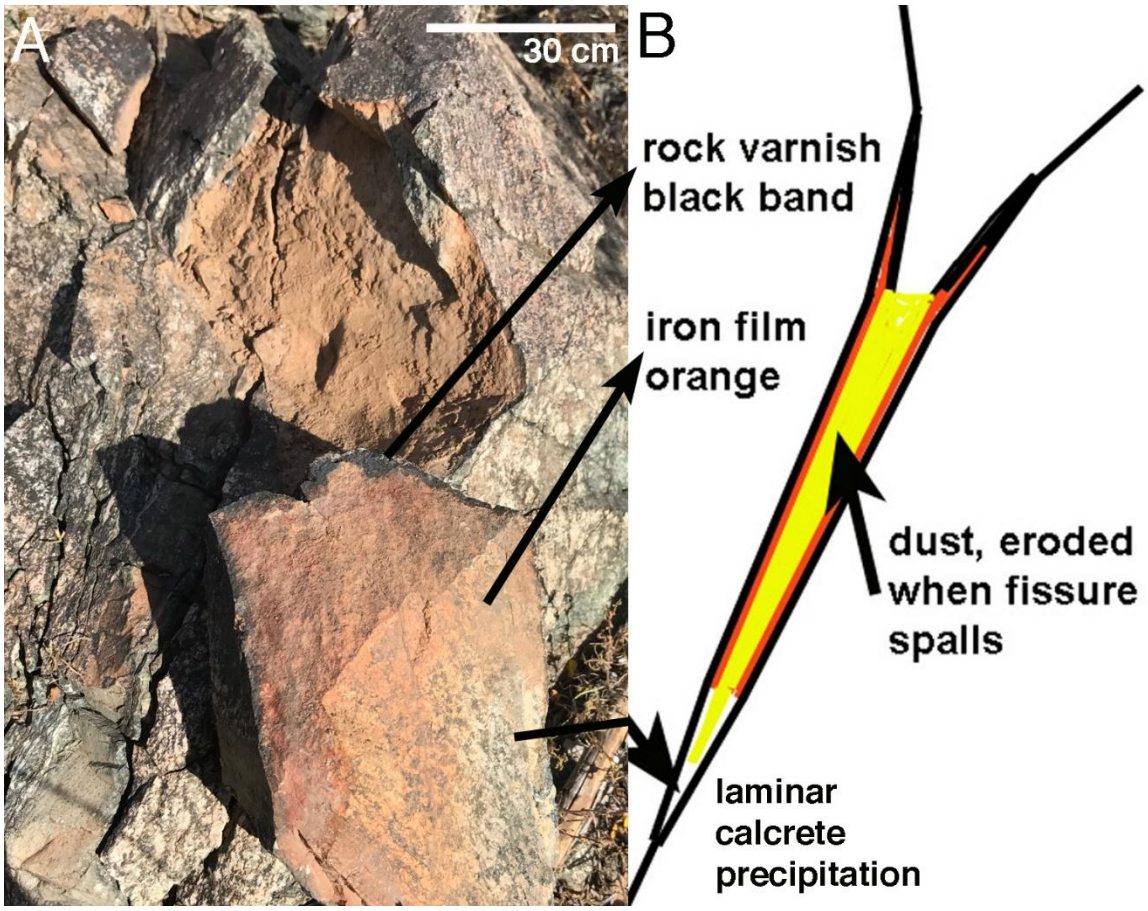


**Figure 2.3.** Dirt cracking proceeds through both laminar calcrete precipitation and the wetting and drying of dust wedges open rock joints. (A) A 0.5 mm fracture was manually pried open at South Mountain, Phoenix. Dust filled the fracture. The two sides of the fracture display rock coatings diagnostic of fractures experiencing dirt cracking. (B) Idealized diagram of rock coating formation associated with fractures opened by dirt cracking.

Granitic rocks underlay extensive areas of metropolitan Phoenix (Figure 2.2). Thus, classic weathering forms of cores stones, tors, domed inselbergs (bornhardts), and kopje occur throughout the Phoenix area (Figure 2.3). Jointing is particularly important in the morphogenesis of granitic terrains (Molnar et al., 2007). Molnar et al. (2007, p. 12) postulated that jointing rests at the core of geomorphic weakness: "Here we speculate that a corollary to the arguments given above about the role of tectonics as a crusher of rock is that in those places where rock has dodged the rock crusher, it may be stronger and less easily removed by erosive agents" (Molnar et al., 2007, p. 12). Jointing is particularly important in arid weathering-limited landscapes (Abrahams et al., 1985; Howard and Selby, 2009; Viles, 2013).

Core stones and tors are common in the wealthier areas of metropolitan Phoenix, such as north Scottsdale, Fountain Hills, and east Mesa. Core stones are the spheroidal less decayed boulders that emerge at the surface as grus erodes (Figure 2.4B) (Twidale, 1982). Domed inselbergs, also known as bornhardts, are bald, and steep-sided domes with a range of shapes and size (Twidale, 1981) (e.g. Figure 2.4A). Bornhardts like those seen in metropolitan Phoenix (e.g. Figure 2.4A) maintain a lower joint density than the surrounding granite. Meanwhile, the surrounding granitic rocks with high joint density experienced active mineral decay to grus. However, the existing joints in bornhardts eventually do separate, leading to rock slides and eventually collapse into a landform known as a kopje (e.g. Figure 2.4C) similar to those studied in Africa and Australia (Michael et al., 2008).

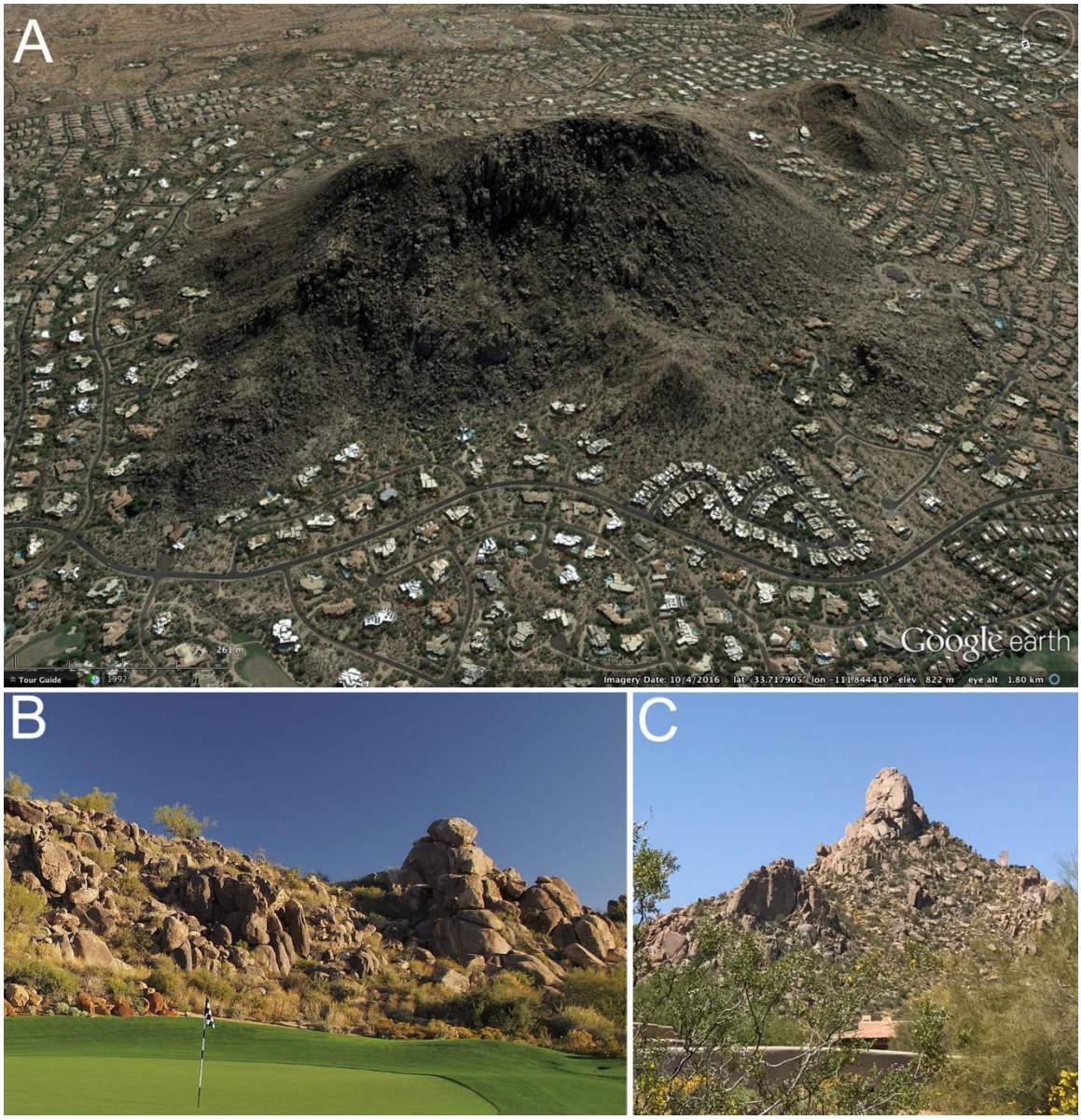


**Figure 2.4.** Landforms resulting from decay of granite in a desert setting in Scottsdale create an aesthetic setting for the wealthy in metropolitan, Phoenix. (A) Troon Mountain, a bornhardt, is surrounded by large home and mansions. (B) Golf courses place greens adjacent to spheroidal core stones and tors. (C) Large homes and mansions surround the collapsed bornhardt known as Pinnacle Peak, a kopje.

Desert pavements consist of a smooth surface with closely packed, interlocking pebbles, cobbles, and sometimes with scattered boulders (Figure 2.5A). Pavements

provide insight into the antiquity of the underlying landform (Seong et al., 2016a), aid in the preservation of ancient artifacts (Adelsberger et al., 2013), and provide information about environmental history (Dietze et al., 2016) and desert soils (Peterson et al., 1995). Although introductory textbooks often attribute desert pavements to deflation winnowing of fines, the desert pavements in the Phoenix area are not a result of wind erosion. In the case of the entire Sonoran Desert, very little evidence of aeolian abrasion exists (Seong et al., 2016a). For example, desert pavements at South Mountain Preserve, Phoenix, have: coatings of rock varnish that deflation would have abraded away (Figure 2.5A); vesicular Av soil horizons from the accumulation of dust underneath surface clasts (Figures 2.5B and 2.5C); closely spaced clasts separated by silt and clay surfaces; and no evidence of ventifacts.

The desert pavement in the Phoenix area was initiated when floods or debris flows deposited loose and unconsolidated clasts on the surface (Figure 2.5D). Aeolian fines slowly move into the matrix between the large clasts deposits (Figure 2.5C), and the size of clasts become smaller mostly from dirt-cracking processes (Figure 2.3). As dust accumulates and clast sizes decreases, the relief of the original bar-and-swale topography gradually reduces (Figure 2.5E). The key to stable pavements (e.g. Figure 2.5A) in the Phoenix area is: a combination of a relatively flat surface; the accumulation of allochthonous dust; a lack of headward retreating swales or gullies (Seong et al., 2016a); and most critically a minimal amount of human activity as even just one vehicle driving over a pavement surface can do damage (Figure 2.5F).

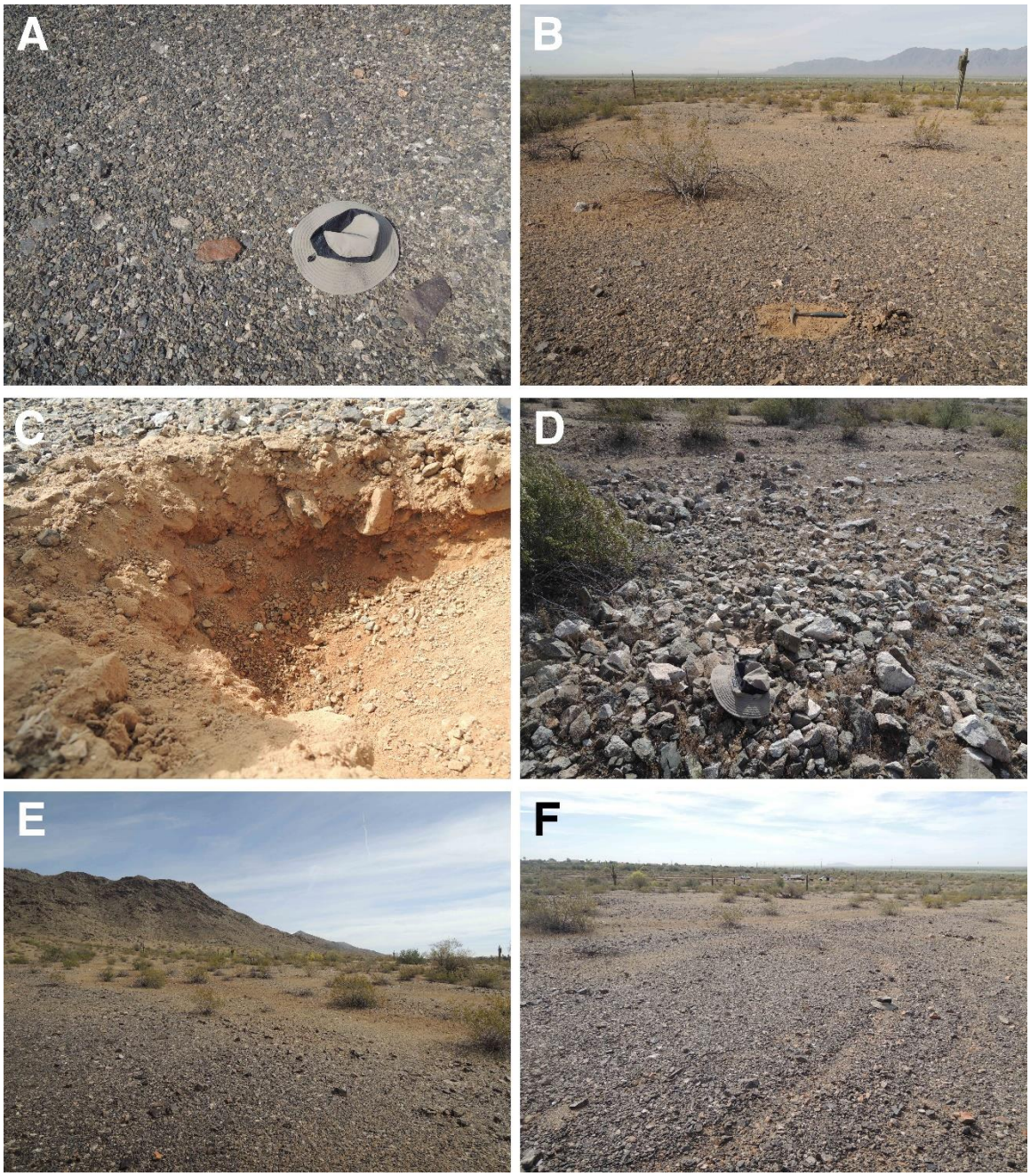


**Figure 2.5.** Desert pavement surfaces at South Mountain, Phoenix. (A) Pleistocene desert pavement showing weathered clasts that are closely packed and interlocked. (B) Dust accumulation underneath surface clasts seen after removal of the pavement clasts with rock hammer for scale. (C) Vesicular soil horizon termed the Av horizon and the underlying Bk horizon with carbonate-covered clasts. (D) Floods deposit typically maintain a rough bar and swale form. (E) Over time, the relief of the bar-and-swale topography decreases as swales fill in and bars erode. (F) Desert pavement by off-road driving by just one vehicle (arrow).

Biological soil crusts (BSCs) consist of assemblages of living organisms on soil or rock surfaces in arid and semiarid areas. Typically composed of cyanobacteria, fungi, lichens, and algae, they cover a wide variety of undisturbed Sonoran Desert soils (Figure 2.6) and protect desert surfaces from erosional shear stresses imposed by overland flow and strong winds (Allen, 2005, 2010).

When soil is wet, the mucilage of cyanobacteria swell and filaments of cyanobacteria move up toward the soil surface (Belnap et al., 2001). This repeated swelling and frequent movement leaves copious sheath material in the uppermost soil layers that, in turn, maintains soil structure after the BSCs are dehydrated and soil particles become loose (Belnap, 2003). Thus, BSCs and especially filamentous cyanobacteria, adhere to and aggregate with soil particles, and their cohesion increases surface stability and prevents erosion in arid and semiarid lands (Belnap, 2003; Bowker et al., 2008).

Although BSCs are extremely well adapted to the harsh growing conditions in deserts, they can be significantly altered by disturbances, such as grazing, recreational activities (hiking, biking, and off-road driving), and military activities (Belnap and Gillette, 1998) (Figure 2.6). Faist et al. (2017) examined BSC hydrologic responses to disturbance at different crustal development stages on sandy soils on the Colorado Plateau through a simulated rainfall experiment. They found that trampling well-developed dark cyano-lichen-dominated crusts increased total sediment loss by nearly four times in comparison to intact controls during a 30 min simulated precipitation event, suggesting that well-developed, intact dark BSCs generally decrease runoff and sediment

loss and considerably increase aggregate stability (Faist et al., 2017). While BSCs are extremely vulnerable to disturbance, their recovery time can be relatively slow. No growth of BSCs occurred in the central Namib, for example, over an eight year period of observation (Viles, 2008).

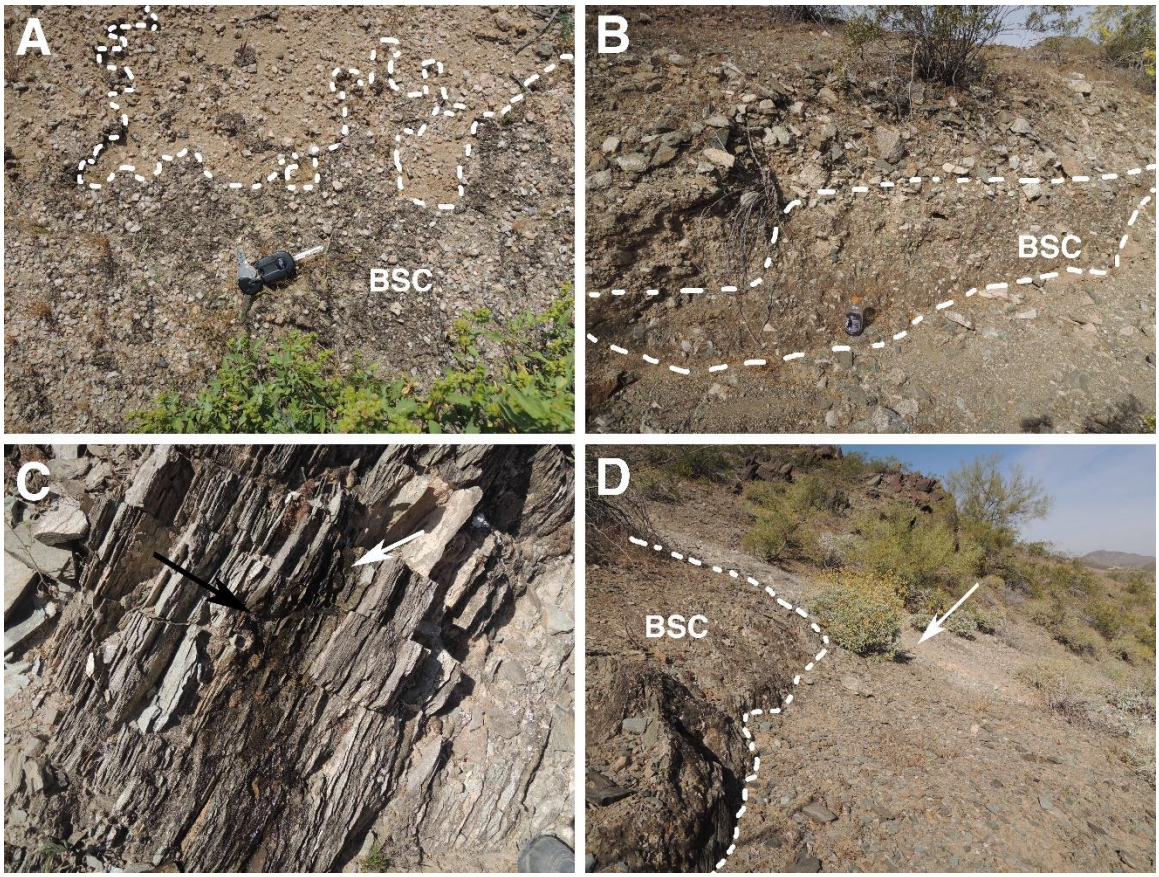


**Figure 2.6.** Biological crusts on soil and rock surfaces in metropolitan Phoenix. (A) Biological crusts on a soil surface with car keys for scale. The upper portion of the image was disturbed by the compressive force of cattle grazing, although some recovery has occurred as seen in the lower half of the image (underneath dashed line) over the past 12 years since cattle grazing ceased. (B) BSCs growing on the side of the east-facing side of a desert wash, an aspect that reduces exposure to directly sunlight in the warmest part of the day. (C) BSCs on a rock surface, where the surface was wetted resulting in a greening up by the algae (whit arrow), where fungi did not green up (black arrow). (D) BSCs disturbed along a hiking trail, but still evident away from the trail.

A variety of different rock coatings occur throughout the metropolitan Phoenix area, but manganese-rich rock varnish darkens the vast majority of exposed rock faces. Figure 2.7A illustrates the typical appearance of rock varnish. Figure 2.7B presents an ultrathin section of varnish, revealing the presence of fine micrometer-scale laminations or "microlaminations." These layers form as a result of Holocene and Pleistocene climatic changes (Liu and Broecker, 2007; Liu and Broecker, 2008). Where these layers have been calibrated by independent ages (Liu, 2017), it is possible to assign millennial-scale ages to landforms (Liu and Broecker, 2013). In the case of Figure 2.7C, a varnish started to form about 8.1 ka, indicated by wet Holocene (WH) layer WH9 at the base of the varnish.

Human activity has left a distinct chemical imprint on rock varnishes. The iron and manganese hydroxides that provide the varnish color also scavenged the lead used in gasoline in the early part of the 20th century. This lead accumulates in the surface-most micron of the varnish (Figure 2.7C), as evidenced by electron microprobe measurements (e.g., 0.44% PbO in Figure 2.7C). This is far greater than background levels seen in natural varnish of <0.03% PbO. Although this Anthropocene signal may seem a bad thing at first, representing widespread contamination, the lead actually provides a useful chronometric marker able to identify purely 20th century flooding surfaces as well as authentication of rock engravings (Dorn et al., 2012).

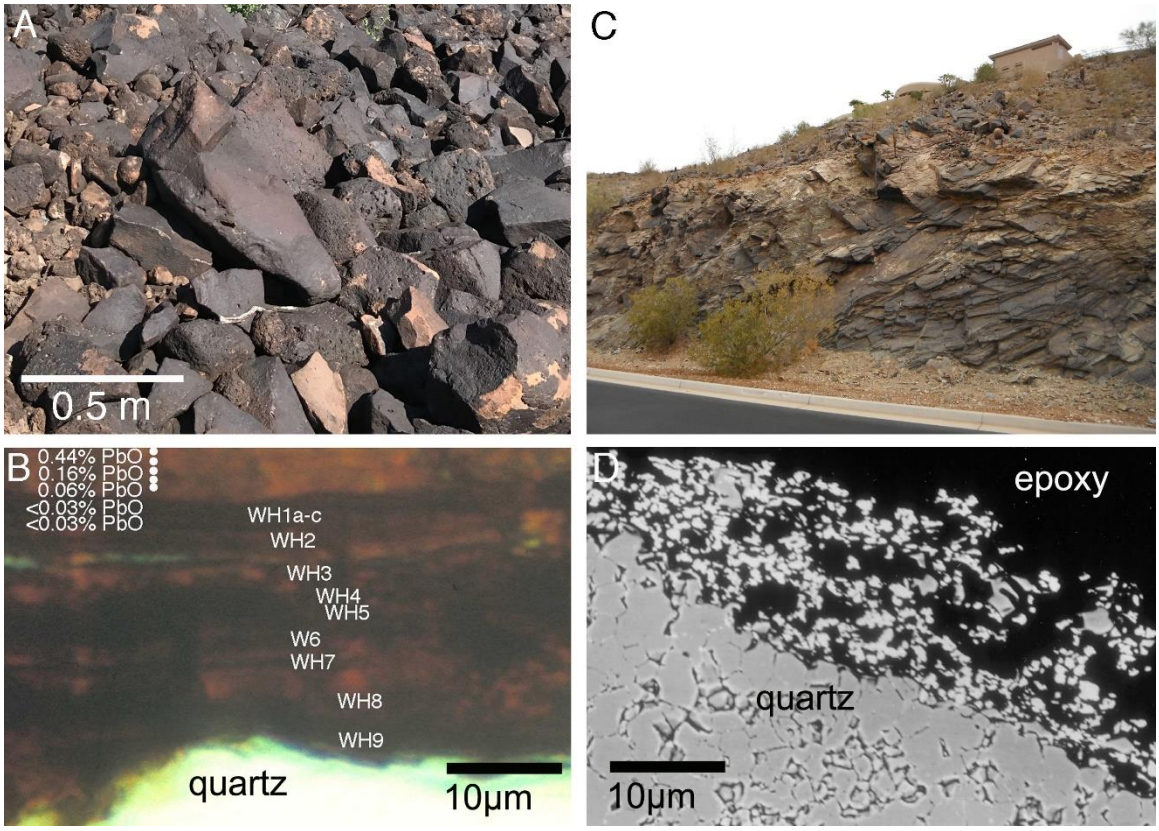


**Figure 2.7.** Rock varnish as the dominant natural rock coating in metropolitan Phoenix. (A) Colluvial boulder field at Shaw Butte darkened by rock varnish. The occasional orange iron film represents rocks spalled by the dirt cracking process (Figure 2.3). (B) Microlaminations form discrete black, orange, and yellow layers in rock varnish thin sections. (C) Urbanization tends to create scars across rock faces, but developers in affluent communities applied "artificial varnish" to minimize the aesthetic impact of a road cut. D) Back-scattered electron microscope image of artificial varnish from image C that is experiencing ongoing dissolution, generating the granule-like appearance.

The dominance of rock varnish makes it easy to spot anthropogenic disturbances associated with construction because the underlying rock is always much lighter in color, including basalts. Some developers in affluent communities decided to try an experimental treatment of artificial varnish (Elvidge and Moore, 1980) to reduce the aesthetic impact of road construction, as seen in the road cut shown in Figure 2.7B. This

artificial varnish is slowly dissolving into granules (Figure 2.7D). In contrast to natural varnish, artificial varnish has not been binded with clay minerals that in turn help cement natural varnish to the underlying rock (Dorn and Oberlander, 1982).

## INTERPLAY OF AEOLIAN, FULVIAL, AND ANTHROPOGENIC PROCESSES

The interaction between aeolian and fluvial processes can be an important factor in the shaping of dryland environments (Bullard and Livingstone, 2002). Source bordering dunes represent a common landform in many dryland environments, such as dunes closely bordering a river (Page et al., 2001). When these fluvial sediments are exposed to the air during a prolonged dry period, winds are more likely to affect sediment transport, and wind velocity and particle size are critical factors to entrain sediments.

Two large exoreic river systems cross the Phoenix metropolitan area. The Salt River runs through the center, while the Gila River flows along the southern boundary. A small area of source bordering dunes and a sand sheet occurs north of the Gila River (Figure 2.8). Sediments collected from the Gila River show considerably less rounding than sediments collected from the source bordering dunes (Figure 2.9).


**Figure 2.8.** Source bordering dunes near the Gila River in the southern part of the Phoenix Metropolitan area. Areas denoted by the dashed lines locate areas with distinct dune forms. However, the land between these areas is covered by a sand sheet.

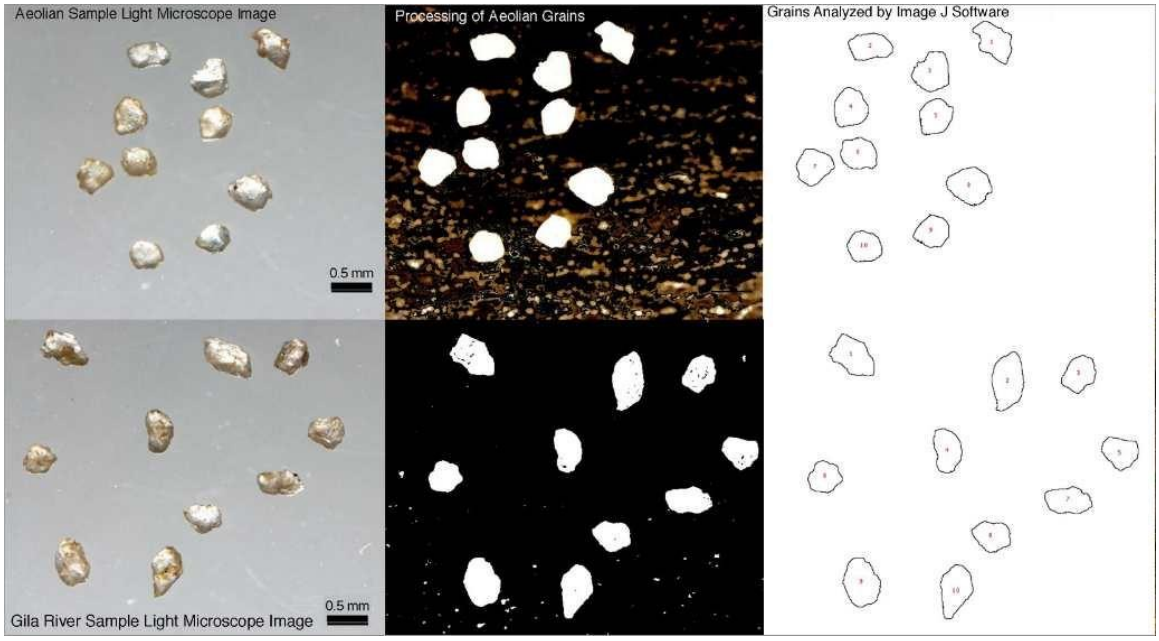


**Figure 2.9.** Grain size analysis of aeolian and fluvial sediments using the ImageJ software. The aeolian sample (upper row) from source-bordering dunes display more rounding than the fluvial sediments from the Gila River (lower row). The grains are first imaged with light microscopy (left column), then subject to digital image processing (middle column), and the resultant grain perimeter is used by the ImageJ software to generate shape parameters. The result of grain shape analysis shows that the aeolian sediments have a higher value in roundness (0.78–0.79) and a lower ratio in aspect ratio (1.29–1.30) than fluvial sediment that has 0.70–0.72 in roundness and 1.45–1.50 in aspect ratio.

This area experienced a variety of land uses, including cattle grazing, irrigated agriculture, road construction, and the building of subdivisions. Concomitantly, human activities along the Gila River altered the natural river system, hydrological processes, and, thus, sediment supply to these source-bordering dunes. For instance, the construction of the Coolidge Dam in the upper course of Gila River in 1928 greatly reduced the flood frequency and magnitude, so that sediment supply has decreased. At the same time, an invasive species, Tamarisk, invaded the riparian zone of the Gila River and spread

rapidly in the 1900s (Graf, 1988). The presence of Tamarisk affects both aeolian and fluvial processes in terms of reducing the sediments in transport and the shear stress on the soil surface. These anthropogenic effects likely decreased the sediment transport to the Gila source-bordering dunes. However, extreme weather events, such as the 1993 flood in Phoenix, triggered by El Niño, reactivated the formation of sandbars and changed the channel form to a braided stream pattern along the Gila River due to increased sediment supply. Figure 2.10 summarizes some of the major controls influencing the potential supply of sediment along the Gila located next to the dunes.

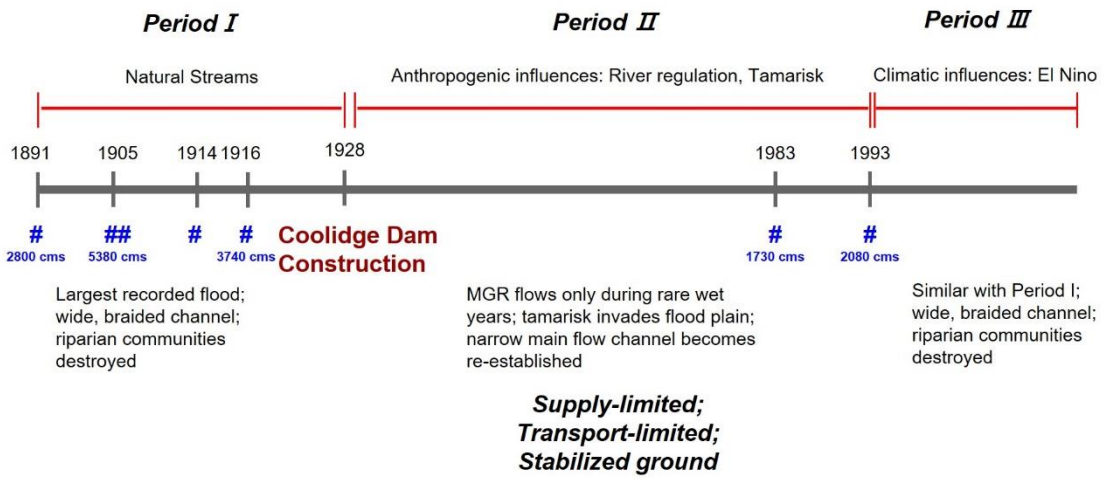


**Figure 2.10.** Timeline of anthropogenic alteration and large flood events along the Gila River. Period I: Gila River was a natural channel with frequent seasonal flooding. Period II: Anthropogenic activities altered the natural channel system of Gila River, largely reducing sediment supply for both aeolian and fluvial transport as well as flood frequency. Period III: Extreme climatic events caused large floods along the Gila River, reactivated aeolian and fluvial-transport processes due to the increased sediment availability.

Extensive areas of the cities of Chandler, Gilbert, Mesa, and Tempe in the metropolitan area are covered by several meters of fine sandy material. This material

could have been derived in part by aeolian transport from the Gila River. In addition, there are lenses of river-transported gravels and cobbles derived from bordering mountains. Thus, it is likely that aeolian and fluvial processes resulted in a mixture of a sand sheet intercalating with low-energy rivers. Figure 2.11 illustrates an anthropogenic excavation into this mixed interfingered aeolian and fluvial deposit.

**Figure 2.11.** An excavation exposed a depositional unit between the Salt and the Verde Rivers in metropolitan Phoenix. Some sediments are clearly fluvial with small cobbles, while sandy units show evidence of both fluvial and aeolian transport. 4-m tall Paloverde trees provide scale. The uppermost 1.5 m consists of rock and sand from construction activities.

## MASS WASTING

Talus from rock falls and rock slides covers steep slopes of desert mountain ranges throughout the southwestern USA (Melton, 1965; Parsons et al., 2009). Urban expansion in arid regions globally (Cooke et al., 1982) continues to thrust infrastructure at the base of steep desert slopes. This is certainly the case in the Phoenix area (Dorn, 2014; Harris and Pearthree, 2002), where the wealthy build homes right on the margins of

mountain preserves (Ewan et al., 2004) and often beneath steep bare rock faces (Figure 2.12). Chronometric studies of rock fall in the Phoenix area reveal that rock falls occurred throughout the Holocene (Dorn, 2014) and historically in the Anthropocene.

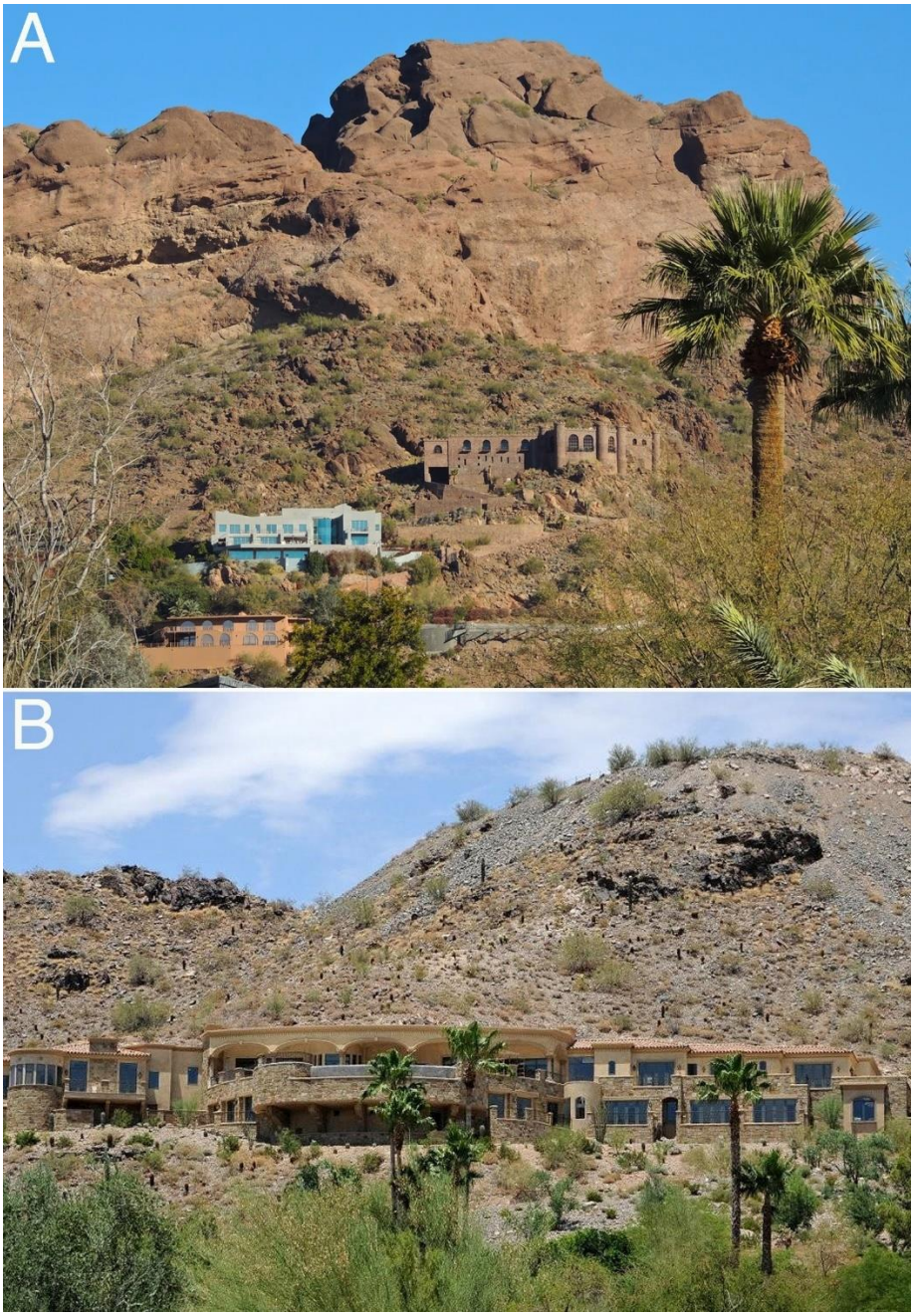


**Figure 2.12.** Historic rock falls place wealthy homes in potential danger in such areas as Camelback Mountain (A) and the Phoenix Mountains (B).

Debris flows are one of the most hazardous landslide types in any region with steep terrain and precipitation, including the Phoenix area (Dorn, 2012, 2016). Debris flows occur when slopes fail to maintain the equilibrium between gravitational drivings and frictional resisting forces (Iverson, 2005). Thus, debris flows typically occur on steep-slope areas between 20 and 45º after prolonged or particularly intense wetting events (Jakob and Hungr, 2005); in the case of the Phoenix area, from thunderstorms, soaking hurricane moisture, or a series of winter frontal storms (Dorn, 2016).

Debris flows have three zones, including initiation, transportation, and deposition (Figure 2.13) (Jakob and Hungr, 2005), and distinctive geomorphic features can be identified in each zone. Distinct head scarps indicate the initiation zone, where slope failures start. Once initiated, chutes develop along the debris-flow channel, and debris-flow materials are transported down the slope. Finally, debris flows produce levees and alluvial fans at the mouths of drainages (Figures 2.13A and 2.13B) (Webb et al., 2008; Youberg et al., 2008). In the case of most debris-flow contexts in Phoenix, the chutes are only a few hundreds of meters long, and the alluvial fans that result exist only at the base of the slopes, as illustrated in Figure 2.13.

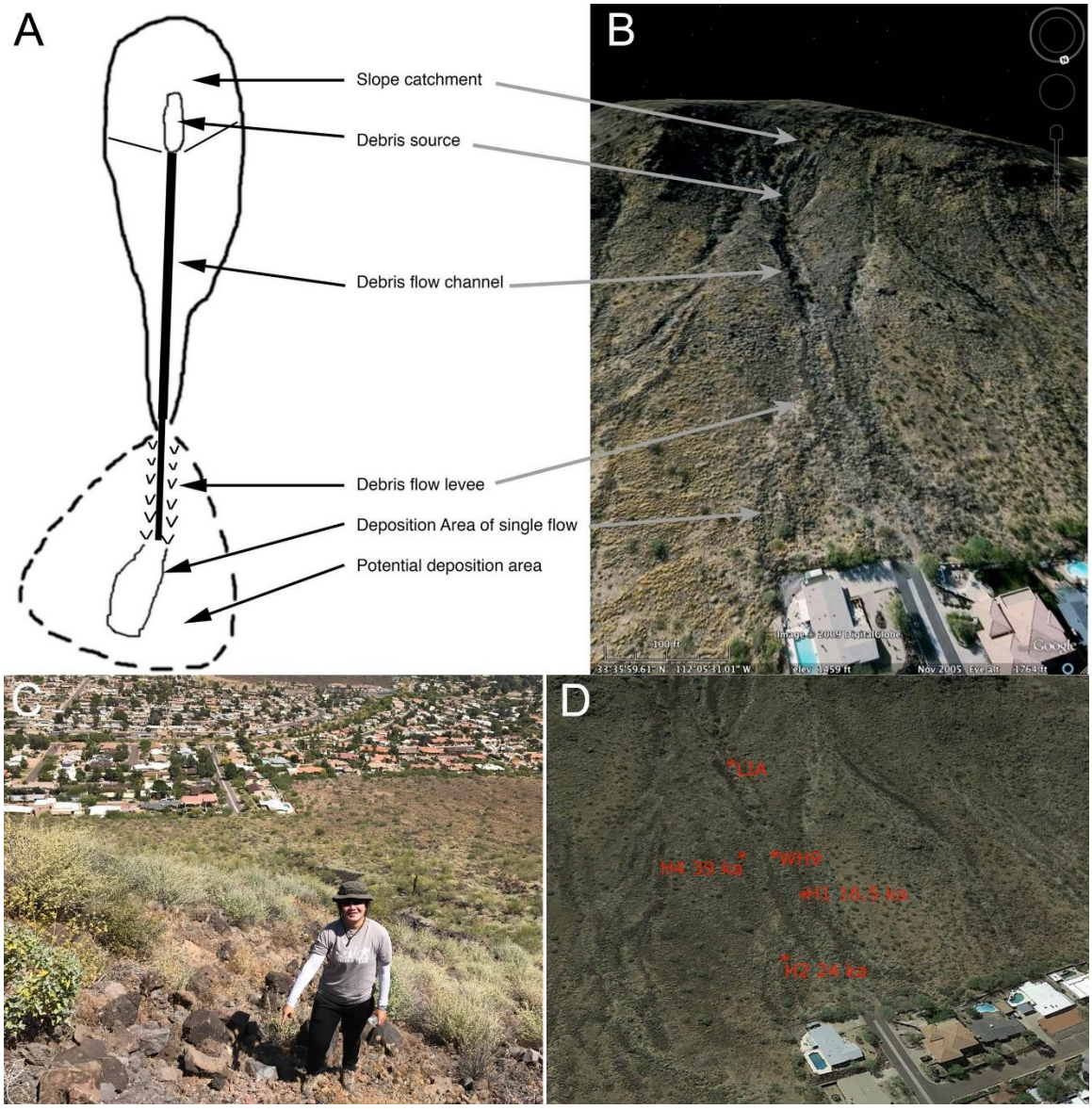


**Figure 2.13.** Shaw Butte in the Phoenix Mountains illustrates how debris flows interface with urbanization. (A) and (B) illustrate the debris-flow system, where small catchments generate debris flows that move down chutes a few hundred meters long, resulting in debris flow deposition near the mountain front. Image C illustrates the source region of the most recent Little Ice Age (LIA) flow that occurred about 0.65 ka. Image D identifies debris-flow deposits that are preserved and occurred about 8.1, 16.5, 24, and 39 ka. However, an unknown number of other debris flows occurred, with evidence destroyed by subsequent events.

Rock slides are another type of mass wasting that involves the displacement of rock materials along a sliding plane, such as a bedding plane and the interface between two different rock types. Granitic rocks experience sheeting, and produce pressure-release shells once the overlying materials have been removed (Bahat et al., 1999). The Phoenix neighborhood of Awhatukee illustrates three different types of mass-wasting events associated with pressure release shells: debris flow (Figure 2.14B), rockfall (Figure 2.14C), and rockslide (Figure 2.14D). What may be surprising is that the homes at the base of these steeply-dipping joint faces have little to no understanding of the potential hazard just meters from their homes.

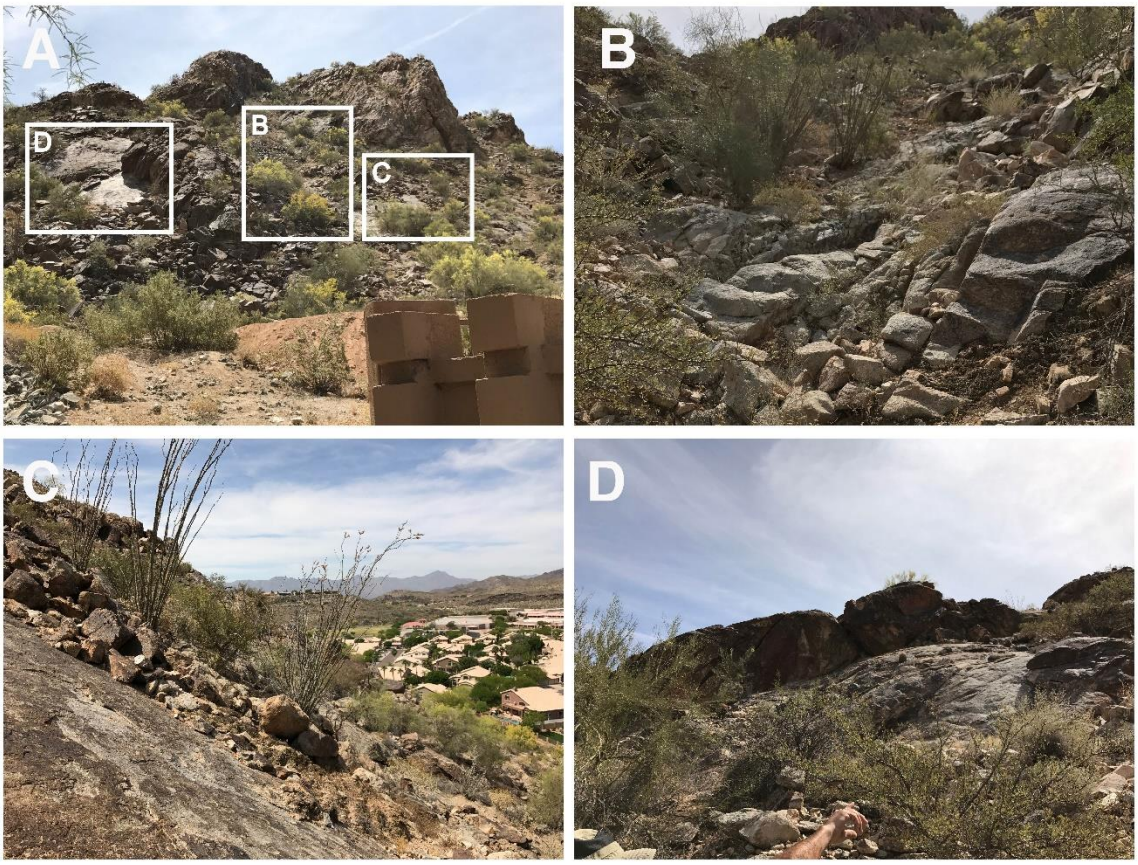


**Figure 2.14.** Image (A) is from the perspective of looking at the mountain slope from the resident's back fence, where (B) debris flow levees, (C) talus from rock falls, and (D) a

rock slide all represent hazards above a suburban neighborhood. Note the massive rock in D that is situated on the pressure-release joint of granitic surface with little to no support to inhibit the next mass-wasting event.

## PEDIMENTATION

The Phoenix metropolitan area hosts iconic pediments with a variety of rock types that makes this area the rival of any other classic pediment sites on Earth (Figure 2.15). Pediments with the classic sharp piedmont angle exist on forest service and city preserve lands, allowing for study of the entire inselberg-pediment landscape (Figures 2.15A, 2.15B, 2.15D, 2.15H)**.** The largest expanse of pediments, however, rests under urban sprawl (Figures 2.15C, 2.15F, 2.15G).

The pediment literature maintains an extensive bias toward granitic study sites (Dohrenwend and Parsons, 2009), including central Arizona (Kesel, 1977; Pelletier, 2010). However, the Phoenix area contains pediments in broad four rock types (Larson et al., 2017): granitic (Figures 2.15A, 2.15B, 2.15D); foliated metamorphic (Figures 2.15C, 2.15G, 2.15H), sedimentary breccia with extensive sandy lenses (Figures 2.15E, 2.15F), and ignimbrite. Given this mixed lithology, explanations of the pediment form requiring differential decay of granitic rocks and fossilized landscapes (Oberlander, 1989) do not work, since similar forms exist side-by-side in rock types other than granite. Furthermore, given the central Arizona evidence that pediment forms are able to adjust to base-level change in the timeframe of the last glacial cycle (Larson et al., 2017), also removes the need for complicated explanations of form requiring two-stage etching (Twidale, 2002).

Our view of pedimentation as a process in the Phoenix area returns to early German geomorphological thinking (Penck, 1924), G.K. Gilbert's classic observations (Gilbert, 1877), and more modern process-geomorphic interpretations (Applegarth, 2004, Larson et al., 2017, Parsons and Abrahams, 1984). Pediments function as transport surfaces (conveyor belts) of materials that are detached and eroded from small mountain masses. Pediments form where drainage areas are too small to develop alluvial fans. The classic piedmont angle, which is seen as a fairly dramatic slope break, results from the greater resistance to detachment and transport of larger slope colluvial particles and bedrock that leads to the generation of steeper slopes. The slopes of pediments once graded to gradually aggrading closed basins throughout the late Miocene and Pliocene, but pediments have been experiencing ongoing adjustment to changing base level throughout the Quaternary (Larson et al., 2014)

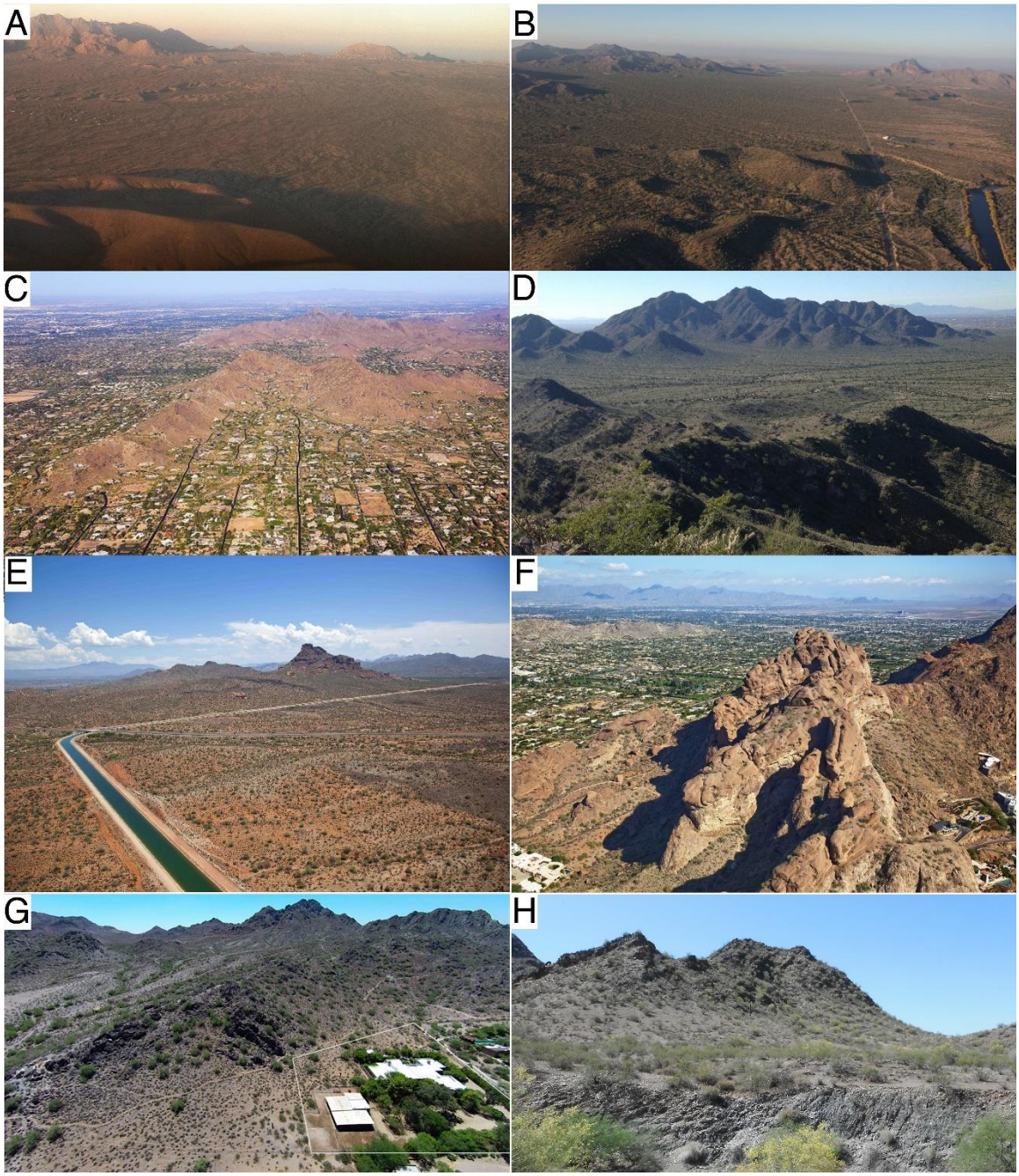


**Figure 2.15.** Pediment-inselberg landscapes of metropolitan Phoenix, illustrating planar pediments in front of small inselberg ranges. (A) granitic eastern McDowell Mountains; (B) granitic northern Usery Mountains; (C) foliated metamorphic Mummy Mountain; (D) granitic San Tan Mountains; (E) breccia Red Mountain; (F) breccia Camelback Mountains; (G) massive metamorphic North Mountain; and (H) foliated metamorphic Phoenix Mountains.

## ALLUVIAL FAN FLOODING

The basic ephemeral channel morphologies of the Sonoran Desert (Sutfin et al., 2014) include bedrock channels in the upper interior of the drainage that transitions to bedrock mixed with alluvium, and ultimately to incised alluvium at an embayment that merges into an alluvial-fan piedmont. For much of the Sonoran Desert, including Phoenix, the alluvial-fan piedmont is incised. The risk for flooding only comes where the channel emerges from the incised area and is then able to experience an avulsion (Fuller, 2012). Such alluvial-fan avulsions only occur below the hydrological apex and not on older abandoned alluvial-fan surfaces.

The Federal Emergency Management Agency (FEMA) uses a procedure for delineating flood-hazard zones on alluvial fans, with fiscal implications for those building on surfaces so delineated on flood insurance-rate maps based on the FEMA approach. Put simplistically, FEMA treats as potentially hazardous all surfaces beneath the topographic apex of a fan. However, vast tracks of land in the 100-yr flood-hazard zone are not truly flood prone if they exist above the hydrological apex. Such a condition occurs when there is a “fan-head trench” that delivers water and sediment in a naturally incised water conduit towards the toe of the fan form. Prior research indicates that the FEMA approach simply does not work in places like Laughlin, Nevada (House, 2005), Tucson, Arizona (Pearthree et al., 1992), and certainly not in the Phoenix area (Fuller, 1990). Figure 2.16 illustrates the offset between the FEMA procedure and reality in the community of Scottsdale, Arizona.


**Figure 2.16.** Development burgeoned on alluvial-fan surfaces during the 1990s, as shown in a comparison of 1991 (A) and 1995 (B) aerial photographs of the southern McDowell Mountains, Scottsdale. In the 1991 image, dots delineate the presence of entrenched channels transporting water and sediment almost 8 km downstream from this fan. Thus, with the hydrological apex located at distance from the topographic apex of the alluvial fan, all of the development is safe from flooding.

STREET FLOODING IN PLANNED AND UNPLANNED HOUSING DEVELOPMENTS

Street flooding is a flash-flooding issue throughout the Phoenix metropolitan area. It typically occurs during the summer monsoon season, when short, but intense, downbursts result in localized overland flow. The local Maricopa County Flood Control District receives property tax funding to route water efficiently through the metropolitan area, working with local municipalities (Figure 2.17). The county and cities can take different cost-benefit strategies to dealing with street flash flooding. Over engineering has often been done by the county. However, local communities have made other choices at times.

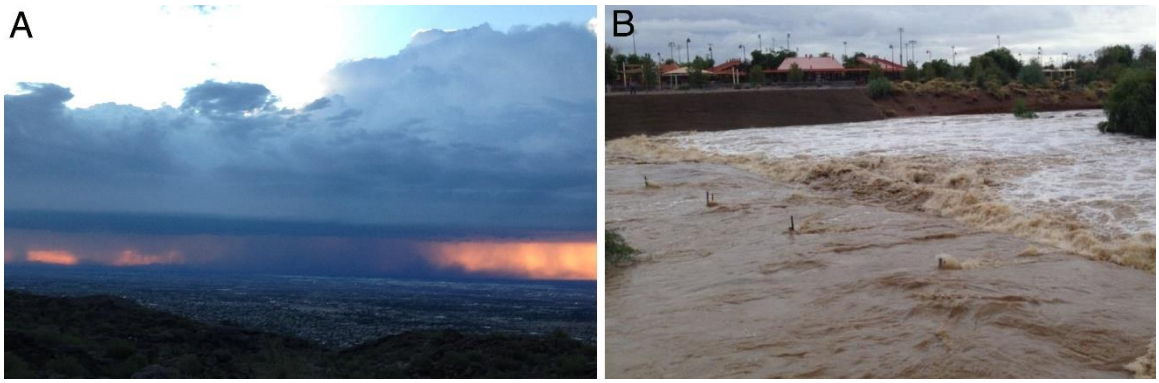


**Figure 2.17.** Monsoon downburst taking place over the western portion of metropolitan Phoenix (A), and corresponding localized flooding being routed through flood-control structures (B).

The homes, infrastructure, and retail space of the Phoenix suburb of Fountain Hills rests on an eroding alluvial fan referred to as a “ballena” (Figure 2.18). However, the roads cross a series of incised ephemeral washes that experience frequent flooding (Rhoads, 1986). The management challenge rests in the cost-benefit tradeoff of

engineering for decadal events, and then let century-scale or millennial-scale flash flooding require infrastructure replacement. This leads to ongoing construction at problem locations, where initial engineering structures have repeatedly failed.

**Figure 2.18.** Fountain Hills is a community built on a ballena, or eroding alluvial fan. Although structures are safe because homes and businesses are placed on ballena tops and side slopes, roads must be engineered to survive occasional flooding in the washes between the ridges.

Much of Phoenix has been built on pediments with low slopes (Figure 2.19). The engineering associated with this development ranges considerably in terms of the investment to deal with ephemeral flooding. In Figure 2.19A, a gun club has built simple berms to deflect flooding around the complex. In contrast, Figure 2.19B displays a wildcat community known as “Rio Verde.” This development is almost entirely unplanned with respect to dealing with runoff. An individual purchasing a plot of land

will build, quite often, without any concern for the flooding issues caused by upstream neighbors, or that they may cause for downstream property owners. More wealthy communities, such as the exclusive Las Sendas neighborhood of Mesa (Figure 2.19C), include structures to deal with the routing of water.

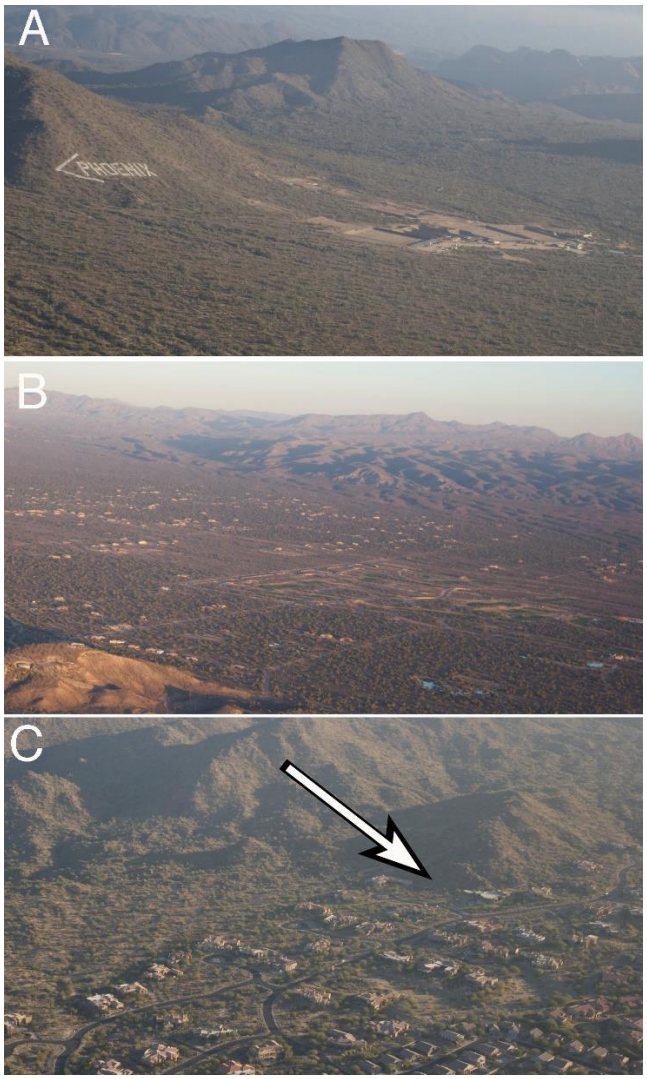


**Figure 2.19.** Development on pediments takes different strategies in dealing with ephemeral flooding. (A) A gun club simply built large levees to divert flow into the surrounding desert. (B) A "wildcat" development called Rio Verde continues to experience localized flooding, since little or no effort focuses on water routing during home or road construction. (C) Affluent subdivisions do consider flash flooding issues, and route water into natural or human-enhanced washes.

The largest river running through metropolitan Phoenix has ceased to pose a flooding hazard. Throughout the 20th century, the Salt River flooded repeatedly, causing considerable losses to property and sometimes lives (Gober, 2005). However, the last time that the Salt River experienced destruction associated with flooding took place in 1993 during a major ENSO event (Figure 2.20C) that corresponded with construction at Roosevelt Dam (Figure 2.20A), requiring the release of water from the reservoir behind. The combination of a very wet winter and a lowered dam level destroyed bridges and a lot of other infrastructure (Figure 2.20B). However, since the Roosevelt Dam's 1993 construction resulted in increased reservoir capacity, flooding has not been an issue since along this major drainage.


**Figure 2.20.** During the winter of 1993, a major ENSO event led to (A) the release of water from the reservoir behind the Roosevelt Dam. The released water destroyed the bridge at Mill Avenue in Tempe (B), as well as other infrastructure along the course of the river through metropolitan Phoenix (C).

## DEBRIS FLOWS

The Phoenix urban area has expanded out into the surrounded mountain fronts, where debris flows take place. In an initial study of the hazard to homes posed by debris flows, Dorn (2012) found that at least 89 houses are located along the pathway of former debris flows or above the debris flow chutes of the Gila Range and the Ma Ha Tuak Range of South Mountain, Camelback Mountain, Mummy Mountain and Shaw Butte areas alone (Figure 2.13).

Debris flows were not generally viewed as a hazard in the Sonoran Desert, until a major debris flow event occurred outside of Tucson (Youberg et al., 2008). Despite evidence to the contrary, those geoscientists living in and around Phoenix generally considered debris flows "acts of god," or extraordinarily rare geological events not worthy of study. This changed after an intense summer thunderstorm on August 12, 2014 and a hurricane that occurred on September 8, 2014 led to short and intensive precipitation events in metropolitan Phoenix, which triggered the occurrence of dozens of debris flows in one mountain range of Phoenix alone (Figure 2.21) (Dorn, 2016).

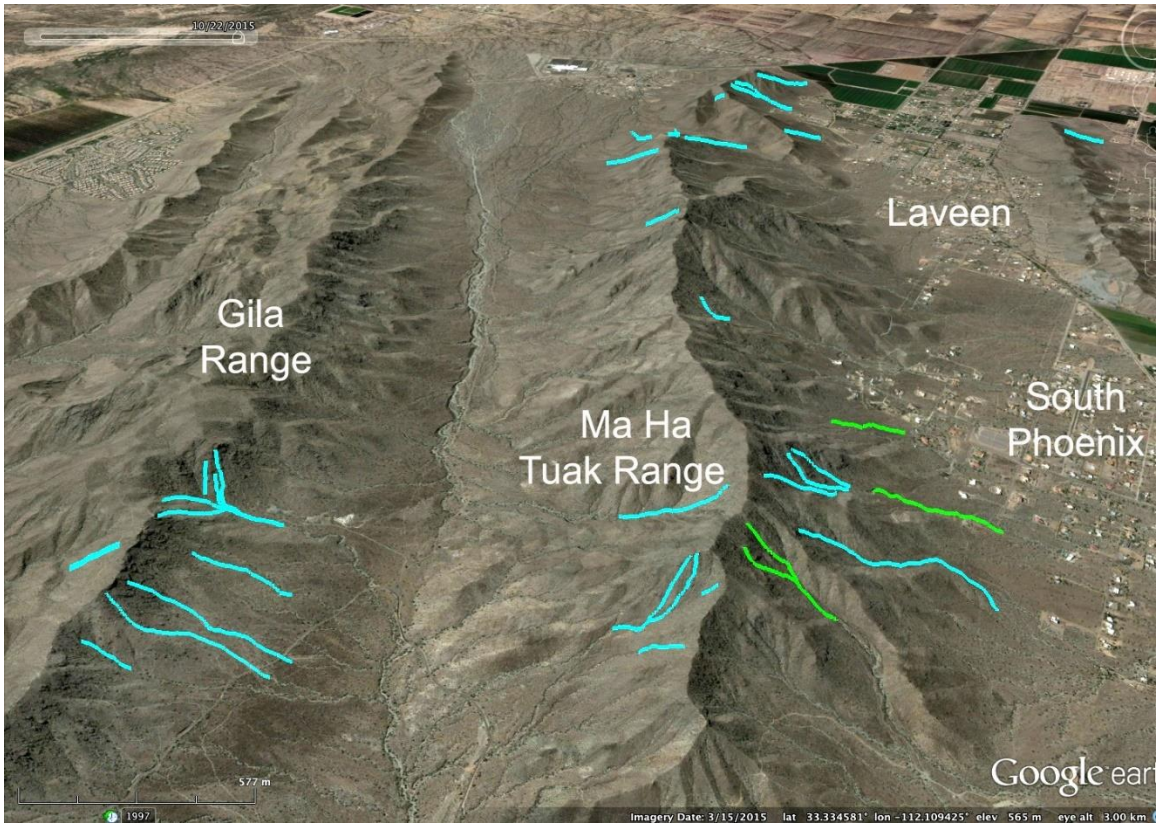


**Figure 2.21.** West-looking view of the debris-flow pathways triggered by the 12th August hurricane thunderstorm (blue) and 8th September summer monsoon event (green) at South Mountain, Phoenix in 2014 (Dorn, 2016).

## HABOOBS AND DUST STORMS

Dust and summer dust storms are part of the urban geomorphic and climate system (Brazel, 1989; Marcus and Brazel, 1992; Péwé et al., 1981). During the spring, strong dry cold fronts deflate dust from agricultural fields and abandon urban lots, producing a substantial dust hazard. During the months of July, August, and September, the Mexican Monsoon's northern boundary impacts the Phoenix area, and produces haboobs (Idso et al., 1972) like the one seen in Figure 2.22, which are associated with the leading edge of cold outflow from convective clouds. Although this is a natural

phenomenon, anthropogenic activities that led to the exposure of bare ground (e.g. exposed house pads, agricultural fields, desertification) all contribute to the available surface area for dust deflation (Eagar et al., 2017).

Dust poses a regular urban hazard in terms of driving, where visibility decreases to the point where a driver is unable to see more than a few meters ahead (Baddock et al., 2013; Hyeres and Marcus, 1981). Desert dust is also associated with a number of human health issues (Goudie, 2014). Valley fever, for example, is produced by the fungus Coccidiodes that lives in soil and dust in the southwestern USA.

**Figure 2.22.** A km-high, nearly 100-km wide haboob approaches Phoenix from the south at sunset.

## SUMMARY PERSPECTIVE ON HUMAN INFLUENCES ON THE ARID GEOMORPHIC SYSTEMS IN THE URBANIZING SONORAN DESERT

From a geomorphic perspective, the Anthropocene, or the proposed new geological epoch when humans have had an overwhelming effect on the Earth system (Waters et al., 2016), requires both empirical evidence and an understanding of exactly how humans alter geomorphic processes. Accordingly, the British Society for Geomorphology maintains a Fixed Term Working Group to advise how geomorphologists to engage in scholarly analysis concerning the Anthropocene as a concept. Practical aspects include a relative magnitude problem, a boundary problem, and a spatial problem associated with "anthropogenic geomorphology" (Brown et al., 2017).

In the context of urban geomorphology (Thornbush, 2015), where human impacts result in enhanced disturbance and increased vulnerability to erosion, an arid city poses very different considerations than urban centers in wetter regions. Urban geomorphic processes in a setting like the Sonoran Desert are potentially altered by a myriad of anthropogenic influences, including: invasive species turning an ecoregion that did not experience massive wildfires naturally into an annual hazard due to invasive annual grass species; altering the armoring effects of soil crusting by widespread destruction of biological soil crusts by periods of cattle grazing; periods of road building and home construction; and other influences, such as off-road vehicles.

An individual walking on desert landforms, before massive land-use change associated with cattle grazing and urban expansion, very likely would have experienced very different surface conditions than found by the average hiker today. Extensive areas

once hosted desert pavements, biological soil crusts (Allen, 2005, 2010), and interlocking colluvium on steeper slopes that provided a net armoring effect (Bowker et al., 2008; Granger et al., 2001; Seong et al., 2016a). Today, only patches of such armored surfaces remain, providing glimpses into the original land surfaces.

According to Brown et al. (2017), "it is clear that the relevance of the Anthropocene concept varies substantially between different branches of geomorphology." While Brown et al. (2017) did not consider rocky desert landscapes, such as the Phoenix metropolitan area, the basic conclusion that "the less obvious effects of humans on the geomorphic systems warrant increased research" certainly applies to the Phoenix metropolitan area and the surrounding Sonoran Desert. Developing a better understanding of the role of human-influenced processes at different scales will be needed to better diagnose the role of human impacts in an arid geomorphic system.

# CHAPTER 3

# SOIL EROSION FROM URBANIZATION PROCESSES IN THE SONORAN DESERT, ARIZONA, USA

(PUBLISHED IN *LAND DEGRADATION & DEVELOPMENT*)

**Citation:** Jeong, A., & Dorn, R. I. (2019). Soil erosion from urbanization processes in the Sonoran Desert, Arizona, USA. *Land Degradation & Development*, *30*(2), 226–238. https://doi.org/10.1002/ldr.3207

## ABSTRACT

Cattle stock ponds on the fringe of metropolitan Phoenix, USA, experienced a wide range of land use changes over the period from 1989-2009. Monitoring sediment accumulation behind 18 earthen berms at each major land-use transition enabled calculations of soil erosion rates and sediment yields from watersheds of different rock types and variable relief. Compared to the period of cattle grazing, the process of urbanization in the Sonoran Desert increased soil erosion from urban-proximate wildfires by up to 4.2x, from exposure of bare ground due to home and commercial real estate development by up to 3.4x, from bare ground exposure due to road and pipeline construction by up to 3.1x over grazing alone. Stock pond watersheds underlain by granitic rock experienced statistically significant higher erosion rates compared to watersheds underlain by metamorphic, basalt, and other rock types. A global compilation of published and unpublished sediment yield data for warm desert (BWh Köppen-Geiger) sites reveals that our data plot consistently with other grazing study areas with an overall slight tendency for higher area-specific sediment yields in smaller drainage areas.

However, our sediment yield data, as well as data form other warm desert sites, do not support previously published generalizations of anomalously high or low sediment yields from warm desert settings. Although the geomorphic setting surrounding different warm desert cities undergoing expansion differs, these results highlight the importance of exposure of bare ground in increasing soil erosion even in an environment with naturally abundant bare ground.

## INTRODUCTION

Soil erosion contributes to land degradation at large (Balaguer-Puig et al., 2018; Nyssen et al., 2008) and small scales (Shi et al., 2014) in all habitable ecoregions (Lal, 1994). Soil erosion in arid lands is the focus of this study and is often attributed to overgrazing (Al-Awadhi et al., 2005), wind erosion (Zhibao et al., 2000), and overland flow of water that generates substantial loss even with low-intensity events (Marques et al., 2008). Critical transitions that greatly increase erosion often involve exposing bare soil through unpaved roads (Marchamalo et al., 2016; Nyssen et al., 2002; Villarreal et al., 2016) and human-caused wildfire (Martínez-Murillo & López-Vicente, 2018).

Compared to other arid regions, the Sonoran Desert in Arizona, USA, has been the location of minimal research on land degradation in general and soil erosion in particular. After Columbian contact, grazing and mining were major agents of land degradation (Radding, 2005) and grazing is still common (Fleischner, 2010). Prior to European invasive grasses, Sonoran Desert wildfires were very infrequent and of low intensity (McLaughlin & Bowers, 1982). Invasive grasses such as Bromus madritensis L.

ssp. rubens and Pennisetum ciliare, however, now generate an abundance of fuel following winter rains that greatly increases the frequency and intensity of Sonoran Desert wildfires (Balch et al., 2013). Arid urban populations in the metropolitan Phoenix and Tucson areas, Arizona, USA, also degrade the surrounding Sonoran Desert through off-road vehicle activity (Villarreal et al., 2016).

This study focuses on soil erosion in a Köppen-Geiger BWh climate at the interface of the Sonoran Desert and the sprawling metropolitan area of Phoenix, Arizona, USA. Relatively sparse published data exist on sediment yield in a BWh setting. In the Negev desert, for example, extremely high sediment yields can occur in small catchments (Schwartz and Greenbaum, 2008), where evidence exists that sediment yield exceeds sediment production by 53%–86% (Clapp et al., 2000). More generally, Einsele and Hinderer (1997) predicted very high specific sediment yields (SSY) of 4000-5000 t/km2/yr at small arid catchments. Scholarship in BWh climates reveals several factors thought to influence erosion rates, including rock type in the Indian arid zone (Sharma and Chatterji, 1982) and slope in southern Arizona (Abrahams et al., 1988). Poesen et al. (1994) highlighted the effects of rock fragments on soil erosion. At microplot ($4 \times 10^{-6}$-100 $m^2$) and macroplot scale (101-104 $m^2$), sediment yield decreases with percent rock fragment cover due to the protection of the underlying soil and the interception of soil particles by rock fragments. Nearing et al. (2005) investigated a humid and a semiarid watershed to better understand how changes in precipitation and vegetation parameters such as rainfall amount, rainfall intensity, rainfall duration, vegetation cover, and canopy cover influence erosion. Zhang et al. (2012) and Dorn (2015) emphasized that extreme precipitation events result in a jump in soil erosion in the southwestern USA.

A reason for the selection of Phoenix as a BWh study site is that prior to an expansion of urbanization, lands managed by the USA Bureau of Land Management, Arizona State Trust Lands, and the USA Forest Service gave permits for cattle grazing. Thousands of berms built across ephemeral desert washes created stock ponds to collect water for cattle (Langbein et al., 1951). Starting in 1989, the second author initiated the monitoring sediment accumulation in 25 stock ponds that had not yet experienced urbanization, but were in locations where political entities planned urban expansion. Periodic observations of sedimentation in these stock ponds before and after land-use transitions took place over the next two decades, recording changes in sedimentation.

This chapter analyzes four hypotheses related to over two decades of monitoring soil erosion on the urban fringe of metropolitan Phoenix, USA:

H1: During the period of cattle grazing prior to urbanization, the sediment yield would be influenced primarily by natural variables such as drainage area, slope, vegetation cover, precipitation amount and intensity, and rock type.

H2: Sediment yield would increase substantially during the period of land-use changes associated with urbanization including human-set wildfires, exposure of bare ground due to home and commercial real estate development, and exposure of bare ground due to other infrastructural development such as road and pipeline construction.

H3: The sediment yields of small basins in a warm desert, Köppen-Geiger BWh climate setting would not meet the expectations of some scholarship in the literature. Einsele and Hinderer (1997, p. 295) plotted specific sediment yield

vs. drainage area for different climate types. In this idealized plot, arid and semiarid drainage areas had some of the highest sediment yields. In contrast, in an analysis of just three BWh catchments, Jansson (1988) found some of the lowest sediment yields. Rózsa and Novák (2011) mapped sensitivity to human factors globally from the perspective of different Köppen-Geiger climate types and predicted that arid regions with minimal relief (plains and hills) would be amount the least sensitive.

H4: In a compilation of all available sediment yield data from BWh catchments, we hypothesize that the general trend of increasing specific sediment yield in smaller basins observed in Europe (Vanmaercke et al., 2011b), Africa (Vanmaercke et al., 2014), and global comparisons (Einsele & Hinderer, 1997) would hold true for warm desert BWh Köppen-Geiger settings.

## STUDY SITE

The Sonoran Desert in central Arizona experiences precipitation averaging 208 mm split evenly between summer and winter maxima (Climate Office of Arizona, https://azclimate.asu.edu/climate/climate-of-phoenix-summary/). Winter rainfall occurs when the westerlies generate Pacific cold fronts and low-pressure systems. Moist air masses from the Gulfs of Mexico and California, combined with surface heating and upper level tropospheric disturbances, produce summer thunderstorms during the July–September Monsoon season. This climate supports Sonoran Desert trees grow along ephemeral washes and on hillslopes where overland flow concentrates, including palo

verde (*Parkinsonia microphylla*), ironwood (*Olneya tesota*), and elephant trees (*Bursera microphylla*). Desert scrub vegetation found on slopes includes creosote bush (*Larrea tridentata*), brittlebush (*Encelia farinosa*), triangle-leaf bursage (*Ambrosia deltoidea*), catclaw acacia (*Acacia greggii*), desert globe mallow (*Sphaeralcia ambigua*), and ocotillo (*Fouquieria splendens*). Piedmonts and hillslopes also host succulents such as saguaro (*Carnegiea gigantea*), barrel (*Ferocactus cylindraceus*) and hedgehog (*Echniocereus engelmannii*) cactus.

Thousands of stock ponds throughout Arizona collect water for grazing cattle (Langbein et al., 1951). Most consist of an earthen dam blocking small ephemeral channels. Researchers use these stock tanks to study erosion and sedimentation rates in non-desert ecoregions in Arizona such as a semi-arid mesquite grassland (Nichols, 2006).

25 stock ponds were selected for a study of erosion and sedimentation associated with urban expansion with their locations determined by areas targeted for urban growth. The goal of the study initiated in 1989 rested in developing a better understanding the role of land degradation associated with urban sprawl in a warm desert region. Seven of the stock ponds experienced overflow events leading to breaching and loss of the sediment record, and these sites are not included in this paper. However, eighteen stock ponds recorded changes in sedimentation associated with major land-use changes on the urban fringe.

Phoenix, Arizona, is the fifth largest USA city. The population of the metropolitan area grew dramatically after World War II with the advent of air conditioning, and the aerial footprint sprawled commensurately with migrants seeking

employment and a low cost homes. Because Phoenix is located entirely in the Sonoran Desert, the stock ponds on the urban fringe had the potential to yield unique insight in a warm desert ecoregion. The USA National Science Foundation selected metropolitan Phoenix as a type urban site to analyze land use-land cover change (LULCC) in an arid climate. Thus, extensive documentation exists on LULCC for the study period from 1989 to 2009 (Fan et al., 2017) that can be accessed at https://sustainability.asu.edu/caplter/.

Figure 3.1 superimposes the location of the 18 studied stock pond drainage areas on a map showing the expansion of urbanization from 1985 through 2010. Appendix A provides overview of a Google Earth KMZ file of the stock tanks and their associated watersheds. Figure 3.2 illustrates typical shifts in land use as the urbanization expanded out into areas formerly occupied by cattle grazing.

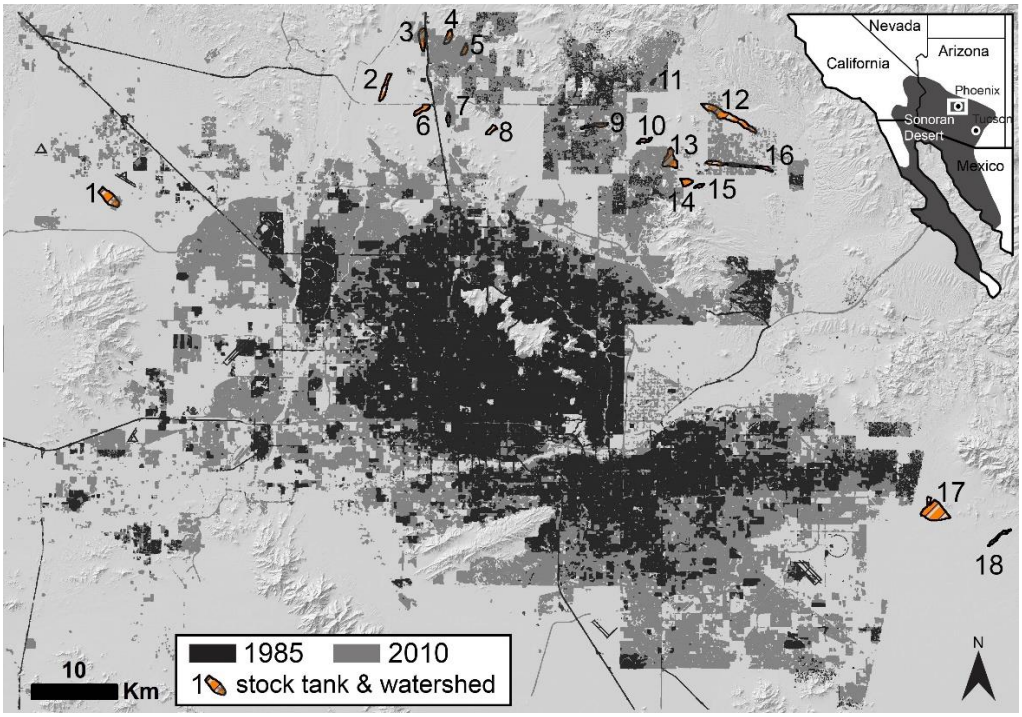


**Figure 3.1.** Map contextualizing the scattered locations of the stock tanks around metropolitan Phoenix. The studied stock ponds are situated in the Sonoran Desert. Urban boundaries in 1985 and 2010 are extracted from land cover classification by Central Arizona–Phoenix Long-Term Ecological Research. Data available at https://sustainability.asu.edu/caplter/data/view/knblter-cap.650.1/. The numbers refer to stock ponds identified in this paper's data tables.

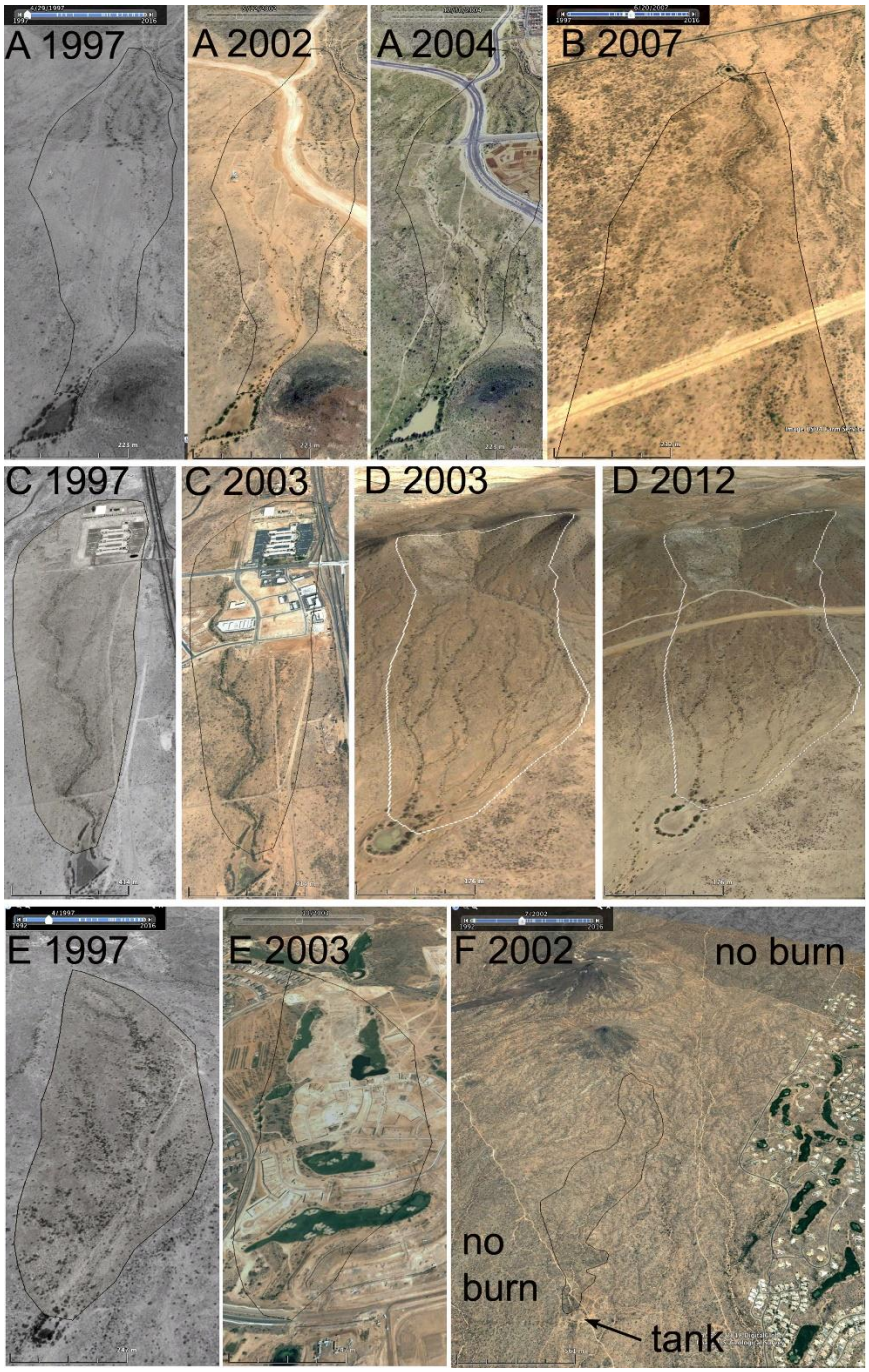


**Figure 3.2.** Examples of land-use changes in stock pond watersheds of the sort that can be explored in greater detail and higher resolution by the reader using Google Earth kmz data (Appendix A). Roads provide a sense of scale. Dates of the Google Earth screenshot imagery are annotated in the upper left corner. (A) Transition from cattle grazing to road construction and housing subdivision development, (B) pipeline construction and proximity to the tank, (C) transition from grazing to commercial development, (D) road construction, (E) wildfire and subdivision development, and (F) stock pond drainage area.

METHODS

*FIELD SAMPLING*

Nine 0.3 m segments of steel rebar were inserted into the sediment accumulation area of the studied stock ponds in a 3x3 grid (Figure 3.3) to understand variability in sedimentation. The rebar was flush to the surface, covered by dirty cardboard. Upon experiencing a major land-use change, each stock pond was revisited to measure sediment accumulation depths on top of the rebar. The rebar was relocated with the assistance of a metal detector. Since sediment bulk density varies with sediment texture, multiple sampling assists in analyzing variability over space and time (Verstraeten & Poesen, 2001). Like others (Bellin et al., 2011), we anticipated that there would be no significant increases in bulk density with depth, but this assumption was tested by collecting bulk density samples at the same time when the sedimentation was measured.

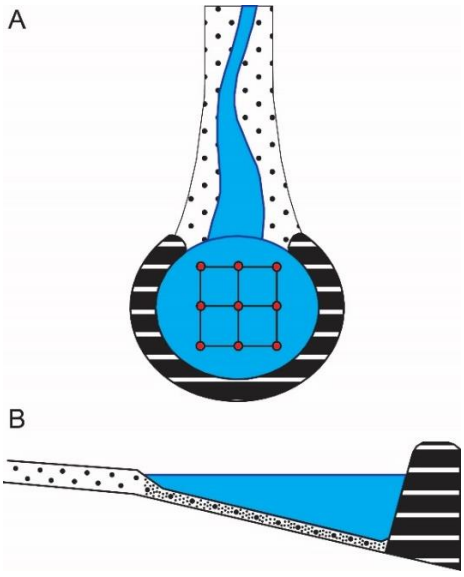


**Figure 3.3.** Generalized diagram presenting 3 × 3 grid of sediment sampling and rebar placement locations in an idealized stock pond. (A) Plan view and (B) cross section illustrating the course nature of sediment in channels just prior to entering the stock pond. However, where water ponds, the clays and silt in the suspended sediment load mix with bedload.

*LABORATORY MEASUREMENTS*

We sampled three points for each stock pond as others have also done for bulk density and particle-size analysis (Bellin et al., 2011). The cylinders method determined the bulk density of all samples (Blake, 1965). The hydrometer method measured the percent silt and clay of all samples (Bouyoucos, 1962). The reported error term derives from the standard deviation.

*CALCULATION OF SOIL EROSION RATE*

Calculating annual soil erosion rate in meters requires the area of the stock pond watershed in $m^2$ ($A_D$), the surface area where the sediment accumulated behind the berm in $m^2$ ($A_b$), the depth of sediment accumulation in m (D), and the number of years of sediment accumulation (Ys).

$= (A_b * D)/ A_D)/Ys$

We converted soil erosion rate to millimeters per thousand years by multiplying the annual soil erosion rate in meters by $10^6$.

A major error concern involves how to analyze the aeolian contribution. Dust storms transport desert dust in the Sonoran Desert (Péwé, 1981). Because an analysis of soils in southern Arizona suggests that up to 20% of the mineral material could derive from dust (Lybrand & Rasmussen, 2018), the silt and clay accumulating in the stock ponds could potentially all derive from aeolian dust deposition or it could derive weathered bedrock. Thus, two sediment yields (and erosion rates) are presented. One is the maximum with the assumption that there was no aeolian dust deposition. One is the

minimum with the assumption that all of the silt and clay derived from aeolian deposition.

For both the maximum and minimum sediment yields (erosion rates), there is a ± assigned from the standard deviation of nine depth measurements for each time slice. This standard deviation of the average depth then translates as a ± percentage the reported sediment yield.

*DETERMINATION OF SPECIFIC SEDIMENT YIELD*

The area-specific sediment yield (SSY) in the studied eighteen stock ponds is calculated as follows (Verstraeten & Poesen, 2001):

$$SSY = SM / (A_D * TE * Y) * 10^6$$

where *SSY* is specific sediment yield (t $km^{-2}$ $y^{-1}$), *SM* is sediment mass (t), *dBD* is average dry bulk density of the sediment (t $m^{-3}$), $A_D$ is drainage area of the watershed of each stock pond ($m^2$), *TE* is sediment trap efficiency (%) and *Y* is time period of measurement (y). In the case of the 18 stock ponds, the sediment trap efficiency (*TE*) is 100% because we rejected all 7 stock ponds that breached. We found no evidence that the studied stock ponds were excavated during the period of study.

The maximum sediment ($SM_{max}$) can be calculated as follows:

$$SM_{max} = SV_{max} * dBD = A_P * D_{avg} * dBD$$

where *Ap* is sedimentation area and $D_{avg}$ is the averaged depth of the sediments measured from nine grid points (Figure 3.3). *SV* is the measured sediment volume in the

stock pond during the given time period *Y* ($m^3$). The minimum sediment yield is then calculated as follows:

$$SM_{min} = SM_{max}*(1 - percent\ silt\ and\ clay)$$

*DATA ACQUISITION AND CORRELATION BETWEEN CATCHMENT PROPERTIES AND EROSION RATE*

We collected quantitative data for each of the selected catchments (Appendix B) with the goal of determining statistically significant correlations between a catchment property and erosion rate. Appendix C presents all data used in the correlation analyses. Pearson's pair-wise correlation was calculated for all pairs of quantitative variables to measure linearity between and among catchment properties (cf. Shi et al., 2013, p 173).

The digital elevation model (DEM) with a resolution of 10 m delineated morphological characteristics of each catchment. ArcGIS software generated data on drainage area, average slope, maximum relief. ImageJ software converted historical aerial photograph images in different time periods to 8-bit images to determine percent perennial vegetation cover (Appendix D). The Maricopa County Flood Control District gathers precipitation data at a variety of rain gauges (http://alert.fcd.maricopa.gov/showrpts_mc.html), typically within a few hundred meters of each catchment. Using this rainfall data, we calculated mean annual precipitation (MAP), summer convective (monsoon) seasonal precipitation from 6/15-9/30 (Appendix E). Study of a well-monitored semiarid watershed in southern Arizona (Polyakov et al., 2010) revealed that sediment transport occurred when rainfall exceeded 10 mm for 30

min ($I_{30}$). Thus, for each sediment accumulation interval, we compiled the total amount of rainfall with $I_{30}$. Additionally, we split the study period into approximately two decadal periods (period 1: 1989-1999; period 2: 2000-2009) and calculated MAP and $I_{30}$ from three nearest rain gauges to all stock tanks to reduce the influence of dry and wet years (Appendix B).

The largest potential error in carrying out a correlation between catchment property and erosion rate involves land use uncertainty. All of the catchments experienced cattle grazing, and almost all of them also experienced potential land degradation events such as wildfire, dirt road creation, and construction. In order to tease out the significance of catchment properties, we rejected all time intervals that involved land use other than cattle grazing.

*COLLECTING QUALITATIVE CATCHMENT PROPERTIES*

Two important influences on soil erosion rates cannot be analyzed using a linear correlation, because rock type and land uses do not translate into interval data. To better understand the importance of rock type and land use on erosion, we used a difference of means t-test. For rock types, we obtained lithological information by ground truthing geological maps. While granitic rocks break down into grus, or sand-sized particles, the other rock types (basalt, ignimbrite, metasedimentary, metavolcanic) decay into a mixture of fines (clay and silt), some sand, but also cobbles and boulders. Thus, an unpaired t-test evaluated whether the specific sediment yield or erosion rate was significantly different between stock pond watersheds that were only granitic and those that were non-granitic.

We identified different land use and land-used changes using prior research (e.g. Fan et al., 2017), field observations, and historic aerial photographs. We classified different land uses into grazing, low-density residential, high-density residential, commercial, construction, and mixed use. We also classified non-urbanized areas as either impacted by cattle grazing or a wildfire event. Because the same stock pond watershed experienced different land-use changes, each time slice was treated as a separate data point. An unpaired t-tests compared the specific sediment yield from basins experiencing grazing; building construction of houses, subdivision and commercial properties; infrastructure of road and pipeline building that exposes bare ground; and wildfire.

## RESULTS

### *OVERVIEW*

During the first 10-year period, both MAP and $I_{30}$ were higher (Appendix B). The average MAP of all stock pond sites in the first decade (258 mm) when grazing was more dominant lowered substantially (212 mm) in second 10-year period (2000-2009) dominated by urbanization. Appendix B also breaks down erosion rates and area-specific sediment yields for all study areas and all time slices studied. Despite decreases in MAP and $I_{30}$ (with 2 site exceptions) in the second decade of study (Appendix B), erosion associated with urbanization processes increased significantly. The following data present a ratio of soil erosion under the new land use compared to soil erosion during the period of just grazing. Exposure of bare ground from construction — whether road, housing or

commercial developments — accelerated erosion over the grazing period by 1.3x, 1.7x, 1.8x, 2.9x, 3.1x, and 3.1x for the Asher Hills, Peralta, Circle Tank, Anthem, Cline, and Bronco tanks respectively. The first period after a wildfire erosion accelerated by 2.1x, 2.4x, 2.7x, 2.8x, 3.1x, and 3.7x for the Cave Creek, Anthem,128$^{th}$ street, 128 street 2$^{nd}$, Anthem, and Rock tanks respectively. The second time slice after a wildfire saw a reduced effect of accelerated erosion over the pre-fire grazing condition of 1.4x, 1.4x, and 2.3x for the 128$^{th}$ street, 128 street 2$^{nd}$, and Rock tanks. The next sections explore the statistical significance of different factors that could potentially impact soil erosion.

*CONTROLS ON EROSION RELATED TO URBANIZATION RELATED LAND-USE CHANGES*

All but one of the study areas experienced cattle grazing at the start of this study. Thus, this results section explores how different factors (drainage area, average slope, relief, vegetation cover, precipitation) impact sediment yield during the period of cattle grazing. A correlation matrix (Table 3.1) presents Pearson's correlation coefficients between sediment yield data (i.e. maximum erosion rate, SY or sediment yield, SSY or area-specific sediment yield) and climatic and morphometric properties of each catchment.

The metrics of soil erosion during cattle grazing did not show any statistically significant relationship with precipitation or vegetation cover. All of the correlations between maximum erosion rate or Emax, SSY, SY and the precipitation metrics of annual, summer and most intense rainfall were not statistically significant. Vegetation

density revealed the same story of no statistically significant correlations with soil erosion.

Only basin morphometry revealed statistically significant correlations with soil erosion metrics. Sediment yield was significantly and positively correlated with drainage area (Ad) ($r = 0.97$, $p < 0.05$) and relief ($r = 0.68$, $p < 0.1$), but average slope (Savg) did not show a clear correlation.

The bulk density (BD) of the accumulated sediment did show a slight positive correlation with the maximum erosion rate ($r = 0.70$, $p < 0.1$), a statistically significant correlation with vegetation cover ($r = 0.81$, $p < 0.05$), and an even stronger relationship with SSY ($r = 0.82$, $p < 0.05$). These positive relationships suggest that there was a tendency for more sand and gravel deposition, as opposed to silt and clay, at sites with a higher sediment yield, more vegetation cover, and a higher erosion rate.

**Table 3.1.** Correlation matrix between the sediment yield and some stock tank catchment variables, Phoenix metropolitan area, Sonoran Desert, Arizona, USA. Appendix C provides supporting documentation for this Table.

| | *Emax* | *Ad* | *Savg* | *Relief* | *BD* | *VC* | *MAP* | *MSP* | *I30* | *SY* | *SSY* |
|---|---|---|---|---|---|---|---|---|---|---|---|
| Emax | 1 | | | | | | | | | | |
| Ad | 0.42 | 1 | | | | | | | | | |
| Savg | -0.16 | -0.28 | 1 | | | | | | | | |
| Relief | 0.45 | 0.59 | 0.40 | 1 | | | | | | | |
| BD | 0.70* | 0.21 | -0.47 | -0.01 | 1 | | | | | | |
| VC | 0.37 | 0.30 | -0.28 | 0.14 | 0.81** | 1 | | | | | |
| MAP | 0.13 | 0.25 | -0.01 | 0.19 | -0.17 | -0.13 | 1 | | | | |
| MSP | -0.07 | 0.14 | 0.20 | 0.18 | -0.35 | -0.14 | 0.89** | 1 | | | |
| I30 | 0 | 0.26 | 0.02 | 0.15 | -0.02 | 0.33 | 0.23 | 0.50 | 1 | | |
| SY | 0.61 | 0.97** | -0.26 | 0.68* | 0.32 | 0.34 | 0.27 | 0.12 | 0.25 | 1 | |
| SSY | 0.98** | 0.37 | -0.24 | 0.36 | 0.82** | 0.51 | 0.05 | -0.16 | 0 | 0.56 | 1 |

Note: Emax, maximum erosion rate (mm $ka^{-1}$); Ad, drainage area; Savg, average slope; Relief, maximum height difference in catchment; BD, bulk density; VC, percent vegetation cover; MAP, mean annual precipitation; MSP, mean summer seasonal precipitation, I30, the total amount of peak 30-minute rainfall exceeded 10 mm for 30 min; SY, sediment yield (t $yr^{-1}$); SSY, area-specific sediment yield (t $km^{-2}$)
*Significant at $p<0.1$,
**Significant at $p<0.05$,
***Significant at $p<0.01$.

Since rock type can be an important factor influencing sediment yield, the stock tank periods experienced only grazing were grouped into granitic and other lithologies. Half of the stock tank watersheds are underlain by only granitic lithologies, ranging from granite to granodiorite with some diorite. Then, half of the stock tank watersheds are underlain by a mix of rock types, typically including rhyolitic tuff (ignimbrite), basalt, metavolcanic and metasedimentary rocks. A t-test comparing sediment yields of granitic vs. other rock types influenced by only grazing reveals a difference, but no statistically significant difference for granite (Mean, M= 103.7, Standard Deviation, SD= 791.1)

versus other rock types (M= 68.9, SD= 1001.0) conditions; $t(12)= 2.14$, $p > 0.05$. However, there was a statistically significant difference for maximum erosion rates between granitic (M= 71.83, SD= 256.97) and other rock types (M= 50.88, SD= 319.55), $t(12) = 2.27$, $p \leq 0.05$. This difference is shown graphically in Figure 3.4A.

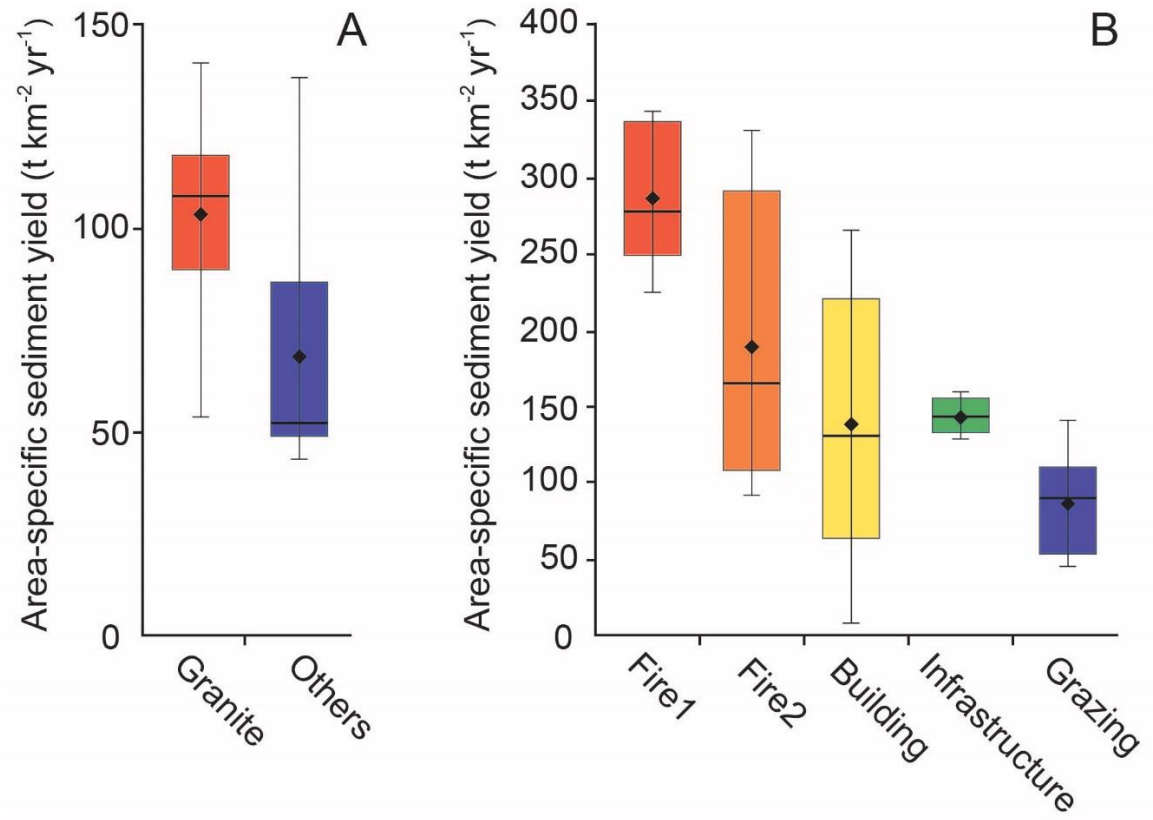


**Figure 3.4.** Box and whisker plots of specific sediment yield associated with variables are inappropriate for linear regression but appropriate for T-test comparisons. (A) A comparison of specific sediment yields for granitic and nongranitic stock tank watersheds influenced only by grazing land use. (B) A comparison of specific sediment yields for stock tank periods of time dominantly influenced by different land uses. Fire1 refers to the period of time immediately after a wildfire (typically 3–5 years). Fire2 refers to the period of time after Fire1 where some revegetation has occurred. Building refers to stock tanks experiencing the exposure of bare ground due to building homes and commercial real estate. Infrastructure refers to stock tanks experiencing the exposure of bare ground due to major infrastructural developments such as road and pipeline construction.

*SEDIMENT YIELD INCREASES FROM URBANIZATION IN A WARM DESERT*

Urban expansion in the Phoenix BWh Sonoran Desert setting resulted in a variety of substantive changes to the dominant land use. From the perspective of established sediment-yield forcings reviewed in the introduction, three major land use changes resulted in the exposure of bare ground in different studied periods.

Wildfires set by human abuses on the urban fringe, unfortunately, occurred in several stock tank watersheds. In two watersheds, it was possible to subdivide time slices after wildfires into 3-5 year intervals. The initial time slice after the fire is designated Fire1 in Figure 3.4B. The time slices that experienced vegetation recovery after Fire1 is grouped into Fire2 in Figure 3.4B.

Bare ground exposure also occurred in association with two sorts of construction related activities. The Building category in Figure 3.4B is from home and commercial real estate construction. The Infrastructure category in Figure 3.4B is from road and pipeline construction.

Statistically significant differences specific sediment yield in T-tests occurred between grazing and all other dominant land uses associated with different periods of time, as revealed visually by box and whisker plots (Figure 3.4B). There was a significant difference in specific sediment yield for Grazing (Mean, M= 85.0, Standard Deviation SD= 1103.3) and Infrastructure construction (M= 143.6, SD= 140.6) conditions; t(18)= 1.73, p= 0.001. There was a significant difference in specific sediment yield for Grazing and Building (M= 150.9, SD= 6245.7) conditions; t(24)= 2.91, p= 0.004. The largest

difference occurred between Grazing and all wildfire (M= 246.8, SD= 7097.38) conditions, both Fire1 and Fire2 grouped together; t(23)= 6.75, p= 0.000.

## DISCUSSION

### *NATURAL CONTROLS ON SONORAN DESERT SEDIMENT YIELDS*

This study of sediment yields on the sprawling fringe of metropolitan Phoenix, USA, revealed very little clarity with regard to natural controls (Table 3.1). The list of no correlation with metrics of soil erosion (maximum erosion rate, sediment yield, or area-specific sediment yield) in the period of just cattle grazing is quite long: annual precipitation, summer convective precipitation, most intense rainfall, vegetation density, and average slope.

We offer no clear explanation for why our study did not conform to the first hypothesis of the paper and the expectation of research carried out elsewhere that variables like precipitation and vegetation cover are important: in a well-studied semi-arid catchment in southern Arizona (Nichols, 2006); in micro-catchments in Iran (Vaezi et al., 2017); and for regional studies of sediment yield in Europe (Vanmaercke et al. , 2011b) and Africa (Vanmaercke et al., 2014).

Four speculative possibilities emerged to explain the lack of statistical clarity. First, pathways of sediment connectivity in the stock tank watersheds can be often highly irregular — similar to the findings of Marchamalo et al. (2016)— where pockets of sediment can rest behind vegetative dams that are suddenly released. Second, data are not available on rain drop size, and prior research (Marques et al., 2008; Nyssen et al., 2005)

reveals its importance. Third, off-road vehicle use influences sediment yield (Villarreal et al., 2016), and it is possible that undetected vehicle use could have influenced observed correlations.

A fourth potential reason for the lack of correlation is that our analysis assumed that cattle grazing was a constant between the different stock ponds, despite being unable to find data on the number and frequency of cattle grazed. However, cattle grazing was on the decline on the periphery of Phoenix for decades prior to this study. The reason is that the cattle grazing in the late 19$^{th}$ and early 20$^{th}$ centuries ate palatable perennial forage grasses leaving mostly unpalatable forage. Thus, discussions with ranchers and land-use managers indicate that by the 1989-1995 period, cattle grazing was minimal in the study areas. However, because grazing intensity can be an important factor (Al-Awadhi et al., 2005; Vaezi et al., 2017; Vanmaercke et al., 2010), the lack of quantitative data on grazing intensity could have influenced our correlation analysis.

T-tests, in contrast, did reveal a statistically significant finding. Rock type was an important control on erosion rate with granitic watersheds yielding more sediment than mixtures of metamorphic, basaltic and rhyolite rock types. The importance of rock type is consistent with the findings in other research (Sadeghi et al., 2017; Vanmaercke et al., 2011a), including in an urbanizing catchment (Ferreira et al., 2017).

### *URBANIZATION INFLUENCES ON SONORAN DESERT SEDIMENT YIELDS*

Rózsa and Novák (2011) mapped sensitivity to human factors globally from the perspective of different Köppen-Geiger climate types and predicted that arid regions with

minimal relief (plains and hills) would be the least sensitive to anthropogenic influences. The various LULCC changes between 1989 and 2009 associated with the urban sprawling of Phoenix, USA (Fan et al., 2017), took place on alluvial and pediment surfaces with minimal relief (Jeong et al., 2018a). In contrast to prior expectation, our data for the Sonoran Desert reveals a great sensitivity of low-relief desert landforms to soil erosion. Figure 3.4B graphically portrays the findings for the urban fringe of Phoenix, USA. When each study site's data (Appendix B) are treated as a separate data point, human-set wildfires can increase sediment yields typically 1.7 to 4.2 fold over grazing; exposure of bare ground due to building homes and commercial real estate development can increase sediment yields typically by 0.2 to 3.4 fold over grazing; and exposure of bare ground due to infrastructural development from road and pipeline construction can increase sediment yields typically by 1.4 to 3.1 over grazing. What is not known is the acceleration of soil erosion from grazing over natural background catchment wide denudation rates. Thus, there is little doubt that urbanization processes significantly increased soil erosion well beyond even the impact of grazing, the prior land use, at the sprawling edge of a desert metropolis.

The acceleration of erosion from urbanization in this Bwh climate was likely dampened due to the climatic conditions that occurred during the study period from 1989 to 2009. The first decade, dominated by grazing in the study sites, was wetter than the second decade more dominated by urbanization LULCC. Yet, despite less annual rainfall and less cumulative time of intense rainfall, sudden and aerially extensive (e.g. Figure 3.2) exposure of bare ground from urbanization processes significantly increased soil erosion and SSY.

Our findings are in contrast with the results of Nearing et al. (2005) who examined the response of seven soil erosion models to basic precipitation and vegetation-related parameters, because higher SSY occurred in the second decade of the study period due to urbanization processes, despite less annual rainfall and less cumulative intense rainfall. Still, these findings are consistent with prior research emphasizing the importance of human activity in general (Vanmaercke et al., 2015), on human-caused wildfire (Martínez-Murillo & López-Vicente, 2018), on building new roads (Marchamalo et al., 2016; Nyssen et al., 2002), on vehicle disturbance (Villarreal et al., 2016), and the importance of rock type in an urbanizing catchment (Ferreira et al., 2017).

The findings of this study have implications for conservation practices in the Sonoran Desert and similar urbanizing settings in other BWh climates. At the present time, there are no requirements to mitigate soil erosion on slopes associated with urbanizing processes. Conservation practices focus on impacts to channels. Discussions with land managers reveals an awareness of a paucity of research on the soil erosion impacts of urbanization in the Sonoran Desert. In constructing Figure 3.5, we compiled prior knowledge on the soil erosion rates in the Sonoran Desert; most of these data were associated with unpublished research associated with development projects. No prior effort had been made to compile or analyze available data. Thus, a broader implication of this research rests in tasking such local and national governmental agencies as the Maricopa County Flood Control District and the Army Corp of Engineers to develop appropriate conservation practices to mitigate the soil erosion impacts of urbanization in BWh climates. This is because sediment yield produced from arid urbanization impacts

flood control structures that exist at all scales from streets to regional impoundment dams.

Figure 3.5 contextualizes the magnitude of the anthropogenic effect seen on the urban fringe of metropolitan Phoenix, USA, in the Sonoran Desert. The same data presented in Figure 3.4B are contrasted with all available data from BWh drainage areas globally in Figure 3.5. Appendix F presents all data used to construct Figure 3.5. Figure 3.5 reveals that the magnitude of area-specific sediment yields associated with different land uses in the Phoenix area rest within observations of BWh drainages experiencing agricultural and grazing land uses. This finding implies that other BWh drainages that undergo a LULCC conversion from grazing to urban could experience an even greater acceleration of soil erosion observed here, if precipitation amounts and intensity do not decrease — as occurred in the Phoenix area.

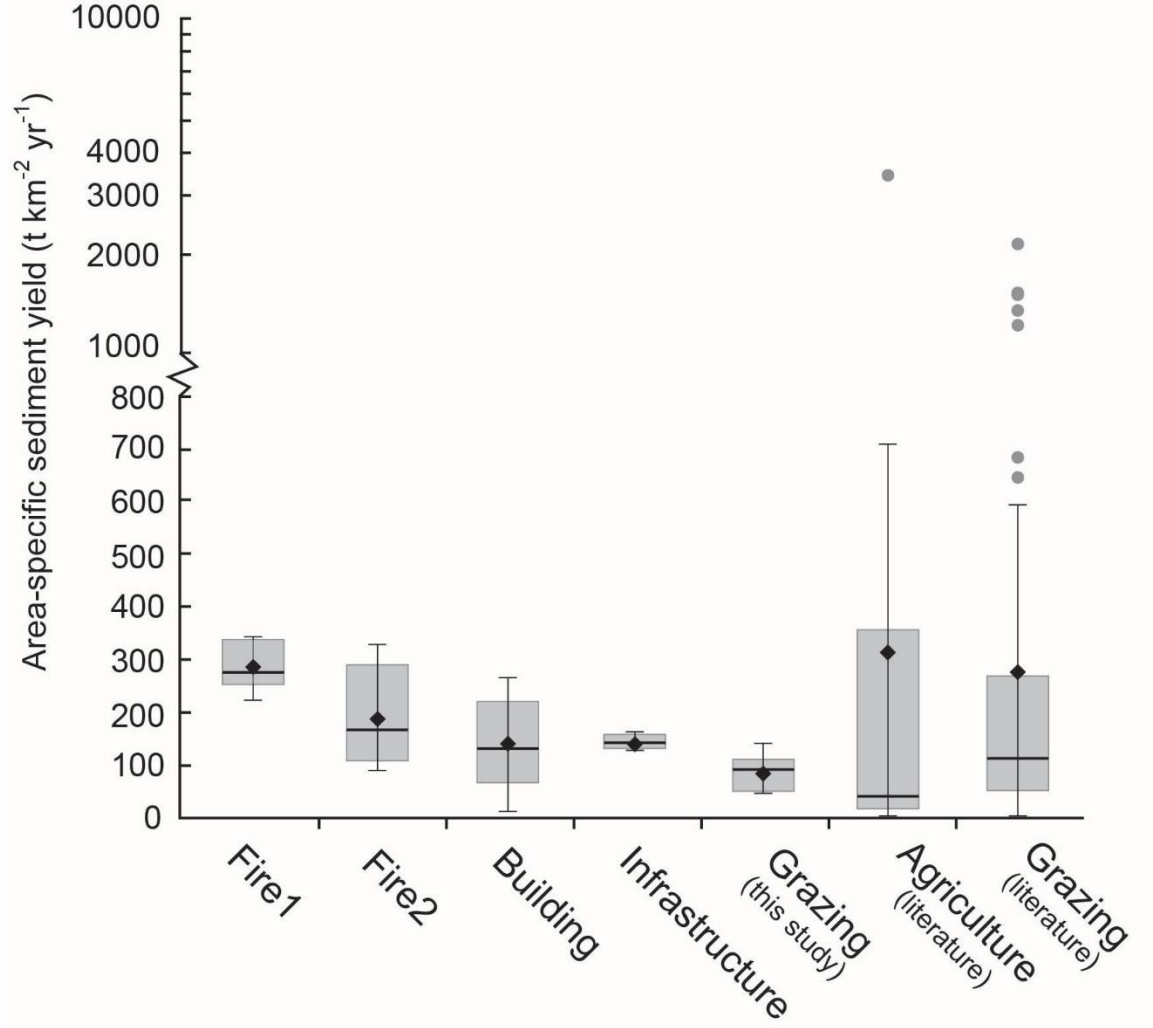


**Figure 3.5.** Box plot of the importance of different land uses surrounding metropolitan Phoenix (where Fire1, Fire2, building, and infrastructure are explained in the caption of Figure 3.4) is placed in comparison with a more global data set of agricultural and grazing land uses in the BWh warm desert setting. Note the break and shift in scale from linear to log in order to portray outliers in the global data set.

*SEDIMENT YIELDS IN KÖPPEN-GIEGER WARM DESERT (BWh) SETTINGS*

Jansson (1988)'s global survey of sediment yield compiled variations by Köppen-Geiger climate groups. At the time, the BWh climate type had an *n* of 3 drainage basins uniquely in warm deserts with very low sediment yields with a median of 25 and a mean of 34 t/km$^2$ per year if sediment yield. Ultimately, in the global analysis, the BW "group has been excluded because of few data" (Jansson, 1988, p. 94). Einsele and Hinderer (1997) also conducted a global analysis of sediment yield focused on estimating the lifetimes of reservoirs and other depressions. In their analysis, they created a plot (Einsele & Hinderer, 1997, p. 295) placing arid to semiarid sediment yields among the highest for various climates. These global generalizations appear contradictory.

Thus, to place our Sonoran Desert BWh findings in a global context, we compiled all available BWh sediment yield data (Appendix F). Most of the African BWh data were compiled by (Vanmaercke et al., 2014). The other data derive from published and also unpublished sources (e.g. theses, consulting reports). Figure 3.6 presents all available area-specific sediment yield data from BWh warm desert climate settings. Data from this study are identified by the circle with different land uses portrayed by different shadings. Data from the Americas, the Middle East, Australia, and Africa are differentiated by land use where such data were available. Taken altogether, this compilation of BWh warm desert sediment yield is consistent with the observation of Einsele and Hinderer (1997) basin size and sediment yield as a slight negative relationship. However, the magnitude of the sediment yield approximation by Einsele and Hinderer (1997), portrayed by the gray shading (Arid to semiarid in Figure 3.6) is far greater than our compiled observations.

Compared to the analysis of African (Vanmaercke et al., 2014) and Europe (Vanmaercke et al., 2011b), the log-log scatterplot of sediment yield data points for BWh in Figure 3.6 rests in the middle of both the African and Europe log-log scatter plots. Although individual study sites may yield particularly high or low sediment yields, taken as a whole, the BWh warm desert climate does not seem to be particularly anomalous or unique, as is sometimes suggested.

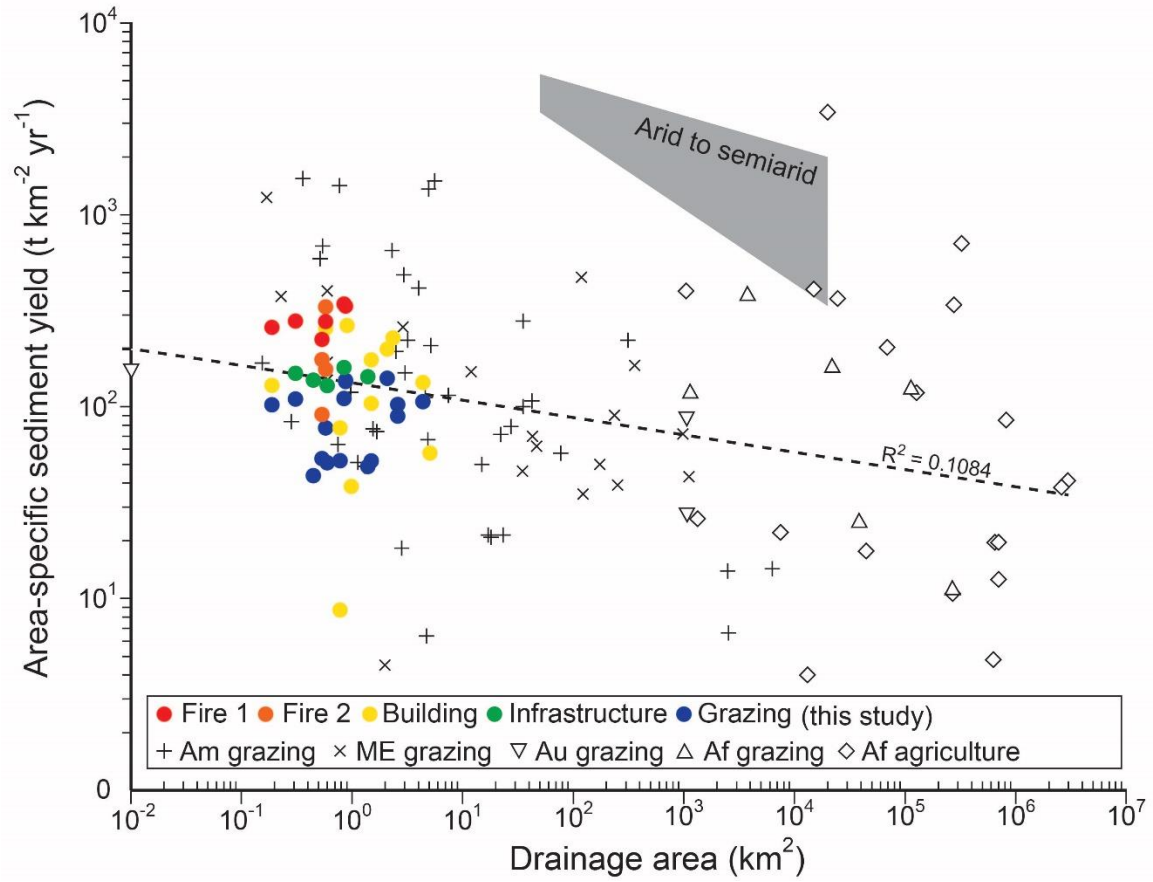


**Figure 3.6.** Log–log scatterplot and linear regression of all available specific sediment yield from the Köppen-Geiger BWh warm desert climate type. The gray shading indicates the sediment yield portrayal by Einsele and Hinderer (1997). Data from the literature are portrayed by symbols on the lower row of the legend, where Am refers to sites in the Americas, ME from the Middle East, Au from Australia, and Af from Africa. Circles in the top row of the legend were derived from Table 3.2 in this study; Fire1, Fire2, building, and infrastructure are explained in the caption of Figure 3.4. Appendix F provides data used to construct this figure.

Thus, Figure 3.6 is consistent with the third hypothesis, the early generalizations about the sediment yield in deserts being particularly anomalous cannot be confirmed by our Sonoran Desert research or by a compilation of available data from BWh catchments. Similarly, Figure 3.6 is consistent with the fourth hypothesis, that the general trend of increasing specific sediment yield in smaller basins observed in Europe (Vanmaercke et al., 2011b), Africa (Vanmaercke et al., 2014), and global comparisons (Einsele & Hinderer, 1997) holds true for warm desert BWh settings.

## CONCLUSION

"Human activities (i.e. deforestation, ploughing, livestock grazing, removal of remnant vegetation, road building) led to an overall increase in erosion process intensity" in the Northern Ethiopian Highlands (Nyssen et al., 2008: 706). Although the setting and land use this Sonoran Desert study is very different, our fundamental conclusion is quite similar. Monitoring sediment accumulation behind 18 earthen berms at each major land-use transition enabled calculations of soil erosion rates. Using a correlation matrix, we examined statistically significant correlations between catchment properties and erosion rates. Unpaired t-tests revealed statistically significant differences between stock pond watersheds that were only granitic and those that were non-granitic.

Unpaired t-tests also compare the specific sediment yield from basins experiencing: grazing; construction of isolated houses, subdivisions and commercial properties; infrastructure of road and pipeline building that exposes bare ground; and wildfires. Wildfires set by urbanites increased sediment yields by up to 4.2x, exposure of

bare ground due to road and pipeline building increased sediment yields by up to 3.4x, and housing and commercial real-estate developments all led to an overall increase in sediment yield of up to 3.4x above grazing on the urban fringe of metropolitan Phoenix, Sonoran Desert, western USA.

The broader significance of this research rests with the need for USA county and federal regulatory agencies to consider policies that mitigate soil erosion from exposed bare ground during urban expansion in BWh climates. Concomitantly, mitigation strategies might also be warranted for other warm desert settings experiencing urbanization (Garba, 2004; Liu et al., 2010; Xian et al., 2008; Yagoub, 2004).While each desert region is unique with respect to the geomorphology surrounding the city (Cooke et al., 1982), the magnitude of sediment yield observed in this study could be of use in urban planning in other warm desert settings. Barbero-Sierra et al. (2013, p. 95) made the case that urban sprawl "has become the most active desertification agent in Spain" by soil sealing. The soil erosion and sediment yield associated with two decades of sprawling urbanization of metropolitan Phoenix, USA could be interpreted in the same way, but in a two-stage process. First came the exposure of bare ground with enhanced soil erosion. Then, came the sealing of soil when the pavement and construction was completed.

# CHAPTER 4

# SEDIMENT ACCUMULATION EXPECTATIONS FOR GROWING DESERT CITIES: A REALISTIC DESIRED OUTCOME TO BE USED IN CONSTRUCTING APPROPRIATELY SIZED FLOOD CONTROL STRUCTURES

(SUBMITTED TO *ENVRIONMENTAL RESEARCH LETTERS*)


## ABSTRACT

Many rapidly urbanizing desert cities (RUDC) around the globe experience an acute risk of flooding. To reduce this risk, properly engineered Flood Control Structures (FCS) must account for sediment accumulation as well as flood waters. While the Phoenix area used regional data from non-urban, non-desert watersheds to generate sediment yield rates (SYR), the proposed desired outcome for RUDCs is to base FCS on SYR that recognize and use the Wolman model of how urbanization impacts SYR. Wolman (1967) recognized that prior to urbanization, land-use land cover changes increase sediment yields slightly prior to urbanization. Then, sediment yields spike during a relatively short period of bare-ground exposure, followed by sealing of the urban surface resulting in a great reduction in sediment yield. This research presents a new analysis of empirical data for the Phoenix metropolitan region, where two regression models provide estimates of a more realistic sediment accumulation for arid regions and also urbanization of desert cities: i) linear regression between drainage area and sediment yield based on a compilation of more than 150 global sediment yield data for warm deserts (BWh Köppen-Geiger) climate; and ii) linear regression relating percent urban

growth with sediment yield using available data on urbanization-generated sediment associated with growth of a desert city. The new model can be used to predict the realistic sediment accumulation for helping provide data where few data exists in parts of arid Africa, southwest Asia, and India.

## INTRODUCTION

Floods are common in many rapidly urbanizing desert cities (RUDC) and often cause extensive loss of life and property, where more deaths can occur from flash floods than dehydration (Warner 2004). The sorts of urban sprawling that take place on alluvial surfaces with minimal relief (Jeong et al 2018a) put inhabitants at high risk of flooding (Middletone and Sternberg 2013). UNISDR (2012) reported more than half of Jordan's disaster related mortalities during 1981-2010 could be explained by flash flooding, where the 2008 floods alone in Yemen led to increased national poverty (UNSIDR 2010). Flash floods are often associated landslides on steep slopes where poorer inhabitants living in self-built informal housing in Bolivian Altiplano and the combination of natural disasters led a number of fatalities (O'Hare and Rivas 2005). Flash floods in the Indian state of Rajasthan caused by once-in-a-200-year event in the Thar Desert killed more than 150 people and the cost of damage was estimated at more than US $290 million (Telegraph 2006). In another example, flash flooding in September of 2015, at least 15 people perished in flash flooding near Utah-Arizona border (The Guardian 2015).

Resilient urban planning efforts certainly recognize the need for flood control, and hence flood control structures (FCS) (Muller 2007, Djordjević et al 2011, Liao 2012).

The sediment volume is an important design parameter for FCS design. Unlike water volume, that can be drained off by spillways, sediment volume behind the FCS is continuously stored, that reduces the life expectancy of FCS. Thus, accurate estimation of sediment volume is an essential design factor for FCS. Over-estimation of sediment volume will lead unnecessary costs to build and maintain the FCS, but under-estimation can result a reduction of life expectancy of FCS due to rapid fill-up behind FCS, or worse yet failure. Sweasy Dam on the Mad River of northern California exemplifies a circumstance where too much sedimentation threatened reservoir sustainability. Approximately 25 years after dam construction, the Sweasy Dam was completely filled and no longer functional; it was removed in 1970 (Mount 1995).

A large volume of data on sediment yields support decision making by enabling establishment of empirical equations for better estimation of sediment yield in developed settings such as the southwestern USA. However, it is a challenge for RUDCs in lesser developed settings in Africa, Middle East, India, and Asia because of limited data are available. Based on a global data compilation of sediment yield in warm deserts (the Köppen-Geiger BWh climate setting) by Jeong and Dorn (2019) and Vanmaercke et al (2014), only eleven published data points have been collected from urban settings outside of the U.S.A. (Appendix G); all other measurements are from agricultural fields or grazing lands. Thus, the focus of this paper rests in establishing a new desired outcome for engineering FCS for growing desert cities that largely lack empirical data on sediment yields.

The Phoenix Metropolitan Region (PMR) is often used as a case study for the analysis of urban climate changes (Georgescu et al 2009, Chow et al 2014, Shaffer et al, 2015), the impact of ecosystem services and disservices (Hall et al 2009, Walker et al 2009, Zhuo et al 2012), urban biodiversity (Banville and Bateman 2012, Bateman et al 2015) and issues of urban sprawl and water quality (Hale et al 2015). The PMR, however, is an atypical desert city from the perspective of urban flood planning. Where as many growing desert cities lack data on sediment yield (Dedkov and Mozzherin 1984, Gallaire 1986, Laronne 1990, Terfous et al 2003, Nyssen et al 2004, Liénou 2007, FAO 2008, Amogu 2009, Billi and el Badri Ali 2010), decisions on the size of FCS and sediment delivery infrastructure in PMR were made based on an abundance of data.

The new desired outcome is to estimate sediment yields for growing desert cities informed by the "Wolman model" and using published and unpublished data from warm desert watersheds both in Phoenix and globally. Wolman (1967) recognized that prior to urbanization, land-use land cover (LULC) changes increase sediment yields that then spike during a relatively short period of bare-ground exposure, followed by sealing of the urban surface that then dramatically reduces sediment yield. This paper presents a new analysis of empirical data for the Phoenix metropolitan region, showing just how FCS are experiencing sedimentation (FCDMC 2015a), and proposes a strategy whereby RUDC can estimate sedimentation rates.

STUDY AREA

Phoenix, Arizona, is the fifth largest USA city. The population of the metropolitan area has increased an order-of-magnitude since 1950s with the advent of air conditioning (Grimm et al 2013), and PMR sprawled (Figure 4.1) commensurately with migrants seeking employment and low-cost homes. Phoenix is located entirely in the Sonoran Desert classified as a warm desert, Köppen-Geiger BWh climate setting and has precipitation averaging 208 mm split evenly between summer and winter maxima (Climate Office of Arizona, https://azclimate.asu.edu/climate/climate-of-phoenix-summary/).

The FCS are sustainable only if they have sufficient water storage space; thus, properly engineered structures must account for sediment accumulation as well as flood waters because sedimentation reduces the storage capacity of the structures. The flood control district of Maricopa County (FCDMC) operates and maintains 22 flood control dams (Appendix G and table 4.1). Among the 22 dams, 15 dams were built from 1954 to 1991 by United States Department of Agriculture-Soil Conservation Service (USDA-SCS) for 100-year flood protection in agricultural areas. Five dams were built from 1974 to 1985 by U.S. Army Corps of Engineers (USACE) for standard project flood ranged in the vicinity of a 200 to 500-year event (FEMA ____). One dam was designed by the FCDMC (FCDMC 2015b), where the total storage capacity was calculated from a gage height-volume relation curve by FCDMC (https://www.maricopa.gov/3768/Water-level-Data). Except Powerline, Vineyard Rd, and Rittenhouse FRS (EMNRCD and FCDMC 2013), most of FCS in PMR have not been recently surveyed to measure present sedimentation, and many of them even have never been surveyed since they were built.

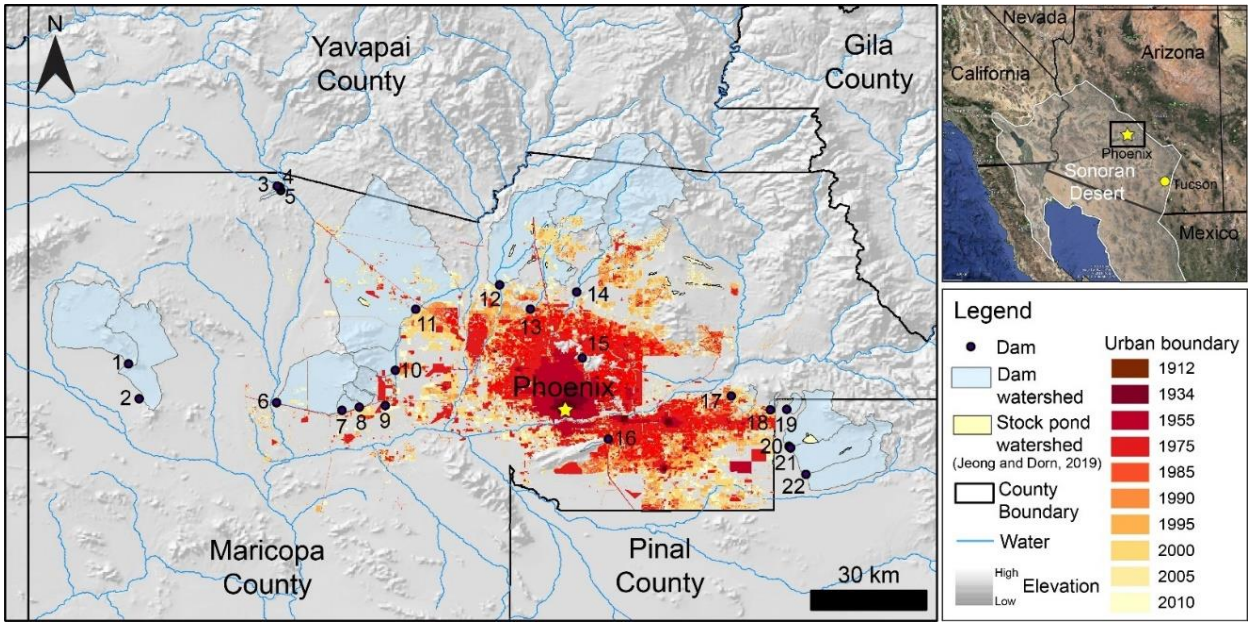


**Figure 4.1.** Map of the Phoenix Metropolitan Region (PMR) showing the locations of main dams and their watersheds. Urban sprawl of PMR over the period from 1912 to 2010 shows the dam watersheds have experienced a wide range of land-use changes. Sediment yield data associated with the urban sprawl was reported by Jeong and Dorn (2019). The data used to estimate sediment accumulation behind 22 main dams in PMR using extrapolation. See method section for details. The numbers refer to dams identified in this paper's data tables. Urban boundaries from 1912 to 2010 are extracted from land cover classification by Central Arizona–Phoenix Long-Term Ecological Research. Data available at https://sustainability.asu.edu/caplter/data/view/knb-lter-cap.1.11 and https://sustainability.asu.edu/caplter/data/view/knblter-cap.650.1/. Because of the limited extent of the land use/land cover maps, some dam catchments on the margin of central Phoenix did not included in the extent of urban sprawl.

The latest hydraulics design manual for building FCS in the PMR focuses on empirically derived equations to estimate sediment yields from non-urbanizing basins (FCDMC 2015a). For the estimation of sediment accumulation in PMR, FCDMC used 21 sediment yield data monitored from 1942 to 1974 (Figure 4.2 and Appendix G). Unfortunately, 10 of the 24 watersheds are located in non-desert regions of California and New Mexico (FCDMC 2015a). Also, the measurement period does not the period of urban acceleration of erosion (Figure 4.2) or any decadal climate changes in the PMR. In

contrast, sediment yield data from 1989 to 2013 (Figure 4.2) reported by Jeong and Dorn (2019) present an opportunity to test Woman's model for PMR because their data recorded changes in sedimentation associated with major land-use changes on the urban fringe during the measurement period (Figure 4.1). Land use–land cover change (LULCC) for the period had a 30 m resolution (Fan et al 2017).

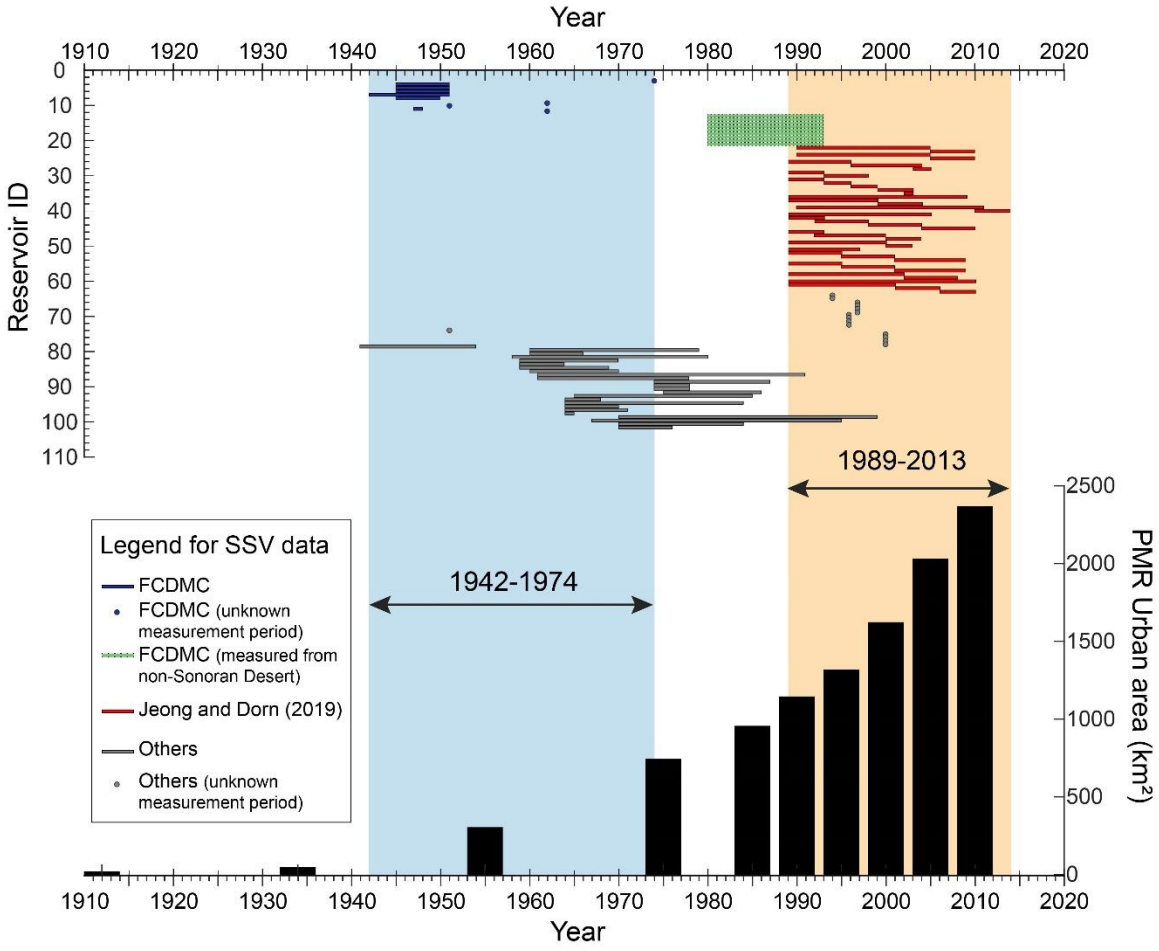


**Figure 4.2.** Period of reservoir sedimentation surveys in the Sonoran Desert where PMR situated in. Note the sparseness of data for the latter part of the 20th century that used as representative area-specific sedimentation volume (SSV) when major dams of PMR built (FCDMC 2015a), which is inconsistent with rapid urban growth of PMR. The reservoir identification numbers held on Appendix G. PMR urban area was calculated by LULCC map provided by Central Arizona–Phoenix Long-Term Ecological Research. Circles marked the published year because measurement period is not reported, indicating the SSV measurement probably earlier than the published year.

## METHODS

Properly functioning FCS require an accurate estimate of sediment yield. This is especially true for RUDCs where floods and flash floods are major risks (The World Bank 2014). Due to the lack of data for present FCS sedimentation in PMR, compiled watershed sediment yield data is used to construct models to estimate sediment yield for the FCS. This paper compares the commonly used model to estimate sediment yield using the relation between sediment yield and drainage area under 'without urban sprawl condition' with a proposed model using the relation between sediment yield and annual urban growth under 'with urban sprawl condition' to recognize urbanization's impact on sediment yield and to assess how the changed sediment yield could affect the scale of FCS. The estimation of annual sediment yield also enables calculation of an annual rate of storage loss and expected life of FCS when the storage capacity of FCS is known (Table 4.1). The predicted sediment yield for FCS in PMR will be compared to the designed sediment yield (Table 4.2) for FCS built by USACE that were designed for 100 years of sediment accumulation (USACE 1982, 1984b), except for the Saddleback FRS and Powerline FRS that was designed for 50 years of sediment accumulation (USDA-SCS 1977, EMNRCD and FCDMC 2013).

Published sediment yield data from soil erosion are presented in different ways, sometimes to different audiences whether they are scientists or policy makers (Leopold 1968, Zhang and Huang 2015, Li *et al* 2015, UNCCD 2008). Since different approaches to the presentation of sediment yield data can generate confusion, this paper defines SSY as an annual area-specific sediment yield measured in units of weights (Mg $km^{-2}$ $yr^{-1}$ or

tons acre$^{-1}$ yr$^{-1}$) and area-specific sedimentation volume (SSV) as the annual area-specific sediment yield measured in units of volume ($m^3$ $km^{-2}$ $yr^{-1}$ or acre-feet $mile^{-2}$ $yr^{-1}$).

**Table 4.1.** The 22 flood control dams operated and maintained by FCDMC in PMR

| ID | Dam Name | Latitude (°) | Longitude (°) | Watershed | Built by | Year completed | Stream gage installation date | $A_D$ (km$^2$) | $A_D$ (mile$^2$) | Total storage capacity (m$^3$) | Total storage capacity (acre-feet) |
|---|---|---|---|---|---|---|---|---|---|---|---|
| 1 | Harquahala FRS | 33.5487 | -113.0977 | Lower Centennial | SCS[a] | 1991 | 3/1/1994 | 264.55 | 102.30 | 36039572 | 29218 |
| 2 | Saddleback FRS | 33.4666 | -113.0726 | Lower Centennial | SCS[a] | 1982 | 12/16/1988 | 76.55 | 29.60 | 8317356 | 6743 |
| 3 | Casandro Dam | 33.9674 | -112.7488 | Lower Hassayampa | FCDMC[b] | 1996 | 8/15/1996 | 3.10 | 1.20 | 283454 | 230 |
| 4 | Sunset FRS | 33.9649 | -112.7426 | Lower Hassayampa | SCS[a] | 1976 | 2/12/1989 | 1.63 | 0.63 | 251753 | 204 |
| 5 | Sunnycove FRS | 33.9571 | -112.7402 | Lower Hassayampa | SCS[a] | 1976 | 7/1/1986 | 3.59 | 1.39 | 451330 | 366 |
| 6 | Buckeye FRS #1 | 33.4578 | -112.7500 | Lower Hassayampa | SCS[a] | 1975 | 7/26/1983 | 198.09 | 76.60 | 26567186 | 21538 |
| 7 | Buckeye FRS #2 | 33.4396 | -112.5965 | Lower Hassayampa | SCS[a] | 1975 | 11/11/1992 | 14.74 | 5.70 | 2383823 | 1933 |
| 8 | Buckeye FRS #3 | 33.4471 | -112.5559 | Lower Hassayampa | SCS[a] | 1975 | 11/23/1992 | 22.50 | 8.70 | 3952317 | 3204 |
| 9 | White Tanks FRS #4 | 33.4506 | -112.4944 | White Tanks B | SCS[a] | 1954 | 1/9/1986 | 48.10 | 18.60 | 3131929 | 2539 |
| 10 | White Tanks FRS #3 | 33.5340 | -112.4710 | White Tanks B | SCS[a] | 1954 | 3/12/1986 | 53.01 | 20.50 | 7405814 | 6004 |
| 11 | McMicken Dam | 33.6773 | -112.4233 | Trilby | USACE[c] | 1956 | 3/20/1983 | 626.33 | 242.20 | 46160399 | 37423 |
| 12 | New River Dam | 33.7348 | -112.2264 | Upper New River | USACE[c] | 1985 | 4/15/1986 | 442.21 | 171.00 | 146322305 | 118626 |
| 13 | Adobe Dam | 33.6777 | -112.1539 | Skunk Creek | USACE[c] | 1982 | 10/28/1982 | 225.76 | 87.30 | 90457256 | 73335 |
| 14 | Cave Buttes Dam | 33.7179 | -112.0453 | Cave Creek | USACE[c] | 1980 | 1/25/1984 | 506.08 | 195.70 | 120020934 | 97303 |
| 15 | Dreamy Draw Dam | 33.5626 | -112.0316 | Upper ACDC | USACE[c] | 1974 | 1/24/1984 | 3.49 | 1.35 | 909075 | 737 |
| 16 | Guadalupe FRS | 33.3719 | -111.9705 | South Mountain | SCS[a] | 1975 | 6/29/1989 | 4.50 | 1.74 | 597251 | 484 |
| 17 | Spook Hill FRS | 33.4731 | -111.6817 | Lower Verde | SCS[a] | 1980 | 3/13/1984 | 35.17 | 13.60 | 7310836 | 5927 |
| 18 | Signal Butte FRS | 33.4403 | -111.5904 | Lower Verde | SCS[a] | 1987 | 11/10/1987 | 42.41 | 16.40 | 4193832 | 3400 |
| 19 | Apache Junction FRS | 33.4415 | -111.5517 | Lower Verde | SCS[a] | 1988 | 9/15/1988 | 14.48 | 5.60 | 2767929 | 2244 |
| 20 | Powerline FRS | 33.3548 | -111.5461 | Upper East Maricopa Floodway | SCS[a] | 1967 | 12/2/1992 | 119.47 | 46.20 | 9038941 | 7328 |
| 21 | Vineyard Rd FRS | 33.3508 | -111.5425 | Upper East Maricopa Floodway | SCS[a] | 1968 | 11/2/1983 | 138.87 | 53.70 | 11769373 | 9542 |
| 22 | Rittenhouse FRS | 33.2889 | -111.5066 | Upper East Maricopa Floodway | SCS[a] | 1969 | 9/27/1988 | 121.80 | 47.10 | 9549849 | 7742 |

[a] SCS: United States Department of Agriculture-Soil Conservation Service (USDA-SCS).

[b] USACE: U.S. Army Corps of Engineers.

[c] FCDMC: flood control district of Maricopa County.

**Table 4.2.** 100 year-capacity loss and expected life of FCS based on the total capacity of FCS and sediment yields predicted by two models. The reported error term derives from the 95 percent confidential interval. Abbreviation: n.a., not available.

| | | | | | | | Model1: without urban sprawl condition | | | | Model 2: with urban sprawl condition | | | |
|---|---|---|---|---|---|---|---|---|---|---|---|---|---|---|
| ID | Dam Name | $A_D$ (km$^2$) | $A_D$ (mile$^2$) | Designed SSV (ac-ft mi$^{-2}$ yr$^{-1}$) | 100-yr capacity loss (%) | Expected life (yrs) | Predicted SSV (m$^3$ km$^{-2}$ yr$^{-1}$) | Predicted SSV (ac-ft mi$^{-2}$ yr$^{-1}$) | 100-yr capacity loss (%) | Expected life (yrs) | Predicted SSV (m$^3$ km$^{-2}$ yr$^{-1}$) | Predicted SSV (ac-ft mi$^{-2}$ yr$^{-1}$) | 100-yr capacity loss (%) | Expected life (yrs) |
| 1 | Harquahala FRS | 264.55 | 102.30 | | | | 56.78 ± 11.39 | 0.119 ± 0.024 | 4.2 ± 0.1 | 2399 ± 48 | n.a. | n.a. | n.a. | n.a. |
| 2 | Saddleback FRS | 76.55 | 29.60 | 0.409[a] | 18 | 558 | 64.59 ± 11.86 | 0.136 ± 0.025 | 5.9 ± 0.1 | 1682 ± 31 | n.a. | n.a. | n.a. | n.a. |
| 3 | Casandro Dam | 3.10 | 1.20 | | | | 90.15 ± 17.51 | 0.189 ± 0.037 | 9.9 ± 0.2 | 1013 ± 20 | 78.1 ± 14.31 | 0.164 ± 0.030 | 8.6 ± 1.6 | 1170 ± 214 |
| 4 | Sunset FRS | 1.63 | 0.63 | | | | 96.40 ± 19.78 | 0.202 ± 0.042 | 6.2 ± 0.1 | 1603 ± 33 | 102.79 ± 21.65 | 0.216 ± 0.045 | 6.7 ± 1.4 | 1503 ± 317 |
| 5 | Sunnycove FRS | 3.59 | 1.39 | | | | 88.78 ± 17.05 | 0.186 ± 0.036 | 7.1 ± 0.1 | 1414 ± 27 | 110.1 ± 31.74 | 0.231 ± 0.067 | 8.8 ± 2.5 | 1140 ± 329 |
| 6 | Buckeye FRS #1 | 198.09 | 76.60 | | | | 58.51 ± 11.46 | 0.123 ± 0.024 | 4.4 ± 0.1 | 2292 ± 45 | 174.08 ± 99.40 | 0.366 ± 0.209 | 13 ± 7.4 | 770 ± 440 |
| 7 | Buckeye FRS #2 | 14.74 | 5.70 | | | | 76.67 ± 13.71 | 0.161 ± 0.029 | 4.7 ± 0.1 | 2109 ± 38 | 75.7 ± 15.46 | 0.159 ± 0.032 | 4.7 ± 1.0 | 2136 ± 436 |
| 8 | Buckeye FRS #3 | 22.50 | 8.70 | | | | 73.37 ± 13.05 | 0.154 ± 0.027 | 4.2 ± 0.1 | 2394 ± 43 | 59.38 ± 15.61 | 0.125 ± 0.033 | 3.4 ± 0.9 | 2958 ± 778 |
| 9 | White Tanks FRS #4 | 48.10 | 18.60 | | | | 67.79 ± 12.21 | 0.142 ± 0.026 | 10.4 ± 0.2 | 960 ± 17 | 158.26 ± 75.12 | 0.332 ± 0.158 | 24.3 ± 11.5 | 411 ± 195 |
| 10 | White Tanks FRS #3 | 53.01 | 20.50 | | | | 67.11 ± 12.12 | 0.141 ± 0.025 | 4.8 ± 0.1 | 2082 ± 38 | 75.56 ± 14.31 | 0.159 ± 0.030 | 5.4 ± 1.0 | 1849 ± 350 |
| 11 | McMicken Dam | 626.33 | 242.20 | | | | 51.91 ± 11.29 | 0.109 ± 0.024 | 7.0 ± 0.2 | 1420 ± 31 | 456.39 ± 322.30 | 0.958 ± 0.677 | 61.9 ± 43.7 | 161 ± 114 |
| 12 | New River Dam | 442.21 | 171.00 | 0.288[b] | 4 | 2412 | 53.82 ± 11.32 | 0.113 ± 0.024 | 1.6 ± 0.0 | 6148 ± 129 | 219.76 ± 133.77 | 0.461 ± 0.281 | 6.6 ± 4.0 | 1506 ± 916 |
| 13 | Adobe Dam | 225.76 | 87.30 | 0.309[c] | 4 | 2723 | 57.72 ± 11.43 | 0.121 ± 0.024 | 1.4 ± 0.0 | 6942 ± 137 | 280.58 ± 183.33 | 0.589 ± 0.385 | 7 ± 4.6 | 1428 ± 933 |
| 14 | Cave Buttes Dam | 506.08 | 195.70 | 0.300[d] | 6 | 1660 | 53.07 ± 11.30 | 0.111 ± 0.024 | 2.2 ± 0.0 | 4468 ± 95 | 596.18 ± 433.04 | 1.252 ± 0.909 | 25.1 ± 18.3 | 398 ± 289 |
| 15 | Dreamy Draw Dam | 3.49 | 1.35 | 0.267[e] | 5 | 2048 | 89.05 ± 17.14 | 0.187 ± 0.036 | 3.4 ± 0.1 | 2924 ± 56 | 86.47 ± 15.93 | 0.182 ± 0.033 | 3.3 ± 0.6 | 3012 ± 555 |
| 16 | Guadalupe FRS | 4.50 | 1.74 | | | | 86.73 ± 16.39 | 0.182 ± 0.034 | 6.5 ± 0.1 | 1530 ± 29 | 74.82 ± 16.05 | 0.157 ± 0.034 | 5.6 ± 1.2 | 1774 ± 381 |
| 17 | Spook Hill FRS | 35.17 | 13.60 | | | | 70.04 ± 12.51 | 0.147 ± 0.026 | 3.4 ± 0.1 | 2968 ±53 | 173.87 ± 85.80 | 0.365 ± 0.180 | 8.4 ± 4.1 | 1196 ± 590 |
| 18 | Signal Butte FRS | 42.41 | 16.40 | | | | 68.69 ± 12.32 | 0.144 ± 0.026 | 6.9 ± 0.1 | 1440 ± 26 | 65.97 ± 11.11 | 0.139 ± 0.023 | 6.7 ± 1.1 | 1499 ± 252 |
| 19 | Apache Junction FRS | 14.48 | 5.60 | | | | 76.81 ± 13.74 | 0.161 ± 0.029 | 4.0 ± 0.1 | 2489 ± 45 | 78.62 ± 15.53 | 0.165 ± 0.033 | 4.1 ± 0.8 | 2431 ± 480 |
| 20 | Powerline FRS | 119.47 | 46.20 | 0.103[f] | 6 | 1542 | 61.67 ± 11.63 | 0.129 ± 0.024 | 8.2 ± 0.2 | 1227 ± 23 | n.a. | n.a. | n.a. | n.a. |
| 21 | Vineyard Rd FRS | 138.87 | 53.70 | | | | 60.71 ± 11.57 | 0.127 ± 0.024 | 7.2 ± 0.1 | 1396 ± 27 | n.a. | n.a. | n.a. | n.a. |
| 22 | Rittenhouse FRS | 121.80 | 47.10 | | | | 61.55 ± 11.62 | 0.129 ± 0.024 | 7.8 ± 0.1 | 1274 ± 24 | n.a. | n.a. | n.a. | n.a. |

*MODEL 1: SEDIMENT YIELD PREDICTION UNDER WITHOUT URBAN SPRAWL CONDITION*

An inverse relation exists between SSY and drainage area (Dendy and Bolton 1976, Lahlou 1988, Milliman and Syvitski 1992, Einsele and Hinderer 1997), and Milliman and Syvitski (1992) confirmed a clear negative relation between SSY and drainage basin area based on 280 global data points. Thus, using this relationship has the benefit that the measurement of basin area is relatively simple, and hence it is frequently used for prediction of SSY in ungauged basins (De Vente *et al* 2007). The negative relation is generally explained by widely-used concept of the sediment delivery ratio (Walling 1983); as basin area increases, the relative portion of flat and gentle slopes increases and act work as sediment sinks rather than sources (Verstraeten *et al* 2003). The negative relation also exists between SSV and drainage area because sediment delivery ratios decline in the downstream direction (Graf *et al* 2010). In model 1, the SSV of FCS is best approximated by a power function.

The problem with this model is that other local environmental conditions could also influence the SSY. For example, scholarship reveals several factors thought to influence erosion rates, that could restrict use of this model: rock type in the Indian arid zone (Sharma and Chatterji 1982, Ferreira *et al* 2017); sediment remobilization in valleys (Church and Slaymaker 1989); and prominent channel erosion over hillslope erosion in highly vegetated areas (Dedkov and Mozzherin 1992, Church *et al* 1999, Prosser *et al* 2001, Dedkov 2004). Therefore, similar environmental settings should be compared when predicting SSV with Model 1. The following subsections describe the SSV

compilation data of Koeppen's BWh warm desert setting, as well as methods used to predict SSV of FCS for desert cities that lack high-resolution datasets.

*DESCRIPTION OF THE SEDIMENT YIELD DATABASE IN KÖPPEN-GEIGER WARM DESERT (BWh) SETTINGS*

All available BWh SSV data were compiled for calculating storage capacity loss and life expectancies of FCS (Appendix G). Most of the African BWh data were compiled by Vanmaercke et al (2014). The other data derive from published and also unpublished sources (e.g. theses, consulting reports). Figure 3 presents all available annual SSV data from BWh warm desert climate settings.

*PREDICTION OF SEDIMENT YIELD USING REGRESSION MODEL BASED ON SEDIMENTATION VOLUME-DRAINAGE AREA RELATION*

Taken altogether, this compilation of BWh warm desert sediment yield is consistent with the observation of prior research that basin size and sediment yield maintains a slight negative relationship. Drainage area, however, only explains 12% of the observed variability in SSV (Figure 4.3). The relation between SSV ($m^3\ km^{-2}\ yr^{-1}$) and drainage area ($A_D$) ($km^2$) for the 153 catchments in the Bwh warm desert setting is:

$$SSV = 101.42 * A_D^{-0.104} \qquad (1)$$

with an $R^2$ value of 0.12. Then, the regression used to estimate SSV for the 22 main FCS in PMR (Table 4.2). The annual rate of storage loss (ASL) was calculated using this equation:

$$ASL = (A_D * SSV / TSC) * 100 \quad (2)$$

where ASL is measured as a percent of storage volume lost per year through sedimentation (Graf *et al* 2010), TSC indicates the total storage capacity of FCS ($m^3$). FCS in PMR was designed to provide a total cumulative sediment storage capacity for 50-years or 100-years of sediment storage (USDA-SCS 1977, USACE 1981, 1982, 1984a, 1984b, EMNRCD and FCDMC 2013), thus 100-yr storage loss (100-yr SL) was calculated by 100 times the ASL. The expected life of a flood control structure (ELF) is inversely related to its annual rate of its storage loss:

$$ELF = 100 / ASL \quad (3)$$

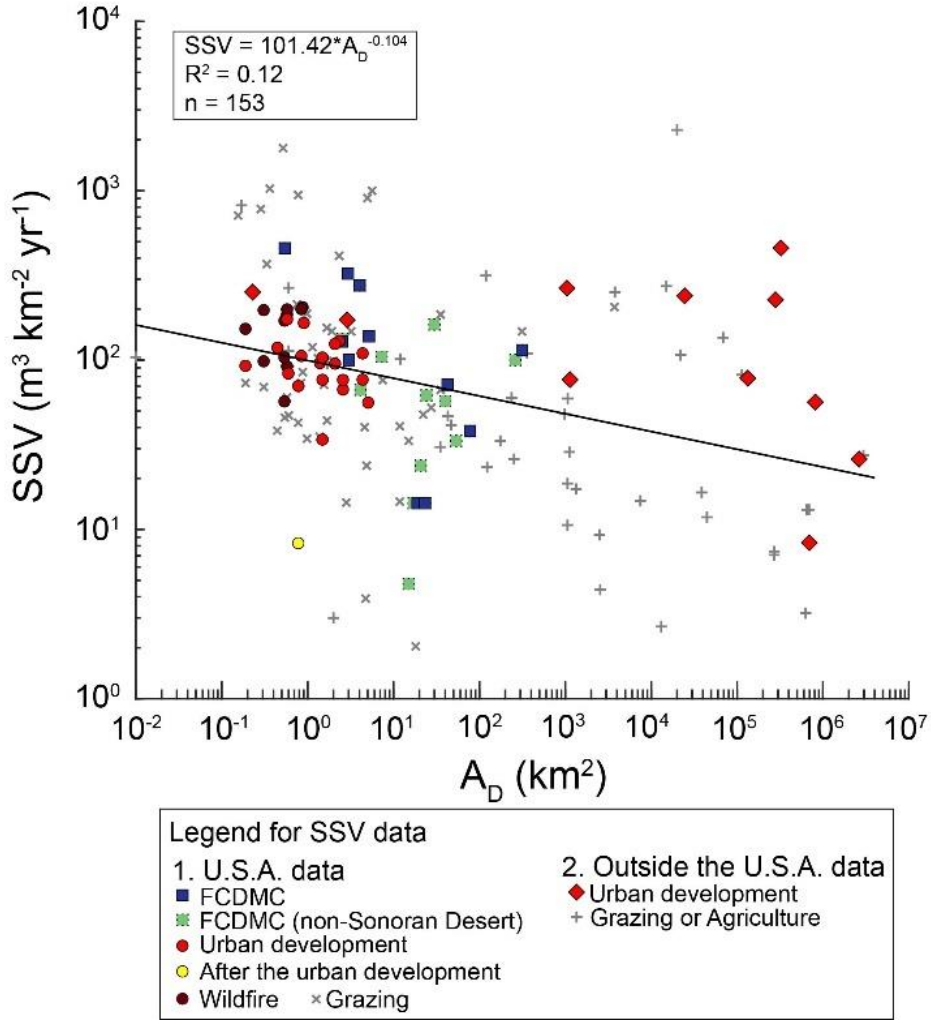


**Figure 4.3.** Log–log scatterplot and linear regression of all available area-specific sedimentation volumes (SSV) and drainage area($A_D$) from the Bwh warm desert setting. Data used to derive the empirical equation to predict SSV of FCS by FCDMC are identified by squares, and data from Jeong and Dorn (2019) are identified by circles with different land uses portrayed by different colors. Data from the Americas, the Middle East, Australia, and Africa are differentiated by land use where such data were available (Appendix G).

*MODEL 2: SEDIMENT YIELD PREDICTION UNDER WITH URBAN SPRAWL CONDITION*

Housing and commercial real-estate development in the PMR led to a lot of bare ground exposure that led to as much as a 3.4-fold increase in sediment yield above and

beyond the effects of grazing (Jeong and Dorn 2019). An individual case exemplifies the Wolman (1967) model for the RUDC of Phoenix, USA. The SSV of the watershed supplying sediment to a cattle stock tank called "Peralta tank" was 42 $m^3$ $km^{-2}$ $yr^{-1}$ during the period of grazing. Sediment yield then rapidly increased to 70 $m^3$ $km^{-2}$ $yr^{-1}$ during the time of active subdivision construction, and decreased to 8 $m^3$ $km^{-2}$ $yr^{-1}$ when sediment sources were sealed by a lot of concrete and pavement (Appendix G and Figure 4.3). Based on the Wolman model, the key land use parameters impacting SSV were annual urban growth and annual imperviousness. The following subsections describe methods used to calculate the land use parameters and the relation with SSV from small desert watersheds. The goal of Model 2 is to estimate SSV for FCS in PMR.

*MEASURING URBANIZATION IMPACT ON THE SSV FROM DESERT WATERSHEDS*

Figure 4.4 illustrates the conceptual model used here to quantify LULCC-related parameters using GIS procedures. Urbanization processes entail exposure of bare ground due to home and commercial real estate development, or other infrastructural development such as road and pipeline construction. Bare ground exposure then accelerates soil erosion by enhancing rain splash (Jeong and Dorn 2019) and overland flow. To estimate the magnitude of bare ground exposure or urban growth during the time period from T1 to T2 (BG1 in Figure 4.4), the area of intersection of natural land cover (natural vegetation and soil/desert) in T1 and urban land cover (asphalt/road, concrete/buildings, urban mixture and residential) in T2 was calculated using GIS. The imperviousness for the time period from T1 to T2, followed by sealing of the urban

surface, then resulted in a great reduction in sediment yield in T2 (U2). Then, the length of the time period (L1) allowed calculation of annual urban growth (AUG) and imperviousness (AI).

The PMR is a NSF site for long-term ecological research in an arid urban setting; two LULCC datasets with a 30 m resolution from CAP LTER quantified urban growth and imperviousness: i) LULC in 1912, 1934, 1955, 1975 and 1995 (https://sustainability.asu.edu/caplter/data/view/knb-lter-cap.1.11); and ii) LULC in 1985, 1990, 1995, 2000, 2005 and 2010 (https://sustainability.asu.edu/caplter/data/view/knblter-cap.650.1/). These data were supplemented by analysis of historic aerial photography from the Maricopa County Tax Assessor website (https://gis.maricopa.gov/GIO/HistoricalAerial/index.html) and Google Earth. Table 4.3 shows data from 18 stock pond catchments (Jeong and Dorn 2019) used to make the regression equation.

For the FCS drainage basins, no urban growth occurred within their drainage basins during 1912-1955. Therefore, based on the two datasets, 8 time periods were established: T1 (1955-1975), T2 (1975-1985), T3 (1975-1995), T4 (1985-1990), T5 (1990-1995), T6 (1995-2000), T7 (2000-2005) and T8 (2005-2010). However, the coverage of the two LULC datasets are different; LULCC for some time periods was not fully spatially covered. FCS ID 1, 2, 20, 21, and 22 in table 4.3 was excluded for quantification of urban growth and imperviousness, because the LULC does not fully cover the whole basin area. For FCS ID 3, 4, and 5, the former LULC dataset spatially covers whole drainage basin, but the latter dataset does not cover it; thus, only T1 and T3

could be used. The FCS ID 18 and 19 drainage basins were only covered by the latter dataset; thus, T4, T5, T6, T7 and T8 were used. For the remaining FCS where the two datasets fully cover the whole drainage area, T1, T2, T4, T5, T6, T7 and T8 were used unless there was no urban growth for each time periods (Table 4.4).

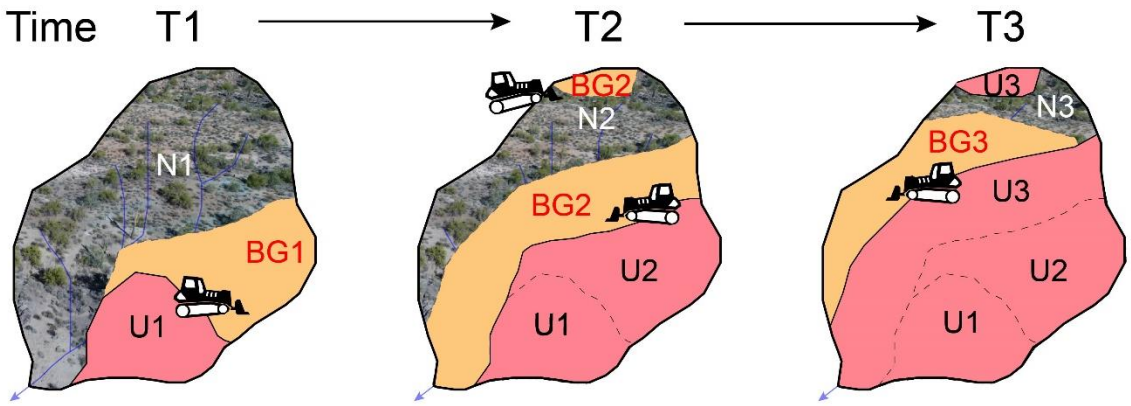


| Time Period | Length of Time Period | Surface Condition | Landuse Change Index |
|---|---|---|---|
| T1→T2 | T2 - T1 = L1 | Exposed bare ground (BG1)<br>Sealed surface (imperviousness) | Annual urban growth: N1 ∩ U2 / L1<br>Annual imperviousness:<br>(U1 + (U2 - U1)) / L1 |
| T2→T3 | T3 - T2 = L2 | Exposed bare ground (BG2)<br>Sealed surface (imperviousness) | Annual urban growth: N2 ∩ U3 / L2<br>Annual imperviousness:<br>(U2 + (U3 - U2)) / L2 |

**Figure 4.4.** Conceptual model to quantify land use-related parameters using GIS. The dashed line is the imaginary line that does not exist on the land use/land cover classification map, which is to show the exposed bare ground. The exposed bare ground during the time period from T1 to T2 (BG1) can be calculated by the intersection of natural land cover in T1 and urban land cover in T2. The imperviousness for the time period from T1 to T2 can be quantified by urban land cover in T2 (U2). The annual urban growth and imperviousness was calculated from dividing by the length of time period. See method section for details.

**Table 4.3.** Data from 18 stock pond catchments (Jeong and Dorn, 2019) used to make the regression equation

| ID | River/Catchment Name | MP | MP length (y) | Lat (°) | Lon (°) | A ($mi^2$) | A ($km^2$) | SDR (%) | Anual urban growth (km2) | Annual Imperviousness (km2) | SSV (acre-feet/$mi^2$/yr) | SSV ($m^3/km^2/yr$) | 1SD error of SSV | Eroded volume (m3/km2/yr) | 1SD error of Eroded volume | Data for EV-AUG regression? | Data for EV-AI regression? |
|---|---|---|---|---|---|---|---|---|---|---|---|---|---|---|---|---|---|
| 1 | Cigar | 1990-2004 | 15 | 33.685117 | -112.534267 | 1.00 | 2.60 | 60.83 | 0.015 | 0.015 | 0.14 | 66.54 | 5.81 | 109.39 | 9.56 | Yes | Yes |
| 2 | Cigar | 2005-2009 | 5 | 33.685117 | -112.534267 | 1.00 | 2.60 | 60.83 | 0.061 | 0.283 | 0.16 | 75.82 | 6.35 | 124.65 | 10.44 | Yes | Yes |
| 3 | Saguaro | 2005-2009 | 5 | 33.800925 | -112.204050 | 0.54 | 1.40 | 64.79 | 0.005 | 0.005 | 0.20 | 95.29 | 6.64 | 147.06 | 10.25 | Yes | Yes |
| 4 | Cline | 1989-1995 | 7 | 33.853465 | -112.149325 | 0.58 | 1.50 | 64.33 | 0.007 | 0.023 | 0.07 | 33.68 | 3.72 | 52.35 | 5.79 | Yes | Yes |
| 5 | Cline | 1996-2003 | 8 | 33.853465 | -112.149325 | 0.58 | 1.50 | 64.33 | 0.039 | 0.115 | 0.16 | 75.91 | 4.64 | 118.00 | 7.21 | Yes | Yes |
| 6 | Cline | 2003-2004 | 2 | 33.853465 | -112.149325 | 0.58 | 1.50 | 64.33 | 0.061 | 0.383 | 0.22 | 102.74 | 11.10 | 159.70 | 17.25 | Yes | Yes |
| 7 | Anthem 2 | 2002 | 1 | 33.850572 | -112.101617 | 0.22 | 0.58 | 71.15 | 0.074 | 0.222 | 0.36 | 172.76 | 16.53 | 242.79 | 23.23 | Yes | Yes |
| 8 | Bronco | 1999-2003 | 5 | 33.774765 | -112.117174 | 0.17 | 0.45 | 73.16 | 0.003 | 0.003 | 0.25 | 117.43 | 22.23 | 160.52 | 30.38 | Yes | Yes |
| 9 | Circle | 2010-2013 | 4 | 33.767891 | -112.069517 | 0.23 | 0.60 | 70.89 | 0.005 | 0.005 | 0.17 | 82.72 | 18.73 | 116.68 | 26.41 | Yes | Yes |
| 10 | Charlie | 1989-2004 | 16 | 33.773722 | -111.949346 | 0.35 | 0.91 | 67.79 | 0.032 | 0.042 | 0.35 | 164.52 | 25.80 | 242.68 | 38.06 | Yes | Yes |
| 11 | Cave Creek | 2000-2003 | 4 | 33.821477 | -111.860042 | 0.07 | 0.19 | 80.62 | 0.003 | 0.003 | 0.19 | 91.75 | 8.37 | 113.81 | 10.38 | Yes | Yes |
| 12 | Buckhorn | 1989-1999 | 11 | 33.771593 | -111.726559 | 1.70 | 4.40 | 57.73 | 0.027 | 0.000 | 0.16 | 76.06 | 2.31 | 131.75 | 4.00 | Yes | Yes |
| 13 | Buckhorn | 2000-2002 | 3 | 33.771593 | -111.726559 | 1.70 | 4.40 | 57.73 | 0.073 | 0.052 | 0.23 | 108.78 | 4.91 | 188.42 | 8.50 | Yes | Yes |
| 14 | The Rocks | 1989-1996 | 8 | 33.735184 | -111.843395 | 0.91 | 2.36 | 61.42 | 0.039 | 0.042 | 0.27 | 128.61 | 13.22 | 209.38 | 21.53 | Yes | Yes |
| 15 | 128th St | 2001-2008 | 8 | 33.719610 | -111.805910 | 0.33 | 0.85 | 68.28 | 0.000 | 0.000 | 0.22 | 104.99 | 13.63 | 153.77 | 19.96 | Yes | Yes |
| 16 | AsherHills | 1989-2001 | 13 | 33.731003 | -111.703998 | 0.81 | 2.10 | 62.15 | 0.004 | 0.004 | 0.20 | 94.53 | 18.09 | 152.09 | 29.10 | Yes | Yes |
| 17 | AsherHills | 2002-2007 | 6 | 33.731003 | -111.703998 | 0.81 | 2.10 | 62.15 | 0.047 | 0.119 | 0.26 | 123.67 | 4.60 | 198.97 | 7.40 | Yes | Yes |
| 18 | Gold Cyn | 1989-2009 | 21 | 33.367485 | -111.515636 | 1.97 | 5.10 | 56.91 | 0.013 | 0.013 | 0.12 | 55.65 | 11.63 | 97.80 | 20.43 | Yes | Yes |
| 19 | Peralta | 2001-2005 | 5 | 33.334978 | -111.429506 | 0.30 | 0.78 | 68.88 | 0.016 | 0.016 | 0.15 | 69.76 | 5.13 | 101.28 | 7.44 | Yes | Yes |
| 20 | Peralta | 2006-2009 | 4 | 33.334978 | -111.429506 | 0.30 | 0.78 | 68.88 | 0.000 | 0.079 | 0.02 | 8.23 | 2.59 | 11.95 | 3.77 | No | Yes |

**Table 4.4.** Prediction of sediment yield by model 2 for each time period. Note: T1 (1955-1975), T2 (1975-1985), T3 (1975-1995), T4 (1985-1990), T5 (1990-1995), T6 (1995-2000), T7 (2000-2005), T8 (2005-2010), n.a.: not available. n.g.: no growth. The unit of annual urban growth (AGU) is $mi^2\ yr^{-1}$ and SSV is ac-ft $mi^{-2}\ yr^{-1}$.

| ID | Dam Name | Ad ($mile^2$) | SDR (%) | Designed SSV | Dam completed (yr) | AUG in T1 | SSV in T1 | AUG in T2 | SSV in T2 | AUG in T3 | SSV in T3 | AUG in T4 | SSV in T4 | AUG in T5 | SSV in T5 | AUG in T6 | SSV in T6 | AUG in T7 | SSV in T7 | AUG in T8 | SSV in T8 | ΣLx | Predicted SSV |
|---|---|---|---|---|---|---|---|---|---|---|---|---|---|---|---|---|---|---|---|---|---|---|---|
| 1 | Harquahala FRS | 102.30 | 38.8 | | 1991 | n.a. | n.a. | n.a. | n.a. | n.a. | n.a. | n.a. | n.a. | n.a. | n.a. | n.a. | n.a. | n.a. | n.a. | n.a. | n.a. | n.a. | n.a. |
| 2 | Saddleback FRS | 29.60 | 44.0 | 0.409 | 1982 | n.a. | n.a. | n.a. | n.a. | n.a. | n.a. | n.a. | n.a. | n.a. | n.a. | n.a. | n.a. | n.a. | n.a. | n.a. | n.a. | n.a. | n.a. |
| 3 | Casandro Dam | 1.20 | 59.8 | | 1996 | 0.002 | 0.158 | n.a. | n.a. | 0.006 | 0.170 | n.a. | n.a. | n.a. | n.a. | n.a. | n.a. | n.a. | n.a. | n.a. | n.a. | 40 | 0.164 |
| 4 | Sunset FRS | 0.63 | 63.8 | | 1976 | 0.003 | 0.172 | n.a. | n.a. | 0.027 | 0.259 | n.a. | n.a. | n.a. | n.a. | n.a. | n.a. | n.a. | n.a. | n.a. | n.a. | 40 | 0.216 |
| 5 | Sunnycove FRS | 1.39 | 58.9 | | 1976 | 0.003 | 0.157 | n.a. | n.a. | 0.046 | 0.305 | n.a. | n.a. | n.a. | n.a. | n.a. | n.a. | n.a. | n.a. | n.a. | n.a. | 40 | 0.231 |
| 6 | Buckeye FRS #1 | 76.60 | 40.0 | | 1975 | 0.207 | 0.583 | 0.000 | 0.100 | n.a. | n.a. | 0.055 | 0.228 | 0.005 | 0.111 | 0.002 | 0.104 | 0.112 | 0.362 | 0.251 | 0.685 | 55 | 0.366 |
| 7 | Buckeye FRS #2 | 5.70 | 51.4 | | 1975 | n.g. | n.a. | n.g. | n.a. | n.a. | n.a. | n.g. | n.a. | n.g. | n.a. | n.g. | n.a. | 0.0 | 0.132 | 0.019 | 0.186 | 10 | 0.159 |
| 8 | Buckeye FRS #3 | 8.70 | 49.4 | | 1975 | n.g. | n.a. | n.g. | n.a. | n.a. | n.a. | n.g. | n.a. | n.g. | n.a. | n.g. | n.a. | 0.0 | 0.126 | 0.000 | 0.124 | 10 | 0.125 |
| 9 | White Tanks FRS #4 | 18.60 | 46.0 | | 1954 | n.g. | n.a. | 0.058 | 0.271 | n.a. | n.a. | 0.028 | 0.189 | 0.008 | 0.136 | 0.013 | 0.150 | 0.196 | 0.642 | 0.205 | 0.665 | 35 | 0.332 |
| 10 | White Tanks FRS #3 | 20.50 | 45.6 | | 1954 | 0.023 | 0.176 | n.g. | n.a. | n.a. | n.a. | n.g. | n.a. | n.g. | n.a. | 0.0 | 0.120 | 0.002 | 0.120 | 0.020 | 0.166 | 35 | 0.159 |
| 11 | McMicken Dam | 242.20 | 35.1 | | 1956 | 0.113 | 0.319 | 0.243 | 0.584 | n.a. | n.a. | 0.286 | 0.673 | 0.381 | 0.867 | 0.351 | 0.805 | 1.224 | 2.593 | 1.499 | 3.158 | 55 | 0.958 |
| 12 | New River Dam | 171.00 | 36.6 | 0.288 | 1985 | 0.031 | 0.158 | 0.029 | 0.153 | n.a. | n.a. | 0.014 | 0.122 | 0.039 | 0.176 | 0.300 | 0.732 | 0.897 | 2.007 | 0.473 | 1.102 | 55 | 0.461 |
| 13 | Adobe Dam | 87.30 | 39.4 | 0.309 | 1982 | 0.004 | 0.109 | 0.030 | 0.167 | n.a. | n.a. | 0.041 | 0.192 | 0.086 | 0.297 | 0.247 | 0.667 | 1.151 | 2.748 | 0.742 | 1.807 | 55 | 0.589 |
| 14 | Cave Buttes Dam | 195.70 | 36.0 | 0.300 | 1980 | 0.137 | 0.378 | 0.221 | 0.554 | n.a. | n.a. | 0.374 | 0.875 | 0.627 | 1.407 | 1.154 | 2.516 | 1.308 | 2.840 | 1.627 | 3.510 | 55 | 1.252 |
| 15 | Dreamy Draw Dam | 1.35 | 59.1 | 0.267 | 1974 | 0.005 | 0.164 | 0.022 | 0.225 | n.a. | n.a. | 0.006 | 0.169 | 0.002 | 0.155 | 0.005 | 0.164 | 0.021 | 0.220 | 0.011 | 0.185 | 55 | 0.182 |
| 16 | Guadalupe FRS | 1.74 | 57.6 | | 1975 | 0.001 | 0.146 | 0.009 | 0.173 | n.a. | n.a. | 0.005 | 0.160 | 0.013 | 0.188 | 0.001 | 0.148 | 0.002 | 0.150 | 0.002 | 0.152 | 55 | 0.157 |
| 17 | Spook Hill FRS | 13.60 | 47.4 | | 1980 | 0.024 | 0.184 | 0.010 | 0.147 | n.a. | n.a. | 0.024 | 0.186 | 0.056 | 0.274 | 0.186 | 0.634 | 0.363 | 1.121 | 0.235 | 0.769 | 55 | 0.365 |
| 18 | Signal Butte FRS | 16.40 | 46.5 | | 1987 | n.a. | n.a. | n.a. | n.a. | n.a. | n.a. | 0.004 | 0.127 | 0.007 | 0.135 | 0.017 | 0.162 | 0.009 | 0.142 | 0.004 | 0.126 | 25 | 0.139 |
| 19 | Apache Junction FRS | 5.60 | 51.5 | | 1988 | n.a. | n.a. | n.a. | n.a. | n.a. | n.a. | 0.004 | 0.140 | 0.006 | 0.145 | 0.031 | 0.222 | 0.016 | 0.177 | 0.004 | 0.141 | 25 | 0.165 |
| 20 | Powerline FRS | 46.20 | 42.1 | 0.103 | 1967 | n.a. | n.a. | n.a. | n.a. | n.a. | n.a. | n.a. | n.a. | n.a. | n.a. | n.a. | n.a. | n.a. | n.a. | n.a. | n.a. | n.a. | n.a. |
| 21 | Vineyard Rd FRS | 53.70 | 41.5 | | 1968 | n.a. | n.a. | n.a. | n.a. | n.a. | n.a. | n.a. | n.a. | n.a. | n.a. | n.a. | n.a. | n.a. | n.a. | n.a. | n.a. | n.a. | n.a. |
| 22 | Rittenhouse FRS | 47.10 | 42.0 | | 1969 | n.a. | n.a. | n.a. | n.a. | n.a. | n.a. | n.a. | n.a. | n.a. | n.a. | n.a. | n.a. | n.a. | n.a. | n.a. | n.a. | n.a. | n.a. |

*SEDIMENT DELIVERY RATIO*

As described in the development of Model 1, a negative relation exists between SSV and $A_D$. The regression model based on sedimentation volume-drainage area, however, does not consider the negative relation between SSV and $A_D$. Thus, unreasonably high SSV could be estimated when the regression equation is used for extrapolation, because drainage areas of FCS are much bigger than stock ponds drainage areas (Table 4.1 and Table 4.3). Therefore, the concept of sediment delivery ratio (SDR) related to $A_D$ is adopted for Model 2. The latest FCDMC Hydraulics manual (FCDMC 2015a) provides an equation to calculate SDR based on the SDR curve as a function of drainage area (USDA 1972) with modification using data from southwest semiarid regions. FCDMC shifted the original USDA curve using data from Walnut Gulch watersheds near Tucson, AZ that the sediment delivery ratio is 0.41 for a drainage area of 57.53 square miles (Lane *et al* 2000). The SDR equation provided by FCDMC is (FCDMC 2015a):

$$SDR = -14.08(\log_{10}A_D) + 2.44(\log_{10}A_D)^2 - 0.45(\log_{10}A_D)^3 + 60.85 \qquad (4)$$

where the unit of SDR is percent and $A_D$ is mile$^2$. The regression equation is applicable only for $A_D$ larger than 0.04 and smaller than 500 mile$^2$. Stock pond SSV were then converted to eroded volume (EV) from the watersheds, using this equation:

$$EV = SSV / (SDR*0.01) \qquad (5)$$

Then, for the larger drainage basins of FCS, the SSV was calculated based on the predicted EV based on regression equation from stock ponds data, using this equation:

$$SSV = EV*SDR*0.01 \qquad (6)$$

The following subsections describe the regression model between EV ($m^3$ $km^{-2}$ $yr^{-1}$) and annual urban growth, as well as between EV and annual imperviousness (Figure 4.4).

*PREDICTION OF URBAN ACCLERATION OF SEDIMENT YIELD*

Based on Wolman's (1967) model, I hypothesized that the two LULCC parameters annual urban growth and imperviousness may be related to EV (Figure 4.5). The p-value for annual urban growth (0.017) is lower than the alpha level of 0.05 and shows statistical significance (Figure 4.5a), but the p-value for annual imperviousness (0.293) is greater than 0.05, indicating that it is not statistically significant (Figure 4.5b). Unlike Wolman's (1967) model prediction, there is no observed inverse relation between EV and annual imperiousness, which may likely because of the increased runoff in urbanized watersheds and high sediment transport efficiency of urban drainage network (Russell *et al* 2017). Therefore, only the regression between EV and annual urban growth was used to model prediction of SSV for FCS (figure 4.5a). The relation between EV ($m^3$ $km^{-2}$ $yr^{-1}$) and annual urban growth (AUG) ($km^2$) for the 18 catchments experiencing urbanization in the Sonoran Desert and PMR is (figure 4.5a and Table 4.3):

$$EV = 1074.1*AUG + 118.94 \quad (7)$$

with an $R^2$ value of 0.29. Then, the SSV was calculated by eq. 6 for each available time periods. The SSV predicted by regression model based on EV-AUG relation (eq. 7) (Table 4.3) were normalized by the length of time periods:

$$\text{Predicted SSV} = [SSV(T1)*L1 + SSV(T2)*L2 + \ldots + SSV(Tx)*Lx] / (L1 + L2 + \ldots + Lx) \quad (8)$$

The storage capacity loss and life expectancies of FCS were estimated using eq. (2) and (3) (Table 4.3). The predicted SSV for each time periods (SSV(Tx)) are presented in Table 4.4.

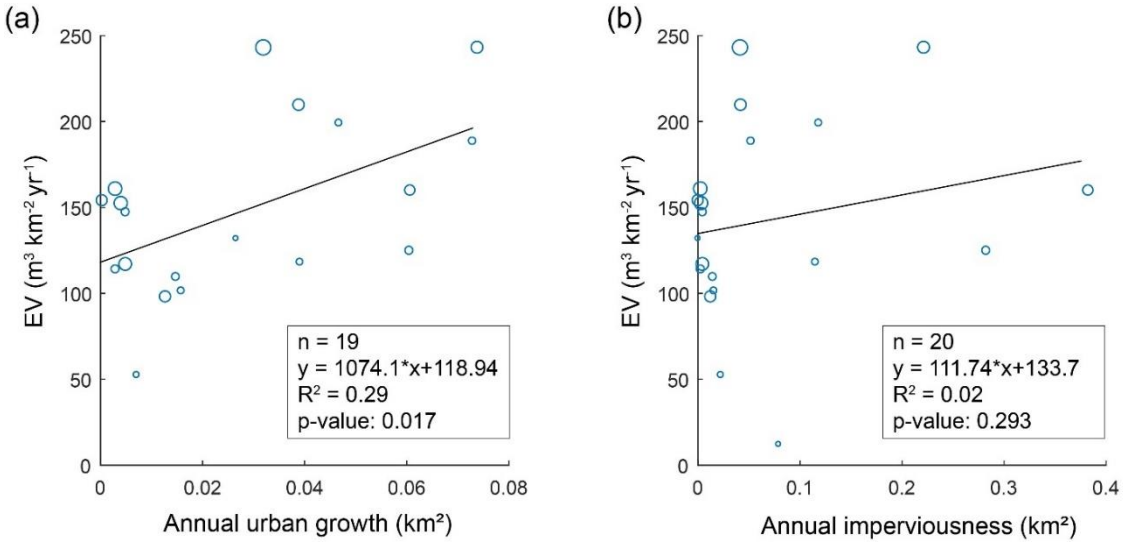


**Figure 4.5.** The scatterplot with 1σ standard error ellipse and linear regression between a) eroded sedimentation volume (EV) and annual urban growth (AUG); b) EV and annual imperviousness (AI). Table 4.3 provides data used to construct this figure.

## RESULTS

### *SEDIMENT YIELD PREDICTION FROM THE TWO MODELS*

Overall, the result from model 2 shows a significant increase in SSV where sites experienced urbanization (Figure 4.1 and Table 4.2). The urbanization impact on sediment yields is clearly shown where FCS ID 6, 9, 11, 12, 13, 14 and 17 that experienced urbanization had much higher SSV (Figure 4.1). In contrast, FCS ID 3, 4, 5,

7, 8, 15, 16, 18 and 19 did not experience urbanization (Figure 4.1), and there were only minor differences in predictions by model 1 and model 2 (Figure 4.6).

Based on model 2 predictions, Cave Buttes Dam (FCS ID14) has the highest SSV, followed by McMicken Dam (FCS ID11) that experienced considerable urban growth (Figure 4.1 and Table 4.4). In contrast, the model 1 prediction shows the highest SSV from Sunset FRS (FCS ID4) followed by Casandro Dam (FCIS ID3) that both have small drainage areas (Table 4.2).

Eleven FCS (FCS ID 4-6, 9-14, 17, 19) had larger predicted SSV from model 2 than model 1 by up to 11.3x (mean: 3.8x), but six FCS (FCS ID 3, 7-8, 15-16, 18) had larger predicted SSV from model 1 than model 2 by up to 1.2x (mean: 1.1x) (Table 4.2). These findings reveals that urbanization's impact on sediment yield is far more dominant than drainage area.

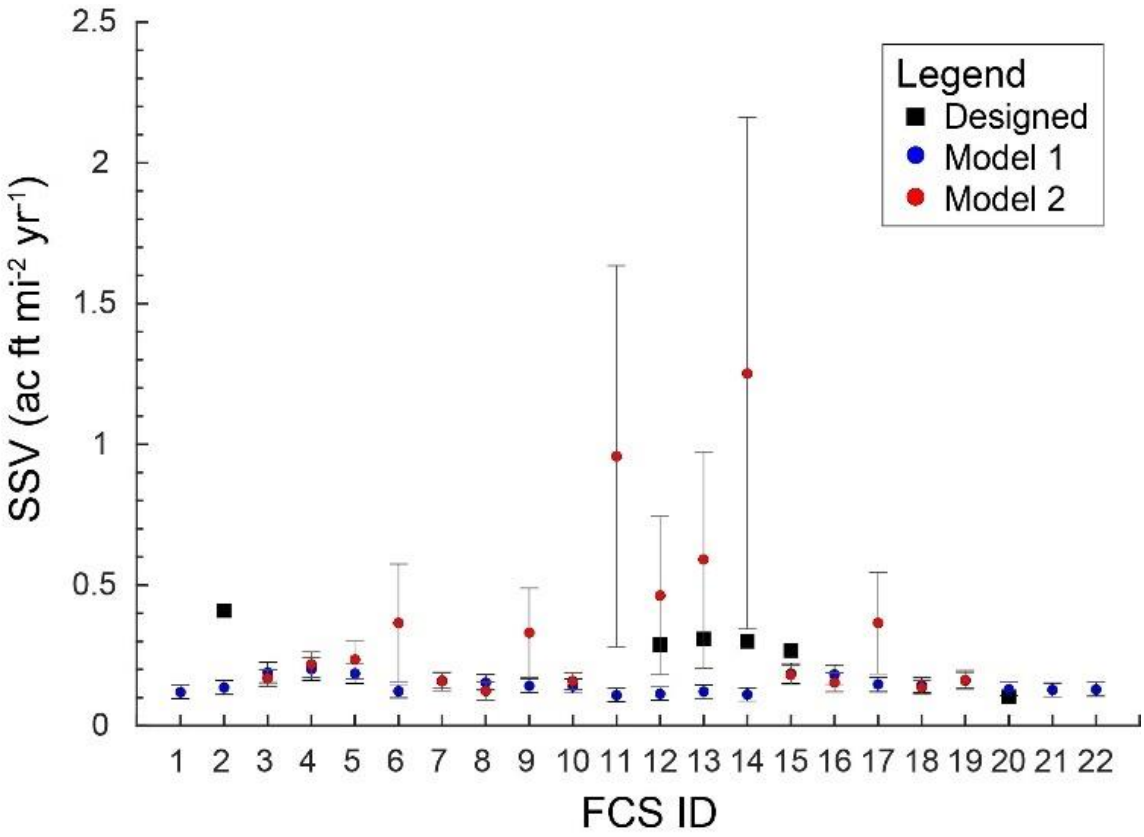


**Figure 4.6.** Comparison between the designed SSV when FCS built and predicted SSV based on the two regression models with the 95 percent confidential interval. Table 4.2 provides data used to construct this figure.

The sustainability of FCS depend on storage loss (SL) over a 100 year period (100yr-SL) and ELF using eq. (2) and eq. (3). Figure 4.2 and table 4.2 present these data. The highest 100yr-storage loss is predicted by model 2 for McMicken Dam (FCS ID11), followed by Cave Buttes Dam (FCS ID14) (Figure 4.7). The ELF of the two dams are 161 ± 114 and 398 ± 289 years, respectively. Model 1 predicted the highest 100yr-SL from White Tanks FRS #4 (FCS ID9), followed by Casandro Dam (FCS ID3) and the ELF of the two dams are 960 ± 17 and 1013 ± 20 years, respectively (Figure 4.7). Projects for sustainable sediment managements were planned and accomplished where sedimentation issues had been identified based on accumulated data. For example, for the

Rittenhouse Basin, the first phase of excavation was planned to increase the capacity of the East Maricopa Floodway along with a regular maintenance plan to mitigate the effects of erosion and sedimentation. This resulted in the McMicken Dam Fissure Risk Zone Remediation Project (FCDMC 2006).

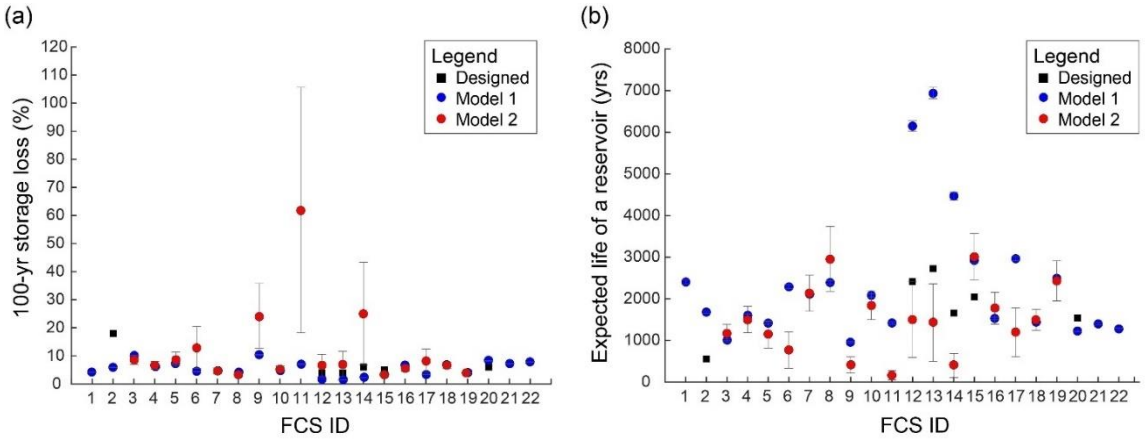


**Figure 4.7.** (a) Comparison between the designed 100-yr storage loss when FCS built and predicted 100-yrs storage loss based on the two regression models with the 95 percent confidential interval. (b) Comparison between the designed expected life when FCS built and predicted expected life based on the two regression models with the 95 percent confidential interval. Table 4.2 provides data used to construct this figure.

The predicted SSV from the two models identified considerable spatial variation in the sustainability of FCS in the PMR (Figure 4.8). The most vulnerable FCS were once far from the urban boundary (Figure 4.8a, c), but urban growth has resulted greater vulnerability of FCS in drainage areas experiencing this growth (Figure 4.8b, d). In contrast, Dreamy Draw Dam (FCS ID 15) and the Guadalupe FCS (FCS ID 16) are slightly overbuilt (Figure 4.6). This is because of a combination of two factors: they are in locations where urban growth was decades ago; and they are in locations where much of the watersheds are now natural preserves that are free from the urban acceleration of erosion.

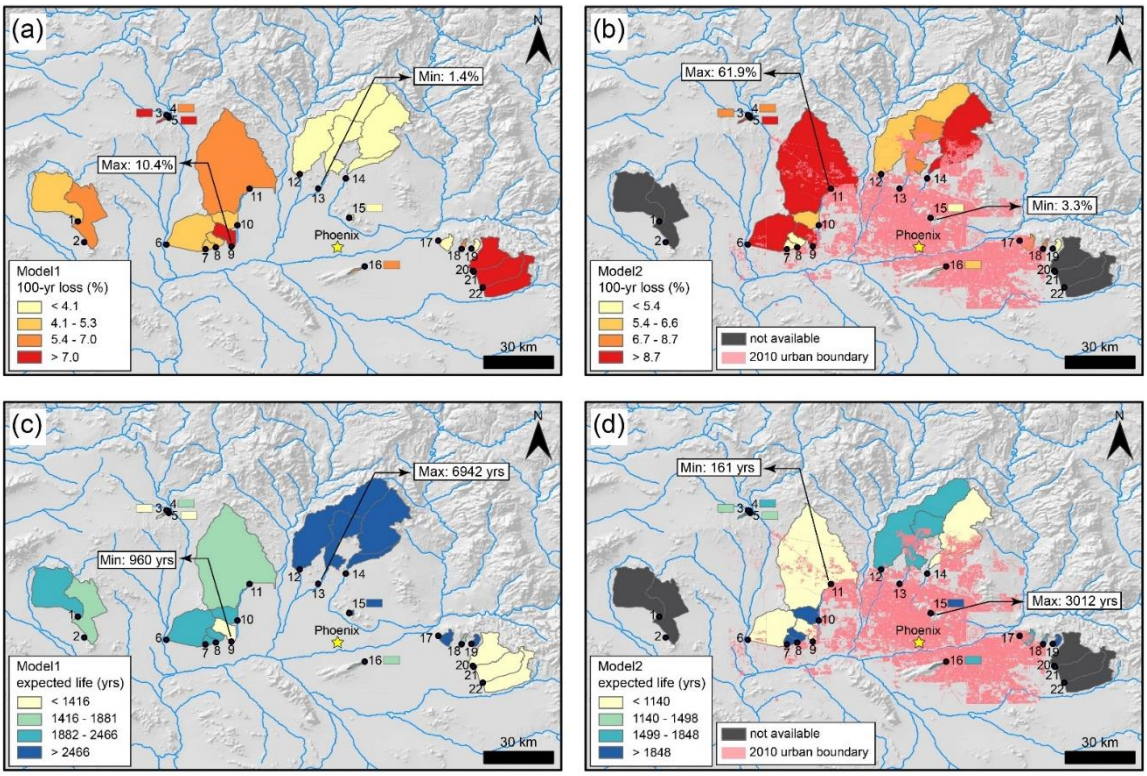


**Figure 4.8.** (a) Distribution of 100-year loss of FCS storage predicted by model 1 in the PMR. (b) Distribution of 100-year loss of FCS storage predicted by model 2 in the PMR. (c) Distribution of expected life of FCS predicted by model 1 in the PMR. (d) Distribution of expected life of FCS predicted by model 1 in the PMR. Table 4.2 provides data used to construct this figure.

*COMPARISON WITH DESIGNED SEDIMENT YIELD*

The area-specific sedimentation volume (SSV) used when the FCS were originally designed ('designed SSV') is higher than predicted by model 1 for Saddleback FRS (FCS ID 2), but lower for powerline FRS (FCS ID 20). The predicted SSV of Dreamy Dram Dam (FCS ID 15) from both model 1 and model 2 is lower than designed SSV. The designed SSV for FCS ID 12, 13, 14 was higher than predicted SSV from model 1, but lower than predicted SSV from model 2 (Figure 4.6).

The designed SSV underestimated area-specific sedimentation volume up to 4.2x for three FCS (FCS ID 12-14) when using model 2 and overestimated SSV up to 3.0x for five FCS (FCS ID 2, 12-15) when using model 1. The general tendency of underestimated designed SSV compared to model 2 prediction and overestimated designed SSV compared to model 1 prediction may indicate that storage capacity might have been appropriate for the time of FCS completion. However, urban sprawl condition has been an ongoing process for the planned life of the structures (50 years for FCS built by SCS and 100 years for FCS built by USACE; Table 4.5).

The designed storage capacity for sedimentation under conditions of a 'future with urban sprawl" maybe too small; this requires efforts to reduce sediment inflow to the reservoir or remove sedimentation from behind FCS such as by dredging. Consider the designed SSV (0.300 ac-ft $mi^{-2}$ $yr^{-1}$) of Cave Buttes Dam (FCS ID14) estimated from USACE (1982) when the dam was built in 1980 (Table 4.1). The original design SSV is only a bit lower than the model 2 SSV (0.378 ac-ft $mi^{-2}$ $yr^{-1}$) during the T1 (1955-1975) period of an 'existing condition' (Table 4.4). Based on model 1 SSV (0.111 ac-ft $mi^{-2}$ $yr^{-1}$) its storage capacity for sedimentation was over-built in a 'future without urban sprawl condition', but its SSV increased significantly after the same was constructed (SSV in T2, T4-T8 in 'future with urban sprawl condition' Table 4.4, Figure 4.1 and 4.2). The urban acceleration of erosion led to a 4.2x higher SSV than designed SSV (Table 4.2), and this reduces the expected design life for sediment storage from 100 years to 23 years.

Other examples come from an analysis of the storage capacity for sedimentation behind New River Dam (FCS ID12), Adobe Dam (FCS ID13) and Dreamy Draw Dam

(FCS ID15). These structures were over-built at the time of FCS completion based on the model 2 (Table 4.4), but the SSV of New River Dam and Adobe Dam increased significantly due to urbanization starting in 1995 (Table 4.4), leading to the insufficient storage for sedimentation (Table 4.2). In contrast, Dreamy Draw Dam had sufficient storage for sedimentation, even after urbanization (Table 4.2 and Table 4.4).

Very little published research exists on the importance of rapid urbanization for sediment projection in a desert city. However, the identification of earth fissures and land subsidence around three Phoenix-area flood control structures led to the need to re-estimate sedimentation rates during the period of rapid urbanization. Powerline, Vineyard and Rittenhouse FRS (FCS ID 20, 21, 22) were classified as high hazard potential structures by Arizona Department of Water Resources (ADWR) due to the proximity of earth fissures and land subsidence (EMNRCD and FCDMC 2013). Thus, SSV was re-estimated by consulting engineers in 2008 and FCDMC in 2010, 2014 and 2016 (Maricopa County 2010). The new SSV was estimated as 0.600 ac-ft $mi^{-2}$ $yr^{-1}$ (FCS ID 20), 0.611 ac-ft $mi^{-2}$ $yr^{-1}$ (FCS ID21), and 0.597 ac-ft $mi^{-2}$ $yr^{-1}$ (FCS ID22) for the Powerline, Vineyard and Rittenhouse structures, respectively (JE Fuller 2008). Then, a 2010 study (FCDMC, 2010a, 2010b, 2010c) estimated SSV for these three respective structures at 0.238 ac-ft $mi^{-2}$ $yr^{-1}$ (FCS ID20), 0.272 ac-ft $mi^{-2}$ $yr^{-1}$ (FCS ID21), and 0.151 ac-ft $mi^{-2}$ $yr^{-1}$ (FCS ID22). Both JE Fuller (2008) and the FCDMC (2010) estimate higher SSV than designed. These independent studies provide broad confirmation of the importance of urbanization on increasing sediment yields in a rapidly urbanizing desert city.

**Table 4.5.** Designed life of FCS in PMR and FCS capacity loss for designed life

| ID | Dam Name | $A_D$ (km²) | $A_D$ (mile²) | Built by | Designed SSV (ac-ft mi$^{-2}$ yr$^{-1}$) | Designed sedimentation life (yrs) | Total storage capacity (acre-feet)[a] | Designed storage capacity for sedimentation (acre-feet) | Capacity loss for designed life (%) | **Model1: without urban sprawl condition** Predicted SSV (ac-ft mi$^{-2}$ yr$^{-1}$) | Capacity loss for designed life (%) | **Model2: with urban sprawl condition** Predicted SSV (ac-ft mi$^{-2}$ yr$^{-1}$) | Capacity loss for designed life (%) |
|---|---|---|---|---|---|---|---|---|---|---|---|---|---|
| 2 | Saddleback FRS | 76.55 | 29.60 | SCS | 0.409 | 50 | 4247 | 120 | 3 | 0.136 | 3 | n.a. | n.a. |
| 12 | New River Dam | 442.21 | 171.00 | USACE | 0.288 | 100 | 118626 | 4925 | 4 | 0.113 | 2 | 0.461 | 7 |
| 13 | Adobe Dam | 225.76 | 87.30 | USACE | 0.309 | 100 | 18350 | 2700 | 15 | 0.121 | 1 | 0.589 | 7 |
| 14 | Cave Buttes Dam | 506.08 | 195.70 | USACE | 0.300 | 100 | 46600 | 5700 | 12 | 0.111 | 2 | 1.252 | 25 |
| 15 | Dreamy Draw Dam | 3.49 | 1.35 | USACE | 0.267 | 100 | 317 | 36 | 11 | 0.187 | 3 | 0.182 | 3 |
| 20 | Powerline FRS | 119.47 | 46.20 | SCS | 0.103 | 50 | 7328 | 350 | 5 | 0.129 | 4 | n.a. | n.a. |

[a] It is based on the total storage capacity when the FCS was designed.

# DISCUSSION

## *THE DESIRED OUTCOME OF RELIABLE SEDIMENT YIELD FORCASTING IN RAPDILY URBANIZING DESERT CITIES*

Forecasting the reliable future sediment yield is an essential part of designing storage capacity for sedimentation of FCS (Verstraeten *et al* 2003, Minear and Kondolf 2009, Vanmaercke *et al* 2011, Haregeweyn *et al* 2012, Wisser *et al* 2013, Vanmaercke *et al* 2015). Rather than measuring sedimentation volume of reservoirs by bathymetry surveying (e.g. Rakhmatullaev *et al* 2011), or back-estimated sediment curve from reservoir sedimentation survey data taken at several points in time and water inflow data (Tebbi *et al* 2012), many researchers use models to predict the reliable sediment yield in rapidly urbanizing desert cities due to the lack of existing sediment yield data and benefits of minimizing time and costs and applicability for designing a new flood control structure (Wasson 1994, Meamarian *et al* 2003, Griffiths *et al* 2006, Vanmaercke *et al* 2011, Fathizad *et al* 2014, Abdullah *et al* 2017).

There are a variety of models used to estimate soil erosion that fills in flood control structures. The basic conclusion of this study is that none of the existing models truly or appropriately consider the effects of urbanization. The drainage area – sediment yield relationship is commonly employed (e.g. Wasson 1994, Griffiths *et al* 2006; Vanmaercke *et al* 2011) and does not factor land use changes. The Revised Universal Soil Loss Equation (RUSLE) (Renard *et al* 1997) is also often used to predict soil erosion (e.g. Abdullah *et al* 2017) and sediment yield (e.g. Fathizad *et al* 2014) using the sediment delivery ratio. However, the C factor in the RUSLE accounts for land use-land cover and management impacts on soil erosion, and the C-factor was based on empirical

data from North America and might be impractical in other regions where land cover conditions and cropping practices differ (Zhao *et al* 2017). Models are also are designed for the plot scale or, at most, small catchments (Boardman 2006, Syvitski and Millman 2007) that do not have the capability for sediment delivery through channels to FCS (Nearing *et al* 2005). A semi-quantitative model developed by the Pacific Southwest Inter-Agency Committee (PSIAC) (PSIAC 1968) uses a rating technique through field visits, complemented with data on surface geology, soils, climate, runoff, topography, ground cover, upland erosion, channel erosion and sediment transport and land use (e.g. Fathizad *et al* 2014; Abdullah *et al* 2017); however, acceleration of soil erosion and sediment yield was not included in the land use factor. A global empirical model, BQART developed by Syvitski and Milliman (2007), was also used to calculate long-term suspended sediment loads where the anthropogenic factor (Eh) is part of factor B in the BQART model. However, the BQART model was trained by 294 global river basins with $10^2$-$10^7$ $km^2$ drainage area. Importantly, the BQART model estimates human and urbanization impacts on sediment yield using an indirect method (population density and GNP per capita) rather than direct method such as urban growth rate proposed in this paper (Figure 4.4).

In summary, the previous methods to predict sediment yield have limitations that include: 1) considerable costs and time to measure local sediment yield data (e.g. bathymetric survey in reservoir, installation of gauging station); 2) drainage area scale issue (e.g. RUSLE, BQART); 3) urban acceleration of erosion is not considered (e.g. sediment yield-drainage area relation, PSIAC), or the relevant factor may not fit for different local setting (e.g. RUSLE), or it is predicted based on indirect variable such as

population density and GNP per capita (BQART). The prior models used to predict sediment yield in rapidly urbanizing desert cities, significantly, do not include a direct method to quantify urban growth and its impact on sediment yield, this despite evidence that urban growth is important factor leading to one to two orders of magnitude increases in sediment yield depending on prior land use (Russell *et al* 2017).

This research reveals that a sediment prediction without considering the urban sprawl condition led to a significant underestimation of sediment yield (Figure 4.6), resulting in reducing available storage for flood control (Figure 4.7 and 4.8). Sedimentation more rapid than planned handicaps flood control structures from fulfilling their most important purpose of flood risk reduction in rapidly urbanizing desert cities.

The results presented in this paper emphasizes that assessing urban growth and its impact on sediment yield is necessary for forecasting the reliable future sediment yield. Most urbanizing desert cities around the globe do not have local financial and technical resources to carry out the detailed empirical research presented in this study (The World Bank 2014). A cost-efficient and simple method to predict reliable future sediment yield is an important priority. The urban solution for forecasting reliable sediment yield in rapidly urbanizing desert cities would be using model 2 suggested in this paper because the model included a direct method to quantify urban growth and its impact on sediment yield. However, prior to employing model 2, the prior step is to predict future urban growth of desert cities using a variety of existing approaches (e.g. Al-Ahmadi *et al* 2009, Tayyebi *et al* 2014, Yagoub and Bizreh 2014, Alqurashi *et al* 2016). Then, with an informed understanding of predicted urban growth, model 2 will be able to suggest upper

bounds of sediment yield accelerated by geomorphic processes associated with desert urbanization. Model 2 would then provide appropriate output for designing sustainable flood control structures in rapidly urbanizing desert cities.

## CONCLUSION

Flood risk reductions are a crucial goal for rapidly urbanizing desert cities (RUDC) to become economically, socially, and environmentally more resilient. The hazard of flooding often causes extensive loss of life and property and even increases national poverty (UNSIDR 2010). An environmental justice issue in RUDC can occur where there is an inequitable distribution of risk associated with flooding. Within the cities, poorer inhabitants living in self-built informal housing on urban edge particularly are at risk (O'Hare and Rivas 2005), and the inhabitants can seldom afford to move to low-risk area with better housing conditions.

A growing need for flood control in RUDC has led to resilient urban planning efforts to build flood control structures (FCS) (Muller 2007, Djordjević *et al* 2011, Liao 2012), but there has been increased concern over FCS sustainability in RUDC mainly derived from sediment accumulation problem behind FCS that can reduce usable capacity even before reservoirs completely filled with sediment (Morris and Fan 1998). The sedimentation problem is closely linked to the land use–land cover change in urban systems because bare ground exposure associated with urban growth (Wolman 1967) has increased one to two order of soil erosion depending on prior land use on global basis (Russell *et al* 2017) and the eroded soils will be transported by water and eventually will

be stored in FCS. Therefore, forecasting reliable sediment yield under urban sprawl conditions is a desired outcome for RUDC's sustainability.

The new approach proposed in this paper uses sediment yield data from urban fringe of the Phoenix metropolitan region, southwest USA, that has been experiencing a wide range of land-use changes over a study period of two decades. During this period of empirical data gathering, urban growth rates were quantified using remote sensing and GIS. In the proposed approach, the relation between sediment yield and urban growth rate is easily applicable for predicting sediment yield under urban sprawl, but only for desert cities. The proposed model is cost-efficient and simple, so it will improve sustainable flood control structure construction. When combined with an analysis of urban growth futures, the proposed desired outcome would reduce RUDC vulnerability to flood risks, particularly where the cities do not have local financial and technical resources that result in backlogs in infrastructure construction (The World Bank 2014).

After implementation of the desired outcome, an eventual goal for RUDCs would be sustainable sediment management. Sustainable sediment management is broadly classified into three categories (Kondolf *et al* 2014): 1) sediment yield reduction; 2) sediment routing; and 3) sediment removal. The city of Taiz in Yemen exemplifies one approach to sustainable sediment management when it built 21 sedimentation traps upstream (The World Bank 2014), which was an initial step towards resilience. In Japan, for example, the oldest sediment bypass tunnel was installed in 1908 and has been successfully diverting coarse sediment. However, this technique involves a high fiscal cost in construction (Sumi *et al* 2004). Sediments may also be removed by dredging

which is a commonly used technique and the pollution-free sediments can be re-used for agriculture (Haregeweyn *et al* 2012); but digging up and transporting costs can be high (Randle *et al* 2017). Based on the fiscal reality of many rapidly urbanizing desert cities, perhaps the most feasible management approach would be a sediment yield reduction approach as implemented in the Phoenix metropolitan area and enforced by regulating construction permits to comply with the Arizona Pollutant Discharge Elimination System (AZPDES) stormwater permitting process for construction activities (FCDMC 2015c).

# CHAPTER 5

# SOIL EROSION ASSOCIATED WITH URBAN SPRAWL COMPARED TO NATURAL BACKGROUND RATES

(FOR SUBMISSION TO *NATURE GEOSCIENCE*)


## ABSTRACT

Urbanization processes are increasingly recognized as potential drivers of environmental change with the pace of influence tied to an increasingly urban world. We present here the first comparison of soil erosion from urbanization to natural background rates of erosion measured through cosmogenic $^{10}$Be catchment-wide denudation rates. Through exposure of bare ground from 1989 to 2013, urban sprawl accelerated erosion 1.3x to 15x above natural background rates of ~ 76 Mg km$^{-2}$ yr$^{-1}$ for the Phoenix metropolitan region, Sonoran Desert, USA. This acceleration likely represents a minimum potential impact because drought conditions occurred during the historic monitoring period. After statistical modeling natural soil erosion and urbanization effects, a spatial model reveals patterns of urban acceleration of soil erosion at the sprawling perimeter of the Phoenix region. We then contextualize our analysis of the erosive effects of a rapidly expanding desert city by presenting the first comparison of the urban acceleration of erosion above natural background rates for urban centers in different climatic regions.

## INTRODUCTION

Wolman (1967) presented a conceptual model of a sudden spike of soil erosion associated with exposure of bare ground from construction followed by impervious surface sealing (Wolman, 1967). Prior to urbanization's soil erosion spike, Wolman's model used as background land uses such as agriculture and deforestation, since the setting of the original paper was in the eastern USA. Since Wolman's proposed model, a great abundance of research confirmed the existence of the bare-ground spike (e.g. Hooke 1994; Douglas and Lawson, 2001; Russell et al., 2017). No prior research, however, has yet compared urbanization's impact on soil erosion to pre-human conditions. This research is the first attempt to compare the natural background rates of erosion, measured by catchment wide denudation rate technique (von Blanckenburg, 2006), to pre-urban land uses such as cattle grazing, and then to the impact of urban sprawl. The importance of the topic of soil erosion in urban settings rests in soil erosion's associated with a variety of environmental and infrastructure management issues (see Table 5.1).

**Table 5.1.** Environmental and infrastructural management issues in urban area associated with soil erosion and sedimentation

| **1. Environmental issues: soil as a major sink for toxic chemicals** | | |
|---|---|---|
| **Toxic chemicals** | **Environmental issues** | **References** |
| Lead | Human health | Weitzman et al. (1993); Mielke and Reagan (1998); Markus and McBratney (2001); McGrath et al. (2004); Zhuo et al. (2012) |
| | Environmental Justice | Kraft and Scheberle (1995); Lanphear et al. (1996); Clark et al. (2006); McClintock (2012); Zhuo et al. (2012) |
| Cadmium | Human health | Lagerwerff and Specht (1970); John (1973); Chaney et al. (1999); Li et al. (2006); Six and Smolders (2014) |
| Other heavy meatals | Human health | Lagerwerff and Specht (1970) |
| **2. Infrastructure management issues: infrastructure sustainability** | | |
| **Infrastructures** | **Management issues** | **References** |
| Reservoir | Reservoir storage capacity loss, dam failure and flood control | Mount (1995); Annandale (2006); Graf et al. (2010); Kondolf et al. (2014); Podolak and Doyle (2015) |
| Road | Roadside gully formation | Croke and Mockler (2001); Jungerius et al. (2002); Nyssen et al. (2002) |
| Culvert | Plugged culvert by sedimentation | Cafferata and Cafferata (2004); Gillespie et al. (2014) |

A fundamental difficulty in this prior research has been the reliance on human-disturbed land uses such as disturbed forests, accelerated burning of scrublands, grazing, and even isolated agriculture as a background condition preceding urbanization (Wolman, 1967). In contrast, catchment-wide denudation rates (CWDR) using cosmogenic isotopes provide watershed erosion rates over a long enough period that could truly represent natural conditions (von Blanckenburg, 2006). CWDR is not sensitive to anthropogenic impacts as long as soil is being removed only from a mixed

soil layer where cosmogenic nuclides concentration is uniform with depth (Brown et al., 1995; Granger et al., 1996). Hence, CWDR is increasingly used to provide 'pre-human' background rates over $10^3$ to $10^5$ years to compare with a variety of land uses (Gellis et al., 2004; Reusser et al., 2015). No prior research, however, has compared CWDR to understand urbanization's impact of soil erosion. Here, we use CWDR to first develop a model of natural background rates of erosion for the Phoenix metropolitan region (PMR), USA, and then use a two-decade long record of erosion at the sprawling edge of the PMR to construct a statistical model of the impact of urbanization on soil erosion.

Cities initiate and expand in all environmental settings (Seto et al., 2011), and urban sprawl in drylands is no exception (Masoumi et al., 2018; Iqurashi and Kumar, 2014; Wang et al., 2018), and the PMR is an icon of urban sprawl (Gober, 2005) (Figure 5.1), set geomorphologically on alluvial fan and pediment low-slope piedmont landforms (Jeong et al., 2018a), in the Sonoran Desert where only scarce data exist on CWDR (Seong et al., 2016b). At first glance, a desert city might be viewed as a potential outlier urban setting to quantify the urban acceleration of erosion above natural (UAEN) conditions, because its low angle piedmont arid setting is generally thought to generate minimal rates of erosion (Einsele and Hinderer, 1997). We look at the PMR differently, as a setting to provide information on the low end of a future range of UAE using CWDR, since understanding the lower end of UAE provides critical information in erosion mitigation efforts (Brown et al., 2017).

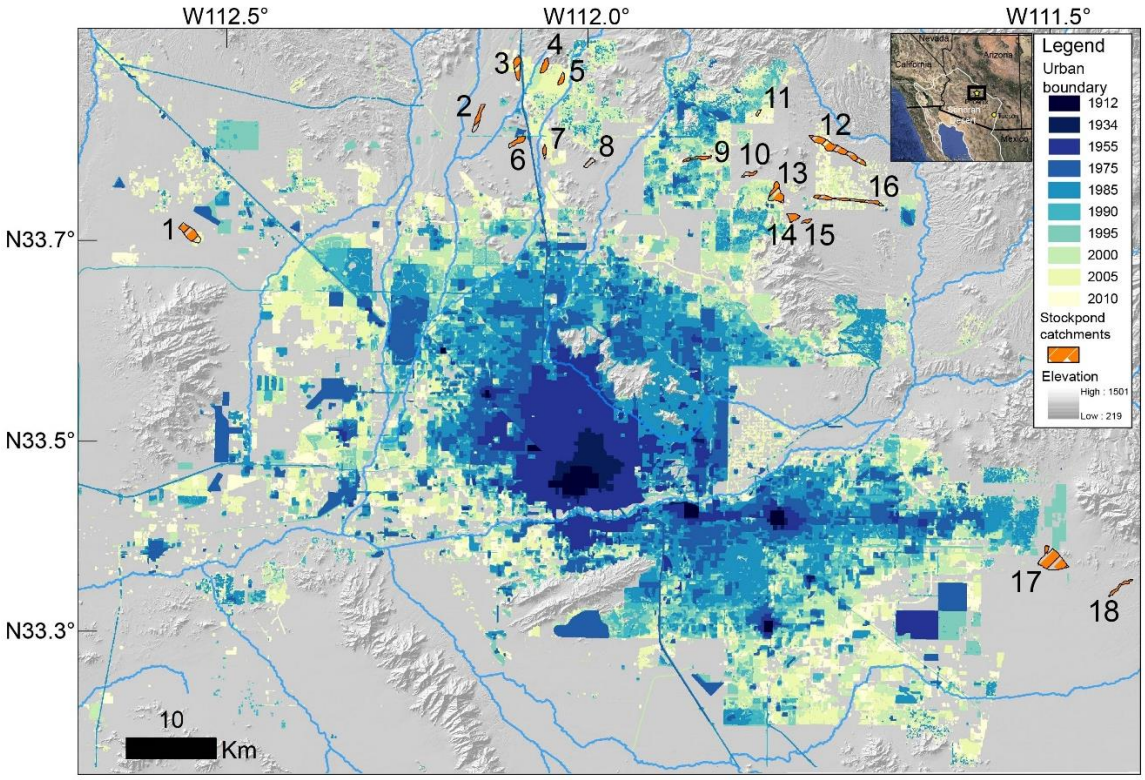


**Figure 5.1.** Urban sprawl of Phoenix metropolitan region (PMR). Map contextualizing the scattered locations of the stock pond catchments with urban sprawl of PMR from 1912 to 2010. The studied stock ponds are situated in the Sonoran Desert. Urban boundaries are extracted from land cover classification by Central Arizona–Phoenix Long-Term Ecological Research. The numbers refer to stock ponds identified in the Table 5.2.

CWDR scholarship reveals that climatic setting does not play a major factor on natural erosion rates (von Blanckenburg, 2006; Portenga and Bierman, 2011). Based on the global compilation of CWDR from cosmogenic nuclides, mean annual precipitation has no significant correlation (von Blanckenburg, 2006; Portenga and Bierman, 2011), and mean annual temperature has either is a very weak negative correlation (Portenga and Bierman, 2011) or no significant correlation (von Blanckenburng, 2006). Rather, slope and basin relief, mean elevation, and seismicity appear to be more important determinants

of background erosion rates (Portenga and Bierman, 2011). Among those, basin slope is the most significant predictor for CWDR and the remaining parameters are highly variable considering their regression power (Portenga and Bierman, 2011). Our rates of CWDR for the lower piedmont slopes (mean slope 0.4-6.5º) of the Sonoran Desert, for example, are similar to CWDR rates for similar geomorphic settings in other climatic settings (Reusser et al., 2015 – Appalachian Piedmont catchment mean slope 3-20º; Croke et al., 2015 – Great Barrier Reef catchment mean slope 1-7º; Schaller et al., 2016 - European fluvial catchments 2-13º). Thus, it is possible to estimate UAEN for other expanding urban regions using a model of CWDR and slope. Literature values for urban erosion rates and this model allows a rough approximation of UAEN to compare with our measurements and modeling in the PMR.

## METHODS

### *Presentation of sediment yield data.*

Sediment yield data from soil erosion are presented in different ways, sometimes to different audiences whether they are scientists or policy makers (Leopold, 1968; Zhang and Huang, 2015; Li et al., 2015; UNCCD, 2008). Since different approaches to the presentation of sediment yield data can generate confusion, the purpose of this section rests in clarifying our decision to present all sediment yield data in terms of area-specific sediment yield (Mg $km^{-2}$ $yr^{-1}$).

In general, sediment yield represents the amount of sediment that has been transported from one location to another measured as mass per time or volume per time

or mass per unit area per time. The exact definition, however, can vary from country to country, among governmental agencies, and among different researchers (see Appendix H).

Appendix H illustrates how soil erosion or sediment yield models vary in their data presentation. Universal Soil Loss Equation (USLE)-types models (USLE, RUSLE, and MUSLE) were designed to predict soil erosion on either plot-scale or catchment scale, so they use the term average annual soil loss as represented by mass per unit area per time, which is often incorporated into other sediment yield models. Sediment yield models (SWAT, AGNPS, and WEPP) differentiate soil erosion and sediment yield by adding sediment delivery ratio term into their model. These models report sediment yield result as either mass per time or mass per unit area per time (Appendix H). Although the output of USLE-types model is different from other sediment models, cross-comparisons exist between USLE-type models and other sediment models (e.g. Nearing et al., 2005; Li et al., 2017).

A key aspect of this study rests in comparing background erosion with modern rates of erosion, where natural background rates use the catchment wide denudation rate (CWDR) approach detailed in the next methods section. CWDR scholarship takes two approaches. One strategy converts modern area-specific sediment yield (Mg $km^{-2}$ $yr^{-1}$) to CWDR (m $Myr^{-1}$) by dividing bedrock density (2.6-2.7 g $cm^{-3}$) (Schaller et al., 2001; Bierman et al., 2005). Another CWDR approach calculates background area-specific sediment yield by multiplying bedrock density and then compared to modern sediment yield correcting for sediment bulk density (1.x g $cm^{-3}$) (Hewawasam et al., 2003; Clapp et al., 2001; Gellis et al., 2004) (Appendix H). Thus, to minimize confusion, we use

exclusively ‘area-specific sediment yield (SSY, Mg $km^{-2}$ $yr^{-1}$) in this paper for modern measurements, and we then convert CWDR to this same unit (SSY, Mg $km^{-2}$ $yr^{-1}$) using bedrock density and sediment bulk density corrections detailed in the next methods section.

*Background area-specific sediment yield derived from cosmogenic nuclide $^{10}Be$.*

The drainage network of each of the selected 18 Phoenix-region catchments combines into a single channel that transfers sediment to a stock tank. Background erosion rate (CWDR) samples were all collected from the single channel just above each stock tank (Figure. 5.1). After sieving, just the 250-750 μm size fraction was chemically treated (Kohl and Nishiizumi, 1992) at the Geochronology Laboratory at Korea University, Seoul, Korea. The treatment repeatedly etches minerals in a dilute HF/HNO3 mixture developed by Kohl and Nishiizumi (1992). We added a $^{9}Be$ carrier with a $^{10}Be/^{9}Be$ ratio < $3.0 \times 10^{-15}$, then separated and purified the Be by ion exchange chromatography and selective precipitation of BeOH at pH > 7. BeOH was oxidized by ignition in a quartz crucibles at 800℃ for 10 min (Jeong et al., 2018b). BeO was then mixed with Nb metal and loaded onto targets for the measurement of the $^{10}Be/^{9}Be$ ratio by the 6MV accelerator mass spectrometry (AMS) at the facility of Korea Institute of Science and Technology (KIST), Seoul, Korea (Jeong et al., 2018b). Isotope ratios were normalized to the $^{10}Be$ standards prepared by Nishiizumi et al. (2007) and the measured isotope ratios were converted to cosmogenic $^{10}Be$ concentrations in quartz using the total $^{10}Be$ in the samples and sample weights.

We calculated the catchment-wide production rate by integrating shielding conditions, latitude–altitude production rate functions (Lal, 1991; Stone, 2000; Heisinger et al., 2002a, 2002b), applying 4.49 ± 0.39 $g^{-1}$ $y^{-1}$ at SLHL (sea-level, high-latitude) for the $^{10}$Be reference spallation production rate in this study (Stone, 2000; Balco et al., 2008). For quantification of CWDR, we used the following equation (Lal, 1991):

$$\mathrm{CWDR} = (P_0/C - \lambda) \cdot z^* \quad (1)$$

where $P_0$ (atoms $g^{-1}$ $yr^{-1}$) is the $^{10}$Be production rate at the surface, averaged for the sediment source basin, C (atoms $g^{-1}$) represents measured $^{10}$Be concentration, λ ($yr^{-1}$) is the decay constant of $^{10}$Be, and z* (cm) is a depth scale of absorption mean free path which is equal to Λ / ρ, where Λ (160 g $cm^{-2}$) is absorption mean free path and ρ (2.65 g $cm^{-3}$) is the density of bedrock.

We converted CWDR into the background area-specific sediment yield (SSY) using the following equation:

$$\text{Background SSY} = \varepsilon \times \rho \quad (2)$$

CWDR represents the catchment-averaged bedrock erosion rate, thus we used bedrock density (ρ = 2.65 g $cm^{-3}$) to calculate cosmogenic nuclide-derived SSY (given as Mg $km^{-2}$ $yr^{-1}$) following scholarship comparing CWDR-converted background SSY with modern SSY did (Appendix H: Clapp et al., 2001; Schaller et al., 2001; Hewawasam et al., 2003; Gellis et al., 2004; Bierman et al., 2005). Table 5.2 presents details of each site needed to calculate production rates, the AMS measurement of $^{10}$Be concentration, the calculation of CWDR in meters per million years, the residence timescale of the sediment

in each catchment in thousands of years, and the calculation of natural background sediment yields. Since different approaches to the presentation of background erosion can generate confusion, we defined background erosion as an annual area-specific sediment yield measured in units of weights (Mg $km^{-2}$ $yr^{-1}$).

**Table 5.2.** Catchment-wide denudation rate (CWDR) based on cosmogenic $^{10}$Be analyses.

| Sample ID | Latitude (º) | Latitude (º) | Mean elevation (m.a.s.l.) | Mean slope (º) | Production rate** (atoms $g^{-1}$ $yr^{-1}$) | $^{10}$Be concentration*** ($10^5$ atoms $g^{-1}$) | Denudation rate (m $Myr^{-1}$) | Timescale**** (kyr) | Background ***** (Mg $km^{-2}$ $yr^{-1}$) |
|---|---|---|---|---|---|---|---|---|---|
| 1. Cigar | 33.685000 | -112.534361 | 462.0 | 0.36 | 5.008 | 5.85 ± 0.06 | 4.48 ± 0.05 | 122.0 ± 10.8 | 11.86 ± 0.13 |
| 2. Saguaro | 33.801417 | -112.204194 | 490.0 | 0.72 | 5.118 | 3.74 ± 0.05 | 7.32 ± 0.09 | 82.9 ± 7.3 | 19.39 ± 0.24 |
| 3. Cline | 33.855750 | -112.149222 | 573.5 | 1.20 | 5.461 | 6.46 ± 0.08 | 4.42 ± 0.05 | 19.3 ± 1.7 | 11.71 ± 0.14 |
| 4. Anthem | 33.850572 | -112.101617 | 574.0 | 6.22* | 5.451 | 2.62 ± 0.04 | 11.29 ± 0.17 | 21.3 ± 1.9 | 29.91 ± 0.44 |
| 5. Anthem 2 | 33.851722 | -112.099861 | 761.5 | 1.76 | 6.276 | 1.89 ± 0.03 | 18.14 ± 0.32 | 43.4 ± 3.8 | 48.08 ± 0.85 |
| 6. Pepe | 33.786100 | -112.159939 | 495.5 | 0.55 | 5.139 | 5.19 ± 0.06 | 5.22 ± 0.06 | 32.0 ± 2.8 | 13.84 ± 0.16 |
| 7. Bronco | 33.775389 | -112.116889 | 496.5 | 0.61 | 5.139 | 4.17 ± 0.05 | 6.56 ± 0.08 | 90.9 ± 8.0 | 17.38 ± 0.21 |
| 8. Circle | 33.771167 | -112.061167 | 573.5 | 6.50* | 5.451 | 2.61 ± 0.06 | 11.34 ± 0.27 | 24.5 ± 2.2 | 30.05 ± 0.72 |
| 9. Charlie | 33.774250 | -111.949444 | 649.0 | 1.19 | 5.763 | 1.83 ± 0.03 | 17.24 ± 0.32 | 19.3 ± 2.0 | 45.68 ± 0.84 |
| 10. Rock | 33.759806 | -111.876472 | 857.0 | 2.57 | 6.719 | 1.29 ± 0.07 | 28.59 ± 1.57 | 21.3 ± 1.9 | 75.76 ± 4.15 |
| 11. Cave Creek | 33.821477 | -111.860042 | 860.0 | 1.93 | 6.739 | 5.99 ± 0.07 | 5.97 ± 0.07 | 45.6 ± 4.0 | 15.83 ± 0.18 |
| 12. Buckhorn | 33.771556 | -111.726667 | 661.5 | 1.53 | 5.813 | 2.62 ± 0.04 | 12.05 ± 0.17 | 120.5 ± 10.7 | 31.93 ± 0.46 |
| 13. The Rocks | 33.735972 | -111.840750 | 812.5 | 2.20 | 6.498 | 1.38 ± 0.03 | 25.95 ± 0.57 | 30.4 ± 2.7 | 68.76 ± 1.52 |
| 14. 128th St | 33.719722 | -111.806333 | 813.5 | 1.70 | 6.498 | 1.25 ± 0.03 | 28.56 ± 0.66 | 103.6 ± 9.2 | 75.7 ± 1.74 |
| 15. 128th St 2 | 33.716417 | -111.791167 | 786.0 | 1.66 | 6.367 | 1.35 ± 0.03 | 26.00 ± 0.67 | 65.7 ± 5.8 | 68.89 ± 1.76 |
| 16. AsherHills | 33.730250 | -111.705028 | 733.5 | 1.28 | 6.125 | 2.63 ± 0.04 | 12.65 ± 0.20 | 74.6 ± 6.6 | 33.53 ± 0.53 |
| 17. Gold Cyn | 33.367667 | -111.514972 | 510.0 | 0.63 | 5.149 | 3.33 ± 0.05 | 8.31 ± 0.12 | 48.6 ± 4.3 | 22.02 ± 0.32 |
| 18. Peralta | 33.334978 | -111.429506 | 594.0 | 1.98 | 5.481 | 1.34 ± 0.03 | 22.52 ± 0.49 | 48.4 ± 4.3 | 59.67 ± 1.30 |

*Anthem and Circle were excluded from regression analysis for PMR background erosion model, due to the steep catchment mean slope. According to Saiz (2010), residential development is severely constrained by the presence of steep-slope terrain with the threshold of 8.5º. 24% of drainage area has slope above 8.5 degree in Anthem and 28% of drainage area has slope above 8.5 degree in Circle.

**Total catchment-wide production rate from spallogenic and muonic production. Reference production rate for SLHL is 4.49 g/yr. (Stone, 2000).

***Normalized with standard 07KNSTD and corrected for process blank. Error propagation was based on Balco et al. (2008). The large value between internal error and external error were selected.

*Measuring modern sediment yields from urban sprawl*

Sediment collection from 18 stock ponds monitored soil erosion as the Phoenix urban fringe expanded between 1989 and 2013 (Figure. 5.1 and Table 5.3). An Appendix A Google Earth File 1 presents the 18 studied stock pond watersheds. The selection of the stock tanks to monitor was based on obtaining local information that a land-use change was planned from the prior use of cattle grazing. Sometimes, that land-use change did not occur or did not take place on the anticipated timescale. The result is a mixture of land-use changes impacting sediment yields as the Phoenix metropolitan area expanded.

In each stock tank, nine 0.3 m segments of steel rebar were pounded flush to the surface of the sediment accumulation area in a 3x3 grid to account for spatial variability in sedimentation. Stock pond were revisited at each major land use change to measure sediment accumulation depths on top of the rebar, located using a metal detector. Bulk density samples were collected from three points at each monitoring event and determined using the hydrometer method with the reported error term in Table 5.3 from the standard deviation.

The area-specific sediment yield (SSY) in the studied eighteen stock ponds is calculated (Verstraeten & Poesen, 2001) as follows:

$$SSY = SM / (A_D*TE*Y)*10^6 \quad (3)$$

where $SSY$ (Mg km$^{-2}$ yr$^{-1}$) is area-specific sediment yield, $SM$ (Mg) is sediment mass, $A_D$ (km$^2$) is drainage area of the watershed of each stock pond, $TE$ (%) is sediment trap efficiency (100% for each stock pond) and $Y$ (yr) is time period of measurement.

Since dust storms are common in the Phoenix region, silt and clay accumulating in the stock ponds could potentially derive from aeolian dust deposition, weathered bedrock, or more likely some unknown combination. Thus, two sediment yields (and erosion rates) are presented in Table 5.3. The maximum sediment yield calculation assumes that there was no aeolian dust deposition, while the minimum sediment yield calculation assumes that all of the silt and clay derived from aeolian deposition with the error term assigned from the standard deviation of nine depth measurements for each time slice. This standard deviation of the average depth then translates as a ± percentage the reported sediment yield.

The maximum sediment ($SM_{max}$) was be calculated as follows:

$$SM_{max} = SV*dBD = A_P*D_{avg}*dBD \quad (4)$$

where $SV$ ($m^3$) is the measured sediment volume in the stock pond during the given time period $Y$ (yr), $dBD$ (g $cm^{-3}$ or t $m^{-3}$) is average dry bulk density of the sediment, $Ap$ ($m^2$) is sedimentation area and $D_{avg}$ (m) is the averaged depth of the sediments measured from nine grid points. The minimum sediment yield was calculated as follows:

$$SM_{min} = SM_{max}*(1 - percent\ silt\ and\ clay) \quad (5)$$

We defined modern area-specific sediment yields from urban sprawl as 'Urban acceleration of erosion (UAE)'. The key comparison involves stock-pond monitored two decades of UAE with background erosion derived from CWDR. Thus, the stock-pond monitored samples required a correction to rock density ($\rho = 2.65$ g $cm^{-3}$) following scholarship making comparisons between UAE and background erosion (Appendix H: Schaller et al., 2001; Bierman et al., 2005). Table 5.3 presents this comparison.

**Table 5.3.** Stock pond catchment characteristics, land use/land cover variables of SSY model for PMR, and data on sediment yields

| Sample ID | Time period | Field description of dominant land use | Initial urban cover | Urban growth | Urban growth | AUGR | AUGR | Different rock types | MAP (mm) (I30) (mm) | | Coordinates | Ad | At | Min UAE* | Max UAE** | Background *** | Min UAEN **** | Max UAEN **** |
|---|---|---|---|---|---|---|---|---|---|---|---|---|---|---|---|---|---|---|
| | | | (%) | (%) | ($km^2$) | (% $yr^{-1}$) | ($km^2$ $yr^{-1}$) | | P1 | P2 | (°) | ($km^2$) | ($m^2$) | (Mg $km^{-2}$ $yr^{-1}$) | (Mg $km^{-2}$ $yr^{-1}$) | (Mg $km^{-2}$ $yr^{-1}$) | | |
| 1. Cigar | 1990-2004 | grazing | 10.68 | 8.54 | 0.22 | 0.57 | 0.01 | metamorphic, basalt, granite | 207(20.9) | 170(15.4) | 33.685117, -112.534267 | 2.6 | 6000 | 77.3 ± 3.8 | 89.2 ± 9.7 | 11.9 ± 0.1 | 6.5 | 7.5 |
| | 2005-2009 | grazing and off-road vehicle use | 0.00 | 11.65 | 0.30 | 2.33 | 0.06 | | | | | | | 89.6 ± 3.2 | 102.4 ± 9.8 | | 7.5 | 8.6 |
| 2. Saguaro | 2005-2009 | grazing & pipeline construction | 0.00 | 1.77 | 0.02 | 0.35 | 0.00 | metamorphic, basalt, granite | 222(25.1) | 181(14.1) | 33.800925, -112.20405 | 1.4 | 5800 | 126.7 ± 4.6 | 143.2 ± 26.0 | 19.4 ± 0.2 | 6.5 | 7.4 |
| 3. Cline | 1989-1995 | Some construction | 1.13 | 3.32 | 0.05 | 0.47 | 0.01 | metamorphic, basalt, granitic | 222(25.1) | 181(14.1) | 33.853465, -112.149325 | 1.5 | 9500 | 44.4 ± 5.4 | 52.0 ± 6.9 | 11.7 ± 0.1 | 3.8 | 4.4 |
| | 1996-2003 | commercial construction | 5.41 | 20.87 | 0.31 | 2.61 | 0.04 | | | | | | | 92.7 ± 3.1 | 103.7 ± 6.4 | | 7.9 | 8.9 |
| | 2003-2004 | subdivision construction | 23.60 | 8.10 | 0.12 | 4.05 | 0.06 | | | | | | | 160.0 ± 10.9 | 174.7 ± 25.4 | | 13.7 | 14.9 |
| 5. Anthem 2 | 2002 | housing | 0.00 | 12.74 | 0.07 | 12.74 | 0.07 | metavolcanic | 222(25.1) | 181(14.1) | 33.850572, -112.101617 | 0.58 | 2700 | 230.1 ± 12.8 | 255.7 ± 41.4 | 48.1 ± 0.9 | 4.8 | 5.3 |
| 7. Bronco | 1999-2003 | road construction | 0.00 | 3.32 | 0.01 | 0.66 | 0.00 | metamorphic, basalt, granite | 222(22.8) | 181(11.5) | 33.774765, -112.117174 | 0.45 | 4100 | 112.5 ± 11.2 | 137.4 ± 32.4 | 17.4 ± 0.2 | 6.5 | 7.9 |
| 8. Circle | 2010-2013 | road construction | 0.00 | 3.32 | 0.02 | 0.83 | 0.00 | metamorphic | 222(22.8) | 181(11.5) | 33.767891, -112.069517 | 0.6 | 5000 | 112.3 ± 4.9 | 128.5 ± 31.1 | 30.1 ± 0.7 | 3.7 | 4.3 |
| 9. Charlie | 1989-2004 | house construction | 1.29 | 56.31 | 0.51 | 3.52 | 0.03 | granitic | 276(40.4) | 237(28.0) | 33.773722, -111.949346 | 0.91 | 10500 | 235.6 ± 11.1 | 264.3 ± 49.1 | 45.7 ± 0.8 | 5.2 | 5.8 |
| 11. Cave Creek | 2000-2003 | house construction | 0.00 | 6.29 | 0.01 | 1.57 | 0.00 | granitic | 276(15.4) | 237(22.9) | 33.821477, -111.860042 | 0.19 | 1200 | 114.3 ± 8.7 | 128.8 ± 23.6 | 15.8 ± 0.2 | 7.2 | 8.2 |
| 12. Buckhorn | 1989-1999 | grazing | 0.00 | 6.65 | 0.29 | 0.60 | 0.03 | granitic | 305(40.4) | 260(28.0) | 33.771593, -111.726559 | 4.4 | 4100 | 91.6 ± 5.4 | 106.2 ± 17.1 | 31.9 ± 0.5 | 2.9 | 3.3 |
| | 2000-2002 | house construction | 0.09 | 4.97 | 0.22 | 1.66 | 0.07 | | | | | | | 115.7 ± 15.2 | 133.4 ± 17.4 | | 3.6 | 4.2 |
| 13. The Rocks | 1989-1996 | house construction | 0.21 | 13.20 | 0.31 | 1.65 | 0.04 | granitic | 310(40.4) | 248(28.0) | 33.735184, -111.843395 | 2.36 | 6500 | 212.9 ± 28.0 | 227.6 ± 25.7 | 68.8 ± 1.5 | 3.1 | 3.3 |
| 14. 128th St | 2001-2008 | road construction | 0.00 | 0.34 | 0.00 | 0.04 | 0.00 | granitic | 310(40.4) | 248(28.0) | 33.719610, -111.80591 | 0.85 | 7000 | 141.3 ± 7.4 | 159.9 ± 29.4 | 75.7 ± 1.7 | 1.9 | 2.1 |
| 16.AsherHills | 1989-2001 | grazing | 0.00 | 2.53 | 0.05 | 0.19 | 0.00 | granitic | 310(17.5) | 248(18.4) | 33.731003, -111.703998 | 2.1 | 9800 | 125.9 ± 11.6 | 140.5 ± 27.6 | 33.5 ± 0.5 | 3.8 | 4.2 |
| | 2002-2007 | house construction | 3.78 | 13.36 | 0.28 | 2.23 | 0.05 | | | | | | | 182.6 ± 7.9 | 199.1 ± 15.0 | | 5.5 | 5.9 |
| 17. Gold Cyn | 1989-2009 | cattle grazing & house construction | 0.00 | 5.26 | 0.27 | 0.25 | 0.01 | ignimbrite, granitic | 254(23.2) | 209(17.9) | 33.367485, -111.515636 | 5.1 | 18000 | 45.3 ± 2.5 | 57.3 ± 13.1 | 22.0 ± 0.3 | 2.1 | 2.6 |
| 18. Peralta | 2001-2005 | subdivision construction | 0.00 | 10.11 | 0.08 | 2.02 | 0.02 | ignimbrite, granitic, breccia | 254(23.2) | 209(17.9) | 33.334978, -111.429506 | 0.78 | 2800 | 61.5 ± 3.9 | 77.4 ± 6.8 | 59.7 ± 1.3 | 1.0 | 1.3 |

Note. AUGR: annual urban growth rate; MAP: mean annual precipitation during the 10-year period of study periods; P1: Period 1 (1989–1999); P2: Period 2 (2000–2009); I30 is the total amount of peak 30-min rainfall exceeded 10 mm for 30 min; Ad: drainage area; At: tank area; Min UAE: minimum urban acceleration of erosion; Max UAE: maximum urban acceleration of erosion; Min UAEN: minimum urban acceleration of erosion above natural background erosion; Max UAEN: maximum urban acceleration of erosion above natural background erosion.

*Min UAE is calculated using Eq. (3) and (5) and the data is published in Jeong and Dorn (2019).

** Max UAE is calculated using Eq. (3) and (4) and the data is published in Jeong and Dorn (2019).

*Measuring urbanization's impact on the Phoenix metropolitan region (PMR)*

Urbanization impacts on cities result in enhanced disturbance and increased vulnerability to erosion, but PMR is a sprawling desert city. The PMR was once sealed by desert pavements, biological soil crusts (BSCs) (Allen, 2005, 2010), and interlocking colluvium on steeper slopes that provided a net-armoring effect (Bowker et al., 2008; Granger et al., 2001; Seong et al., 2016a). Only patches of the armored surfaces currently remain, providing glimpses into the original land surfaces due to the enhanced disturbance by anthropogenic impacts including periods of cattle grazing, periods of road building and home construction, and other influences, such as off-road vehicles (Jeong et al., 2018a). For these reasons, SSY associated with the time period of grazing (Table 5.3) is not an appropriate proxy for natural background erosion.

The urban expansion that followed grazing exposed bare soils that are far more vulnerable to erosion due to the enhanced rain splash and overland flow. For example, BSCs increases surface stability by minimizing detachment of soil particles. McCalla (1946) first showed soil aggregates and BSCs association were more resistant to disintegration by raindrop than aggregates without BSCs, which is supported by much studies reporting BSCs considerably reduced detachment and splash erosion by raindrops and overland flow (Osborn, 1952; Tchoupopnou, 1989; Booth, 1941; Fletcher and Martin, 1948), but the destruction of BSCs by road building and home construction generally decreases infiltration capacity (Harper and St. Clair, 1985; Harper and Marble, 1988; Eldridge, 1993; Warren, 2001; Kidron et al., 2012), increases runoff (Fletcher, 1960) and results in widespread erosion (Neff et al., 2005). With the context of a natural

condition of far greater armoring than the period of cattle grazing, we linked stock pond SSY measurements to urban growth in each of the stock ponds.

Figure 5.2 illustrates the conceptual model used here to quantify LULCC-related parameters using GIS procedures. To quantify the initial urban condition (IU of the year when SSY of stock pond watersheds monitoring started (Table 5.3 and Figure. 5.2), we first calculated either percentage or area of urban LULCC (asphalt/road, concrete/buildings, urban mixture and residential) in LULCC from 1985 to 2010 at five year intervals. When measurements fell between the five-year intervals, and the available historic imagery could not discern the exact time of the urban growth, we distributed urban growth evenly. Thus, urban growth (UG) (percentage and square kilometers) is quantified by calculating the transition from natural LULCC (natural vegetation and soil/desert) to urban LULCC. We also quantified time normalized urban growth rate (AUGR) by dividing the UG into the number of years of each monitoring period (Table 5.3 and Figure. 5.2).

In order to model background erosion and UAE for the entire Phoenix metropolitan region (PMR), we quantified the LULCC-related parameters for entire PMR using GIS procedures (Figure 5.3). The PMR is a NSF site for long-term ecological research in an arid urban setting; two LULCC datasets with a 30 m resolution from CAP LTER quantified initial urban cover and urban growth and: i) LULC in 1912, 1934, 1955, 1975 and 1995 (https://sustainability.asu.edu/caplter/data/view/knb-lter-cap.1.11); and ii) LULC in 1985, 1990, 1995, 2000, 2005 and 2010 (https://sustainability.asu.edu/caplter/data/view/knblter-cap.650.1/). These data were

supplemented by analysis of historic aerial photography from the Maricopa County Tax Assessor website (https://gis.maricopa.gov/GIO/HistoricalAerial/index.html) and Google Earth. Based on the two datasets, 9 time periods were established: T1 (1912-1934), T2 (1955-1975), T3 (1975-1985), T4 (1975-1995), T5 (1985-1990), T6 (1990-1995), T7 (1995-2000), T8 (2000-2005) and T9 (2005-2010).

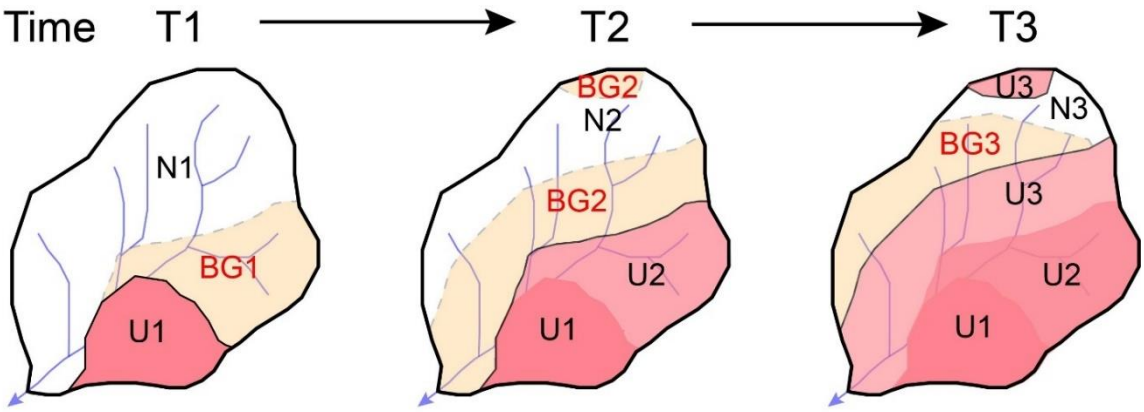


| Time period | Length of time period | Surface condition | Landuse change index |
|---|---|---|---|
| T1→T2<br>T2→T3 | | Initial urban cover (U1)<br>Initial urban cover (U2) | Initial urban cover (imperviousness): U1<br>Initial urban cover (imperviousness): U2 |
| T1→T2<br>T2→T3 | | Exposed bare ground (BG1)<br>Exposed bare ground (BG2) | Urban growth: N1 ∩ U2<br>Urban growth: N2 ∩ U3 |
| T1→T2<br>T2→T3 | T2 - T1 = L1<br>T3 - T2 = L2 | Exposed bare ground (BG1)<br>Exposed bare ground (BG2) | Annual urban growth rate: N1 ∩ U2 / L1<br>Annual urban growth rate: N2 ∩ U3 / L2 |

**Figure 5.2.** Conceptual model to quantify land use-related parameters using GIS. The dashed line is the imaginary line that does not exist on the land use/land cover classification map, which is to show the exposed bare ground. The initial urban cover during the time period from T1 to T2 can be quantified as U1. The urban growth during the time period from T1 to T2 (BG1) can be calculated by the intersection of natural land cover in T1 and urban land cover in T2. The annual urban growth was calculated from dividing by the length of time period. See method section for details.

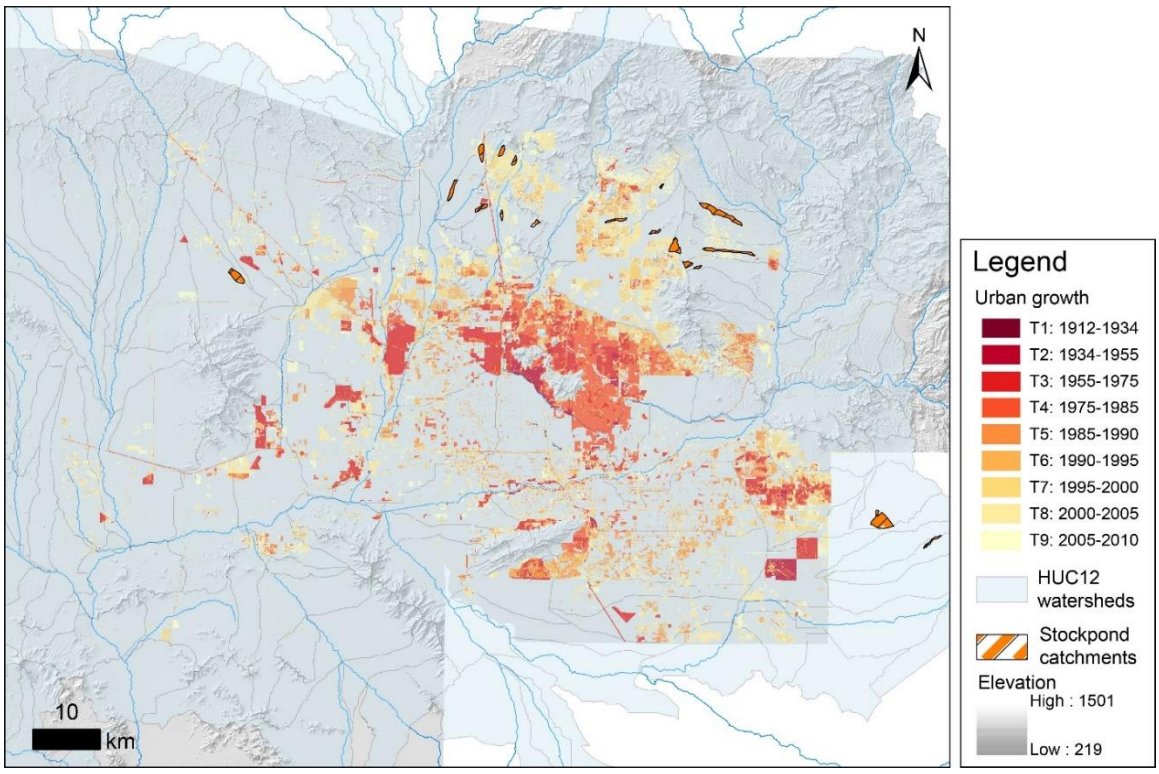


**Figure 5.3.** Urban growth from 1912 to 2010 and 12-digit hydrologic unit code (HUC) subwatersheds of PMR (USGS and USDA-NRCS, 2013) used for quantifying relevant LULCC and natural variables for erosion modelling

*Modeling background erosion for the entire metropolitan Phoenix*

In order to model background erosion for the entire PMR, we analyzed variables potentially related to background erosion rates. Metrics such as slope, basin relief, and mean elevation might be important determinants of CWDR and rock type is less dominant (Portenga and Bierman, 2011). We explored how different factors (mean slope, mean elevation, relief, drainage area, drainage density) impact CWDR. A correlation matrix presents Pearson's correlation coefficients between CWDR and morphometric properties of each catchment (Table 5.4). Of note, we excluded two CWDRs for a bivariate correlation test, because these two watersheds had comparatively steep

catchment mean slopes (6.6º and 6.2º) because the residential development backed up against mountain desert slopes. Generally, in Phoenix, residential development is severely constrained by the presence of steep-slope terrain with the threshold of 8.5º (Saiz, 2010). Thus, the presence of backing desert mountains made these catchments inappropriate for inclusion in any statistical tests.

CWDR was significantly and positively correlated with mean slope ($r = 0.77$, $p < 0.05$) and mean elevation ($r = 0.70$, $p < 0.05$), but drainage area, relief and drainage density did not show a clear correlation. Mean slope and mean elevation was significantly and positively correlated ($r = 0.88$, $p < 0.01$). Because the two predictors, mean slope and mean elevation is significantly correlated, we rejected mean elevation as a predictor for CWDR to avoid multicollinearity (Table 5.4).

**Table 5.4.** Correlation matrix between the CWDR and some stock tank catchment variables, Phoenix metropolitan area, Sonoran Desert, Arizona, USA

| | *CWDR* | *Mean slope* | *Mean elevation* | *Relief* | *Drainage area* | *Drainage density* |
|---|---|---|---|---|---|---|
| CWDR | 1 | | | | | |
| Mean slope | 0.77** | 1 | | | | |
| Mean elevation | 0.70** | 0.88*** | 1 | | | |
| Relief | 0.08 | 0.20 | 0.22 | 1 | | |
| Drainage area | -0.27 | -0.31 | -0.33 | 0.44 | 1 | |
| Drainage density | 0.34 | 0.25 | 0.39 | -0.20 | -0.49* | 1 |

Note: n = 16, *Significant at $p < 0.1$. **Significant at $p < 0.05$. ***Significant at $p < 0.01$.

Since rock type is nominal data, we completed analyses of Student's t-Tests to understand the importance of rock type on CWDR. Half of the stock pond watersheds are

underlain by only granitic lithologies, ranging from granite to granodiorite with some diorite and the other half of the stock pond watersheds are underlain by a mix of rock types, typically including rhyolitic tuff (ignimbrite), basalt, metavolcanic, and metasedimentary rocks (Jeong and Dorn, 2019). A t test comparing CWDRs of granitic versus other rock types reveals statistically significant difference for granite (M = 52.01, SD = 23.25) versus other rock types (M = 25.49, SD = 18.15) conditions, $t(13) = 2.54$, $p < 0.05$ (Table 5.5a). This difference is shown graphically in Figure 5.4a. However, we also rejected rock type as a predictor for CWDR because rock type and mean slope were highly correlated. We also did t test comparing mean slopes of granitic versus other rock types reveals statistically significant difference for granite (M = 1.76, SD = 0.46) versus other rock types (M = 0.98, SD = 0.6) conditions, $t(13) = 2.91$, $p < 0.05$ (Table 5.5b). This difference is shown graphically in Figure 5.4b. Different weathering characteristics of granitic and non-granitic rock types may result in multicollinearity. Whereas granitic rocks break down into grus, or sand-sized particles and maintain steep slope, the other rock types (basalt, ignimbrite, metasedimentary, and metavolcanic) decay into a mixture of fines (clay and silt), some sand, but also cobbles and boulders. Thus, we adopted only mean slope as a predictor for background erosion ($R^2 = 0.59$, $p < 0.001$) out of these variables (Figure 5.5).

$$\textit{Background erosion} = 28.537*(\textit{mean slope}) - 0.254 \quad (6)$$

Modelling background erosion for the entire PMR was conducted with the following procedures:

1) Quantify exposed bare ground (BG) layers during the time period (T1-T9) using GIS (Figure 5.3)

2) Based on the HUC12 subwatersheds, calculate mean slopes for all BG layers (Figure.5.3)

3) Using equation 6, calculate background erosion for entire PMR

**Table 5.5.** Student's t-Tests results for rock types

| | ***a*** *CWDR* | | ***b*** *Mean slope* | |
|---|---|---|---|---|
| | *Granite* | *Others* | *Granite* | *Others* |
| Mean | 52.01 | 25.49 | 1.76 | 0.98 |
| Variance | 540.65 | 329.28 | 0.21 | 0.36 |
| Observations | 8 | 8 | 8 | 8 |
| Hypothesized Mean Difference | 0 | | 0 | |
| df | 13 | | 13 | |
| t Stat | 2.54 | | 2.91 | |
| P(T<=t) one-tail | 0.012 | | 0.006 | |
| t Critical one-tail | 1.77 | | 1.77 | |
| P(T<=t) two-tail | 0.025 | | 0.012 | |
| t Critical two-tail | 2.16 | | 2.16 | |

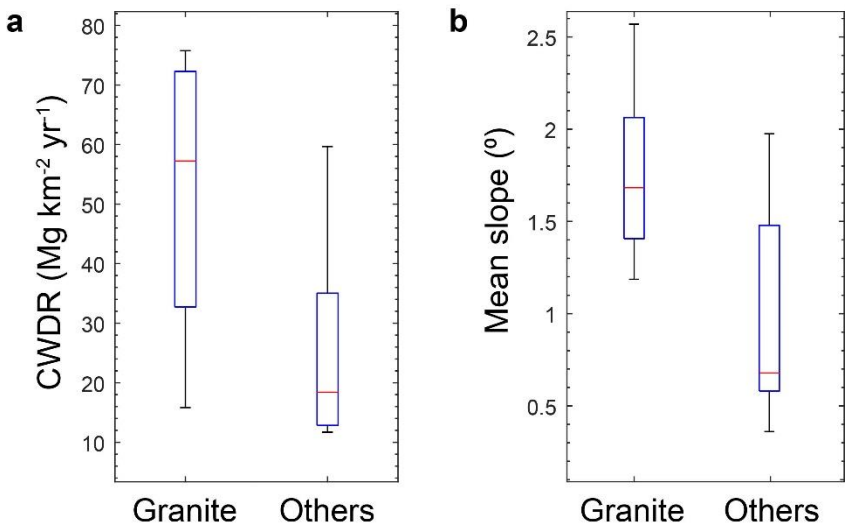


**Figure 5.4.** Box and whisker plots. (a) Box and whisker plots to compare CWDR of granite and other rock type. (b) Box and whisker plots to compare mean slope of granite and other rock type. Box ranges from 25th to 75th percentiles. Whiskers represent data range. Red lines are medians.

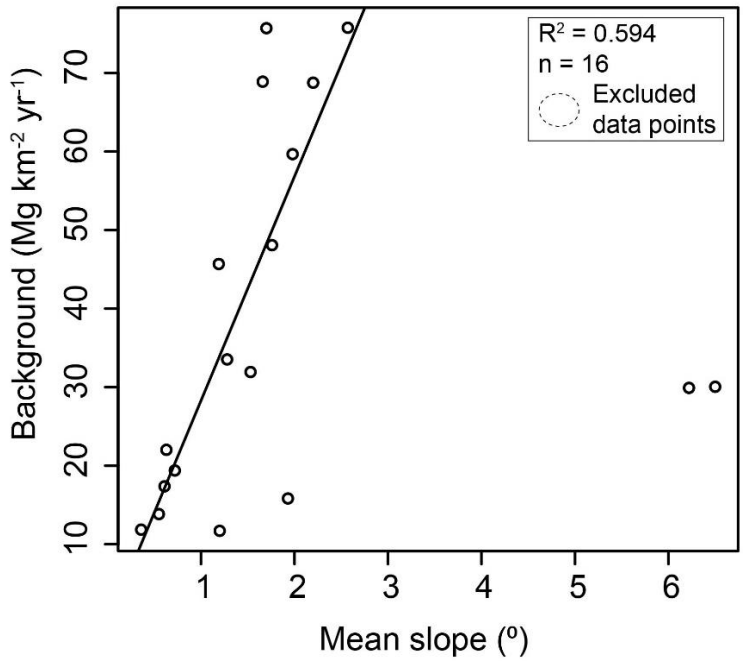


**Figure 5.5.** Linear regression model to examine the relationship between mean slope and background erosion rate.

*Modeling urban acceleration of erosion for the entire metropolitan Phoenix*

In order to model UAE for the entire PMR, we analyzed variables potentially related to UAE. We explored how different LULCC and catchment geomorphological factors (initial urban cover, annual urban growth rate, drainage area, mean slope, relief and drainage density) impact UAE. A correlation matrix presents Pearson's correlation coefficients between UAE and the variables (Table 5.6). UAE was significantly and positively correlated with annual urban growth rate in unit of % $yr^{-1}$ (AUGR1) ($r = 0.59$, $p < 0.05$). Annual urban growth rate in unit of % $yr^{-1}$ (AUGR1) and annual urban growth rate in unit of $km^2$ $yr^{-1}$ (AUGR2) was significantly and positively correlated ($r = 0.66$, $p < 0.05$). For modelling, we adopted AUGR2 instead AUGR1 because measurement of urban growth using percentage is not likely independent from the size of watersheds. We also adopted mean slope as a predictor for UAE because it represents natural influences of erosion, although it does not have significant correlation with UAE. Figure 5.6 shows the bivariate regression between AUGR1, AUGR2, mean slope and UAE. The final model to predict UAE is developed using multiple regression analysis, examining the relationship between AUGR2, slope and UAE (Table 5.7).

$$UAE = 1075.421*(AUGR2) + 7.925*(mean\ slope) + 99.388 \quad (7)$$

The multiple regression model with all two predictors produced $R^2 = 0.21$ (Adjusted $R^2 = 0.11$), $F(2,16) = 2.06$, $p < 0.5$.

**Table 5.6.** Correlation matrix between the UAE and some stock tank catchment variables, Phoenix metropolitan area, Sonoran Desert, Arizona, USA

| *Name* | *UAE* | *IUC* | *AUGR1* | *AUGR2* | *DA* | *MSlp* | *RF* | *DD* |
|---|---|---|---|---|---|---|---|---|
| UAE | 1 | | | | | | | |
| IUC | 0.05 | 1 | | | | | | |
| AUGR1 | 0.59** | 0.12 | 1 | | | | | |
| AUGR2 | 0.42 | 0.29 | 0.66** | 1 | | | | |
| DA | -0.34 | -0.03 | -0.28 | 0.26 | 1 | | | |
| MSlp | 0.10 | -0.17 | 0.01 | -0.15 | -0.30 | 1 | | |
| RF | 0.11 | -0.17 | -0.15 | 0.17 | 0.40 | 0.34 | 1 | |
| DD | 0.06 | -0.41 | -0.14 | -0.40 | -0.36 | 0.38 | 0.03 | 1 |

Note: n = 19, *Significant at p < 0.1. **Significant at p < 0.05. ***Significant at p < 0.01. UAE: urban acceleration of erosion (Mg km$^{-2}$ yr$^{-1}$); IUC: initial urban cover (%); AUGR1: annual urban growth rate (% yr$^{-1}$); AUGR2: annual urban growth rate (km$^2$ yr$^{-1}$); DA: drainage area (km$^2$); Mslp: Mean slope (º); RF: relief (m); DD: drainage density (km$^{-1}$).

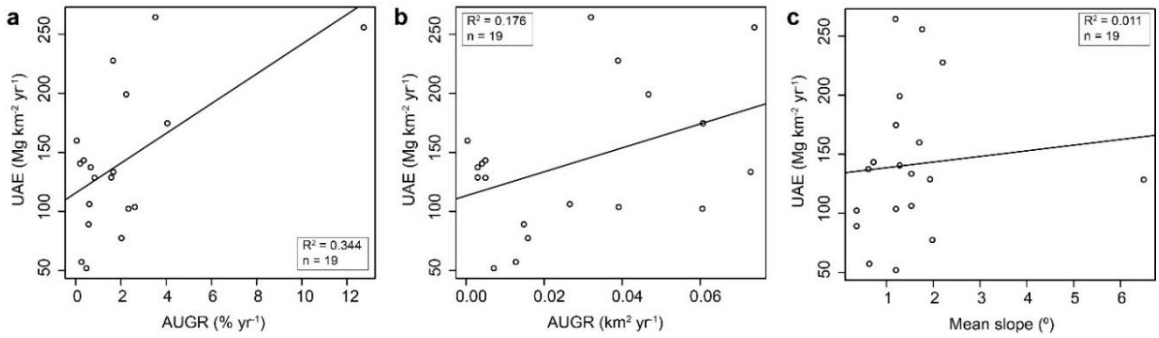


**Figure 5.6.** Scatterplot and linear regression to examine the relationship between (a) AUGR1 and UAE, (b) AUGR2 and UAE, (c) mean slope and UAE.

**Table 5.7.** Linear regression analysis for estimation of urban acceleration of erosion (UAE)

| | *Dependent variable:* | | | |
|---|---|---|---|---|
| | UAE | | | |
| Model | (1) | (2) | (3) | (4) |
| AUGR (% $yr^{-1}$) | 12.581** | | | |
| | (4.216) | | | |
| AUGR ($km^2$ $yr^{-1}$) | | 1012.34. | | 1075.421. |
| | | (530.52) | | (543.648) |
| Mean slope | | | 4.769 | 7.925 |
| | | | (11.166) | (10.439) |
| Constant | 115.741*** | 113.29*** | 133.810*** | 99.388** |
| | (14.429) | (19.58) | (22.326) | (26.988) |
| Observations | 19 | 19 | 19 | 19 |
| $R^2$ | 0.344 | 0.176 | 0.011 | 0.205 |
| Adjusted $R^2$ | 0.305 | 0.128 | -0.048 | 0.106 |

Note: .0.05<P<0.1 *0.01<P<0.05 ** 0.001<P<0.01 *** P<0.001. We adopted model 4 for estimation of urban acceleration of erosion.

Modelling UAE for the entire PMR was conducted with the following procedures:

1) Quantify exposed bare ground (BG) layers during the time period (T1-T9) using GIS (Figure 5.3)

2) Calculate AUGR2 during the time period (T1-T9) for all BG layers (Figure.5.3)

3) Based on the HUC12 subwatersheds, calculate mean slopes for all BG layers (Figure.5.3)

4) Using equation 7, calculate UAE for entire PMR

## RESULTS AND DISCUSSION

### *Urban acceleration of soil erosion in sprawling desert watersheds*

Cosmogenic nuclide $^{10}$Be-derived CWDRs from 18 small desert watersheds on low-angle piedmont settings in PMR (Figure 5.1) presented an opportunity to quantify pre-human natural background erosion for PMR ("background erosion", hereafter). Background erosion rates estimated from cosmogenic nuclides range from 12 to 76 Mg km$^{-2}$ yr$^{-1}$ with a mean of 38 Mg km$^{-2}$ yr$^{-1}$ and are integrated over a mean soil residence time of 19–122 kyr (Table 5.2). These slow rates of soil erosion are because these natural piedmont surfaces once hosted biological soil crusts, and interlocking colluvium on steeper slopes, providing a net armoring effect (Jeong et al., 2018).

Urban sprawl, however, disturbed the surfaces and exposed bare ground during the home and commercial real estate development, or other infrastructural development such as road and pipeline construction, that in turn accelerates soil erosion by enhancing rain splash and overland flow (Jeong and Dorn 2019). Bare ground associated with urban sprawling processes of residential and real estate development (Figure 5.2) increases sediment yields typically ~15-fold over background rates (Table 5.3). Figure 5.7 exemplifies historic changes in just one of the watersheds. Appendix K presents this information for all of the watersheds impacted by urban sprawl. Normally, Wolman's (1967)'s erosion spike is compared with historical land use such as grazing or logging, but in Figure. 5.7 and Appendix K, the CWDR background erosion exists as a point of comparison.

**c** ID03: Cline (1989-2004)

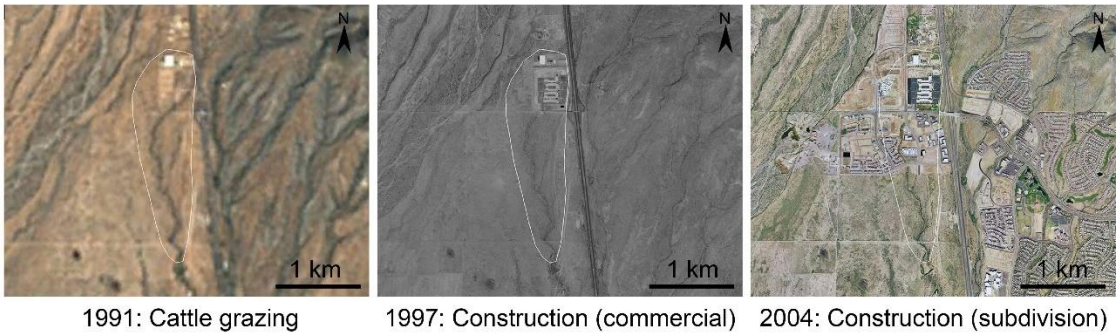


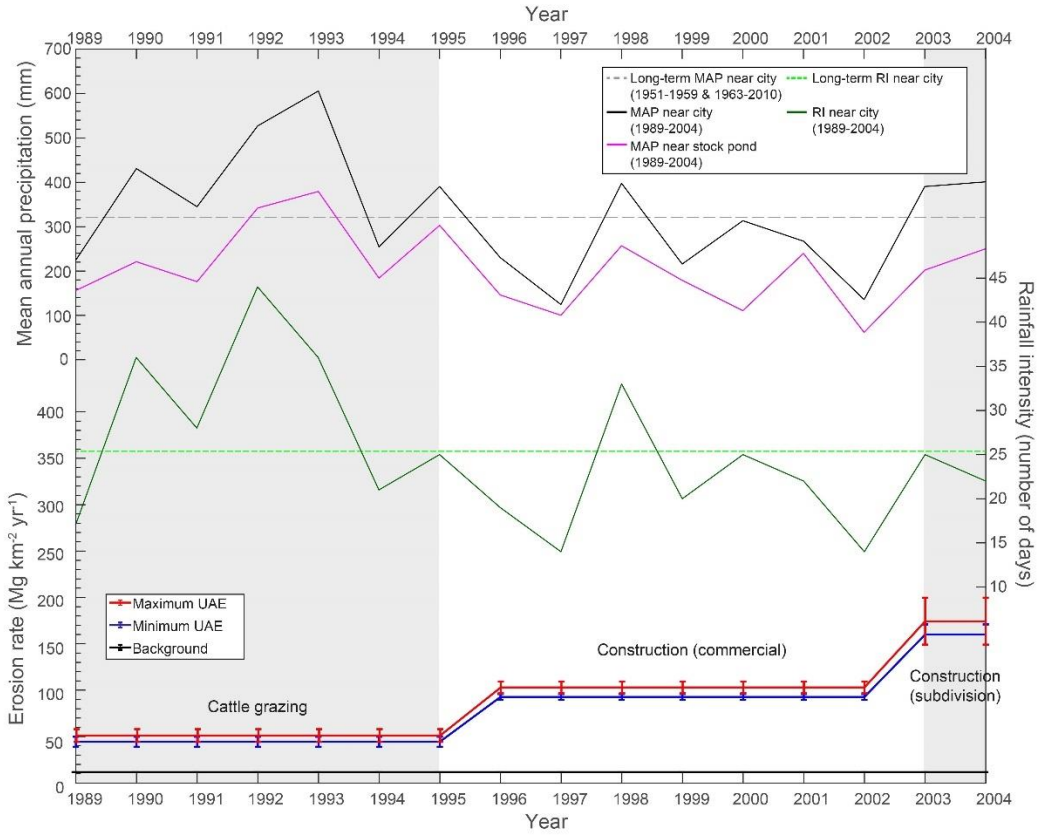


**Figure 5.7.** The change of land-use, precipitation variables, and erosion rates during the monitoring period. This is one example from ID 3 Cline catchment. The UAE jumped twice associated with the land-use changes. Compared to background erosion rate, UAEN is 4x during cattle grazing, 9x during commercial construction, and 15x during subdivision construction, respectively. However, the UAE was likely diminished due to the climatic conditions that occurred during the study period from 1989 to 2013. During the first time period, dominated by grazing in the Cline tank watershed had higher mean annual precipitation and rainfall intensity than the second and third time period, dominated by construction.

Our sediment yield data (Table 5.3) supports that assumption that the magnitude of urban growth within a watershed is a key factor by exposing more bare ground to increase erosion rates. For example, when the Cline tank experienced slow construction for 11 years (AUGR: 0.47% $yr^{-1}$), the area-specific sediment yield (SSY) was 52 Mg $km^{-2}$ $yr^{-1}$ (Figure. 5.7). Then, SSY suddenly jumped two-fold during the desert was skinned with an AUGR of 2.61% $yr^{-1}$) in the next 8 years. SSY then jumped by a factor of 3.4 during subdivision construction (AUGR: 4.05% $yr^{-1}$) only for a 2-year period (Figure. 5.7). Compared to natural background SSY, UAEN is 4x, 9x, and 15x, respectively. However, the UAE was likely diminished due to relatively dry historic climatic conditions that occurred during the study period from 1989 to 2013 (Figure. 5.7 and Appendix I). Because this urban acceleration occurred in periods of drought and less cumulative time of intense rainfall (Figure. 5.7), our findings underscore the interpretation that we measured the minimum end of the range of potential soil erosion for rapidly expanding desert cities.

These findings provide the first confirmation of Wolman's conceptual model, originally developed for a forested region-turned urban (Wolman, 1967), for a rapidly expanding desert city. The Wolman model ends with sealing the surface, and the area-specific sediment yields (SSY) of Peralta stock tank (ID18 in Appendix I) of 52 Mg $km^{-2}$ $yr^{-1}$ during the pre-urban grazing period, rapidly increased to 77 Mg $km^{-2}$ $yr^{-1}$ during active construction, and decreased to 9 Mg $km^{-2}$ $yr^{-1}$ after 5 years subdivision development because sediment sources in disturbed catchment are replaced by sealed surface.

*Model urban acceleration of soil erosion for the Phoenix metropolitan region*

We modeled both background erosion and UAE for bare ground layers associated with urban growth from 1912 to 2010 (Figure 5.3). Overall the background erosion rates for PMR range from 3 to 436 Mg $km^{-2}$ $yr^{-1}$ with a mean of 115 Mg $km^{-2}$ $yr^{-1}$ and median of 90 Mg $km^{-2}$ $yr^{-1}$ (Figure 5.8). The spatial distribution of background erosion rates in PMR (Figure 5.9a) shows that are area located near mountain fronts at the urban fringe or preserved area have steeper slopes and hence higher background erosion rates.

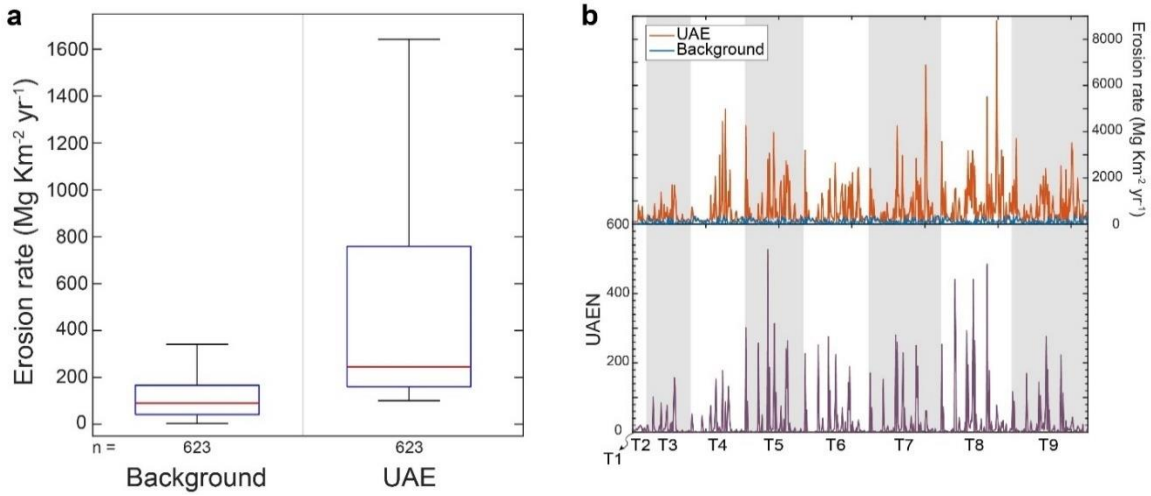


**Figure 5.8.** Erosion modelling results for the entire PMR. (a) Box and whisker plots of background erosion and UAE. Box ranges from 25th to 75th percentiles. Whiskers represent data range, excluding statistical outliers. Red lines are medians. n indicates the number of bare ground layers (Figure 5.3). (b) Histogram of background erosion, UAE and UAEN for time periods: T1 (1912-1934), T2 (1955-1975), T3 (1975-1985), T4 (1975-1995), T5 (1985-1990), T6 (1990-1995), T7 (1995-2000), T8 (2000-2005) and T9 (2005-2010).

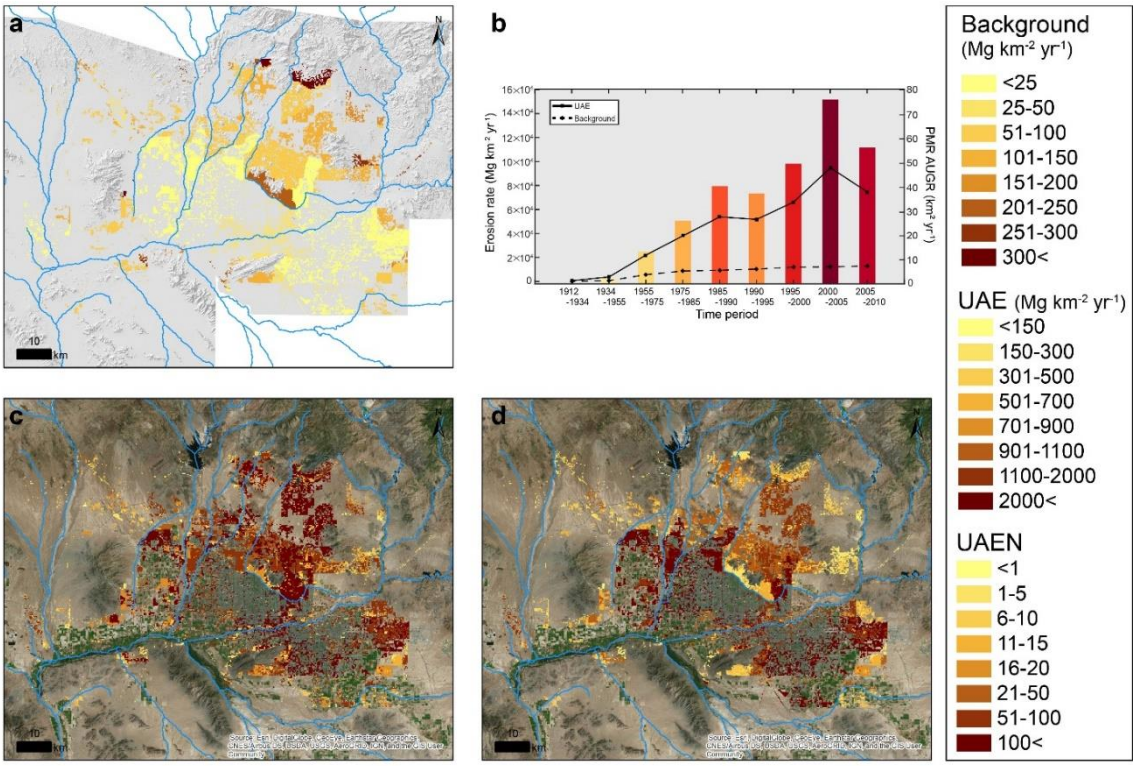


**Figure 5.9.** Spatial distribution of background erosion rate and UAEN and temporal change of UAE and background erosion rate in PMR. (a) Spatial distribution of background erosion rate. (b) Temporal change of background erosion and UAE in PMR from 1912 to 2010 associated with PMR annual urban growth rate. (c) Spatial distribution of UAE (d) Spatial distribution of UAEN. Less than 1 means background erosion is greater than UAE. Base map was imported from ESRI, producer of ArcGIS software and public datasets. Accessed through the Arizona State University license. Appendix J provides larger maps.

The urban sprawl of PMR from 1912 to 2010 accelerated erosion rates almost three-order-of magnitude depending on the annual urban growth rate (Figure 5.9b). The fastest urban growth occurred during 2000-2005 period (AUGR: 76 $km^2$ $yr^{-1}$) and the UAE yields 94,815 Mg $km^{-2}$ $yr^{-1}$ (Table 5.8). The rate of urban growth slowed down during 2005-2010 period (AUGR: 56 $km^2$ $yr^{-1}$), so that UAE decreased to 74,621 Mg $km^{-2}$ $yr^{-1}$ (Table 5.8), but is substantial UAE compared to background erosion. In contrast, during the early urbanization period from 1912 to 1934, the urban expansion was

significantly slower (AUGR: 0.02 $km^2$ $yr^{-1}$) leading to 548 Mg $km^{-2}$ $yr^{-1}$ of UAE (Table 5.8 and Figure 5.9c and Appendix J). During the modeling period, the total UAE for PMR ranged from 101 to 8803 Mg $km^{-2}$ $yr^{-1}$ with a mean of 651 Mg $km^{-2}$ $yr^{-1}$ and median of 245 Mg $km^{-2}$ $yr^{-1}$ (Figure 5.8). In contrast to the spatial distribution of background erosion, higher UAE areas usually correspond with the low-angle piedmont areas where urban expansion accelerated in the 1960s due to the advent of air conditioning (Grimm et al., 2013) (Fig. 5.1 and 5.9 and Appendix J) and the discordance of spatial distribution of background and UAE (Figure 5.9a and 5.9c and Appendix J) suggests geomorphic settings on as low-angle piedmont slopes can still be vulnerable to soil erosion during urban sprawling.

**Table 5.8.** Transition of UAE, Background erosion and UAEN in PMR from 1912 to 2010 derived from regression analysis

| Time period | Background (Mg $km^{-2}$ $yr^{-1}$) | UAE (Mg $km^{-2}$ $yr^{-1}$) | UAEN |
|---|---|---|---|
| T1: 1912-1934 | 100 ± 115 | 548 ± 411 | 5.5 |
| T2: 1934-1955 | 541 ± 336 | 3738 ± 2066 | 6.9 |
| T3: 1955-1975 | 5667 ± 1972 | 21987 ± 12484 | 3.9 |
| T4: 1975-1985 | 8666 ± 2765 | 37985 ± 22879 | 4.4 |
| T5: 1985-1990 | 9234 ± 2953 | 53830 ± 32779 | 5.8 |
| T6: 1990-1995 | 10276 ± 3279 | 51723 ± 31090 | 5.0 |
| T7: 1995-2000 | 11896 ± 3732 | 66205 ± 40166 | 5.6 |
| T8: 2000-2005 | 12082 ± 3764 | 94815 ± 58324 | 7.8 |
| T9: 2005-2010 | 12924 ± 4069 | 74621 ± 44526 | 5.8 |

Another way to think of these findings is that UAEN can be an indicator to assess the vulnerability of urban acceleration to soil erosion (Figure 5.9d) Less than 1 means background erosion is greater than UAE and more than 1 shows that the magnitude of urban acceleration of erosion above natural background erosion. During the modelling period, the total UAEN for PMR range from 0.5 to 527x with a mean of 26x and median of 3x (Figure 5.10).

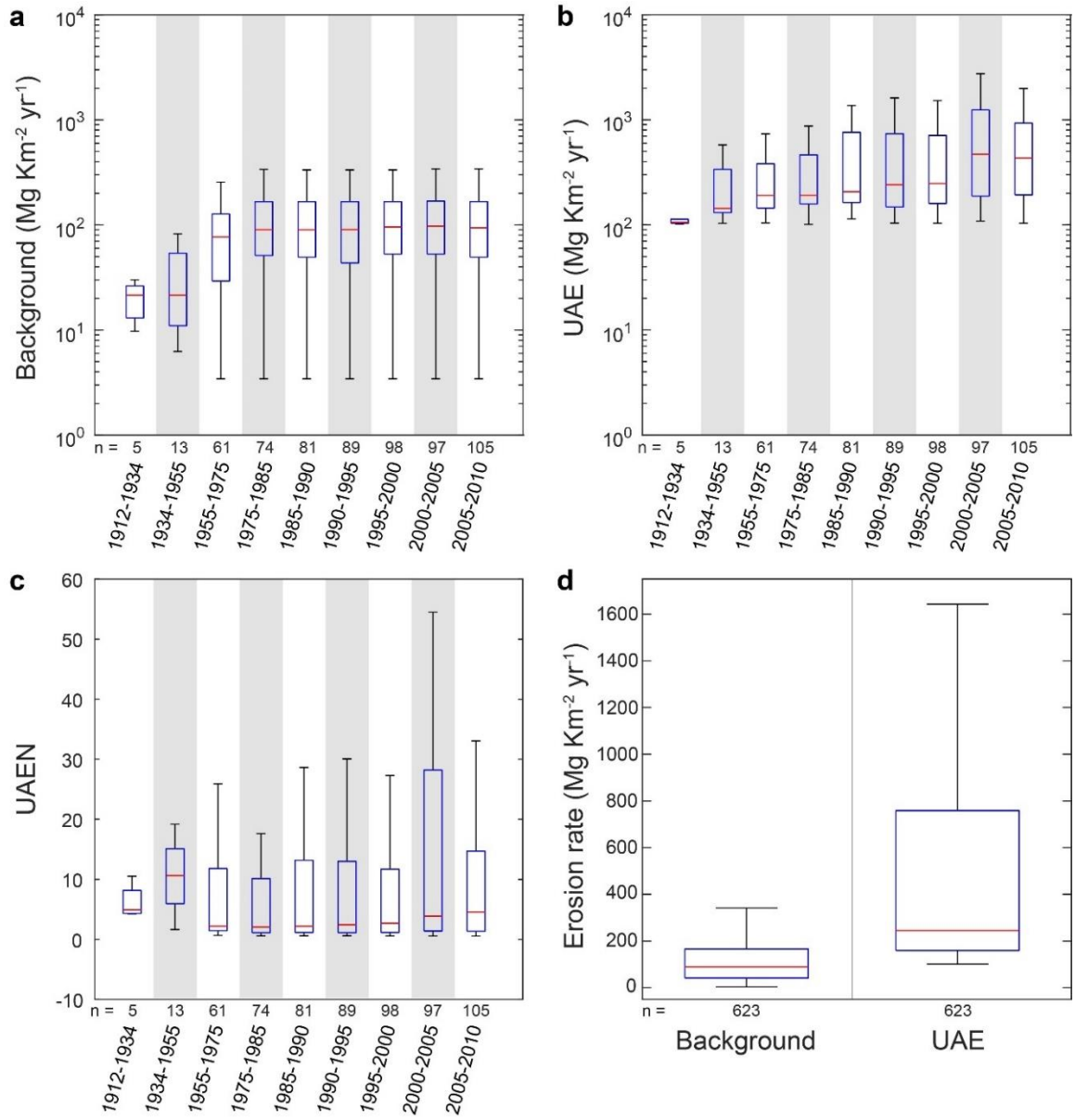


**Fig. 5.10.** Box and whisker plot for background, UAE and UAEN change over time periods. Box ranges from 25th to 75th percentiles. Whiskers represent data range, excluding statistical outliers. Red lines are medians. n indicates the number of bare ground layers. (a) background erosion rate change over the time periods. (b) UAE change over the time periods. (c) UAE index change over the time periods. (d) Background and UAE from all individual bare ground layers that experienced urbanization. The median background erosion rate is 90 Mg $km^{-2}$ $yr^{-1}$ that is only a bit lower than reported median background erosion rate in arid climate zone (93 Mg $km^{-2}$ $yr^{-1}$) based on compilation of cosmogenic nuclide derived catchment-wide denudation rates by Portenga and Bierman (2011).

*Global soil erosion implications of ongoing urban sprawling*

Soil erosion from urban sprawl in Sonoran Desert can be contextualized by cities in other climatic regions if we relax a key assumption. The Phoenix case study rigorously compared natural CWDR soil erosion rates to the same watersheds experiencing urban sprawl at different times and at different rates. While many soil erosion rates accelerated by urbanization process are reported globally (Appendix K), little CWDR research occurred in the same urbanizing watersheds, which impedes global comparison of UAEN. However, our CWDR from Phoenix case study provides an opportunity for the global comparison of UAEN with these assumptions:

Assumption 1: Cities are located on the low-slope landforms based on Saiz (2010)'s founding that residential development is severely constrained by the presence of steep-slope terrain with the threshold of 8.5º.

Assumption 2: Slope is the most important predictor for background erosion (Portenga and Bierman, 2011). Therefore, our CWDR for the lower piedmont slopes (mean slope 0.4-6.5º) of the Sonoran Desert can be used to estimate CWDR for other cities in other climatic settings where urban development also occurred on lower piedmont slopes.

If the CWDR data are truly comparable, then the Phoenix case study places it on the lower end of urban acceleration above background rates of erosion (Fig. 5.11). Such a finding, if supported by comparisons of the same watersheds, should not be surprising for a few reasons. First, the UAE effects in Phoenix were measured during drought

conditions. Second, the urban sprawl occurred on low slopes of desert piedmont settings appropriate for subdivision growth.

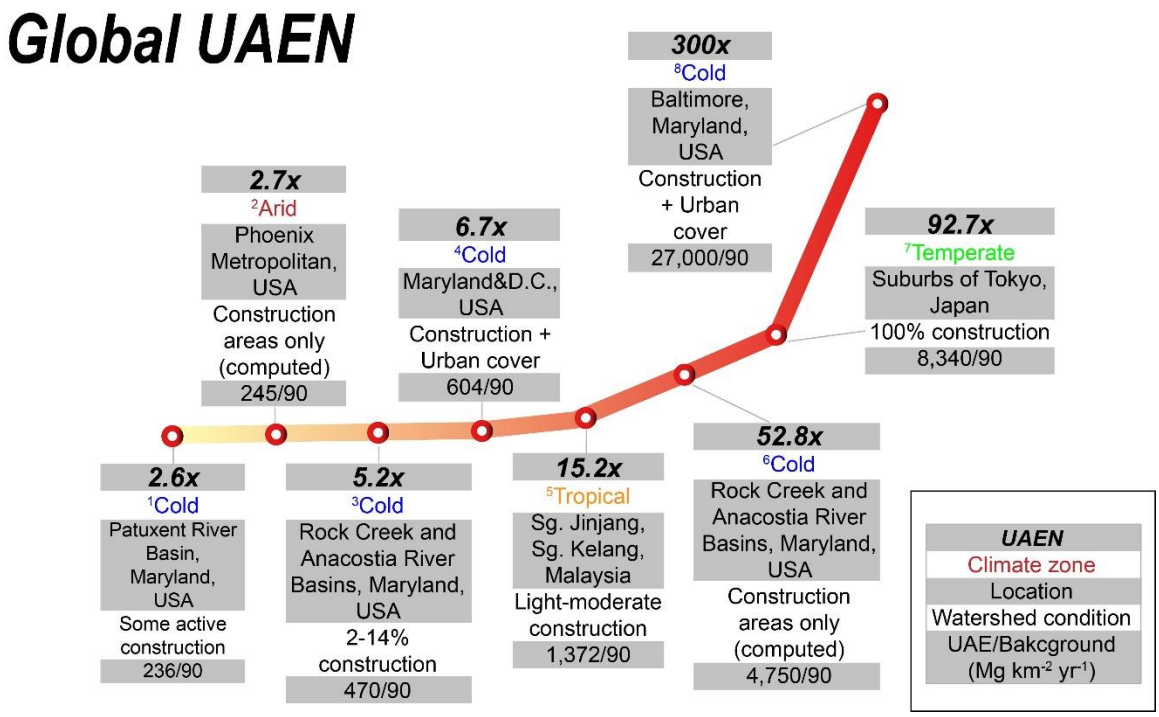


**Figure 5.11.** Comparison of UAEN on a global basis. For the background erosion, CWDR from PMR case study was used. For the UAE, Russell et al. (2017) compiled global erosion rates impacted by construction, and only data points that reported median erosion rates were adopted in this study. Extended data table provide details. We hypothesized that our case study will provide the lower bound of UAEN. While Phoenix model calculated UAE only for computed construction areas, other UAE in other regions were measured from construction and other land-use mixed watershed except for ID6 Maryland case and 7 Japan case. Therefore, the UAE measured from the mixed land-use watershed may be underestimated and thus, UAEN.

## CONCLUSION

Measuring human amplification of soil erosion requires an understanding of natural background erosion rates (Gellis et al., 2004). Erosion rates accelerated by various human actions in the United States have been reported in abundant literature such as erosion rates induced by mining, grazing, logging, deforestation, and urbanization, but traditional methods to measure sediment yield using sediment loads in the stream or reservoir do not always reflect background rates of erosion (Trimble, 1977), while concentrations of *in situ*-produced $^{10}$Be measured in fluvial sediments provide an opportunity to estimate catchment wide denudation rates (CWDR) over timescales of $10^3$ to $10^5$ years (von Blanckenburg, 2006). There was no comparisons of natural background using CWDR to urban acceleration of erosion unlike non-urban settings such as agricultural fields, deforested area, although urbanization processes accelerates erosion by one to two orders of magnitude compared to the other land uses (Russell et al., 2017). Furthermore, considering that urbanization's unceasing expansion will add one new city of a million every five days until 2050 more than tripling urban land from 2000 to 2050 (d'Amour et al., 2017; Seto et al., 2011), quantification of background erosion rates is a critical task for cities worldwide. Based on measurements of contemporary sediment yield and CWDRs on small desert watersheds in Phoenix metropolitan region, our erosion modelling for Phoenix metropolitan region showed that 2.7x increase of erosion rate by urbanization compared to natural background, and this Phoenix case study places it on the lower end of urban acceleration above background rates of erosion. Brown et al. (2017) argued that "the less obvious effects of humans on geomorphic systems warrant

increased research", certainly applies to the north-central Sonoran Desert, that could provide the 'knowledge for mitigation' to our society.

# CHAPTER 6

# CONCLUSION

The goal of this dissertation rests in developing a better understanding of soil erosion in the geomorphic setting of desert piedmonts, both erosional pediments and depositional alluvial fans. The study area of piedmonts in what is now the Phoenix metropolitan region broadly experienced four very different periods of land use history: the natural landscape prior to human alteration; hunter-gatherer indigenous use followed by Hohokam urbanization near the Salt River; cattle grazing associated with Euro-American settlement since the 19$^{th}$ century; and urban growth that accelerated greatly since the advent of air conditioning in second half of the 20th (Gober and Trapido-Lurie, 2005; Sheridan, 2007). The hunter-gatherers and Hohokam indigenous land use did not focus on the pediments and alluvial fans, but rather on the urban core adjacent to the Salt River. Thus, this dissertation explores soil erosion in the 'natural background' period, in the cattle grazing period, and in the urban sprawl period.

The major findings of research are as follows:

1) (CHAPTER 2) Before massive land-use change associated with cattle grazing and urban expansion, desert piedmonts of alluvial fans and pediments experienced very different surface conditions than found by the average hiker today. Extensive areas once hosted desert pavements, biological soil crusts, and interlocking colluvium on steeper slopes, providing a net armoring effect. Today, only patches of such armored surfaces remain due to the anthropogenic impacts.

2) (CHAPTER 3) Human activities (i.e. devegetation, livestock grazing, invasive plant species, road building) led to an overall increase in erosion process intensity in the Sonoran Desert and the Phoenix metropolitan region. Compared to the period of cattle grazing, the process of urbanization in the Sonoran Desert increased soil erosion from urban-proximate wildfires by up to 4.2x, from exposure of bare ground due to home and commercial real estate development by up to 3.4x, from bare ground exposure due to road and pipeline construction by up to 3.1x over grazing alone.
3) (CHAPTER 3) Stock pond watersheds underlain by granitic rock experienced statistically significant higher erosion rates compared to watersheds underlain by metamorphic, basalt, and other rock types. This statistically significant result, however, is autocorrelated with slope as granitic pediments are underwent a base-level lowering when the Salt and Verde rivers integrated.
4) (CHAPTER 3) A new global compilation of published and unpublished sediment yield data for warm desert (BWh Köppen-Geiger) sites reveals that data from the Phoenix piedmont watersheds plot consistently with other grazing study areas with an overall slight tendency for higher area-specific sediment yields in smaller drainage areas. However, our sediment yield data, as well as data form other warm desert sites, do not support previously published generalizations of anomalously high or low sediment yields from warm desert settings.
5) (CHAPTER 3) Although the geomorphic setting surrounding different warm desert cities undergoing expansion differs, these results highlight the importance

of exposure of bare ground in increasing soil erosion even in an environment with naturally abundant bare ground.

6) (CHAPTER 4) There are environmental and infrastructural management issues associated with erosion and sediment yield in rapidly urbanizing desert cities. A growing need for flood control in rapidly urbanizing desert cities has led to resilient urban planning efforts to build and manage flood control structures, but there has been increased concern over flood control structures sustainability in rapidly urbanizing desert cities mainly derived from sediment accumulation problem behind flood control structures that can reduce usable capacity even before reservoirs completely filled with sediment. The sedimentation problem is closely linked to the land use–land cover change in urban systems because bare ground exposure associated with urban growth has increased one to two order of soil erosion depending on prior land use on global basis and the eroded soils will be transported by water and eventually will be stored in flood control structures.
7) (CHAPTER 4) Forecasting reliable sediment yield under urban sprawl conditions is a desired outcome for rapidly urbanizing desert cities. The proposed model to predict reliable sediment yield behind flood control structures using the relationship between annual urban growth rate and sediment yield, has the potential to help rapidly urbanizing desert cities reduce the costs of building flood control structures by relying on basic relationships instead of establishing a network of empirical research sites.
8) (CHAPTER 5) The Phoenix metropolitan region offers the context for the first comparison of soil erosion from urbanization to natural background rates of

erosion measured through cosmogenic $^{10}$Be catchment-wide denudation rates. No other direct comparisons exist for the same watersheds impacted by urbanization and measured by CWDR. Through exposure of bare ground from 1989 to 2013, urban sprawl accelerated erosion 1.3x to 15x above natural background rates of ~ 76 Mg km$^{-2}$ yr$^{-1}$ for the Phoenix metropolitan region, Sonoran Desert, USA. This acceleration likely represents a minimum potential impact because drought conditions occurred during the historic monitoring period.

9) (CHAPTER 5) A spatial model reveals patterns of urban acceleration of soil erosion at the sprawling perimeter of the Phoenix region from 1912 to 2010. The background erosion rates for Phoenix metropolitan region range from 3 to 436 Mg km$^{-2}$ yr$^{-1}$ with a mean of 115 Mg km$^{-2}$ yr$^{-1}$ and median of 90 Mg km$^{-2}$ yr$^{-1}$. In contrast, the urban acceleration of erosion ranged from 101 to 8803 Mg km$^{-2}$ yr$^{-1}$ with a mean of 651 Mg km$^{-2}$ yr$^{-1}$ and median of 245 Mg km$^{-2}$ yr$^{-1}$, and the total urban acceleration of erosion above natural background for Phoenix metropolitan region range from 0.5 to 527x with a mean of 26x and median of 3x.

10) (CHAPTER 5) If we relax the need to compare the exact same watersheds analyzed for urban effects and CWDR, then it becomes possible to compare CWDR-analyzed watersheds near other urban centers. In a comparison of literature-based CWDR and urban erosive effects, this Phoenix case study rests on the lower end of urban acceleration above background rates of erosion associated with urban centers in different climatic regions.

11) In analyzing and reviewing geomorphology literature associated with the Anthropocene, Brown et al. (2017) wrote that “the less obvious effects of humans

on geomorphic systems warrant increased research". This statement certainly applies to the north-central Sonoran Desert. Brown et al. (2017)'s analysis connections between the Anthropocene and geomorphology largely eschewed the sorts of low-slope desert piedmonts found in the Sonoran Desert. Yet when researchers explore the envelope of anthropogenic effects, it can become extraordinarily useful to look at the non-spectacular cases that rarely make news reports in *Science* or *Nature*. Based on the findings of this dissertation, the lower end of urbanization's impact on soil erosion does appear to indeed be low-slope piedmonts of the Sonoran Desert. Yet even in this relatively tranquil setting, urbanization's acceleration impact can be tremendous, sometimes reaching over an order of magnitude.

# REFERENCES


Abdullah, M., Feagin, R., & Musawi, L. (2017). The use of spatial empirical models to estimate soil erosion in arid ecosystems. *Environmental Monitoring and Assessment, 189*(2), 78.

Abrahams, A. D., Parsons, A. J., & Hirsh, P. J. (1985). Hillslope gradient-particle size relations: evidence for the formation of debris slopes by hydraulic processes in the Mojave Desert. *The Journal of Geology*, *93*(3), 347-357.

Abrahams, A. D., Parsons, A. J., & Luk, S. H. (1988). Hydrologic and sediment responses to simulated rainfall on desert hillslopes in southern Arizona. *Catena*, *15*(2), 103-117.

Adelsberger, K. A., Smith, J. R., McPherron, S. P., Dibble, H. L., Olszewski, D. I., Schurmans, U. A., & Chiotti, L. (2013). Desert pavement disturbance and artifact taphonomy: a case study from the Eastern Libyan Plateau, Egypt. *Geoarchaeology*, *28*(2), 112-130.

Al-Ahmadi, K., Heppenstall, A., Hogg, J., & See, L. (2009). A fuzzy cellular automata urban growth model (FCAUGM) for the city of Riyadh, Saudi Arabia. Part 2: scenario testing. *Applied Spatial Analysis and Policy*, *2*(2), 85–105.

Alqurashi, A. F., & Kumar, L. (2014). Land use and land cover change detection in the Saudi Arabian desert cities of Makkah and Al-Taif using satellite data. *Advances in Remote Sensing*, *3*(3), 106–119.

Alqurashi, A., Kumar, L., & Al-Ghamdi, K. (2016). Spatiotemporal modeling of urban growth predictions based on driving force factors in five Saudi Arabian cities. *ISPRS International Journal of Geo-Information*, *5*(8), 139.

Al-Awadhi, J. M., Omar, S. A., & Misak, R. F. (2005). Land degradation indicators in Kuwait. *Land Degradation & Development*, *16*(2), 163–176.

Allen, C. D., Betancourt, J. L., & Swetnam, T. W. (1998). Landscape changes in the southwestern United States: techniques, long-term data sets, and trends. *Perspectives on the Land-Use History of North America: A Context for Understanding Our Changing Environment. Fort Collins (CO): US Geological Survey*, 71-84.

Allen, C. D. (2005). Micrometeorology of a smooth and rugose biological soil crust near Coon Bluff, Arizona. *Journal of the Arizona-Nevada Academy of Science*, 21-28.

Allen, C. D. (2010). Biogeomorphology and biological soil crusts: a symbiotic research relationship. *Géomorphologie: relief, processus, environnement*, *16*(4), 347-358.

Amogu, O. (2009). La dégradation des espaces sahéliens et ses conséquences sur l'alluvionnement du fleuve Niger moyen.

Annandale, G. W. (2006). Reservoir sedimentation. *Encyclopedia of Hydrological Sciences*.

Applegarth, M. T. (2004). Assessing the influence of mountain slope morphology on pediment form, south-central Arizona. *Physical Geography*, *25*(3), 225-236.

Arnold, J. G., Srinivasan, R., Muttiah, R. S., & Williams, J. R. (1998). Large area hydrologic modeling and assessment part I: model development 1. *JAWRA Journal of the American Water Resources Association*, *34*(1), 73–89.

Baddock, M. C., Strong, C. L., Murray, P. S., & McTainsh, G. H. (2013). Aeolian dust as a transport hazard. *Atmospheric environment*, *71*, 7-14.

Bahat, D., Grossenbacher, K., & Karasaki, K. (1999). Mechanism of exfoliation joint formation in granitic rocks, Yosemite National Park. *Journal of Structural Geology*, *21*(1), 85-96.

Balaguer-Puig, M., Marqués-Mateu, Á., Lerma, J. L., & Ibáñez-Asensio, S. (2018). Quantifying small-magnitude soil erosion: Geomorphic change detection at plot scale. *Land Degradation & Development*, *29*(3), 825–834.

Balamurugan, G. (1991). Tin mining and sediment supply in Peninsular Malaysia with special reference to the Kelang River basin. *Environmentalist*, *11*(4), 281–291.

Balch, J. K., Bradley, B. A., D'Antonio, C. M., & Gómez-Dans, J. (2013). Introduced annual grass increases regional fire activity across the arid western USA (1980-2009). *Global Change Biology*, *19*(1), 173–183.

Balco, G., Stone, J. O., Lifton, N. A., & Dunai, T. J. (2008). A complete and easily accessible means of calculating surface exposure ages or erosion rates from 10Be and 26Al measurements. *Quaternary Geochronology*, *3*(3), 174–195.

Banville, M. J., & Bateman, H. L. (2012). Urban and wildland herpetofauna communities and riparian microhabitats along the Salt River, Arizona. *Urban Ecosystems*, *15*(2), 473–488.

Barbero-Sierra, C., Marques, M.-J., & Ruíz-Pérez, M. (2013). The case of urban sprawl in Spain as an active and irreversible driving force for desertification. *Journal of Arid Environments*, *90*, 95–102.

Bateman, H. L., Stromberg, J. C., Banville, M. J., Makings, E., Scott, B. D., Suchy, A., & Wolkis, D. (2015). Novel water sources restore plant and animal communities along an urban river. *Ecohydrology*, *8*(5), 792–811.

Bellin, N., VanAcker, V., Wesemael B., van, Solé-Benet, A., & Bakker, M. M. (2011). Natural and anthropogenic controls on soil erosion in the internal betic Cordillera (southeast Spain), (2), 190–8162.

Belnap, J. (2003). The world at your feet: desert biological soil crusts. *Frontiers in Ecology and the Environment*, *1*(4), 181-189.

Belnap, J., Büdel, B., & Lange, O. L. (2001). Biological soil crusts: characteristics and distribution. In *Biological soil crusts: structure, function, and management* (pp. 3-30). Springer, Berlin, Heidelberg.

Belnap, J., & Gillette, D. A. (1998). Vulnerability of desert biological soil crusts to wind erosion: the influences of crust development, soil texture, and disturbance. *Journal of arid environments*, *39*(2), 133-142.

Bierman, P. R., Reuter, J. M., Pavich, M., Gellis, A. C., Caffee, M. W., & Larsen, J. (2005). Using cosmogenic nuclides to contrast rates of erosion and sediment yield in a semi-arid, arroyo-dominated landscape, Rio Puerco Basin, New Mexico. *Earth Surface Processes and Landforms: The Journal of the British Geomorphological Research Group*, *30*(8), 935–953.

Billi, P., & el Badri Ali, O. (2010). Sediment transport of the Blue Nile at Khartoum. *Quaternary International*, *226*(1–2), 12–22.

Blake, G. R. (1965). Bulk Density 1. In C. A. Black, D. D. Evans, L. E. White, L. E. Engsminger, & F. E. Clark (Eds.), *Methods of soil analysis. Part 1. Physical and mineralogical properties, including statistics of measurement and sampling* (pp. 374–390). Maddison, WI: American Society of Agronomy.

Boardman, J. (2006). Soil erosion science: Reflections on the limitations of current approaches. *Catena*, *68*(2–3), 73–86.

Booth, W. E. (1941). Algae as pioneers in plant succession and their importance in erosion control. *Ecology*, *22*(1), 38–46.

Borrelli, P., Van Oost, K., Meusburger, K., Alewell, C., Lugato, E., & Panagos, P. (2018). A step towards a holistic assessment of soil degradation in Europe: Coupling on-site erosion with sediment transfer and carbon fluxes. *Environmental Research*, *161*, 291–298.

Bouyoucos, G. J. (1962). Hydrometer Method Improved for Making Particle Size Analyses of Soils 1. *Agronomy Journal*, *54*(5), 464.

Bowker, M. A., Belnap, J., Chaudhary, V. B., & Johnson, N. C. (2008). Revisiting classic water erosion models in drylands: the strong impact of biological soil crusts. *Soil Biology and Biochemistry*, *40*(9), 2309-2316.

Brazel, A. J. (1989). Dust and climate in the American Southwest. In *Paleoclimatology and paleometeorology: Modern and past patterns of global atmospheric transport* (pp. 65-96). Springer, Dordrecht.

Brown, A. G., Tooth, S., Bullard, J. E., Thomas, D. S. G., Chiverrell, R. C., Plater, A. J., … Rose, J. (2017). The geomorphology of the Anthropocene: emergence, status and implications. *Earth Surface Processes and Landforms*, *42*(1), 71–90.

Bullard, J. E., & Livingstone, I. (2002). Interactions between aeolian and fluvial systems in dryland environments. *Area*, *34*(1), 8-16.

Cafferata, P., & Cafferata, P. H. (2004). *Designing Watercourse Crossings for Passage of 100 Year Flood Flows, Wood, and Sediment*. California Department of Forestry and Fire Protection.

Chaney, R. L., Ryan, J. A., Li, Y.-M., & Brown, S. L. (1999). Soil cadmium as a threat to human health. In *Cadmium in soils and plants* (pp. 219–256). Springer.

Chin, A. (2006). Urban transformation of river landscapes in a global context. *Geomorphology*, *79*(3–4), 460–487.

Chow, W. T. L., Salamanca, F., Georgescu, M., Mahalov, A., Milne, J. M., & Ruddell, B. L. (2014). A multi-method and multi-scale approach for estimating city-wide anthropogenic heat fluxes. *Atmospheric Environment*, *99*, 64–76.

Church, M., Ham, D., Hassan, M., & Slaymaker, O. (1999). Fluvial clastic sediment yield in Canada: scaled analysis. *Canadian Journal of Earth Sciences*, *36*(8), 1267–1280.

Church, M., & Slaymaker, O. (1989). Disequilibrium of Holocene sediment yield in glaciated British Columbia. *Nature*, *337*(6206), 452.

Clapp, E. M., Bierman, P. R., Nichols, K. K., Pavich, M., & Caffee, M. (2001). Rates of sediment supply to arroyos from upland erosion determined using in situ produced cosmogenic 10 Be and 26 Al. *Quaternary Research*, *55*(2), 235–245.

Clapp, E. M., Bierman, P. R., Schick, A. P., Lekach, J., Enzel, Y., & Caffee, M. (2000). Sediment yield exceeds sediment production in arid region drainage basins. *Geology*, *28*(11), 995-998.

Clark, H. F., Brabander, D. J., & Erdil, R. M. (2006). Sources, sinks, and exposure pathways of lead in urban garden soil. *Journal of Environmental Quality*, *35*(6), 2066–2074.

Coney, P. J., & Harms, T. A. (1984). Cordilleran metamorphic core complexes: Cenozoic extensional relics of Mesozoic compression. *Geology*, *12*(9), 550-554.

Cooke, R. U., Brunsden, D., Doornkamp, J. C. & Jones, D. (1982). *Urban geomorphology in drylands.* Oxford: Oxford University Press.

Croke, J., Bartley, R., Chappell, J., Austin, J. M., Fifield, K., Tims, S. G., … Furuichi, T. (2015). 10Be-derived denudation rates from the Burdekin catchment: The largest contributor of sediment to the Great Barrier Reef. *Geomorphology*, *241*, 122–134.

Croke, J., & Mockler, S. (2001). Gully initiation and road-to-stream linkage in a forested catchment, southeastern Australia. *Earth Surface Processes and Landforms: The Journal of the British Geomorphological Research Group*, *26*(2), 205–217.

De Vente, J., Poesen, J., Arabkhedri, M., & Verstraeten, G. (2007). The sediment delivery problem revisited. *Progress in Physical Geography*, *31*(2), 155–178.

d'Amour, C. B., Reitsma, F., Baiocchi, G., Barthel, S., Güneralp, B., Erb, K.-H., … Seto, K. C. (2017). Future urban land expansion and implications for global croplands. *Proceedings of the National Academy of Sciences*, *114*(34), 8939–8944.

Dedkov, A. (2004). The relationship between sediment yield and drainage basin area. *IAHS PUBLICATION*, *288*, 197–204.

Dedkov, A., & Mozzherin, V. (1984). Erosia i Stok Nanosov na Zemle (Erosion and sediment yield on the Earth). Izdatelstvo Kazanskogo Universiteta, 264 pp. *Russian with an English Summary*.

Dedkov, A. P., & Moszherin, V. I. (1992). Erosion and sediment yield in mountain regions of the world. *Erosion, Debris Flows and Environment in Mountain Regions*, *209*, 29–36.

Dendy, F. E., & Bolton, G. C. (1976). Sediment yield-runoff-drainage area relationships in the United States. *Journal of Soil and Water Conservation*.

Dietze, M., Dietze, E., Lomax, J., Fuchs, M., Kleber, A., & Wells, S. G. (2016). Environmental history recorded in aeolian deposits under stone pavements, Mojave Desert, USA. *Quaternary Research*, *85*(1), 4-16.

Djordjević, S., Butler, D., Gourbesville, P., Mark, O., & Pasche, E. (2011). New policies to deal with climate change and other drivers impacting on resilience to flooding in urban areas: the CORFU approach. *Environmental Science & Policy*, *14*(7), 864–873.

Dohrenwend, J. C., & Parsons, A. J. (2009). Pediments in arid environments. In *Geomorphology of desert environments* (pp. 377-411). Springer, Dordrecht.

Dorn, R. I. (2014). Chronology of rock falls and slides in a desert mountain range: Case study from the Sonoran Desert in south-central Arizona. *Geomorphology*, *223*, 81-89.

Dorn, R. I. (2012). Do debris flows pose a hazard to mountain-front property in metropolitan Phoenix, Arizona?. *The Professional Geographer*, *64*(2), 197-210.

Dorn, R. I. (2016). Identification of debris-flow hazards in warm deserts through analyzing past occurrences: Case study in South Mountain, Sonoran Desert, USA. *Geomorphology*, *273*, 269-279.

Dorn, R.I. (2015). Impact of consecutive extreme rainstorm events on particle transport: Case study in a Sonoran Desert range, western USA. *Geomorphology* 250: 53-62.

Dorn, R. I. (2011). Revisiting dirt cracking as a physical weathering process in warm deserts. *Geomorphology*, *135*(1-2), 129-142.

Dorn, R. I., Moore, G., Pagán, E. O., Bostwick, T. W., King, M., & Ostapuk, P. (2012). Assessing early Spanish explorer routes through authentication of rock inscriptions. *The Professional Geographer*, *64*(3), 415-429.

Dorn, R. I., & Oberlander, T. M. (1982). Rock varnish. *Progress in Physical Geography*, *6*(3), 317-367.

Douglas, I., & Lawson, N. (2000). The human dimensions of geomorphological work in Britain. *Journal of Industrial Ecology*, *4*(2), 9–33.

Eagar, J. D., Herckes, P., & Hartnett, H. E. (2017). The characterization of haboobs and the deposition of dust in Tempe, AZ from 2005 to 2014. *Aeolian Research*, *24*, 81-91.

East Maricopa Natural Resource Conservation District (EMNRCD) and Flood Control District of Maricopa County (FCDMC). (2013). FINAL SUPPLEMENTAL WATERSHED PLAN AND ENVIRONMENTAL ASSESSMENT FOR THE POWERLINE FLOOD RETARDING STRUCTURE. (http://apps.fcd.maricopa.gov/Projects/PPM/downloads/PVR/VineyardRittenhouseFinalSuppWatershedPlanandEASigned.pdf)

Einsele, G., & Hinderer, M. (1997). Terrestrial sediment yield and the lifetimes of reservoirs, lakes, and larger basins. *Geologische Rundschau* 86: 288-310.

Eldridge, D. J. (1993). Cryptogam cover and soil surface condition: effects on hydrology on a semiarid woodland soil. *Arid Land Research and Management*, *7*(3), 203–217.

Elvidge, C. D., & Moore, C. B. (1980). Restoration of petroglyphs with artificial desert varnish. *Studies in Conservation*, *25*(3), 108-117.

Ewan, J., Ewan, R. F., & Burke, J. (2004). Building ecology into the planning continuum: case study of desert land preservation in Phoenix, Arizona (USA). *Landscape and Urban Planning*, *68*(1), 53-75.

Faist, A. M., Herrick, J. E., Belnap, J., Van Zee, J. W., & Barger, N. N. (2017). Biological soil crust and disturbance controls on surface hydrology in a semi-arid ecosystem. *Ecosphere*, *8*(3).

Fan, C., Myint, S. W., Rey, S. J., & Li, W. (2017). Time series evaluation of landscape dynamics using annual Landsat imagery and spatial statistical modeling: Evidence from the Phoenix metropolitan region. *International Journal of Applied Earth Observation and Geoinformation*, *58*, 12-25.

FAO. (2008). AQUASTAT Global River Sediment Yields Database. (http://www.fao.org/nr/water/aquastat/sediment/index.stm) (accessed: Feb 9, 2019)

Fathizad, H., Karimi, H., & Alibakhshi, S. M. (2014). The estimation of erosion and sediment by using the RUSLE model and RS and GIS techniques (Case study: Arid and semi-arid regions of Doviraj, Ilam province, Iran). *International Journal of Agriculture and Crop Sciences*, *7*(6), 303.

FEMA. (_____). THE 100 YEAR FLOOD MYTH. (https://training.fema.gov/hiedu/docs/hazrm/handout%203-5.pdf)

Ferreira, C. S. S., Walsh, R. P. D., Blake, W. H., Kikuchi, R., & Ferreira, A. J. D. (2017). Temporal Dynamics of Sediment Sources in an Urbanizing Mediterranean Catchment. *Land Degradation & Development*, *28*(8), 2354–2369.

Fleischner, T. L. (2010). Livestock grazing and wildlife conservation in the American West: historical policy and conservation biology perspectives. *Wild Rangelands: Conserving Wildlife While Maintaining Livestock in Semi-Arid Ecosystems*, 235–265.

Fletcher, J. E. (1960). Some effects of plant growth on infiltration in the southwest. *Water Yield in Relation to Environment in the Southwestern US*, 51–63.

Fletcher, J. E., & Martin, W. P. (1948). Some effects of algae and molds in the rain-crust of desert soils. *Ecology*, *29*(1), 95–100.

Flood Control District of Maricopa County (FCDMC). (2006). Annual Report Fiscal Year 2005/2006 McMicken Dam Fissure Risk Zone Remediation Project. (https://www.maricopa.gov/ArchiveCenter/ViewFile/Item/798)

Flood Control District of Maricopa County (FCDMC). (2015b). Dam Safety Program. *Annual ASCE/ASHE State Conference.*

Flood Control District of Maricopa County (FCDMC). (2015c). Drainage Design Manual for Maricopa County Erosion Control (https://www.maricopa.gov/4324/Download)

Flood Control District of Maricopa County (FCDMC). (2015a). Drainage Design Manual for Maricopa County Hydraulics (https://www.maricopa.gov/4324/Download)

Flood Control District of Maricopa County (FCDMC). (2010a). Sediment Yield Estimation for Powerline Flood Retarding Structure.

Flood Control District of Maricopa County (FCDMC). (2010c). Sediment Yield Estimation for Rittenhouse Flood Retarding Structure.

Flood Control District of Maricopa County (FCDMC). (2010b). Sediment Yield Estimation for Vineyard Road Flood Retarding Structure.

Fuller, J. E. (1990). Misapplication of the FEMA alluvial fan model: A case history. In *Hydraulics/Hydrology of Arid Lands (H²AL)* (pp. 367-372). New York: American Society Civil Engineers.

Fuller, J. E. (2012). Evaluation of avulsion potential on active alluvial fans in central and western Arizona. *Arizona Geological Survey, Contributed Report*, *12*.

Fox, H. L. (1976). The urbanizing river: a case study in the Maryland Piedmont. *Geomorphology and Engineering*, 245–271.

Gallaire, R. (1986). Le Niger à Kandadji: Synthèse des EtudesRep. *ORSTOM, Paris*.

Garba, S. B. (2004). Managing urban growth and development in the Riyadh metropolitan area, Saudi Arabia. *Habitat International*, *28*(4), 593–608.

Gellis, A. C., Pavich, M. J., Bierman, P. R., Clapp, E. M., Ellevein, A., & Aby, S. (2004). Modern sediment yield compared to geologic rates of sediment production in a semi-arid basin, New Mexico: assessing the human impact. *Earth Surface Processes and Landforms: The Journal of the British Geomorphological Research Group*, *29*(11), 1359–1372.

Georgescu, M., Miguez-Macho, G., Steyaert, L. T., & Weaver, C. P. (2009). Climatic effects of 30 years of landscape change over the Greater Phoenix, Arizona, region: 1. Surface energy budget changes. *Journal of Geophysical Research: Atmospheres*, *114*(D5).

Gilbert, G. K. (1877). *Geology of the Henry mountains*. Washington D.C.: U.S. Geological and Geographical Survey.

Gillespie, N., Unthank, A., Campbell, L., Anderson, P., Gubernick, R., Weinhold, M., … Wells, S. (2014). Flood effects on road–stream crossing infrastructure: economic and ecological benefits of stream simulation designs. *Fisheries*, *39*(2), 62–76.

Glacken, C. J. (1967). *Traces on the Rhodian shore: Nature and culture in Western thought from ancient times to the end of the eighteenth century* (Vol. 170). Univ of California Press.

Gober, P., & Burns, E. K. (2002). The size and shape of Phoenix's urban fringe. *Journal of Planning Education and Research*, *21*(4), 379–390.

Gober, P., & Trapido-Lurie, B. (2005). *Metropolitan Phoenix: Place making and community building in the desert*. University of Pennsylvania Press.

Goudie, A. S. (2014). Desert dust and human health disorders. *Environment international*, *63*, 101-113.

Goudie, A. S., & Viles, H. A. (2016). *Geomorphology in the Anthropocene*. Cambridge University Press.

Graf, W. L. (1988). *Fluvial processes in dryland rivers* (p. 346). New York: Springer-Verlag.

Graf, W. L., Wohl, E., Sinha, T., & Sabo, J. L. (2010). Sedimentation and sustainability of western American reservoirs. *Water Resources Research*, *46*(12).

Granger, D. E., Riebe, C. S., Kirchner, J. W., & Finkel, R. C. (2001). Modulation of erosion on steep granitic slopes by boulder armoring, as revealed by cosmogenic 26Al and 10Be. *Earth and Planetary Science Letters*, *186*(2), 269-281.

Griffiths, P. G., Hereford, R., & Webb, R. H. (2006). Sediment yield and runoff frequency of small drainage basins in the Mojave Desert, USA. *Geomorphology*, *74*(1–4), 232–244.

Grimm, N. B., Redman, C. L., Boone, C. G., Childers, D. L., Harlan, S. L., & Turner, B. L. (2013). Viewing the urban socio-ecological system through a sustainability lens: Lessons and prospects from the central Arizona–Phoenix LTER programme. In *Long term socio-ecological research* (pp. 217–246). Springer.

Haff, P.K., (2010). Hillslopes, rivers, plows, and trucks: mass transport on Earth's surface by natural and technological processes. *Earth Surf. Process. Landforms 35*, 1157–1166.

Hale, R. L., Turnbull, L., Earl, S. R., Childers, D. L., & Grimm, N. B. (2015). Stormwater infrastructure controls runoff and dissolved material export from arid urban watersheds. *Ecosystems*, *18*(1), 62–75.

Hall, S. J., Ahmed, B., Ortiz, P., Davies, R., Sponseller, R. A., & Grimm, N. B. (2009). Urbanization alters soil microbial functioning in the Sonoran Desert. *Ecosystems*, *12*(4), 654–671.

Hall, K., Thorn, C., & Sumner, P. (2012). On the persistence of ‘weathering’. *Geomorphology*, *149*, 1-10.

Harper, K. T., & Marble, J. R. (1988). A role for nonvascular plants in management of arid and semiarid rangelands. In *Vegetation science applications for rangeland analysis and management* (pp. 135–169). Springer.

Harper, K. T., & St Clair, L. L. (1985). *Cryptogamic Soil Crusts on Arid and Semiarid Rangelands in Utah: Effects of Seedling Establishment and Soil Stability-Final Report.: Final Report on BLM Contact No. BLM AA 851-CTI-48*. Department of Botany and Range Science, Provo, Utah, USA.

Harris, R. C., & Pearthree, P. A. (2002). *A Home Buyer's Guide to Geologic Hazards in Arizona* (Vol. 13). Arizona Geological Survey.

Haregeweyn, N., Fikadu, G., Tsunekawa, A., Tsubo, M., & Meshesha, D. T. (2012). The dynamics of urban expansion and its impacts on land use/land cover change and small-scale farmers living near the urban fringe: A case study of Bahir Dar, Ethiopia. *Landscape and Urban Planning*, *106*(2), 149–157.

Heisinger, B., Lal, D., Jull, A. J. T., Kubik, P., Ivy-Ochs, S., Knie, K., & Nolte, E. (2002a). Production of selected cosmogenic radionuclides by muons: 2. Capture of negative muons. *Earth and Planetary Science Letters*, *200*(3–4), 357–369.

Heisinger, B., Lal, D., Jull, A. J. T., Kubik, P., Ivy-Ochs, S., Neumaier, S., … Nolte, E. (2002b). Production of selected cosmogenic radionuclides by muons: 1. Fast muons. *Earth and Planetary Science Letters*, *200*(3–4), 345–355.

Hewawasam, T., von Blanckenburg, F., Schaller, M., & Kubik, P. (2003). Increase of human over natural erosion rates in tropical highlands constrained by cosmogenic nuclides. *Geology*, *31*(7), 597–600.

Holt, W. E., Chase, C. G., & Wallace, T. C. (1986). Crustal structure from three-dimensional gravity modeling of a metamorphic core complex: A model for uplift, Santa Catalina–Rincon mountains, Arizona. *Geology*, *14*(11), 927-930.

Hooke, R.L., (1994). On the efficacy of humans as geomorphic agents. *GSA Today 4*, 217.

Hooke, R., (1999). Spatial distribution of human geomorphic activity in the United States: comparison with rivers. *Earth Surf. Process. Landforms 24*, 687–692.

House, P. K. (2005). Using geology to improve flood hazard management on alluvial fans - an example from Laughlin Nevada. *Journal of the American Water Resources Association*, *41*(6), 1431-1447.

Howard, A. D., & Selby, M. J. (2009). Rock slopes. In *Geomorphology of desert environments (pp. 189-232). Springer, Dordrecht.*

Hyers, A. D., & Marcus, M. G. (1981). Land use and desert dust hazards in central Arizona. *Pe we, TL (Ed.), Desert Dust: Origin, Characteristics, and Effect on Man. Geological Society of America, Boulder, Colorado*, 267-280.

Idso, S. B., Ingram, R. S., & Pritchard, J. M. (1972). An American haboob. *Bulletin of the American Meteorological Society*, *53*(10), 930-935.

*Iverson, R. M. (2005).* Debris-flow mechanics. In Savage, W., Baum, R (Eds.), *Debris-flow hazards and related phenomena* (pp. 105-134). Berlin: Springer.

Jakob, M., Hungr, O., & Jakob, D. M. (2005). *Debris-flow hazards and related phenomena* (Vol. 739). Berlin: Springer.

Jansson, M. B. (1988). A global survey of sediment yield. *Geografiska Annaler, Series A*, *70*(1–2), 81–98. https://doi.org/10.1080/04353676.1988.11880241

JE Fuller Hydrology and Geomorphology, Inc. (2008). Desert Drive Area Study, Volume II Existing Conditions Inundation and Sedimentation Analysis.

Jeong, A., Cheung, S. Y., Walker, I. J., & Dorn, R. I. (2018a). Urban geomorphology of an arid city: case study of Phoenix, Arizona. In *Urban Geomorphology* (pp. 177-204). Elsevier. https://doi.org/10.1016/B978-0-12-811951-8.00010-2

Jeong, A., & Dorn, R. I. (2019). Soil erosion from urbanization processes in the Sonoran Desert, Arizona, USA. *Land Degradation & Development*, *30*(2), 226–238. https://doi.org/10.1002/ldr.3207

Jeong, A., Lee, J. I., Seong, Y. B., Balco, G., Yoo, K.-C., Yoon, H. I., … Yu, B. Y. (2018b). Late Quaternary deglacial history across the Larsen B embayment, Antarctica. *Quaternary Science Reviews*, *189*, 134-148. https://doi.org/10.1016/j.quascirev.2018.04.011

John, M. K. (1973). Cadmium uptake by eight food crops as influenced by various soil levels of cadmium. *Environmental Pollution (1970)*, *4*(1), 7–15.

Jungerius, P. D., Matundura, J., & Van De Ancker, J. A. M. (2002). Road construction and gully erosion in West Pokot, Kenya. *Earth Surface Processes and Landforms*, *27*(11), 1237–1247.

Kesel, R.H. (1977). Some aspects of the geomorphology of inselbergs in central Arizona, USA. *Zeitschrift für Geomorphologie*, *21*, 119–46.

Kidron, G. J., Barinova, S., & Vonshak, A. (2012). The effects of heavy winter rains and rare summer rains on biological soil crusts in the Negev Desert. *Catena*, *95*, 6–11.

Kinoshita, T., & Yamazaki, Y. (1974). Increase of sediment transport due to large-scale urbanization. *IAHS Publ*, *113*, 130–136.

Kohl, C. P., & Nishiizumi, K. (1992). Chemical isolation of quartz for measurement of in-situ-produced cosmogenic nuclides. *Geochimica et Cosmochimica Acta*, *56*(9), 3583–3587.

Kondolf, G. M., Gao, Y., Annandale, G. W., Morris, G. L., Jiang, E., Zhang, J., … Guo, Q. (2014). Sustainable sediment management in reservoirs and regulated rivers: Experiences from five continents. *Earth's Future*, *2*(5), 256–280.

Kraft, M. E., & Scheberle, D. (1995). Environmental justice and the allocation of risk: the case of lead and public health. *Policy Studies Journal*, *23*(1), 113–122.

Laflen, J. M., Lane, L. J., & Foster, G. R. (1991). WEPP: A new generation of erosion prediction technology. *Journal of Soil and Water Conservation*, *46*(1), 34–38.

Lagerwerff, J. V, & Specht, A. W. (1970). Contamination of roadside soil and vegetation with cadmium, nickel, lead, and zinc. *Environmental Science & Technology*, *4*(7), 583–586.

Lahlou, A. (1996). Environmental and socio-economic impacts of erosion and sedimentation in North Africa. *IAHS Publications-Series of Proceedings and Reports-Intern Assoc Hydrological Sciences*, *236*, 491–500.

Lal, D. (1991). Cosmic ray labeling of erosion surfaces: in situ nuclide production rates and erosion models. *Earth and Planetary Science Letters*, *104*(2–4), 424–439.

Lal, R. (1994). Global overview of soil erosion. In C. R. R.S. Baker, G.W. Gee (Ed.), *Soil and Water Science: Key to Understanding our Global Environment*. Maddison, WI: Soil Science Society of America.

Lane, L. J., Kidwell, M. R., & Weltz, M. A. (2000). Watershed sediment yield and rangeland health. *International Journal of Sediment Research*, *15*(1), 51–59.

Langbein, W., Hains, C., & Culler, R. (1951). Hydrology of stock-water reservoirs in Arizona. *U.S. Geological Survey Circular*, (110), 1–18.

Lanphear, B. P., Weitzman, M., & Eberly, S. (1996). Racial differences in Urban children's environmental exposures to lead. *American Journal of Public Health*, *86*(10), 1460–1463.

Laronne, J. B. (1990). Probability distribution of event sediment yields in the northern Negev, Israel. In *Soil erosion on agricultural land. Proceedings of a workshop sponsored by the British Geomorphological Research Group, Coventry, UK, January 1989.* (pp. 481–492). John Wiley & Sons Ltd.

Larson, P. H., Dorn, R. I., Palmer, R. E., Bowles, Z., Harrison, E., Kelley, S., ... & Douglass, J. (2014). Pediment response to drainage basin evolution in south-central Arizona. *Physical Geography*, *35*(5), 369-389.

Larson, P. H., Kelley, S. B., Dorn, R. I., & Seong, Y. B. (2016). Pace of Landscape Change and Pediment Development in the Northeastern Sonoran Desert, United States. *Annals of the American Association of Geographers*, *106*(6), 1195-1216.

Leopold, L. B. (1968). *Hydrology for urban land planning: A guidebook on the hydrologic effects of urban land use* (Vol. 554). US Department of the Interior, Geological Survey.

Li, J., Deng, J., Gu, Q., Wang, K., Ye, F., Xu, Z., & Jin, S. (2015). The accelerated urbanization process: A threat to soil resources in eastern China. *Sustainability*, *7*(6), 7137–7155.

Li, J. T., Qiu, J. W., Wang, X. W., Zhong, Y., Lan, C. Y., & Shu, W. S. (2006). Cadmium contamination in orchard soils and fruit trees and its potential health risk in Guangzhou, China. *Environmental Pollution*, *143*(1), 159–165.

Li, P., Mu, X., Holden, J., Wu, Y., Irvine, B., Wang, F., … Sun, W. (2017). Comparison of soil erosion models used to study the Chinese Loess Plateau. *Earth-Science Reviews*, *170*, 17–30.

Liao, K.-H. (2012). A theory on urban resilience to floods—a basis for alternative planning practices. *Ecology and Society*, *17*(4).

Liénou, G. (2007). Impacts de la variabilité climatique sur les ressources en eau et les transports de matières en suspension de quelques bassins versants représentatifs au Cameroun. *These de Doctorat PhD, Université de Yaoundé I*.

Liu, T. (2008). VML dating lab. *http://www.vmldating.com/ last accessed April 22, 2017*.

Liu, T., & Broecker, W. S. (2007). Holocene rock varnish microstratigraphy and its chronometric application in the drylands of western USA. *Geomorphology*, *84*(1-2), 1-21.

Liu, T., & Broecker, W. S. (2013). Millennial-scale varnish microlamination dating of late Pleistocene geomorphic features in the drylands of western USA. *Geomorphology*, *187*, 38-60.

Liu, T., & Broecker, W. S. (2008). Rock varnish microlamination dating of late Quaternary geomorphic features in the drylands of western USA. *Geomorphology*, *93*(3-4), 501-523.

Liu, Y., Zhang, X., Lei, J., & Zhu, L. (2010). Urban expansion of oasis cities between 1990 and 2007 in Xinjiang, China. *International Journal of Sustainable Development & World Ecology*, *17*(3), 253–262.

Lozano-García, M. S., Ortega-Guerrero, B., & Sosa-Nájera, S. (2002). Mid-to late-Wisconsin pollen record of San Felipe basin, Baja California. *Quaternary Research*, *58*(1), 84-92.

Lybrand, R. A., & Rasmussen, C. (2018). Climate, topography, and dust influences on the mineral and geochemical evolution of granitic soils in southern Arizona. *Geoderma*, *314*, 245–261.

Marchamalo, M., Hooke, J. M., & Sandercock, P. J. (2016). Flow and Sediment Connectivity in Semi-arid Landscapes in SE Spain: Patterns and Controls. *Land Degradation & Development*, *27*(4), 1032–1044.

Marcus, M. G., & Brazel, A. J. (1992). Summer dust storms in the Arizona Desert. In Janelle, D. G. (Ed.) *Geographical Snapshots of North America* (pp. 411-415). New York: Guilford Press.

Maricopa County. (2010). Sediment Yield Analysis for Powerline, Vineyard Road and Rittenhouse Flood Retarding Structures (https://members.naco.org/FileUpload/Awards/Storage/2017/107163/2017NACo_PVR_SedimentYieldAnlaysis_finalVersion.pdf)

Maricopa County Flood Control District. (n.d.). Historic Precipitation Data. Retrieved June 5, 2018, from http://alert.fcd.maricopa.gov/showrpts_mc.html

Markus, J., & McBratney, A. B. (2001). A review of the contamination of soil with lead: II. Spatial distribution and risk assessment of soil lead. *Environment International*, *27*(5), 399–411.

Marques, M. J., Bienes, R., Pérez-Rodríguez, R., & Jiménez, L. (2008). Soil degradation in central Spain due to sheet water erosion by low-intensity rainfall events. *Earth Surface Processes and Landforms*, *33*(3), 414–423.

Marsh, G. P. (1864). Man and Nature: Or Physical Geography as Modified by Human Action (New York: C. Scribner).

Martínez-Murillo, J. F., & López-Vicente, M. (2018). Effect of Salvage Logging and Check Dams on Simulated Hydrological Connectivity in a Burned Area. *Land Degradation & Development*, *29*(3), 701–712.

Masoumi, H. E., Hosseini, M., & Gouda, A. A. (2018). Drivers of urban sprawl in two large Middle-eastern countries: literature on Iran and Egypt. *Human Geographies--Journal of Studies & Research in Human Geography*, *12*(1).

McAuliffe, J. R., & Van Devender, T. R. (1998). A 22,000-year record of vegetation change in the north-central Sonoran Desert. *Palaeogeography, Palaeoclimatology, Palaeoecology*, *141*(3-4), 253-275.

McCalla, T. M. (1946). The Influence of Microorganisms and Some Organic Substances on Water Percolation through a Layer of Peorian Loess 1. *Soil Science Society of America Journal*, *10*(C), 175–179.

McClintock, N. (2012). Assessing soil lead contamination at multiple scales in Oakland, California: Implications for urban agriculture and environmental justice. *Applied Geography*, *35*(1–2), 460–473.

McGrath, D., Zhang, C., & Carton, O. T. (2004). Geostatistical analyses and hazard assessment on soil lead in Silvermines area, Ireland. *Environmental Pollution*, *127*(2), 239–248.

McLaughlin, S. P., & Bowers, J. E. (1982). Effects of wildfire on a Sonoran Desert plant community. *Ecology*, 246–248.

Meamarian, H., Tajbakhsh, S. M., & Esmaeilzadeh, H. (2003). The Sediment yield potential estimation of Kashmar urban watershed using MPSIAC model in the GIS framework. In *Proceeding of India map conference* (pp. 22–24). Citeseer.

Melton, M. A. (1965). Debris-covered hillslopes of the southern Arizona desert: consideration of their stability and sediment contribution. *The Journal of Geology*, *73*(5), 715-729.

Michael, D. R., Cunningham, R. B., & Lindenmayer, D. B. (2008). A forgotten habitat? Granite inselbergs conserve reptile diversity in fragmented agricultural landscapes. *Journal of Applied Ecology*, *45*(6), 1742-1752.

Mielke, H. W., & Reagan, P. L. (1998). Soil is an important pathway of human lead exposure. *Environmental Health Perspectives*, *106*(suppl 1), 217–229.

Middleton, N. J., & Sternberg, T. (2013). Climate hazards in drylands: A review. *Earth-Science Reviews*, *126*, 48–57.

Milliman, J. D., & Syvitski, J. P. M. (1992). Geomorphic/tectonic control of sediment discharge to the ocean: the importance of small mountainous rivers. *The Journal of Geology*, *100*(5), 525–544.

Minear, J. T., & Kondolf, G. M. (2009). Estimating reservoir sedimentation rates at large spatial and temporal scales: A case study of California. *Water Resources Research*, *45*(12).

Molnar, P., Anderson, R. S., & Anderson, S. P. (2007). Tectonics, fracturing of rock, and erosion. *Journal of Geophysical Research: Earth Surface*, *112*(F3).

Montgomery, D. R. (2007). Soil erosion and agricultural sustainability. *Proceedings of the National Academy of Sciences*, *104*(33), 13268–13272.

Morris, G. L., & Fan, J. (1998). *Reservoir sedimentation handbook: design and management of dams, reservoirs, and watersheds for sustainable use*. McGraw Hill Professional.

Mount, J. F. (1995). *California rivers and streams: the conflict between fluvial process and land use*. Univ of California Press.

Muller, M. (2007). Adapting to climate change: water management for urban resilience. *Environment and Urbanization*, *19*(1), 99–113.

Nagy, M. L., Pérez, A., & Garcia-Pichel, F. (2005). The prokaryotic diversity of biological soil crusts in the Sonoran Desert (Organ Pipe Cactus National Monument, AZ). *FEMS Microbiology Ecology*, *54*(2), 233-245.

National Research Council. (1998). New strategies for America's Watersheds. Washington, DC: National Academy Press. 311 p.

Nations, D., & Stump, E. (1981). *Geology of Arizona*. Dubuque, Iowa: Kenndall/Hunt Pub.

Nearing, M. A., Jetten, V., Baffaut, C., Cerdan, O., Couturier, A., Hernandez, M., ... & Souchère, V. (2005). Modeling response of soil erosion and runoff to changes in precipitation and cover. *Catena*, *61*(2-3), 131-154.

Neff, J. C., Reynolds, R. L., Belnap, J., & Lamothe, P. (2005). Multi-decadal impacts of grazing on soil physical and biogeochemical properties in southeast Utah. *Ecological Applications*, *15*(1), 87–95.

Nichols, M. H. (2006). Measured sediment yield rates from semiarid rangeland watersheds. *Rangeland Ecology & Management*, *59*(1), 55–62.

Nishiizumi, K., Imamura, M., Caffee, M. W., Southon, J. R., Finkel, R. C., & McAninch, J. (2007). Absolute calibration of 10Be AMS standards. *Nuclear Instruments and Methods in Physics Research Section B: Beam Interactions with Materials and Atoms*, *258*(2), 403–413.

Nyssen, J., Poesen, J., Moeyersons, J., Deckers, J., Haile, M., & Lang, A. (2004). Human impact on the environment in the Ethiopian and Eritrean highlands—a state of the art. *Earth-Science Reviews*, *64*(3–4), 273–320.

Nyssen, J., Poesen, J., Moeyersons, J., Haile, M., & Deckers, J. (2008). Dynamics of soil erosion rates and controlling factors in the Northern Ethiopian Highlands–towards a sediment budget. *Earth Surface Processes and Landforms*, *33*(5), 695–711.

Nyssen, J., Poesen, J., Moeyersons, J., Luyten, E., Veyret-Picot, M., Deckers, J., … Govers, G. (2002). Impact of road building on gully erosion risk: a case study from the northern Ethiopian highlands. *Earth Surface Processes and Landforms, 27*(12), 1267–1283.

Nyssen, J., Vandenreyken, H., Poesen, J., Moeyersons, J., Deckers, J., Haile, M., … Govers, G. (2005). Rainfall erosivity and variability in the Northern Ethiopian Highlands. *Journal of Hydrology, 311*(1–4), 172–187.

Oberlander, T. M. (1997). Slope and pediment systems. In Thomas, D. S. G. (Ed.) *Arid zone geomorphology* (pp. 135-163). London: Belhaven Press.

O'Hare, G., & Rivas, S. (2005). The landslide hazard and human vulnerability in La Paz City, Bolivia. *The Geographical Journal, 171*(3), 239–258. https://doi.org/10.1111/j.1475-4959.2005.00163.x

Ollier, C. D. (1965). Dirt cracking—a type of insolation weathering. *Australian Journal of Science, 27*(8), 236-237.

Osborn, B. (1952). Storing rainfall at the grass roots. *Journal of Range Management, 5*(6), 408–414.

Overby, S., Baker Jr, M.B., (1995). Sediment and nutrient regime from a central Arizona chaparral watershed, in: Hydrology and Water Resources in Arizona and the Southwest. Arizona-Nevada Academy of Science.

Page, K. J., Dare-Edwards, A. J., Owens, J. W., Frazier, P. S., Kellett, J., & Price, D. M. (2001). TL chronology and stratigraphy of riverine source bordering sand dunes near Wagga Wagga, New South Wales, Australia. *Quaternary International, 83*, 187-193.

Parsons, A. J., & Abrahams, A. D. (1984). Mountain mass denudation and piedmont formation in the Mojave and Sonoran Deserts. *American Journal of Science, 284*(3), 255-271.

Parsons, A. J., Abrahams, A. D. & Howard, A. D. (2009). Rock-mantled slopes. In Parsons, A. J., Abrahams, A. D. (Eds.) *Geomorphology of Desert Environments* (pp. 233-263). New York: Springer.

Pearthree, P. A., Demsey, K. A., Onken, J. A., Vincent, K. R. & House, P. K. (1992) Geomorphic assessment of the flood-prone areas on the southern piedmont of the Tortilita Mountains, Pima County, Arizona. *Arizona Geological Survey Open File Report 91-11,* 1-32.

Pelletier, J. D. (2010). How do pediments form?: A numerical modeling investigation with comparison to pediments in southern Arizona, USA. *Bulletin, 122*(11-12), 1815-1829.

Penck, W (1924) *Die Morphologische Analyse: Ein Kapital der physikalischen Geologie*. Stuttgart: Engelhorn.

Peterson, F. F., Bell, J. W., Dorn, R. I., Ramelli, A. R., & Ku, T. L. (1995). Late Quaternary geomorphology and soils in Crater Flat, Yucca Mountain area, southern Nevada. *Geological Society of America Bulletin*, *107*(4), 379-395.

Péwé, T. L., Péwé, R. H., Journaux, A. & Slatt, R. M (1981). Desert Dust: Characteristics and rates of deposition. *Spec. Pap. Geol. Soc. Am.*, *186*, 169–190.

Podolak, C. J. P., & Doyle, M. W. (2015). Reservoir sedimentation and storage capacity in the United States: Management needs for the 21st century. *Journal of Hydraulic Engineering*, *141*(4), 2515001.

Poesen, J. W., Torri, D., & Bunte, K. (1994). Effects of rock fragments on soil erosion by water at different spatial scales: a review. *Catena*, *23*(1-2), 141-166.

Polyakov, V. O., Nearing, M. A., Nichols, M. H., Scott, R. L., Stone, J. J., & Mcclaran, M. P. (2010). Long-term runoff and sediment yields from small semiarid watersheds in southern Arizona. *Water Resources Research*, *46*(9), doi.org/10.1029/2009WR009001

Portenga, E. W., & Bierman, P. R. (2011). Understanding Earth's eroding surface with 10 Be. *GSA Today*, *21*(8), 4–10.

Prosser, I. P., Rutherfurd, I. D., Olley, J. M., Young, W. J., Wallbrink, P. J., & Moran, C. J. (2001). Corrigendum to: Large-scale patterns of erosion and sediment transport in river networks, with examples from Australia. *Marine and Freshwater Research*, *52*(5), 817.

PSIAC. (1968). *Report of the water management subcommittee on factors affecting sediment yield in the pacific southwest area and selection and evaluation of measures for reduction of erosion and sediment yield*.

Radding, C. (2005). *Landscapes of Power and Identity: comparative histories in the Sonoran Desert and the Forests of Amazonia from Colony to Republic*. Durham, NC: Duke University Press.

Rakhmatullaev, S., Marache, A., Huneau, F., Le Coustumer, P., Bakiev, M., & Motelica-Heino, M. (2011). Geostatistical approach for the assessment of the water reservoir capacity in arid regions: a case study of the Akdarya reservoir, Uzbekistan. *Environmental Earth Sciences*, *63*(3), 447–460. https://doi.org/10.1007/s12665-010-0711-3

Randle T, Boyd P, Jonas M, Vermeeren R, Edison D, Cooper D, … Whelan M. (2017). Frequently Asked Questions about Reservoir Sedimentation and Sustainability. (https://acwi.gov/sos/faqs_2017-05-30.pdf)

Renard, K. G., Foster, G. R., Weesies, G. A., McCool, D. K., & Yoder, D. C. (1997). *Predicting soil erosion by water: a guide to conservation planning with the Revised Universal Soil Loss Equation (RUSLE)* (Vol. 703). United States Department of Agriculture Washington, DC.

Reusser, L., Bierman, P., & Rood, D. (2015). Quantifying human impacts on rates of erosion and sediment transport at a landscape scale. *Geology*, *43*(2), 171–174.

Reynolds, S. J. (1985). *Geology of the South Mountains, central Arizona*. Arizona Bureau of Geology and Mineral Technology, Geological Survey Branch.

Rhoads, B. L. (1986). Flood hazard assessment for land-use planning near desert mountains. *Environmental Management*, *10*(1), 97-106.

Richard, S. M., Reynolds, S. J., Spencer, J. E., & Pearthree, P. A. (2000). Geologic map of Arizona: Arizona Geological Survey Map M-35, 1 sheet, scale 1: 1000, 000. *The Arizona Geological Survey, Tucson, AZ*.

Rózsa, P., & Novák, T. (2011). Mapping anthropic geomorphological sensitivity on a global scale. *Zeitschrift Fur Geomorphologie*. https://doi.org/10.1127/0372-8854/2011/0055-0038

Russell, K. L., Vietz, G. J., & Fletcher, T. D. (2017). Global sediment yields from urban and urbanizing watersheds. *Earth-Science Reviews*, *168*, 73–80.

Sadeghi, S. H., Najafi, S., & Bakhtiari, A. R. (2017). Sediment contribution from different geologic formations and land uses in an Iranian small watershed, case study. *International Journal of Sediment Research*, *32*(2), 210–220.

Saiz, A. (2010). The geographic determinants of housing supply. *The Quarterly Journal of Economics*, *125*(3), 1253–1296.

Schaller, M., Ehlers, T. A., Stor, T., Torrent, J., Lobato, L., Christl, M., & Vockenhuber, C. (2016). Spatial and temporal variations in denudation rates derived from cosmogenic nuclides in four European fluvial terrace sequences. *Geomorphology*, *274*, 180–192.

Schwartz, U., & Greenbaum, N. (2008). Extremely high sediment yield from a small arid catchment—Giv'at Hayil, northwestern Negev, Israel. *Israel Journal of Earth Sciences*, *57*.

Seong, Y. B., Dorn, R. I., & Yu, B. Y. (2016a). Evaluating the life expectancy of a desert pavement. *Earth-Science Reviews*, *162*, 129-154.

Seong, Y. B., Larson, P. H., Dorn, R. I., & Yu, B. Y. (2016b). Evaluating process domains in small arid granitic watersheds: Case study of Pima Wash, South Mountains, Sonoran Desert, USA. *Geomorphology*, *255*, 108-124.

Seto, K. C., Fragkias, M., Güneralp, B., & Reilly, M. K. (2011). A meta-analysis of global urban land expansion. *PloS One*, *6*(8), e23777.

Shaffer, S. R., Chow, W. T. L., Georgescu, M., Hyde, P., Jenerette, G. D., Mahalov, A., … Ruddell, B. L. (2015). Multiscale modeling and evaluation of urban surface energy balance in the Phoenix metropolitan area. *Journal of Applied Meteorology and Climatology*, *54*(2), 322–338.

Sharma, K. D., & Chatterji, P. C. (1982). Sedimentation in Nadis in the Indian arid zone. *Hydrological Sciences Journal*, *27*(3), 345-352.

Shi, Z. H., Ai, L., Li, X., Huang, X. D., Wu, G. L., & Liao, W. (2013). Partial least-squares regression for linking land-cover patterns to soil erosion and sediment yield in watersheds. *Journal of Hydrology*, *498*, 165–176.

Shi, Z. H., Huang, X. D., Ai, L., Fang, N. F., & Wu, G. L. (2014). Quantitative analysis of factors controlling sediment yield in mountainous watersheds. *Geomorphology*, *226*, 193–201.

Six, L., & Smolders, E. (2014). Future trends in soil cadmium concentration under current cadmium fluxes to European agricultural soils. *Science of the Total Environment*, *485*, 319–328.

Spencer, J. E. (1984). Role of tectonic denudation in warping and uplift of low-angle normal faults. *Geology*, *12*(2), 95-98.

Stone, J. O. (2000). Air pressure and cosmogenic isotope production. *Journal of Geophysical Research: Solid Earth*, *105*(B10), 23753–23759.

Strand, R. I., & Pemberton, E. L. (1982). *Reservoir sedimentation: Technical guideline for Bureau of Reclamation*. Sedimentation and River Hydraulics Section, Hydrology Branch, Division of ….

Stuckless, J. S., & Sheridan, M. F. (1971). Tertiary volcanic stratigraphy in the Goldfield and Superstition Mountains, Arizona. *Geological Society of America Bulletin*, *82*(11), 3235-3240.

Sumi, T., Okano, M., & Takata, Y. (2004). Reservoir sedimentation management with bypass tunnels in Japan. In *Proc. 9th International Symposium on River Sedimentation* (pp. 1036–1043).

Sutfin, N. A., Shaw, J. R., Wohl, E. E., & Cooper, D. J. (2014). A geomorphic classification of ephemeral channels in a mountainous, arid region, southwestern Arizona, USA. *Geomorphology*, *221*, 164-175.

Syvitski, J. P. M., & Milliman, J. D. (2007). Geology, geography, and humans battle for dominance over the delivery of fluvial sediment to the coastal ocean. *The Journal of Geology, 115*(1), 1–19.

Tayyebi, A., Perry, P. C., & Tayyebi, A. H. (2014). Predicting the expansion of an urban boundary using spatial logistic regression and hybrid raster–vector routines with remote sensing and GIS. *International Journal of Geographical Information Science*, *28*(4), 639–659.

Tchoupopnou, E. (1989). Splash from microphytic soil crusts following simulated rain. Utah State University. Department of Range Science.

Tebbi, F. Z., Dridi, H., & Morris, G. L. (2012). Optimization of cumulative trapped sediment curve for an arid zone reservoir: Foum El Kherza (Biskra, Algeria). *Hydrological Sciences Journal*, *57*(7), 1368–1377.

Telegraph. (2006). Desert turns to 'a sea' as flash floods kill 150. (https://www.telegraph.co.uk/news/1527529/Desert-turns-to-a-sea-as-flash-floods-kill-150.html) (accessed: Feb 9, 2019)

Terfous, A., Megnounif, A., & Bouanani, A. (2003). Détermination des dégradation spécifiques dans trois bassins versant des régions mediterraneennes algeriennes. *Hydrology of the Mediterranean and Semiarid Regions. IAHS Publ*, *278*, 366–372.

The Guardian. (2015). Utah flash flood: death toll rises as more victims found in Zion national park. (https://www.theguardian.com/us-news/2015/sep/15/flash-flooding-utah-arizona-deaths) (accessed: Feb 9, 2019)

The World Bank. (2014). Natural Disasters in the Middle East and North Africa: A Regional Overview. (https://www.gfdrr.org/sites/default/files/publication/NDMENA14.pdf)

Thornbush, M. (2015). Geography, urban geomorphology and sustainability. *Area*, *47*(4), 350-353.

Trimble, S. W. (1977). The fallacy of stream equilibrium in contemporary denudation studies. *American Journal of Science*, *277*(7), 876–887.

Twidale, C. R. (1981). Granitic inselbergs: domed, block-strewn and castellated. *Geographical Journal*, 54-71.

Twidale, C. R. (2012). *Granite landforms*. Amsterdam: Elsevier.

Twidale, C. R. (2002). The two-stage concept of landform and landscape development involving etching: origin, development and implications of an idea. *Earth-Science Reviews*, *57*(1-2), 37-74.

United Nations. (2018). World Urbanization Prospects: The 2018 Revision. DESA/Population Division.

United Nations Convention to Combat Desertification (UNCCD). (2008). The 10-Year Strategic Plan and Framework to Enhance the Implementation of the Convention (2008–2018). (https://digitallibrary.un.org/record/668087?ln=en)

United Nations Office for Disaster Risk Reduction (UNISDR). (2012). Disaster Risk-poverty Trends in Jordan, Syria, Yemen: Key Findings and Policy Recommendations. (https://www.preventionweb.net/files/27853_arabriskpovertypolicynotejuly2012.pdf)

United Nations Office for Disaster Risk Reduction (UNISDR). (2010). ISDR secretariat biennial workplan: 2008-2009 final report. (thttps://www.unisdr.org/we/inform/publications/14768)

U.S. Army Corps of Engineers (USACE). (1981). New River and Phoenix City Streams, Arizona, Design Memorandum No. 5, Master Plan and Initial Development Feature Design Memorandum, Dreamy Draw Dam. (https://apps.dtic.mil/dtic/tr/fulltext/u2/a130263.pdf)

U.S. Army Corps of Engineers (USACE). (1982). New River and Phoenix City Streams, Arizona, Design Memorandum No. 6, Master Plan and Initial Development Feature Design Memorandum, Cave Buttes Dam. (https://apps.dtic.mil/dtic/tr/fulltext/u2/a133055.pdf)

U.S. Army Corps of Engineers (USACE). (1984a). New River and Phoenix City Streams, Arizona, Design Memorandum No. 3, General Design Memorandum - Phase 11, Project Design Part 3- New River Dam.

U.S. Army Corps of Engineers (USACE). (1984b). New River and Phoenix City Streams, Arizona, Design Memorandum No. 7, Master Plan and Initial Development Feature Design Memorandum, Adobe Dam. (https://www.maricopacountyparks.net/assets/1/6/Adobe_Dam_Master_Plan.pdf)

U.S. Department of Agriculture (USDA). (1972). Sedimentation *National Engineering Handbook.* (Washington, DC: USDA)

USDA-NRCS. (1983). Sediment sources, yields, ratios. Chapter 6 in National Engineering Handbook, Section 3, Sedimentation. U.S. Department Agriculture, Natural Resources Conservation Service formerly Soil Conservation service (SCS), 6.2-6.19. Washington, D.C.: U.S. Goverment Printing Office.

U.S. Department of Agriculture – Soil Conservation Service (USDA-SCS). (1977). Harquahala Valley Watershed Maricopa and Yuma Counties, Arizona : final environmental impact statement.

U.S. Department of the Interior Bureau of Reclamation. (2009). Reclamation Library – Glossary. https://www.usbr.gov/library/glossary/#S

Vaezi, A. R., Abbasi, M., Bussi, G., & Keesstra, S. (2017). Modeling Sediment Yield in Semi-Arid Pasture Micro-Catchments, NW Iran. *Land Degradation & Development*. [Chichester] : https://doi.org/10.1002/ldr.2526

Vanacker, V., Molina, A., Govers, G., Poesen, J., Dercon, G., Deckers, S., (2005). River channel response to short-term human-induced change in landscape connectivity in Andean ecosystems. *Geomorphology 72*, 340–353.

Van Devender, T. R. (1990). Late Quaternary vegetation and climate of the Sonoran Desert, United States and Mexico. In Betancourt, J. L., Van Devender, T. R., Martin, P. S. (Eds.) *Packrat Middens: The Last 40,000 Years of Biotic Change* (pp. 134-165). Tucson: University of Arizona Press.

Vanmaercke, M., Poesen, J., Broeckx, J., & Nyssen, J. (2014). Sediment yield in Africa. *Earth - Science Reviews*, *136*, 350.

Vanmaercke, M., Poesen, J., Govers, G., & Verstraeten, G. (2015). Quantifying human impacts on catchment sediment yield: A continental approach. *Global and Planetary Change*, *130*, 22.

Vanmaercke, M., Poesen, J., Maetens, W., de Vente, J., & Verstraeten, G. (2011a). Sediment yield as a desertification risk indicator. *Science of the Total Environment*, *409*(9), 1715–1725. https://doi.org/10.1016/j.scitotenv.2011.01.034

Vanmaercke, M., Poesen, J., Radoane, M., Govers, G., Ocakoglu, F., & Arabkhedri, M. (2012). How long should we measure? An exploration of factors controlling the inter-annual variation of catchment sediment yield. *Journal of Soils and Sediments*, *12*(4), 603–619.

Vanmaercke, M., Poesen, J., Verstraeten, G., de Vente, J., & Ocakoglu, F. (2011b). Sediment yield in Europe: Spatial patterns and scale dependency. *Geomorphology*, *130*(3–4), 142–161.

Vanmaercke, M., Zenebe, A., Poesen, J., Nyssen, J., Verstraeten, G., & Deckers, J. (2010). Sediment dynamics and the role of flash floods in sediment export from medium-sized catchments: a case study from the semi-arid tropical highlands in northern Ethiopia. *Journal of Soils and Sediments : JSS.* Landsberg, Germany .

Verstraeten, G., & Poesen, J. (2001). Variability of dry sediment bulk density between and within retention ponds and its impact on the calculation of sediment yields. *Earth Surface Processes and Landforms*, *26*(4), 375–394.

Verstraeten, G., Poesen, J., de Vente, J., & Koninckx, X. (2003). Sediment yield variability in Spain: a quantitative and semiqualitative analysis using reservoir sedimentation rates. *Geomorphology*, *50*(4), 327–348.

Viles, H. A. (2008). Understanding dryland landscape dynamics: do biological crusts hold the key?. *Geography Compass*, *2*(3), 899-919.

Viles, H. A. (2013). Linking weathering and rock slope instability: non-linear perspectives. *Earth Surface Processes and Landforms*, *38*(1), 62-70.

Villarreal, M. L., Webb, R. H., Norman, L. M., Psillas, J. L., Rosenberg, A. S., Carmichael, S., … Sparks, P. E. (2016). Modeling Landscape-scale Erosion Potential Related to Vehicle Disturbances Along the USA–Mexico Border. *Land Degradation & Development*, *27*(4), 1106–1121.

von Blanckenburg, F. (2006). The control mechanisms of erosion and weathering at basin scale from cosmogenic nuclides in river sediment. *Earth and Planetary Science Letters*, *242*(3–4), 224–239. https://doi.org/10.1016/J.EPSL.2005.11.017

Walker, J. S., Grimm, N. B., Briggs, J. M., Gries, C., & Dugan, L. (2009). Effects of urbanization on plant species diversity in central Arizona. *Frontiers in Ecology and the Environment*, *7*(9), 465–470.

Walling, D. E. (2006). Human impact on land–ocean sediment transfer by the world's rivers. *Geomorphology*, *79*(3–4), 192–216.

Walling, D. E. (1983). The sediment delivery problem. *Journal of Hydrology*, *65*(1–3), 209–237.

Wang, L.-Y., Xiao, Y., Rao, E.-M., Jiang, L., Xiao, Y., & Ouyang, Z.-Y. (2018). An assessment of the impact of urbanization on soil erosion in Inner Mongolia. *International Journal of Environmental Research and Public Health*, *15*(3), 550.

Wark, J. W., & Keller, F. J. (1963). *Preliminary study of sediment sources and transport in the Potomac River basin*. Interstate Commission on the Potomac River Basin.

Warner, T. T. (2004). Desert Meteorology, 612 pp. Cambridge Univ. Press, Cambridge, UK.

Warren, S. D. (2001). Biological soil crusts and hydrology in North American deserts. In *Biological soil crusts: structure, function, and management* (pp. 327–337). Springer.

Wasson, R. J. (1994). Annual and decadal variation of sediment yield in Australia, and some global comparisons. *IAHS Publications-Series of Proceedings and Reports-Intern Assoc Hydrological Sciences*, *224*, 269–280.

Waters, C. N., Zalasiewicz, J., Summerhayes, C., Barnosky, A. D., Poirier, C., Gałuszka, A., ... & Jeandel, C. (2016). The Anthropocene is functionally and stratigraphically distinct from the Holocene. *Science*, *351*(6269), aad2622.

Webb, R. H., Magirl, C. S., Griffiths, P. G., & Boyer, D. E. (2008). *Debris Flows and Floods in Southeastern Arizona from Extreme Precipitation in July 2006-Magnitude, Frequency, and Sediment Delivery* (No. 2008-1274). Geological Survey (US).

Weitzman, M., Aschengrau, A., Bellinger, D., Jones, R., Hamlin, J. S., & Beiser, A. (1993). Lead-contaminated soil abatement and urban children's blood lead levels. *Jama*, *269*(13), 1647–1654.

Wischmeier, W. H., & Smith, D. D. (1965). Predicting rainfall erosion losses from cropland. *USDA Agricultural Handbook*, *282*.

Wischmeier, W. H., & Smith, D. D. (1978). Predicting rainfall erosion losses-a guide to conservation planning. *Predicting Rainfall Erosion Losses-a Guide to Conservation Planning.*

Wisser, D., Frolking, S., Hagen, S., & Bierkens, M. F. P. (2013). Beyond peak reservoir storage? A global estimate of declining water storage capacity in large reservoirs. *Water Resources Research*, *49*(9), 5732–5739.

Wolman, M. G. (1967). A cycle of sedimentation and erosion in urban river channels. *Geografiska Annaler: Series A, Physical Geography*, *49*(2–4), 385–395.

Wolman, M. G., & Schick, A. P. (1967). Effects of construction on fluvial sediment, urban and suburban areas of Maryland. *Water Resources Research*, *3*(2), 451–464. https://doi.org/10.1029/WR003i002p00451

Xian, G., Crane, M., & McMahon, C. (2008). Quantifying multi-temporal urban development characteristics in Las Vegas from Landsat and ASTER data. *Photogrammetric Engineering & Remote Sensing*, *74*(4), 473–481.

Yagoub, M. M. (2004). Monitoring of urban growth of a desert city through remote sensing: Al-Ain, UAE, between 1976 and 2000. *International Journal of Remote Sensing*, *25*(6), 1063–1076.

Yagoub, M. M., & Al Bizreh, A. A. (2014). Prediction of land cover change using Markov and cellular automata models: case of Al-Ain, UAE, 1992-2030. *Journal of the Indian Society of Remote Sensing*, *42*(3), 665–671.

York, A. M., Shrestha, M., Boone, C. G., Zhang, S., Harrington, J. A., Prebyl, T. J., … Nolen, B. (2011). Land fragmentation under rapid urbanization: A cross-site analysis of Southwestern cities. *Urban Ecosystems*, *14*(3), 429–455.

Yorke, T. H., & Herb, W. J. (1978). *Effects of urbanization on streamflow and sediment transport in the Rock Creek and Anacostia River basins, Montgomery County, Maryland, 1962-74*. Department of the Interior, Geological Survey.

Youberg, A., Cline, M. L., Cook, J. P., Pearthree, P. A., & Webb, R. H. (2008). Geological mapping of debris-flow deposits in the Santa Catalina Mountains, Pima County, Arizona. *Arizona Geological Survey Open File Report*, *8*, 06.

Young, R. A., Onstad, C. A., Bosch, D. D., & Anderson, W. P. (1989). AGNPS: A nonpoint-source pollution model for evaluating agricultural watersheds. *Journal of Soil and Water Conservation*, *44*(2), 168–173.

Zhang, Y., Hernandez, M., Anson, E., Nearing, M. A., Wei, H., Stone, J. J., & Heilman, P. (2012). Modeling climate change effects on runoff and soil erosion in southeastern Arizona rangelands and implications for mitigation with conservation practices. *Journal of soil and water conservation*, *67*(5), 390-405.

Zhang, W., & Huang, B. (2015). Soil erosion evaluation in a rapidly urbanizing city (Shenzhen, China) and implementation of spatial land-use optimization. *Environmental Science and Pollution Research*, *22*(6), 4475–4490.

Zhao, G., Kondolf, G. M., Mu, X., Han, M., He, Z., Rubin, Z., … Sun, W. (2017). Sediment yield reduction associated with land use changes and check dams in a catchment of the Loess Plateau, China. *CATENA*, *148*, 126–137. https://doi.org/https://doi.org/10.1016/j.catena.2016.05.010

Zhibao, D., Xunming, W., & Lianyou, L. (2000). Wind erosion in arid and semiarid China: an overview. *Journal of Soil and Water Conservation*, *55*(4), 439–444.

Zhuo, X., Boone, C. G., & Shock, E. L. (2012). Soil lead distribution and environmental justice in the Phoenix metropolitan region. *Environmental Justice*, *5*(4), 206–213.

# APPENDIX A

# GOOGLE EARTH KMZ FILE OF THE STOCK TANKS

# AND THEIR ASSOCIATED WATERSHEDS

The selected 18 stock ponds and their associated watersheds are indicated as the name of stock ponds in the Google Earth kmz file, which is referred in the appendix B. The kmz file offers several benefits for readers to better understand the purpose of this study: i) it shows the regional setting where stock ponds are located; ii) it provides the opportunity to identify the location of studied stock tanks and their associated watersheds in the regional setting such as and to compare the size of each stock tank and its watershed indicated in the appendix B; iii) it provides some information regarding the catchment properties such as relief and slope gradient; iv) most importantly, it helps users explore the land use changes occurred during the period of sediment accumulation. The Google Earth provides the tool of time slider which enables to see historical satellite imagery. Therefore, users can examine the typical shifts in land use as the urbanization expanded out into areas formerly occupied by cattle grazing referred in the appendix B using the time slider in the Google Earth and visually look at the bare ground exposure due to the urban development or human-influenced wildfires with the higher resolution such as the examples provided in the figure 3.2. A downloadable version is available online at: https://onlinelibrary.wiley.com/doi/10.1002/ldr.3207.

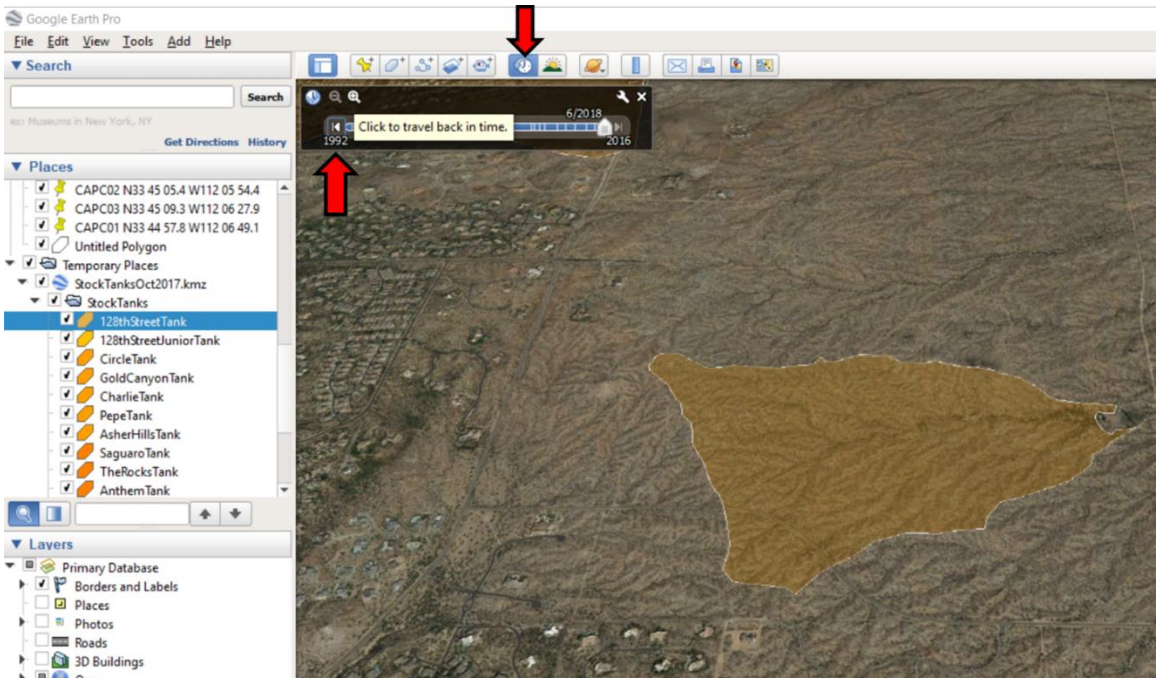


**Note:** Google Earth provide the time slider to observe the historic satellite imagery.

# APPENDIX B

# STOCK POND CATCHMENT CHARACTERSITCS AND DATA ON SOIL EROSION RATES AND SEIDMENT YIELDS

| Stock Tank | Time Period | Dominant Land Use | Different Rock Types | MAP (mm) (I30) (mm) | | Coordinates | Ad | At | Max. ER | Min. ER | Max. SSY |
|---|---|---|---|---|---|---|---|---|---|---|---|
| | | | | P1 | P2 | | ($km^2$) | ($m^2$) | (mm $ka^{-1}$) | (mm $ka^{-1}$) | (t $km^{-2}$ $yr^{-1}$) |
| 1. Cigar Tank | 1990-2004 | grazing | metamorphic, basalt, granite | 207(20.9) | 170(15.4) | 33.685117, | 2.60 | 6000 | 66 ± 5.8 | 57.7 ± 2.8 | 89.2 ± 9.7 |
| | 2005-2009 | grazing and off-road vehicle use | | | | -112.534267 | | | 75.8 ± 6.4 | 66.4 ± 2.4 | 102.4 ± 9.8 |
| 2. Saguaro | 1990-2004 | grazing | metamorphic, basalt, granite | 222(25.1) | 181(14.1) | 33.800925, | 1.40 | 5800 | 35.0 ± 4.8 | 29.7 ± 2.3 | 48.7 ± 7.6 |
| | 2005-2009 | grazing & pipeline construction | | | | -112.20405 | | | 95.3 ± 6.6 | 84.3 ± 3.0 | 143.2 ± 26.0 |
| 3. Cline | 1989-1995 | Some construction | metamorphic, basalt, granitic | 222(25.1) | 181(14.1) | 33.853465, | 1.50 | 9500 | 33.7 ± 3.7 | 28.8 ± 3.5 | 52.0 ± 6.9 |
| | 1996-2003 | commercial construction | | | | -112.149325 | | | 75.9 ± 4.6 | 67.8 ± 2.2 | 103.7 ± 6.4 |
| | 2003-2004 | subdivision construction | | | | | | | 102.7 ± 11.1 | 94.1 ± 6.4 | 174.7 ± 25.4 |
| 4. Anthem | 1989-1992 | grazing | metavolcanic | 222(25.1) | 181(14.1) | 33.862595, | 0.88 | 3000 | 84.2 ± 5.6 | 74.8 ± 9.8 | 136.7 ± 14.6 |
| | 1993-1997 | after wildfire | | | | -112.123726 | | | 203.6 ± 5.1 | 188.6 ± 16.7 | 334.0 ± 25.4 |
| 5. Anthem 2 | 1989-1992 | grazing | metavolcanic | 222(25.1) | 181(14.1) | 33.850572, | 0.58 | 2700 | 59.6 ± 4.0 | 51.6 ± 2.3 | 77.5 ± 7.1 |
| | 1993-1995 | after wildfire period 1 | | | | -112.101617 | | | 184.5 ± 24.9 | 169.4 ± 16.4 | 276.7 ± 45.8 |
| | 1996-1998 | after wildfire period 2 | | | | | | | 197.8 ± 17.2 | 184.4 ± 34.9 | 330.9 ± 32.8 |
| | 1999-2002 | after wildfire period 3 | | | | | | | 91.2 ± 3.9 | 85.2 ± 11.7 | 156.2 ± 14.9 |
| | 2002 | housing | | | | | | | 172.8 ± 16.5 | 155.5 ± 8.7 | 255.7 ± 41.4 |
| 6. Pepe | 1989-2008 | grazing & ongoing house construction | metamorphic, basalt, granite | 222(22.8) | 181(11.5) | 33.786100, | 0.99 | 3300 | 34.0 ± 5.6 | 27.7 ± 3.3 | 38.4 ± 10.0 |
| | | | | | | -112.159939 | | | | | |
| 7. Bronco | 1989-1998 | grazing | metamorphic, basalt, granite | 222(22.8) | 181(11.5) | 33.774765, | 0.45 | 4100 | 37.9 ± 5.8 | 32.4 ± 4.7 | 43.7 ± 8.0 |
| | 1999-2003 | road construction | | | | -112.117174 | | | 117.4 ± 22.2 | 96.1 ± 9.5 | 137.4 ± 32.4 |
| 8. Circle | 1990-2010 | grazing | metamorphic | 222(22.8) | 181(11.5) | 33.767891, | 0.60 | 5000 | 46.8 ± 11.6 | 39.0 ± 3.8 | 51.0 ± 13.7 |
| | 2010-2013 | road construction | | | | -112.069517 | | | 82.7 ± 18.7 | 72.3 ± 3.2 | 128.5 ± 31.1 |
| 9. Charlie | 1989-2004 | house construction | granitic | 276(40.4) | 237(28.0) | 33.773722, | 0.91 | 10500 | 164.5 ± 25.8 | 146.6 ± 6.9 | 264.3 ± 49.1 |
| | | | | | | -111.949346 | | | | | |
| 10. Rock | 1989-1992 | grazing | granitic | 276(40.4) | 237(28.0) | 33.758838, | 0.54 | 2800 | 45.3 ± 4.5 | 38.6 ± 3.0 | 53.6 ± 8.8 |
| | 1992-1997 | after wildfire period 1 | | | | -111.877228 | | | 169.7 ± 14.7 | 150.7 ± 10.8 | 224.0 ± 25.3 |
| | 1998-2003 | after wildfire period 2 | | | | | | | 102.9 ± 5.9 | 93.3 ± 14.6 | 175.7 ± 11.7 |
| | 2004-2009 | after wildfire period 3 | | | | | | | 56.6 ± 3.3 | 52.9 ± 10.7 | 90.9 ± 9.3 |

(Continues)

| Stock Tank | Time Period | Dominant Land Use | Different Rock Types | MAP (mm) (I30) (mm) | | Coordinates | Ad | At | Max. ER | Min. ER | Max. SSY | Min. SSY |
|---|---|---|---|---|---|---|---|---|---|---|---|---|
| | | | | P1 | P2 | | ($km^2$) | ($m^2$) | (mm $ka^{-1}$) | (mm $ka^{-1}$) | (t $km^{-2}$ $yr^{-1}$) | (t $km^{-2}$ $yr^{-1}$) |
| 11. Cave Creek | 1989-1992 | grazing | granitic | 276(15.4) | 237(22.9) | 33.821477, | 0.19 | 1200 | 73.0 ± 8.3 | 63.7 ± 7.7 | 102.2 ± 15.4 | 89.1 ± 10.8 |
| | 1992-1999 | after wildfire | | | | -111.860042 | | | 151.8 ± 10.5 | 142.4 ± 23.4 | 258.5 ± 18.0 | 242.6 ± 39.8 |
| | 2000-2003 | house construction | | | | | | | 91.8 ± 8.4 | 81.4 ± 6.2 | 128.8 ± 23.6 | 114.3 ± 8.7 |
| 12. Buckhorn | 1989-1999 | grazing | granitic | 305(40.4) | 260(28.0) | 33.771593, | 4.40 | 4100 | 76.1 ± 2.3 | 65.6 ± 3.9 | 106.2 ± 17.1 | 91.6 ± 5.4 |
| | 2000-2002 | house construction | | | | -111.726559 | | | 108.8 ± 4.9 | 94.3 ± 12.4 | 133.4 ± 17.4 | 115.7 ± 15.2 |
| 13. The Rocks | 1989-1996 | house construction | granitic | 310(40.4) | 248(28.0) | 33.735184, | 2.36 | 6500 | 128.6 ± 13.2 | 120.3 ± 15.8 | 227.6 ± 25.7 | 212.9 ± 28.0 |
| | | | | | | -111.843395 | | | | | | |
| 14. 128th St | 1989-1994 | grazing | granitic | 310(40.4) | 248(28.0) | 33.719610, | 0.85 | 7000 | 72.6 ± 17.5 | 62.3 ± 8.9 | 110.3 ± 27.1 | 94.7 ± 13.6 |
| | 1995-2000 | after wildfire | | | | -111.80591 | | | 198.5 ± 12.0 | 175.4 ± 6.3 | 342.0 ± 40.4 | 302.3 ± 10.8 |
| | 2001-2008 | road construction | | | | | | | 105.0 ± 13.6 | 92.7 ± 4.9 | 159.9 ± 29.4 | 141.3 ± 7.4 |
| 15. 128th St 2 | 1989-1994 | grazing | granitic | 310(40.4) | 248(28.0) | 33.716550, | 0.31 | 2200 | 69.0 ± 28.6 | 59.6 ± 7.8 | 109.5 ± 45.9 | 94.5 ± 12.4 |
| | 1995-2000 | after wildfire | | | | -111.79117 | | | 195.8 ± 56.2 | 175.6 ± 11.2 | 278.7 ± 94.4 | 250.0 ± 15.9 |
| | 2001-2008 | road construction | | | | | | | 97.7 ± 29.9 | 88.9 ± 8.0 | 149.1 ± 48.4 | 135.7 ± 12.2 |
| 16.AsherHills | 1989-2001 | grazing | granitic | 310(17.5) | 248(18.4) | 33.731003, | 2.10 | 9800 | 94.5 ± 18.1 | 84.7 ± 7.8 | 140.5 ± 27.6 | 125.9 ± 11.6 |
| | 2002-2007 | house construction | | | | -111.703998 | | | 123.7 ± 4.6 | 113.4 ± 4.9 | 199.1 ± 15.0 | 182.6 ± 7.9 |
| 17. Gold Cyn | 1989-2009 | cattle grazing & house construction | ignimbrite, granitic | 254(23.2) | 209(17.9) | 33.367485, | 5.10 | 18000 | 55.7 ± 11.6 | 44.0 ± 2.4 | 57.3 ± 13.1 | 45.3 ± 2.5 |
| | | | | | | -111.515636 | | | | | | |
| 18. Peralta | 1989-2000 | grazing | ignimbrite, granitic, breccia | 254(23.2) | 209(17.9) | 33.334978, | 0.78 | 2800 | 42.2 ± 2.0 | 36.1 ± 2.4 | 52.2 ± 3.8 | 44.7 ± 3.0 |
| | 2001-2005 | subdivision construction | | | | -111.429506 | | | 69.8 ± 5.1 | 55.4 ± 3.6 | 77.4 ± 6.8 | 61.5 ± 3.9 |
| | 2006-2009 | subdivision finished | | | | | | | 8.2 ± 2.6 | 5.9 ± 0.4 | 8.7 ± 2.8 | 6.2 ± 0.4 |

Note. MAP: mean annual precipitation during the 10 year period of study periods, P1: period 1 (1989-1999), P2: period 2 (2000-2009), I30 is the total amount of peak 30-minute rainfall exceeded 10 mm for 30 min, Ad: drainage area, At: tank area, Max. ER: maximum erosion rate, Min. ER: minimum erosion rate, Max. SSY: maximum area-specific sediment yield, Min. SSY: minimum area-specific sediment yield.

# APPENDIX C

## DATA USED IN THE CORRELATION ANALYSIS

## OF TABLE 3.1 IN THE CHAPTER 3

The purpose of the appendix C is to describe the detailed statistical methods used in the paper to find the correlation between and among catchment properties and to evaluate whether there is statistically significant difference in erosion rates or sediment yield between different rock types or land use types. It is reported that variables like precipitation and vegetation cover are important influences on the erosion and sediment yield in a semi-arid catchment in southern Arizona (Nichols, 2006), in micro-catchments in Iran (Vaezi, Abbasi, Bussi, & Keesstra, 2017), in Europe (Vanmaercke, Poesen, Verstraeten, de Vente, & Ocakoglu, 2011) and Africa (Vanmaercke, Poesen, Broeckx, & Nyssen, 2014). Based on these findings in the literature, statistical tests were performed to examine which variables statistically influence to the sediment yield and erosion rates in the last two decades, north-central Sonoran Desert, USA. Pearson's pair-wise correlation analyses were performed using Microsoft Excel Data Analysis tool to determine if there is a statistically significant correlation between a catchment property and erosion rate in section 5.2 in the paper. And an unpaired t-test was used to evaluate whether the specific sediment yield was significantly different between stock pond watersheds that were only granitic and those that were non-granitic in section 5.2 in the paper. The unpaired t-tests was also conducted to statistically compare the specific sediment yield from basins experiencing grazing; building construction of houses, subdivision and commercial properties; infrastructure of road and pipeline building that exposes bare ground; and wildfire.

## 1. Pearson Correlation

- **Raw Data**

| *Tank Name* | *Emax* | *Ad* | *Savg* | *Relief* | *BD* | *VC* | *MAP* | *MSP* | *I30* | *SY* | *SSY* |
|---|---|---|---|---|---|---|---|---|---|---|---|
| 128st. Junior | 69.00 | 310 | 3.4 | 37.32 | 1.59 | 36.54 | 3.37 | 20.44 | 1.21 | 33.94 | 109.47 |
| 128st. | 72.57 | 851 | 3.3 | 31.58 | 1.52 | 32.02 | 399.39 | 107.80 | 1.21 | 93.87 | 110.30 |
| Saguaro | 34.98 | 1400 | 1.4 | 33.26 | 1.39 | 30.89 | 200.08 | 63.33 | 0.53 | 68.24 | 48.74 |
| Buckhorn | 76.06 | 4400 | 3.1 | 203.32 | 1.40 | 30.45 | 361.56 | 105.51 | 1.45 | 467.42 | 106.23 |
| Asher Hill | 94.53 | 2100 | 2.6 | 196.04 | 1.49 | 22.23 | 263.63 | 63.82 | 0.65 | 295.12 | 140.53 |
| Rock Tank | 45.27 | 540 | 5.1 | 67.75 | 1.18 | 14.88 | 387.69 | 149.35 | 1.70 | 28.93 | 53.57 |
| Cigar | 66.54 | 2600 | 0.7 | 17.93 | 1.34 | 10.52 | 217.68 | 69.27 | 0.95 | 231.82 | 89.16 |
| Peralta | 41.17 | 784 | 3.7 | 49.36 | 1.24 | 10.07 | 252.24 | 70.17 | 0.84 | 40.89 | 52.15 |
| Cave Creek | 72.98 | 190 | 3.7 | 25.06 | 1.40 | 8.84 | 319.72 | 81.18 | 0.22 | 19.41 | 102.18 |
| Circle | 46.76 | 600 | 12.9 | 153.41 | 1.09 | 5.68 | 202.90 | 80.09 | 0.75 | 30.58 | 50.97 |
| Bronco | 37.86 | 450 | 1.1 | 15.21 | 1.15 | 3.95 | 230.89 | 64.77 | 0.87 | 19.65 | 43.67 |
| Cline | 33.68 | 1500 | 2.3 | 42.27 | 1.54 | | 326.28 | 80.16 | 1.09 | 77.96 | 51.98 |
| Anthem2 | 59.61 | 580 | 3.3 | 40.19 | 1.30 | | 304.99 | 86.74 | 1.14 | 44.95 | 77.50 |
| Anthem | 84.19 | 880 | 12.2 | 208.61 | 1.62 | | 304.99 | 86.74 | 1.14 | 120.26 | 136.66 |

**Abbreviations**: Emax, maximum erosion rate (mm $ka^{-1}$); Ad, drainage area; Savg, average slope; Relief, maximum height difference in catchment; BD, bulk density; VC, percent vegetation cover; MAP, mean annual precipitation; MSP, mean summer seasonal precipitation, I30, the total amount of peak 30-minute rainfall exceeded 10 mm for 30 min; SY, sediment yield (t $yr^{-1}$); SSY, area-specific sediment yield (t $km^{-2}$)

Among the eighteen studied catchments, fourteen catchments were selected first to control land use-influences on specific sediment yield. Thus, all the Emax, SY and SSY used in the Pearson's pairwise correlation analyses were collected data during the only grazing period. Cline, Anthem2 and Anthem stock tanks were additionally excluded to perform Pearson's pair-wise correlation analyses because Google Earth imagery to calculate the percent vegetation cover (VC) during the grazing period was not available for the stock tanks. We finally performed Pearson's pair-wise correlation analyses with the eleven catchments after the process of careful selection of data.

The Pearson's correlation table with the significance levels (Table 3.1 in the chapter 3) are calculated using Microsoft Excel with the following steps.

- **Step 1. Determine Pearson's correlation coefficient (r)**

| | *Emax* | *Ad* | *Savg* | *Relief* | *BD* | *VC* | *MAP* | *MSP* | *I30* | *SY* | *SSY* |
|---|---|---|---|---|---|---|---|---|---|---|---|
| Emax | 1.000 | | | | | | | | | | |
| Ad | 0.416 | 1.000 | | | | | | | | | |
| Savg | -0.159 | -0.276 | 1.000 | | | | | | | | |
| Relief | 0.446 | 0.586 | 0.398 | 1.000 | | | | | | | |
| BD | 0.700 | 0.206 | -0.467 | -0.009 | 1.000 | | | | | | |
| VC | 0.374 | 0.301 | -0.282 | 0.144 | 0.808 | 1.000 | | | | | |
| MAP | 0.132 | 0.247 | -0.013 | 0.192 | -0.175 | -0.130 | 1.000 | | | | |
| MSP | -0.075 | 0.145 | 0.200 | 0.180 | -0.354 | -0.136 | 0.888 | 1.000 | | | |
| I30 | -0.003 | 0.257 | 0.017 | 0.154 | -0.017 | 0.331 | 0.234 | 0.500 | 1.000 | | |
| SY | 0.611 | 0.965 | -0.261 | 0.681 | 0.320 | 0.336 | 0.265 | 0.123 | 0.245 | 1.000 | |
| SSY | 0.982 | 0.365 | -0.242 | 0.360 | 0.817 | 0.505 | 0.052 | -0.161 | -0.003 | 0.558 | 1.000 |

We calculated the Pearson correlation coefficient (r) using correlation analysis tool in Microsoft Excel for all the pairs of variables (n = 11).

- **Step 2. Determine t-value (t)**

| | *Emax* | *Ad* | *Savg* | *Relief* | *BD* | *VC* | *MAP* | *MSP* | *I30* | *SY* | *SSY* |
|---|---|---|---|---|---|---|---|---|---|---|---|
| Emax | | | | | | | | | | | |
| Ad | 1.236 | | | | | | | | | | |
| Savg | -0.477 | -0.823 | | | | | | | | | |
| Relief | 1.322 | 1.724 | 1.183 | | | | | | | | |
| BD | 2.043 | 0.616 | -1.383 | -0.026 | | | | | | | |
| VC | 1.114 | 0.897 | -0.844 | 0.430 | 2.335 | | | | | | |
| MAP | 0.395 | 0.738 | -0.040 | 0.576 | -0.524 | -0.388 | | | | | |
| MSP | -0.224 | 0.434 | 0.600 | 0.539 | -1.055 | -0.407 | 2.545 | | | | |
| I30 | -0.009 | 0.768 | 0.050 | 0.461 | -0.050 | 0.988 | 0.699 | 1.480 | | | |
| SY | 1.795 | 2.742 | -0.779 | 1.989 | 0.953 | 1.002 | 0.793 | 0.369 | 0.733 | | |
| SSY | 2.785 | 1.087 | -0.725 | 1.071 | 2.358 | 1.494 | 0.157 | -0.482 | -0.009 | 1.646 | |

Then, we determined the t-value for all the pairs of variables using the equation:

$$t = r \times \sqrt{\frac{n-2}{1-r^2}}$$

- **Step 3. Determine p-value**

| | *Emax* | *Ad* | *Savg* | *Relief* | *BD* | *VC* | *MAP* | *MSP* | *I30* | *SY* | *SSY* |
|---|---|---|---|---|---|---|---|---|---|---|---|
| Emax | | | | | | | | | | | |
| Ad | 0.248 | | | | | | | | | | |
| Savg | 0.645 | 0.432 | | | | | | | | | |
| Relief | 0.219 | 0.119 | 0.267 | | | | | | | | |
| BD | 0.071 | 0.553 | 0.200 | 0.980 | | | | | | | |
| VC | 0.294 | 0.393 | 0.421 | 0.677 | 0.044 | | | | | | |
| MAP | 0.702 | 0.480 | 0.969 | 0.579 | 0.613 | 0.707 | | | | | |
| MSP | 0.828 | 0.674 | 0.564 | 0.603 | 0.319 | 0.694 | 0.031 | | | | |
| I30 | 0.993 | 0.462 | 0.961 | 0.656 | 0.961 | 0.349 | 0.502 | 0.173 | | | |
| SY | 0.106 | 0.023 | 0.456 | 0.078 | 0.365 | 0.342 | 0.448 | 0.720 | 0.482 | | |
| SSY | 0.021 | 0.305 | 0.487 | 0.312 | 0.043 | 0.169 | 0.879 | 0.641 | 0.993 | 0.134 | |

The significance (p-value) was determined using built-in data analysis tool of Microsoft Excel based on the two tailed Student's t-distribution:

$$\frac{\bar{X} - \mu}{S/\sqrt{n}}$$

Where $\bar{X}$ is the sample mean, μ is the population mean, S is the population standard deviation and n is the sample size.

We adopted the significance level for this study as 0.1, 0.05, and 0.01.

## 2. Unpaired t-tests

- **Raw Data**

| Granite | Others | Granite | Others | Fire1 | Fire2 | Building | Infrastructure | Fire total | Grazing |
|---|---|---|---|---|---|---|---|---|---|
| (t km$^{-2}$ yr$^{-1}$) | (t km$^{-2}$ yr$^{-1}$) | (mm kyr$^{-1}$) | (mm kyr$^{-1}$) | (t km$^{-2}$ yr$^{-1}$) | (t km$^{-2}$ yr$^{-1}$) | (t km$^{-2}$ yr$^{-1}$) | (t km$^{-2}$ yr$^{-1}$) | (t km$^{-2}$ yr$^{-1}$) | (t km$^{-2}$ yr$^{-1}$) |
| 140.53 | 50.97 | 95.00 | 47.00 | 334.00 | 330.90 | 103.70 | 143.20 | 334.00 | 89.20 |
| 106.23 | 77.50 | 76.00 | 60.00 | 276.70 | 156.20 | 174.70 | 137.40 | 276.70 | 48.70 |
| 110.30 | 136.66 | 73.00 | 84.00 | 224.00 | 175.70 | 255.70 | 128.50 | 224.00 | 136.70 |
| 109.47 | 89.16 | 69.00 | 67.00 | 258.50 | 90.90 | 38.40 | 159.90 | 258.50 | 77.50 |
| 102.18 | 43.67 | 73.00 | 38.00 | 342.00 | | 264.30 | 149.10 | 342.00 | 43.70 |
| 53.57 | 51.98 | 45.00 | 34.00 | 278.70 | | 128.80 | | 278.70 | 51.00 |
| | 48.74 | | 35.00 | | | 133.40 | | 330.90 | 53.60 |
| | 52.15 | | 42.00 | | | 227.60 | | 156.20 | 102.20 |
| | | | | | | 199.10 | | 175.70 | 106.20 |
| | | | | | | 57.30 | | 90.90 | 110.30 |
| | | | | | | 77.40 | | | 109.50 |
| | | | | | | | | | 140.50 |
| | | | | | | | | | 52.20 |
| | | | | | | | | | 102.40 |
| | | | | | | | | | 52.00 |

**Note**: Fire1 refers to the period of time immediately after a wildfire (typically 3-5 years). Fire2 refers to the period of time after Fire1 where some revegetation has occurred. Fire total refers to all the period of time after a wild fire.

We rejected all time intervals that involved land use other than cattle grazing to understand the significance of rock types to SSY. Therefore, the fourteen catchments among eighteen studied catchments were selected. We also classified our SSY data into the different types of land use including grazing; building construction of houses, subdivision and commercial properties; infrastructure of road and pipeline building that exposes bare ground; and wildfire.

The unpaired t-tests were performed using Microsoft Excel data analysis tool ('t-test: two-sample assuming unequal variance') to understand statistical difference between variables based on the equation:

$$t = \frac{(\overline{x_1} - \overline{x_2})}{\sqrt{\frac{(s_1)^2}{n_1} + \frac{(s_2)^2}{n_2}}}$$

Where $\overline{x_1}$ is the mean of sample 1, $s_1$ is the standard deviation of sample 1, $n_1$ is the sample size of sample 1, $\overline{x_2}$ is the mean of sample 2, $s_2$ is the standard deviation of sample 2, $n_2$ is the sample size of sample 2. The significant difference between two variables is achieved when the statistical t value ('t Stat') is greater than critical t value for the two-tailed t test ('t Critical two-tail') or P value ('P two-tail') is less than 0.05.

- **T-test results**

**1) Rock types**

| | *Granite* | *Others* |
|---|---|---|
| Mean | 103.714 | 68.854 |
| Variance | 791.072 | 1001.046 |
| Observations | 6 | 8 |
| Pooled Variance | 913.557 | |
| Hypothesized Mean Difference | 0.000 | |
| df | 12 | |
| t Stat | 2.136 | |
| P(T<=t) one-tail | 0.027 | |
| t Critical one-tail | 1.782 | |
| P(T<=t) two-tail | 0.054 | |
| t Critical two-tail | 2.179 | |

| | *Granite* | *Others* |
|---|---|---|
| Mean | 71.833 | 50.875 |
| Variance | 256.967 | 319.554 |
| Observations | 6 | 8 |
| Pooled Variance | 293.476 | |
| Hypothesized Mean Difference | 0 | |
| df | 12 | |
| t Stat | 2.265 | |
| P(T<=t) one-tail | 0.021 | |
| t Critical one-tail | 1.782 | |
| P(T<=t) two-tail | 0.043 | |
| t Critical two-tail | 2.179 | |

**Note**: Left: t-test result based on the SSY values / Right: t-test result based on the maximum erosion rates (Emax).

Among the different rock types in studied catchments (N = 14), there was no statistically significant difference in SSY between granite (M = 103.71, SD = 791.07) and other rock types (M = 68.85, SD = 1001.05), $t(12) = 2.14$, $p \geq 0.05$. Therefore, we failed to reject the null hypothesis that there is no difference in SSY between granite and other rock types. However, the p value was 0.054 which is close to the critical value of 0.05, so that we performed the unpaired t-tests with the maximum erosion rates to examine the statistical difference between rock types and found a statistically significant difference in Emax between the granite (M = 71.83, SD = 256.97) and other rock types (M = 50.88,

SD = 319.55), t(12) = 2.27, $p \leq 0.05$. Thus, we rejected the null hypothesis and verified that stock pond watersheds underlain by granitic rock experienced statistically significant higher erosion rates compared to watersheds underlain by metamorphic, basalt, and other rock types.

## 2) Land use types

| | *Fire total* | *Grazing* |
|---|---|---|
| Mean | 246.760 | 85.047 |
| Variance | 7097.378 | 1103.254 |
| Observations | 10 | 15 |
| Pooled Variance | 3448.781 | |
| Hypothesized Mean Difference | 0.000 | |
| df | 23 | |
| t Stat | 6.745 | |
| P(T<=t) one-tail | 0.000 | |
| t Critical one-tail | 1.714 | |
| P(T<=t) two-tail | 0.000 | |
| t Critical two-tail | 2.069 | |

| | *Building* | *Grazing* |
|---|---|---|
| Mean | 150.945 | 85.047 |
| Variance | 6245.711 | 1103.254 |
| Observations | 11 | 15 |
| Pooled Variance | 3245.944 | |
| Hypothesized Mean Difference | 0.000 | |
| df | 24 | |
| t Stat | 2.914 | |
| P(T<=t) one-tail | 0.004 | |
| t Critical one-tail | 1.711 | |
| P(T<=t) two-tail | 0.008 | |
| t Critical two-tail | 2.064 | |

| | *Infrastructure* | *Grazing* |
|---|---|---|
| Mean | 143.620 | 85.047 |
| Variance | 140.637 | 1103.254 |
| Observations | 5 | 15 |
| Pooled Variance | 889.339 | |
| Hypothesized Mean Difference | 0.000 | |
| df | 18 | |
| t Stat | 3.803 | |
| P(T<=t) one-tail | 0.001 | |
| t Critical one-tail | 1.734 | |
| P(T<=t) two-tail | 0.001 | |
| t Critical two-tail | 2.101 | |

Regarding different land use types in studied catchments, there was a statistically significant difference in specific sediment yield between grazing (M = 85.05, SD = 1103.25) and all wildfire (M = 246.76, SD = 7097.38); t(23) = 6.75, $p \leq 0.05$. There was a significant difference in specific sediment yield for grazing and building (M = 150.95, SD= 6245.71) conditions; t(24)= 2.91, p = 0.004. There was a 6 significant difference in specific sediment yield for grazing and infrastructure construction (M = 143.62, SD= 140.64) conditions; t(18)= 1.73, p = 0.001. Therefore, we rejected the null hypothesis that there is no difference in SSY between different land use types.

# APPENDIX D

# VEGEATION COVER ANALYSIS

| Stock pond | Time period | Dominant land use | Vegetation cover during cattle grazing period | Date of satellite image on Google Earth<br>Vegetation cover | | | | |
|---|---|---|---|---|---|---|---|---|
| 1. Cigar | 1990-2004 | grazing | | 1997 Apr. | | | | |
| | | | 10.52% | 10.52% | | | | |
| | 2005-2009 | grazing and off-road vehicle use | | 2003 Oct. | 2004 Dec. | 2007 Jun. | | |
| | | | | 18.87% | 12.60% | 12.65% | | |
| 2. Saguaro | 1990-2004 | grazing | | 1997 Apr. | 2003 Nov. | 2004 Dec. | | |
| | | | 30.89% | 21.36% | 26.48% | 44.83% | | |
| | 2005-2009 | grazing & pipeline construction | | 2006 Apr. | 2007 Jun. | 2009 Nov. | | |
| | | | | 42.20% | 23.34% | 35.86% | | |
| 3. Cline | 1989-1995 | Some construction | | | | | | |
| | 1996-2003 | commercial construction | | 1997 Apr. | 2003 Oct. | 2003 Nov. | | |
| | | | | 3.07% | 3.96% | 7.25% | | |
| | 2003-2004 | subdivision construction | | 2004 Dec. | | | | |
| | | | | 5.75% | | | | |
| 4. Anthem | 1989-1992 | grazing | | | | | | |
| | 1993-1997 | after wildfire | | 1997 Apr. | 2003 Oct. | | | |
| | | | | 5.37% | 6.16% | | | |
| 5. Anthem 2 | 1989-1992 | grazing | | | | | | |
| | 1993-1995 | after wildfire period 1 | | | | | | |
| | 1996-1998 | after wildfire period 2 | | 1997 Apr. | | | | |
| | | | | 4.65% | | | | |
| | 1999-2002 | after wildfire period 3 | | | | | | |
| | 2002 | housing | | 2003 Oct. | 2004 Dec. | 2007 Jun. | | |
| | | | | 1.73% | 2.05% | 2.20% | | |
| 7. Bronco | 1989-1998 | grazing | | 1997 Apr. | | | | |
| | | | 3.95% | 3.95% | | | | |
| | 1999-2003 | road construction | | 2002 May | 2003 Oct. | 2004 Dec. | 2007 Jun. | 2009 Nov. |
| | | | | 7.36% | 7.85% | 7.08% | 5.62% | 6.84% |
| 8. Circle | 1990-2010 | grazing | | 1997 Apr. | 2002 May | 2003 Oct. | 2007 Jun. | |
| | | | 5.68% | 4.03% | 10.03% | 4.62% | 4.02% | |

| | | | | | | | | |
|---|---|---|---|---|---|---|---|---|
| | 2010-2013 | road construction | | 2011 Mar. | 2012 May | 2012 Jun. | 2013 Mar. | |
| | | | | 7.36% | 7.85% | 7.08% | 5.62% | |
| 10. Rock | 1989-1992 | grazing | | 1992 Sep. | | | | |
| | | | 14.88% | 14.88% | | | | |
| | 1992-1997 | after wildfire period 1 | | | | | | |
| | 1998-2003 | after wildfire period 2 | | 2002 Jul. | | | | |
| | | | | 8.17% | | | | |
| | 2004-2009 | after wildfire period 3 | | 2004 Apr. | 2007 Jun. | 2009 Nov. | | |
| | | | | 9.43% | 6.46% | 8.90% | | |
| 11. Cave Creek | 1989-1992 | grazing | | 1992 Sep. | | | | |
| | | | 8.84% | 8.84% | | | | |
| | 1992-1999 | after wildfire | | | | | | |
| | 2000-2003 | house construction | | 2003 Oct. | 2004 Dec. | | | |
| | | | | 4.55% | 12.59% | | | |
| 12. Buckhorn | 1989-1999 | grazing | | 1992 Sep. | | | | |
| | | | 30.45% | 30.45% | | | | |
| | 2000-2002 | house construction | | 2003 Oct. | | | | |
| | | | | 20.18% | | | | |
| 14. 128th St | 1989-1994 | grazing | | 1992 Sep. | | | | |
| | | | 32.02% | 32.02% | | | | |
| | 1995-2000 | after wildfire | | | | | | |
| | 2001-2008 | road construction | | 2003 Apr. | 2004 Apr. | 2005 Apr. | 2006 Oct. | 2007 Jun. |
| | | | | 55.68% | 62.95% | 59.66% | 19.48% | 22.06% |
| 15. 128th St 2 | 1989-1994 | grazing | | 1992 Sep. | | | | |
| | | | 36.54% | 36.54% | | | | |
| | 1995-2000 | after wildfire | | | | | | |
| | 2001-2008 | road construction | | 2003 Apr. | 2004 Apr. | 2005 Apr. | 2006 Oct. | 2007 Jun. |
| | | | | 75.99% | 67.32% | 71.52% | 40.55% | 34.28% |
| 16.AsherHills | 1989-2001 | grazing | | 1992 Sep. | | | | |
| | | | 22.23% | 22.23% | | | | |
| | 2002-2007 | house construction | | 2003 Apr. | 2004 Dec. | 2005 Apr. | 2007 Jun. | |
| | | | | 76.57% | 63.12% | 71.55% | 65.93% | |
| 18. Peralta | 1989-2000 | grazing | | 1992 May | | | | |
| | | | 10.07% | 10.07% | | | | |

| | | | | |
|---|---|---|---|---|
| 2001-2005 | subdivision construction | | | |
| 2006-2009 | subdivision finished | | 2007 Jun. | 2010 Feb. |
| | | | 5.76% | 10.78% |

# APPENDIX E

# PRECIPITATION VARIABLES ANALYSIS

| # | Stock Tank | Rain gauge IDs | MAP (89-99) | MAP (00-09) | MSP (89-99) | MSP (00-09) |
|---|---|---|---|---|---|---|
| 1 | Cigar | 72000 | 213 | 172 | 67 | 55 |
| | | 72500 | 221 | 167 | 72 | 45 |
| | | 73000 | 186 | 172 | 73 | 55 |
| | | Avg of 3 gauges | 207 | 170 | 71 | 51 |
| 2 | Saguaro | 62000 | 233 | 175 | 77 | 55 |
| | | 62300 | 278 | 208 | 81 | 54 |
| | | 19500 | 155 | 160 | 35 | 40 |
| | | Avg of 3 gauges | 222 | 181 | 64 | 50 |
| 3 | Cline | 62000 | 233 | 175 | 77 | 55 |
| | | 62300 | 278 | 208 | 81 | 54 |
| | | 19500 | 155 | 160 | 35 | 40 |
| | | Avg of 3 gauges | 222 | 181 | 64 | 50 |
| 4 | Anthem | 62000 | 233 | 175 | 77 | 55 |
| | | 62300 | 278 | 208 | 81 | 54 |
| | | 19500 | 155 | 160 | 35 | 40 |
| | | Avg of 3 gauges | 222 | 181 | 64 | 50 |
| 5 | Anthem2 | 62000 | 233 | 175 | 77 | 55 |
| | | 62300 | 278 | 208 | 81 | 54 |
| | | 19500 | 155 | 160 | 35 | 40 |
| | | Avg of 3 gauges | 222 | 181 | 64 | 50 |
| 6 | Pepe | 62000 | 233 | 175 | 77 | 55 |
| | | 62300 | 278 | 208 | 81 | 54 |
| | | 19500 | 155 | 160 | 35 | 40 |
| | | Avg of 3 gauges | 222 | 181 | 64 | 50 |
| 7 | Bronco | 62000 | 233 | 175 | 77 | 55 |
| | | 62300 | 278 | 208 | 81 | 54 |
| | | 19500 | 155 | 160 | 35 | 40 |
| | | Avg of 3 gauges | 222 | 181 | 64 | 50 |
| 8 | Circle | 62000 | 233 | 175 | 77 | 55 |
| | | 62300 | 278 | 208 | 81 | 54 |
| | | 19500 | 155 | 160 | 35 | 40 |
| | | Avg of 3 gauges | 222 | 181 | 64 | 50 |
| 9 | Charlie | 21000 | 313 | 283 | 80 | 73 |
| | | 76200 | 362 | 268 | 105 | 76 |
| | | 19500 | 155 | 160 | 35 | 40 |
| | | Avg of 3 gauges | 276 | 237 | 74 | 63 |
| 10 | Rock | 21000 | 313 | 283 | 80 | 73 |
| | | 76200 | 362 | 268 | 105 | 76 |
| | | 19500 | 155 | 160 | 35 | 40 |
| | | Avg of 3 gauges | 276 | 237 | 74 | 63 |
| 11 | Cave Creek | 21000 | 313 | 283 | 80 | 73 |
| | | 76200 | 362 | 268 | 105 | 76 |

| | | | | | | |
|---|---|---|---|---|---|---|
| | | 19500 | 155 | 160 | 35 | 40 |
| | | Avg of 3 gauges | 276 | 237 | 74 | 63 |
| | | 21000 | 313 | 283 | 80 | 73 |
| 12 | Buckhorn | 76200 | 325 | 268 | 105 | 76 |
| | | 75500 | 276 | 228 | 71 | 65 |
| | | Avg of 3 gauges | 305 | 260 | 85 | 71 |
| | | 75500 | 276 | 228 | 71 | 65 |
| 13 | The Rocks | 75800 | 329 | 246 | 66 | 67 |
| | | 76200 | 325 | 268 | 105 | 76 |
| | | Avg of 3 gauges | 310 | 248 | 81 | 69 |
| | | 75500 | 276 | 228 | 71 | 65 |
| 14 | 128th St | 75800 | 329 | 246 | 66 | 67 |
| | | 76200 | 325 | 268 | 105 | 76 |
| | | Avg of 3 gauges | 310 | 248 | 81 | 69 |
| | | 75500 | 276 | 228 | 71 | 65 |
| 15 | 128th St2 | 75800 | 329 | 246 | 66 | 67 |
| | | 76200 | 325 | 268 | 105 | 76 |
| | | Avg of 3 gauges | 310 | 248 | 81 | 69 |
| | | 75500 | 276 | 228 | 71 | 65 |
| 16 | Asherhills | 75800 | 329 | 246 | 66 | 67 |
| | | 76200 | 325 | 268 | 105 | 76 |
| | | Avg of 3 gauges | 310 | 248 | 81 | 69 |
| | | 37000 | 230 | 184 | 71 | 57 |
| 17 | GoldCyn | 38500 | 264 | 226 | 79 | 76 |
| | | 39000 | 267 | 218 | 74 | 66 |
| | | Avg of 3 gauges | 254 | 209 | 75 | 66 |
| | | 37000 | 230 | 184 | 71 | 57 |
| 18 | Peralta | 38500 | 264 | 226 | 79 | 76 |
| | | 39000 | 267 | 218 | 74 | 66 |
| | | Avg of 3 gauges | 254 | 209 | 75 | 66 |

Note: MAP, mean annual precipitation; MSP, mean seasonal (summer) precipitation.

**Mean annual precipitation (mm)**

| Gauge ID | 1989 | 1990 | 1991 | 1992 | 1993 | 1994 | 1995 | 1996 | 1997 | 1998 | 1999 | 2000 | 2001 | 2002 | 2003 | 2004 | 2005 | 2006 | 2007 | 2008 | 2009 | 2010 | 2011 | 2012 | 2013 |
|---|---|---|---|---|---|---|---|---|---|---|---|---|---|---|---|---|---|---|---|---|---|---|---|---|---|
| 72000 | | | | | 325 | 158 | 262 | 121 | 129 | 311 | 184 | 79 | 202 | 107 | 288 | 122 | 316 | 155 | 126 | 198 | 126 | | | | |
| 72500 | | | | | 344 | 140 | 329 | 103 | 150 | 290 | 193 | 107 | 294 | 73 | 183 | 129 | 342 | 87 | 133 | 195 | 127 | | | | |
| 73000 | | | | | | 122 | 236 | 190 | 137 | 268 | 163 | 73 | 263 | 124 | 280 | 149 | 358 | 71 | 107 | 173 | 120 | | | | |
| 62000 | 181 | 244 | 160 | 341 | 341 | 247 | 326 | 168 | 75 | 266 | 219 | 113 | 261 | 76 | 181 | 205 | 380 | 142 | 76 | 203 | 116 | 238 | 90 | 126 | 122 |
| 62300 | 248 | 296 | 228 | 448 | 516 | 192 | 356 | 145 | 136 | 288 | 208 | 155 | 288 | 63 | 251 | 312 | 365 | 143 | 107 | 226 | 169 | 319 | 170 | 195 | 212 |
| 19500 | 39 | 123 | 140 | 237 | 281 | 113 | 227 | 125 | 90 | 217 | 110 | 64 | 170 | 46 | 174 | 233 | 344 | 152 | 105 | 201 | 113 | 202 | | 115 | 233 |
| 21000 | 314 | 257 | 268 | 440 | 412 | 152 | 478 | 251 | 171 | 429 | 269 | 167 | 376 | 84 | 287 | 263 | 495 | 234 | 240 | 401 | 285 | | | | |
| 76200 | | 323 | 275 | 565 | 543 | 291 | 465 | 200 | 179 | 413 | | 98 | 361 | 111 | 287 | 288 | 507 | 207 | 240 | 357 | 227 | | | | |
| 75500 | | | 263 | 457 | 433 | 193 | 314 | 132 | 171 | 278 | 243 | 137 | 279 | 60 | 241 | 199 | 434 | 172 | 195 | 360 | 203 | | | | |
| 75800 | | | 310 | 485 | 552 | 292 | 353 | 161 | 185 | 346 | 276 | 133 | 338 | 101 | 273 | 222 | 431 | 188 | 176 | 399 | 202 | | | | |
| 37000 | 137 | 217 | 174 | 456 | 341 | 200 | 279 | 215 | 91 | 250 | 175 | 103 | 289 | 91 | 91 | 221 | 304 | 171 | 123 | 307 | 140 | | | | |
| 38500 | 149 | 231 | 242 | 492 | 415 | 267 | 336 | 230 | 96 | 278 | 164 | 128 | 326 | 101 | 181 | 238 | 378 | 253 | 178 | 305 | 172 | | | | |
| 39000 | 124 | 290 | 279 | 429 | 523 | 260 | 293 | 146 | 117 | 354 | 119 | 93 | 328 | 97 | 121 | 260 | 362 | 190 | 162 | 360 | 205 | | | | |

**Mean seasonal (summer) precipitation (mm)**

| Gauge ID | 1989 | 1990 | 1991 | 1992 | 1993 | 1994 | 1995 | 1996 | 1997 | 1998 | 1999 | 2000 | 2001 | 2002 | 2003 | 2004 | 2005 | 2006 | 2007 | 2008 | 2009 |
|---|---|---|---|---|---|---|---|---|---|---|---|---|---|---|---|---|---|---|---|---|---|
| 72000 | | | | | 37 | 41 | 46 | 75 | 57 | 113 | 102 | 29 | 38 | 74 | 116 | 25 | 27 | 129 | 47 | 51 | 10 |
| 72500 | | | | | 60 | 38 | 80 | 46 | 78 | 86 | 117 | 57 | 63 | 45 | 59 | 18 | 55 | 58 | 32 | 51 | 9 |
| 73000 | | | | | | 32 | 46 | 116 | 67 | 82 | 94 | 24 | 59 | 103 | 107 | 28 | 71 | 47 | 37 | 50 | 19 |
| 62000 | 78 | 165 | 38 | 92 | 18 | 72 | 66 | 108 | 30 | 62 | 116 | 58 | 48 | 53 | 58 | 52 | 88 | 86 | 28 | 63 | 17 |
| 62300 | 85 | 126 | 50 | 86 | 90 | 47 | 77 | 96 | 51 | 61 | 124 | 93 | 51 | 38 | 56 | 93 | 41 | 92 | 33 | 29 | 18 |
| 19500 | 24 | 61 | 23 | 46 | 14 | 7 | 36 | 72 | 32 | 34 | 36 | 4 | 14 | 32 | 31 | 67 | 38 | 81 | 50 | 65 | 14 |
| 21000 | 75 | 75 | 20 | 122 | 24 | 4 | 162 | 169 | 46 | 54 | 130 | 65 | 50 | 48 | 55 | 49 | 56 | 135 | 132 | 96 | 43 |
| 76200 | | 158 | 63 | 227 | 56 | 35 | 139 | 119 | 60 | 74 | 124 | 10 | 46 | 81 | 53 | 47 | 97 | 122 | 122 | 147 | 34 |
| 75500 | | | 71 | 124 | 48 | 24 | 92 | 74 | 77 | 20 | 105 | 50 | 17 | 35 | 38 | 29 | 93 | 123 | 99 | 116 | 45 |
| 75800 | | | 71 | 94 | 30 | 35 | 63 | 76 | 65 | 27 | 129 | 50 | 53 | 67 | 35 | 37 | 84 | 117 | 84 | 111 | 36 |
| 37000 | 23 | 110 | 9 | 153 | 39 | 31 | 64 | 147 | 21 | 61 | 123 | 40 | 57 | 37 | 20 | 86 | 45 | 98 | 54 | 88 | 41 |
| 38500 | 16 | 100 | 32 | 163 | 72 | 62 | 72 | 161 | 30 | 61 | 97 | 66 | 56 | 53 | 26 | 94 | 64 | 183 | 74 | 110 | 37 |
| 39000 | 39 | 139 | 39 | 122 | 81 | 59 | 36 | 83 | 36 | 121 | 57 | 30 | 59 | 48 | 16 | 102 | 73 | 113 | 80 | 98 | 39 |

| # | Stock Tank | Rain gauge IDs | Annual total amount of I30 (mm)[a] Period 1 (1989-1999) | Period 2 (2000-2009) |
|---|---|---|---|---|
| 1 | Cigar | 72000 | 20.9 | 15.4 |
| 2 | Saguaro | 62300 | 25.1 | 14.1 |
| 3 | Cline | 62300 | 25.1 | 14.1 |
| 4 | Anthem | 62300 | 25.1 | 14.1 |
| 5 | Anthem2 | 62300 | 25.1 | 14.1 |
| 6 | Pepe | 65800 | 22.8 | 11.5 |
| 7 | Bronco | 65800 | 22.8 | 11.5 |
| 8 | Circle | 65800 | 22.8 | 11.5 |
| 9 | Charlie | 76200 | 40.4 | 28.0 |
| 10 | Rock | 76200 | 40.4 | 28.0 |
| 11 | Cave Creek | 21000 | 15.4 | 22.9 |
| 12 | Buckhorn | 76200 | 40.4 | 28.0 |
| 13 | The Rocks | 76200 | 40.4 | 28.0 |
| 14 | 128th St | 76200 | 40.4 | 28.0 |
| 15 | 128th St2 | 76200 | 40.4 | 28.0 |
| 16 | Asherhills | 75500 | 17.5 | 18.4 |
| 17 | GoldCyn | 39000 | 23.2 | 17.9 |
| 18 | Peralta | 39000 | 23.2 | 17.9 |

a Total amount of rainfall exceeded 10 mm (0.4 inches) for 30 min normalized by measurement period (years).

| Cigar | | | Saguaro | | | Charlie | | |
|---|---|---|---|---|---|---|---|---|
| Gauge ID: 72000 | | | Gauge ID: 62500 | | | Gauge ID: 20200 | | |
| Date | Time | I30 (inches/30min) | Date | Time | I30 (inches/30min) | Date | Time | I30 (inches/30min) |
| 7/24/1992 | 500 | 1.06 | 10/6/1993 | 1230 | 0.91 | 10/6/1993 | 1300 | 0.79 |
| 8/22/1992 | 1200 | 0.59 | 8/31/1993 | 1600 | 0.47 | 10/6/1993 | 1330 | 0.35 |
| 9/19/1992 | 2300 | 0.47 | 8/29/1993 | 1430 | 0.31 | 8/30/1993 | 630 | 0.31 |
| 12/8/1992 | 330 | 0.28 | 8/31/1993 | 1530 | 0.28 | 11/12/1993 | 2100 | 0.24 |
| 9/19/1992 | 2330 | 0.28 | 8/29/1993 | 1630 | 0.28 | 10/6/1993 | 1230 | 0.20 |
| 5/21/1992 | 900 | 0.24 | 9/2/1994 | 2030 | 0.39 | 12/6/1994 | 200 | 0.31 |
| 12/4/1992 | 430 | 0.20 | 8/19/1994 | 2030 | 0.31 | 10/15/1994 | 930 | 0.28 |
| 8/30/1992 | 1730 | 0.20 | 7/19/1994 | 730 | 0.28 | 7/28/1994 | 2000 | 0.24 |
| 6/3/1992 | 2130 | 0.20 | 10/15/1994 | 830 | 0.24 | 3/7/1994 | 1430 | 0.24 |
| 1/18/1993 | 1500 | 0.55 | 8/19/1994 | 1430 | 0.24 | 12/6/1994 | 130 | 0.20 |
| 8/29/1993 | 100 | 0.39 | 12/29/1994 | 2000 | 0.2 | 9/28/1995 | 300 | 0.75 |
| 10/6/1993 | 1130 | 0.35 | 10/15/1994 | 800 | 0.2 | 9/27/1995 | 2400 | 0.71 |
| 10/6/1993 | 1200 | 0.28 | 9/27/1995 | 2400 | 0.55 | 11/1/1995 | 2030 | 0.51 |
| 2/8/1993 | 1930 | 0.24 | 8/11/1995 | 2330 | 0.55 | 9/28/1995 | 330 | 0.35 |
| 2/28/1993 | 300 | 0.20 | 9/28/1995 | 330 | 0.31 | 11/1/1995 | 2000 | 0.28 |
| 7/17/1994 | 1830 | 0.43 | 8/12/1995 | 30 | 0.24 | 1/26/1995 | 100 | 0.28 |
| 5/24/1994 | 1930 | 0.31 | 6/28/1995 | 1730 | 0.24 | 10/31/1995 | 2330 | 0.24 |
| 5/24/1994 | 1200 | 0.31 | 9/28/1995 | 30 | 0.2 | 3/11/1995 | 1830 | 0.20 |
| 12/25/1994 | 1830 | 0.28 | 8/15/1995 | 1930 | 0.2 | 3/11/1995 | 1800 | 0.20 |
| 10/15/1994 | 630 | 0.28 | 8/11/1995 | 2400 | 0.2 | 2/15/1995 | 330 | 0.20 |
| 10/15/1994 | 700 | 0.20 | 8/11/1995 | 2300 | 0.2 | 9/2/1996 | 100 | 0.39 |
| 3/7/1994 | 1130 | 0.20 | 1/5/1995 | 330 | 0.2 | 7/14/1996 | 2130 | 0.39 |
| 8/14/1995 | 2330 | 0.51 | 1/4/1995 | 2100 | 0.2 | 7/14/1996 | 2200 | 0.35 |
| 1/25/1995 | 2100 | 0.31 | 7/25/1996 | 2100 | 0.35 | 9/11/1996 | 500 | 0.31 |
| 9/6/1995 | 2130 | 0.28 | 7/14/1996 | 2200 | 0.31 | 9/2/1996 | 300 | 0.28 |
| 3/11/1995 | 1700 | 0.28 | 8/18/1996 | 2330 | 0.28 | 9/2/1996 | 130 | 0.28 |
| 1/5/1995 | 230 | 0.24 | 6/30/1996 | 2030 | 0.24 | 8/14/1996 | 1230 | 0.28 |
| 11/1/1995 | 1930 | 0.20 | 8/14/1996 | 1830 | 0.2 | 9/6/1996 | 2000 | 0.24 |
| 8/26/1996 | 2230 | 0.55 | 9/11/1997 | 1130 | 0.71 | 9/9/1996 | 2230 | 0.20 |
| 7/14/1996 | 2330 | 0.43 | 1/13/1997 | 2300 | 0.31 | 8/14/1996 | 1330 | 0.20 |
| 7/25/1996 | 2300 | 0.24 | 1/13/1997 | 400 | 0.24 | 7/25/1996 | 2200 | 0.20 |
| 7/25/1996 | 2200 | 0.20 | 12/7/1997 | 230 | 0.2 | 9/11/1997 | 1130 | 0.31 |
| 1/13/1997 | 1300 | 0.24 | 7/7/1998 | 2400 | 0.35 | 9/11/1997 | 1330 | 0.20 |
| 12/7/1997 | 200 | 0.20 | 9/11/1998 | 730 | 0.28 | 1/13/1997 | 830 | 0.20 |
| 9/11/1997 | 1700 | 0.20 | 7/6/1998 | 2100 | 0.28 | 1/13/1997 | 400 | 0.20 |
| 9/11/1997 | 1030 | 0.20 | 8/24/1998 | 2100 | 0.24 | 10/26/1998 | 730 | 0.39 |
| 9/1/1997 | 1200 | 0.20 | 3/26/1998 | 430 | 0.24 | 3/26/1998 | 1100 | 0.35 |
| 1/13/1997 | 2130 | 0.20 | 2/15/1998 | 200 | 0.24 | 10/25/1998 | 1600 | 0.28 |
| 8/7/1998 | 2330 | 0.98 | 8/17/1998 | 930 | 0.2 | 2/15/1998 | 230 | 0.24 |
| 7/8/1998 | 1930 | 0.55 | 3/26/1998 | 400 | 0.2 | 2/24/1998 | 1930 | 0.20 |
| 7/7/1998 | 1800 | 0.55 | 9/23/1999 | 1430 | 0.47 | 7/14/1999 | 1600 | 0.67 |
| 7/8/1998 | 1900 | 0.39 | 7/15/1999 | 530 | 0.35 | 7/15/1999 | 600 | 0.43 |
| 2/4/1998 | 600 | 0.31 | 9/11/1999 | 2030 | 0.31 | 7/7/1999 | 2030 | 0.43 |
| 8/7/1998 | 2400 | 0.24 | 7/14/1999 | 1530 | 0.31 | 8/27/1999 | 1730 | 0.39 |
| 8/6/1998 | 200 | 0.20 | 7/10/1999 | 1900 | 0.31 | 7/23/1999 | 1830 | 0.35 |
| 7/8/1998 | 2000 | 0.20 | 9/23/1999 | 1400 | 0.28 | 7/15/1999 | 530 | 0.31 |
| 2/4/1998 | 630 | 0.20 | 9/23/1999 | 1300 | 0.28 | 7/7/1999 | 2100 | 0.28 |
| 7/14/1999 | 1500 | 1.22 | 7/14/1999 | 1600 | 0.2 | 9/19/1999 | 1930 | 0.24 |
| 8/15/1999 | 2130 | 0.39 | 7/10/1999 | 2100 | 0.2 | 6/2/1999 | 930 | 0.20 |
| 8/19/1999 | 1930 | 0.24 | 10/22/2000 | 500 | 0.39 | 10/22/2000 | 500 | 0.39 |
| 9/11/1999 | 2330 | 0.20 | 6/20/2000 | 1700 | 0.39 | 10/22/2000 | 700 | 0.35 |
| 8/30/1999 | 1900 | 0.20 | 10/21/2000 | 2230 | 0.31 | 10/22/2000 | 300 | 0.31 |
| 10/30/2000 | 1700 | 0.28 | 8/17/2000 | 1930 | 0.28 | 10/21/2000 | 1930 | 0.20 |
| 6/28/2000 | 1930 | 0.24 | 10/27/2000 | 1500 | 0.24 | 8/14/2001 | 1600 | 0.55 |
| 10/7/2001 | 700 | 0.55 | 10/22/2000 | 30 | 0.2 | 8/9/2001 | 100 | 0.31 |
| 8/17/2001 | 100 | 0.31 | 10/21/2000 | 2200 | 0.2 | 1/27/2001 | 1430 | 0.20 |
| 8/17/2001 | 130 | 0.20 | 7/29/2001 | 2300 | 0.59 | 7/9/2002 | 2030 | 0.20 |

| Cigar | | | Saguaro | | | Charlie | | |
|---|---|---|---|---|---|---|---|---|
| Gauge ID: 72000 | | | Gauge ID: 62500 | | | Gauge ID: 20200 | | |
| Date | Time | I30 (inches/30min) | Date | Time | I30 (inches/30min) | Date | Time | I30 (inches/30min) |
| 7/30/2001 | 30 | 0.20 | 8/9/2001 | 100 | 0.24 | 8/14/2003 | 2000 | 0.39 |
| 3/7/2001 | 700 | 0.20 | 12/4/2001 | 530 | 0.2 | 10/10/2003 | 830 | 0.31 |
| 9/7/2002 | 1830 | 0.35 | 7/29/2001 | 2330 | 0.2 | 2/13/2003 | 2300 | 0.31 |
| 9/7/2002 | 1900 | 0.28 | 9/6/2002 | 2030 | 0.55 | 3/16/2003 | 2000 | 0.28 |
| 10/26/2002 | 1730 | 0.24 | 9/7/2002 | 1800 | 0.39 | 11/12/2003 | 2330 | 0.20 |
| 9/6/2002 | 1900 | 0.24 | 8/26/2003 | 2230 | 0.2 | 2/13/2003 | 2400 | 0.20 |
| 8/4/2002 | 30 | 0.24 | 2/25/2003 | 1830 | 0.2 | 2/13/2003 | 1500 | 0.20 |
| 7/11/2002 | 1830 | 0.24 | 9/19/2004 | 1300 | 0.67 | 3/4/2004 | 1730 | 0.35 |
| 9/6/2002 | 2100 | 0.20 | 9/19/2004 | 1400 | 0.47 | 9/19/2004 | 330 | 0.31 |
| 8/14/2003 | 2100 | 1.69 | 8/16/2004 | 1830 | 0.43 | 3/5/2004 | 230 | 0.31 |
| 8/27/2003 | 30 | 0.35 | 3/5/2004 | 230 | 0.31 | 4/2/2004 | 600 | 0.28 |
| 2/13/2003 | 2100 | 0.35 | 11/8/2004 | 400 | 0.28 | 3/5/2004 | 430 | 0.28 |
| 9/6/2003 | 1530 | 0.31 | 8/16/2004 | 1700 | 0.28 | 3/5/2004 | 330 | 0.24 |
| 9/6/2003 | 1600 | 0.28 | 4/9/2004 | 1700 | 0.24 | 3/5/2004 | 300 | 0.24 |
| 8/14/2003 | 2030 | 0.24 | 3/5/2004 | 330 | 0.24 | 3/5/2004 | 130 | 0.24 |
| 11/12/2003 | 1530 | 0.20 | 3/5/2004 | 200 | 0.24 | 9/19/2004 | 1430 | 0.20 |
| 2/25/2003 | 2400 | 0.20 | 3/4/2004 | 1700 | 0.2 | 4/2/2004 | 730 | 0.20 |
| 8/15/2004 | 1900 | 0.47 | 10/18/2005 | 1130 | 0.35 | 3/5/2004 | 30 | 0.20 |
| 12/29/2004 | 830 | 0.35 | 8/9/2005 | 1500 | 0.35 | 2/23/2004 | 530 | 0.20 |
| 4/2/2004 | 300 | 0.31 | 2/20/2005 | 100 | 0.2 | | | |
| 12/29/2004 | 730 | 0.28 | 8/13/2006 | 1930 | 0.55 | | | |
| 4/2/2004 | 330 | 0.24 | 9/9/2006 | 900 | 0.51 | | | |
| 11/8/2004 | 200 | 0.24 | 8/24/2006 | 930 | 0.35 | | | |
| 11/22/2004 | 600 | 0.20 | 9/9/2006 | 830 | 0.24 | | | |
| 2/19/2005 | 2400 | 0.47 | 7/25/2007 | 1500 | 0.59 | | | |
| 1/3/2005 | 2030 | 0.28 | 11/30/2007 | 1600 | 0.31 | | | |
| 9/2/2006 | 1830 | 0.98 | 12/1/2007 | 230 | 0.28 | | | |
| 8/9/2006 | 1730 | 0.71 | 11/30/2007 | 2400 | 0.28 | | | |
| 9/7/2006 | 2230 | 0.59 | 3/22/2007 | 1500 | 0.28 | | | |
| 9/6/2006 | 2330 | 0.28 | 12/7/2007 | 1730 | 0.24 | | | |
| 8/11/2006 | 2330 | 0.24 | 8/1/2007 | 1730 | 0.24 | | | |
| 8/31/2006 | 2000 | 0.24 | 3/22/2007 | 2200 | 0.24 | | | |
| 9/12/2006 | 1930 | 0.24 | 12/1/2007 | 1230 | 0.2 | | | |
| 8/31/2006 | 1830 | 0.24 | 7/28/2007 | 1700 | 0.2 | | | |
| 9/2/2006 | 1800 | 0.24 | 7/10/2008 | 2400 | 0.47 | | | |
| 8/9/2006 | 1700 | 0.20 | 7/13/2008 | 1730 | 0.43 | | | |
| 7/23/2007 | 1730 | 0.59 | 7/10/2008 | 2300 | 0.43 | | | |
| 3/22/2007 | 1530 | 0.35 | 8/28/2008 | 2030 | 0.31 | | | |
| 11/30/2007 | 2330 | 0.24 | 8/7/2008 | 2030 | 0.31 | | | |
| 11/30/2007 | 1930 | 0.24 | 11/27/2008 | 2000 | 0.28 | | | |
| 7/23/2007 | 1630 | 0.24 | 8/28/2008 | 2200 | 0.28 | | | |
| 12/7/2007 | 1630 | 0.20 | 8/28/2008 | 2130 | 0.24 | | | |
| 1/31/2007 | 400 | 0.20 | 7/10/2008 | 2230 | 0.2 | | | |
| 7/13/2008 | 1700 | 0.39 | 7/19/2009 | 2030 | 0.47 | | | |
| 11/27/2008 | 130 | 0.35 | 8/13/2009 | 130 | 0.31 | | | |
| 9/10/2008 | 1900 | 0.28 | | | | | | |
| 11/27/2008 | 200 | 0.20 | | | | | | |

| Circle, Pepe, Bronco | | | 128 st., 128 St.2, The rocks, Rock, Buckhorn, Charlie | | | Gold canyon, Peralta | | |
|---|---|---|---|---|---|---|---|---|
| Gauge ID: 65800 | | | Gauge ID: 76200 | | | Gauge ID: 39000 | | |
| Date | Time | I30 (inches/30min) | Date | Time | I30 (inches/30min) | Date | Time | I30 (inches/30min) |
| 9/3/1990 | 1900 | 0.87 | 10/21/1989 | 1500 | 0.28 | 8/19/1989 | 330 | 0.55 |
| 8/14/1990 | 1030 | 0.75 | 10/21/1989 | 1330 | 0.24 | 8/14/1989 | 2400 | 0.35 |
| 9/3/1990 | 1930 | 0.51 | 8/17/1989 | 2300 | 0.2 | 4/4/1989 | 1500 | 0.24 |
| 8/15/1990 | 530 | 0.47 | 8/5/1990 | 1830 | 0.55 | 8/7/1989 | 1830 | 0.20 |
| 9/3/1990 | 1800 | 0.43 | 8/30/1990 | 2100 | 0.55 | 1/4/1989 | 730 | 0.20 |
| 7/21/1990 | 1900 | 0.31 | 7/21/1990 | 1930 | 0.47 | 9/3/1990 | 1630 | 0.55 |
| 8/11/1990 | 2200 | 0.24 | 7/2/1990 | 2200 | 0.39 | 9/3/1990 | 1600 | 0.55 |
| 1/17/1990 | 1900 | 0.20 | 11/2/1990 | 1400 | 0.31 | 7/10/1990 | 1900 | 0.31 |
| 9/14/1990 | 2400 | 0.20 | 9/2/1990 | 400 | 0.28 | 9/14/1990 | 2100 | 0.28 |
| 12/19/1991 | 1200 | 0.43 | 7/10/1990 | 2030 | 0.28 | 8/15/1990 | 200 | 0.24 |
| 8/11/1991 | 500 | 0.39 | 9/15/1990 | 1000 | 0.24 | 8/14/1990 | 930 | 0.24 |
| 8/11/1991 | 430 | 0.39 | 9/14/1990 | 2200 | 0.24 | 8/14/1990 | 300 | 0.24 |
| 12/18/1991 | 1600 | 0.35 | 9/3/1990 | 2000 | 0.24 | 8/15/1990 | 130 | 0.20 |
| 12/18/1991 | 1400 | 0.35 | 9/2/1990 | 430 | 0.2 | 4/24/1990 | 830 | 0.20 |
| 11/30/1991 | 1100 | 0.35 | 3/29/1990 | 1430 | 0.2 | 9/5/1991 | 1500 | 0.47 |
| 10/27/1991 | 1400 | 0.35 | 1/17/1990 | 1830 | 0.2 | 10/27/1991 | 1200 | 0.35 |
| 12/10/1991 | 2300 | 0.31 | 9/20/1990 | 700 | 0.2 | 1/4/1991 | 1700 | 0.35 |
| 11/30/1991 | 1200 | 0.28 | 8/24/1991 | 1630 | 0.67 | 1/4/1991 | 1900 | 0.31 |
| 8/27/1991 | 100 | 0.28 | 10/27/1991 | 1230 | 0.51 | 10/27/1991 | 800 | 0.28 |
| 10/27/1991 | 1500 | 0.24 | 8/24/1991 | 1600 | 0.39 | 10/27/1991 | 1000 | 0.24 |
| 8/11/1991 | 530 | 0.24 | 9/5/1991 | 1700 | 0.31 | 1/4/1991 | 2300 | 0.24 |
| 8/11/1991 | 400 | 0.24 | 8/11/1991 | 400 | 0.28 | 11/10/1991 | 1730 | 0.20 |
| 8/11/1991 | 330 | 0.24 | 1/4/1991 | 1800 | 0.28 | 1/4/1991 | 2100 | 0.20 |
| 1/4/1991 | 1600 | 0.24 | 9/5/1991 | 1430 | 0.24 | 8/22/1992 | 630 | 0.55 |
| 8/11/1991 | 200 | 0.20 | 1/4/1991 | 2200 | 0.24 | 8/22/1992 | 600 | 0.51 |
| 1/4/1991 | 1800 | 0.20 | 1/4/1991 | 2000 | 0.2 | 7/24/1992 | 330 | 0.51 |
| 12/10/1991 | 1900 | 0.20 | 3/26/1991 | 1000 | 0.2 | 10/23/1992 | 2100 | 0.43 |
| 11/30/1991 | 300 | 0.20 | 3/20/1991 | 1930 | 0.2 | 8/6/1992 | 2100 | 0.39 |
| 3/28/1992 | 2230 | 0.51 | 8/6/1992 | 2000 | 0.91 | 8/23/1992 | 300 | 0.31 |
| 8/22/1992 | 2230 | 0.47 | 8/6/1992 | 2130 | 0.63 | 3/8/1992 | 2100 | 0.31 |
| 8/22/1992 | 2130 | 0.47 | 8/23/1992 | 300 | 0.63 | 5/8/1992 | 1530 | 0.28 |
| 3/28/1992 | 2200 | 0.43 | 8/22/1992 | 730 | 0.55 | 8/6/1992 | 2130 | 0.24 |
| 2/10/1992 | 2030 | 0.35 | 7/24/1992 | 330 | 0.47 | 8/3/1992 | 30 | 0.20 |
| 1/12/1992 | 2000 | 0.35 | 3/29/1992 | 800 | 0.43 | 1/18/1993 | 1330 | 0.71 |
| 1/6/1992 | 1530 | 0.31 | 8/22/1992 | 700 | 0.43 | 8/24/1993 | 2100 | 0.55 |
| 9/19/1992 | 2200 | 0.28 | 8/22/1992 | 830 | 0.39 | 1/8/1993 | 530 | 0.43 |
| 1/14/1993 | 1930 | 0.83 | 8/22/1992 | 800 | 0.39 | 3/27/1993 | 200 | 0.31 |
| 1/10/1993 | 2100 | 0.55 | 8/22/1992 | 900 | 0.31 | 8/27/1993 | 2100 | 0.28 |
| 10/7/1993 | 200 | 0.24 | 8/6/1992 | 1930 | 0.31 | 10/6/1993 | 1700 | 0.24 |
| 8/29/1993 | 2130 | 0.24 | 7/24/1992 | 300 | 0.28 | 8/27/1993 | 2400 | 0.24 |
| 8/29/1993 | 2200 | 0.20 | 5/23/1992 | 1630 | 0.28 | 11/11/1993 | 1200 | 0.20 |
| 3/26/1993 | 1630 | 0.20 | 8/7/1992 | 230 | 0.24 | 8/27/1993 | 2030 | 0.20 |
| 3/26/1993 | 1330 | 0.20 | 8/6/1992 | 2030 | 0.24 | 2/10/1993 | 200 | 0.20 |
| 1/10/1993 | 2030 | 0.20 | 1/11/1992 | 2400 | 0.2 | 1/18/1993 | 1730 | 0.20 |
| 1/7/1993 | 2000 | 0.20 | 1/11/1992 | 2330 | 0.2 | 1/11/1993 | 130 | 0.20 |
| 11/13/1993 | 1400 | 0.20 | 12/4/1992 | 1630 | 0.2 | 1/7/1993 | 2400 | 0.20 |
| 10/6/1993 | 1330 | 0.20 | 8/12/1992 | 1300 | 0.2 | 7/17/1994 | 1530 | 0.59 |
| 10/6/1993 | 1300 | 0.20 | 10/6/1993 | 1330 | 0.43 | 9/2/1994 | 2300 | 0.51 |
| 2/8/1994 | 1400 | 0.39 | 10/6/1993 | 1230 | 0.35 | 5/25/1994 | 30 | 0.35 |
| 12/25/1994 | 2100 | 0.24 | 3/26/1993 | 1730 | 0.35 | 8/26/1994 | 2200 | 0.28 |
| 11/1/1995 | 2000 | 0.59 | 1/17/1993 | 1230 | 0.31 | 11/12/1994 | 530 | 0.24 |
| 9/28/1995 | 330 | 0.35 | 10/7/1993 | 230 | 0.31 | 7/28/1994 | 1900 | 0.24 |
| 8/19/1995 | 2000 | 0.35 | 10/6/1993 | 230 | 0.31 | 5/24/1994 | 1830 | 0.24 |
| 9/28/1995 | 300 | 0.31 | 10/6/1993 | 1400 | 0.28 | 10/15/1994 | 1300 | 0.20 |
| 1/26/1995 | 30 | 0.28 | 8/30/1993 | 600 | 0.28 | 10/15/1994 | 1230 | 0.20 |
| 3/11/1995 | 2330 | 0.24 | 1/18/1993 | 1330 | 0.28 | 8/20/1995 | 2130 | 0.35 |
| 3/6/1995 | 730 | 0.20 | 1/10/1993 | 2230 | 0.28 | 1/5/1995 | 430 | 0.24 |

| Circle, Pepe, Bronco | | | 128 st., 128 St.2, The rocks, Rock, Buckhorn, Charlie | | | Gold canyon, Peralta | | |
|---|---|---|---|---|---|---|---|---|
| Gauge ID: 65800 | | | Gauge ID: 76200 | | | Gauge ID: 39000 | | |
| Date | Time | I30 (inches/30min) | Date | Time | I30 (inches/30min) | Date | Time | I30 (inches/30min) |
| 9/18/2004 | 2030 | 0.43 | 8/27/1999 | 1730 | 0.75 | 2/12/2005 | 200 | 0.20 |
| 4/2/2004 | 700 | 0.39 | 7/15/1999 | 630 | 0.59 | 1/4/2005 | 930 | 0.20 |
| 4/2/2004 | 600 | 0.39 | 7/14/1999 | 1630 | 0.43 | 1/3/2005 | 1730 | 0.20 |
| 4/2/2004 | 500 | 0.31 | 4/2/1999 | 1130 | 0.39 | 9/7/2006 | 2300 | 0.55 |
| 3/5/2004 | 130 | 0.28 | 7/29/1999 | 1300 | 0.24 | 9/7/2006 | 2330 | 0.39 |
| 9/19/2004 | 1230 | 0.24 | 7/10/1999 | 1830 | 0.2 | 7/30/2006 | 300 | 0.35 |
| 4/2/2004 | 800 | 0.24 | 4/2/1999 | 1100 | 0.2 | 9/9/2006 | 1200 | 0.24 |
| 11/22/2004 | 830 | 0.20 | 10/10/2000 | 600 | 0.59 | 7/27/2006 | 800 | 0.24 |
| 8/11/2004 | 1800 | 0.20 | 10/27/2000 | 1600 | 0.47 | 3/11/2006 | 1030 | 0.20 |
| 3/4/2004 | 2230 | 0.20 | 3/6/2000 | 2000 | 0.39 | 9/1/2007 | 1730 | 0.51 |
| 2/23/2004 | 600 | 0.20 | 3/6/2000 | 100 | 0.39 | 7/21/2007 | 2130 | 0.43 |
| 2/23/2004 | 500 | 0.20 | 3/5/2000 | 2400 | 0.28 | 11/30/2007 | 1930 | 0.31 |
| 11/11/2005 | 900 | 0.28 | 6/19/2000 | 330 | 0.28 | 8/16/2007 | 1730 | 0.31 |
| 1/27/2005 | 130 | 0.28 | 10/10/2000 | 630 | 0.24 | 11/30/2007 | 1700 | 0.28 |
| 1/27/2005 | 200 | 0.24 | 2/14/2001 | 1430 | 0.39 | 8/6/2007 | 1800 | 0.28 |
| 2/12/2005 | 1700 | 0.24 | 7/29/2001 | 2200 | 0.35 | 7/28/2007 | 1630 | 0.28 |
| 2/12/2005 | 600 | 0.24 | 1/9/2001 | 1430 | 0.28 | 11/30/2007 | 2330 | 0.24 |
| 1/11/2005 | 1800 | 0.20 | 8/9/2001 | 30 | 0.2 | 11/30/2007 | 2400 | 0.20 |
| 7/31/2005 | 1900 | 0.20 | 3/7/2001 | 1000 | 0.2 | 7/30/2007 | 1830 | 0.20 |
| 9/7/2006 | 30 | 0.91 | 1/12/2001 | 2200 | 0.2 | 7/30/2007 | 1800 | 0.20 |
| 7/25/2006 | 2330 | 0.47 | 7/14/2002 | 2030 | 0.94 | 7/21/2007 | 2100 | 0.20 |
| 9/7/2006 | 2130 | 0.39 | 7/23/2002 | 2000 | 0.35 | 7/10/2008 | 2130 | 0.94 |
| 9/2/2006 | 1830 | 0.39 | 9/10/2002 | 1930 | 0.31 | 8/28/2008 | 2130 | 0.31 |
| 8/24/2006 | 930 | 0.39 | 7/14/2002 | 2100 | 0.28 | 11/27/2008 | 2100 | 0.28 |
| 9/7/2006 | 100 | 0.31 | 7/14/2002 | 2000 | 0.2 | 11/27/2008 | 500 | 0.24 |
| 9/3/2006 | 2200 | 0.28 | 8/5/2002 | 2100 | 0.2 | 7/11/2008 | 30 | 0.24 |
| 8/24/2006 | 1000 | 0.28 | 8/19/2003 | 1000 | 0.43 | 7/10/2008 | 2200 | 0.24 |
| 8/24/2006 | 900 | 0.24 | 2/25/2003 | 2230 | 0.35 | 1/27/2008 | 2000 | 0.24 |
| 11/30/2007 | 1700 | 0.43 | 10/10/2003 | 930 | 0.31 | 7/10/2008 | 2230 | 0.20 |
| 11/30/2007 | 2400 | 0.39 | 2/25/2003 | 2330 | 0.28 | 5/22/2008 | 1300 | 0.20 |
| 1/31/2007 | 1300 | 0.24 | 2/25/2003 | 1900 | 0.28 | 2/4/2008 | 500 | 0.20 |
| 11/30/2007 | 1800 | 0.20 | 8/14/2003 | 2000 | 0.28 | 7/23/2009 | 2330 | 0.55 |
| 7/23/2007 | 1730 | 0.20 | 3/16/2003 | 2030 | 0.24 | 12/8/2009 | 30 | 0.20 |
| 7/23/2007 | 1700 | 0.20 | 3/1/2003 | 1600 | 0.2 | 4/11/2009 | 700 | 0.20 |
| 3/23/2007 | 300 | 0.20 | 3/1/2003 | 1400 | 0.2 | | | |
| 8/25/2008 | 2030 | 0.47 | 2/25/2003 | 1930 | 0.2 | | | |
| 7/10/2008 | 2030 | 0.43 | 2/13/2003 | 2330 | 0.2 | | | |
| 8/25/2008 | 2100 | 0.39 | 10/10/2003 | 830 | 0.2 | | | |
| 8/25/2008 | 2000 | 0.31 | 8/26/2003 | 2200 | 0.2 | | | |
| 7/20/2008 | 300 | 0.28 | 7/26/2004 | 2000 | 0.28 | | | |
| 9/10/2008 | 2000 | 0.24 | 4/2/2004 | 1200 | 0.28 | | | |
| 9/5/2009 | 930 | 0.31 | 4/2/2004 | 400 | 0.28 | | | |
| 8/13/2009 | 430 | 0.24 | 3/5/2004 | 430 | 0.28 | | | |
| 10/5/2010 | 1330 | 0.47 | 3/4/2004 | 1800 | 0.28 | | | |
| 7/31/2010 | 300 | 0.47 | 12/29/2004 | 1230 | 0.24 | | | |
| 10/5/2010 | 1730 | 0.43 | 12/29/2004 | 1030 | 0.24 | | | |
| 12/22/2010 | 2330 | 0.39 | 3/5/2004 | 130 | 0.24 | | | |
| 7/31/2010 | 330 | 0.39 | 3/5/2004 | 100 | 0.2 | | | |
| 1/19/2010 | 2200 | 0.35 | 12/29/2004 | 1600 | 0.2 | | | |
| 1/21/2010 | 2030 | 0.31 | 12/29/2004 | 1100 | 0.2 | | | |
| 7/22/2010 | 1900 | 0.24 | 12/6/2004 | 1730 | 0.2 | | | |
| 1/19/2010 | 1930 | 0.24 | 11/21/2004 | 330 | 0.2 | | | |
| 8/22/2010 | 30 | 0.20 | 8/15/2004 | 1730 | 0.2 | | | |
| 3/7/2010 | 1630 | 0.20 | 4/2/2004 | 800 | 0.2 | | | |
| 1/21/2010 | 330 | 0.20 | 3/5/2004 | 500 | 0.2 | | | |
| 1/21/2010 | 300 | 0.20 | 8/2/2005 | 2130 | 0.67 | | | |
| 11/5/2011 | 30 | 0.20 | 7/26/2005 | 1700 | 0.63 | | | |
| 8/23/2012 | 200 | 0.55 | 1/5/2005 | 30 | 0.31 | | | |

| Circle, Pepe, Bronco | | | 128 st., 128 St.2, The rocks, Rock, Buckhorn, Charlie | | | Gold canyon, Peralta | | |
|---|---|---|---|---|---|---|---|---|
| Gauge ID: 65800 | | | Gauge ID: 76200 | | | Gauge ID: 39000 | | |
| Date | Time | I30 (inches/30min) | Date | Time | I30 (inches/30min) | Date | Time | I30 (inches/30min) |
| 7/21/2012 | 2000 | 0.39 | 10/17/2005 | 2300 | 0.28 | | | |
| 9/7/2012 | 730 | 0.31 | 8/2/2005 | 2400 | 0.28 | | | |
| 9/7/2012 | 700 | 0.24 | 7/30/2005 | 1400 | 0.28 | | | |
| 8/21/2012 | 2200 | 0.24 | 7/26/2005 | 1800 | 0.28 | | | |
| 7/21/2012 | 1930 | 0.20 | 2/11/2005 | 1830 | 0.28 | | | |
| 9/9/2013 | 1130 | 1.06 | 7/31/2005 | 1800 | 0.24 | | | |
| 8/24/2013 | 330 | 0.28 | 2/19/2005 | 200 | 0.2 | | | |
| 7/19/2013 | 2300 | 0.28 | 1/26/2005 | 1630 | 0.2 | | | |
| 7/19/2013 | 2230 | 0.28 | 9/3/2006 | 2130 | 1.18 | | | |
| 9/9/2013 | 1230 | 0.24 | 9/9/2006 | 1000 | 0.43 | | | |
| 9/9/2013 | 1200 | 0.24 | 7/30/2006 | 30 | 0.35 | | | |
| 3/9/2013 | 130 | 0.20 | 9/9/2006 | 930 | 0.24 | | | |
| | | | 9/2/2006 | 1800 | 0.24 | | | |
| | | | 3/19/2006 | 1200 | 0.2 | | | |
| | | | 10/6/2006 | 800 | 0.2 | | | |
| | | | 7/31/2007 | 1900 | 1.26 | | | |
| | | | 7/31/2007 | 1830 | 0.59 | | | |
| | | | 7/21/2007 | 1930 | 0.51 | | | |
| | | | 11/30/2007 | 1900 | 0.47 | | | |
| | | | 8/3/2007 | 2200 | 0.31 | | | |
| | | | 12/1/2007 | 400 | 0.31 | | | |
| | | | 11/30/2007 | 2300 | 0.31 | | | |
| | | | 7/23/2007 | 1530 | 0.28 | | | |
| | | | 12/1/2007 | 600 | 0.24 | | | |
| | | | 12/1/2007 | 530 | 0.24 | | | |
| | | | 7/23/2007 | 1630 | 0.24 | | | |
| | | | 12/1/2007 | 730 | 0.2 | | | |
| | | | 11/30/2007 | 2330 | 0.2 | | | |
| | | | 7/4/2008 | 1930 | 0.83 | | | |
| | | | 7/13/2008 | 1500 | 0.75 | | | |
| | | | 8/25/2008 | 2200 | 0.67 | | | |
| | | | 7/10/2008 | 2000 | 0.59 | | | |
| | | | 7/13/2008 | 1430 | 0.31 | | | |
| | | | 7/15/2008 | 430 | 0.28 | | | |
| | | | 7/4/2008 | 2000 | 0.2 | | | |
| | | | 8/29/2008 | 2300 | 0.2 | | | |
| | | | 9/8/2009 | 2300 | 0.31 | | | |
| | | | 4/11/2009 | 230 | 0.28 | | | |
| | | | 8/13/2009 | 330 | 0.24 | | | |
| | | | 4/11/2009 | 830 | 0.2 | | | |
| | | | 2/9/2009 | 2130 | 0.2 | | | |

| Cave Creek | | | Asher Hills | | | Cline, Anthem, Anthem2, Saguaro | | |
|---|---|---|---|---|---|---|---|---|
| Gauge ID: 21000 | | | Gauge ID: 75500 | | | Gauge ID: 62300 | | |
| Date | Time | I30 (inches/30min) | Date | Time | I30 (inches/30min) | Date | Time | I30 (inches/30min) |
| 7/27/1989 | 1800 | 0.43 | 8/14/1990 | 930 | 0.63 | 10/5/1989 | 1530 | 0.63 |
| 8/17/1989 | 2230 | 0.39 | 9/20/1990 | 2230 | 0.43 | 8/15/1989 | 2300 | 0.51 |
| 7/27/1989 | 1930 | 0.39 | 9/3/1990 | 2100 | 0.24 | 8/17/1989 | 2200 | 0.31 |
| 12/29/1989 | 30 | 0.31 | 8/14/1990 | 1000 | 0.24 | 10/4/1989 | 630 | 0.24 |
| 3/26/1989 | 730 | 0.28 | 9/3/1990 | 1600 | 0.2 | 8/17/1989 | 100 | 0.24 |
| 7/30/1989 | 2030 | 0.24 | 8/12/1990 | 1930 | 0.2 | 9/3/1989 | 1000 | 0.2 |
| 7/30/1989 | 2000 | 0.24 | 2/28/1991 | 1200 | 0.59 | 3/26/1989 | 230 | 0.2 |
| 7/21/1989 | 2100 | 0.24 | 11/10/1991 | 1130 | 0.51 | 1/4/1989 | 800 | 0.2 |
| 12/29/1989 | 1600 | 0.20 | 9/6/1991 | 1400 | 0.35 | 9/3/1990 | 1800 | 0.67 |
| 9/15/1990 | 1800 | 0.39 | 9/6/1991 | 1300 | 0.35 | 3/29/1990 | 800 | 0.63 |
| 9/20/1990 | 1800 | 0.31 | 3/26/1991 | 1030 | 0.28 | 7/12/1990 | 1630 | 0.55 |
| 3/29/1990 | 700 | 0.24 | 10/27/1991 | 1400 | 0.24 | 7/24/1990 | 400 | 0.35 |
| 9/20/1990 | 1600 | 0.20 | 10/27/1991 | 1330 | 0.24 | 7/7/1990 | 1700 | 0.35 |
| 3/29/1990 | 900 | 0.20 | 10/27/1991 | 1300 | 0.24 | 8/14/1990 | 1100 | 0.31 |
| 10/27/1991 | 1200 | 0.31 | 9/6/1991 | 1600 | 0.24 | 7/2/1990 | 2130 | 0.28 |
| 1/7/1991 | 1900 | 0.31 | 9/6/1991 | 1500 | 0.24 | 11/26/1990 | 1000 | 0.2 |
| 1/7/1991 | 1700 | 0.31 | 10/27/1991 | 1230 | 0.2 | 9/15/1990 | 1900 | 0.2 |
| 10/27/1991 | 1100 | 0.28 | 9/1/1991 | 630 | 0.2 | 8/6/1990 | 1500 | 0.2 |
| 12/11/1991 | 1130 | 0.24 | 8/24/1991 | 1630 | 0.2 | 3/29/1990 | 830 | 0.2 |
| 9/5/1991 | 1800 | 0.20 | 8/24/1991 | 1600 | 0.2 | 10/27/1991 | 1230 | 0.71 |
| 3/20/1991 | 1930 | 0.20 | 8/11/1991 | 430 | 0.2 | 12/10/1991 | 1900 | 0.43 |
| 3/20/1991 | 1800 | 0.20 | 8/22/1992 | 700 | 0.59 | 8/11/1991 | 430 | 0.43 |
| 1/7/1991 | 1500 | 0.20 | 5/23/1992 | 1600 | 0.47 | 12/10/1991 | 2130 | 0.35 |
| 1/7/1991 | 1100 | 0.20 | 7/23/1992 | 2330 | 0.39 | 1/4/1991 | 2000 | 0.28 |
| 8/17/1992 | 1630 | 0.43 | 7/24/1992 | 200 | 0.28 | 12/19/1991 | 1530 | 0.24 |
| 8/11/1992 | 1930 | 0.31 | 10/28/1992 | 830 | 0.24 | 1/4/1991 | 1800 | 0.2 |
| 8/6/1992 | 2000 | 0.31 | 8/6/1992 | 1330 | 0.24 | 1/4/1991 | 1600 | 0.2 |
| 8/22/1992 | 2300 | 0.28 | 8/6/1992 | 1300 | 0.24 | 8/22/1992 | 2200 | 0.31 |
| 8/19/1992 | 2300 | 0.28 | 3/28/1992 | 2130 | 0.24 | 8/22/1992 | 1100 | 0.31 |
| 7/23/1992 | 2330 | 0.24 | 12/4/1992 | 900 | 0.2 | 7/24/1992 | 200 | 0.31 |
| 5/30/1992 | 330 | 0.24 | 12/3/1992 | 2300 | 0.2 | 12/4/1992 | 1300 | 0.24 |
| 5/23/1992 | 1630 | 0.24 | 9/19/1992 | 2330 | 0.2 | 12/4/1992 | 1130 | 0.24 |
| 1/11/1992 | 2330 | 0.24 | 8/6/1992 | 1230 | 0.2 | 8/22/1992 | 2230 | 0.24 |
| 12/4/1992 | 1600 | 0.20 | 3/8/1992 | 2100 | 0.2 | 8/11/1992 | 1830 | 0.24 |
| 8/11/1992 | 1900 | 0.20 | 8/30/1993 | 330 | 0.39 | 7/24/1992 | 130 | 0.24 |
| 5/20/1992 | 1800 | 0.20 | 8/29/1993 | 1230 | 0.35 | 8/31/1993 | 1530 | 1.18 |
| 5/20/1992 | 30 | 0.20 | 10/6/1993 | 1330 | 0.31 | 8/31/1993 | 1600 | 0.87 |
| 1/6/1992 | 600 | 0.20 | 1/14/1993 | 2000 | 0.28 | 10/6/1993 | 1300 | 0.35 |
| 1/8/1993 | 2130 | 0.35 | 1/18/1993 | 1700 | 0.24 | 1/8/1993 | 300 | 0.35 |
| 10/6/1993 | 1430 | 0.28 | 1/10/1993 | 2300 | 0.24 | 8/6/1993 | 2200 | 0.31 |
| 1/8/1993 | 500 | 0.24 | 5/15/1993 | 2000 | 0.2 | 3/26/1993 | 1630 | 0.31 |
| 10/7/1993 | 330 | 0.20 | 1/10/1993 | 2400 | 0.2 | 11/14/1993 | 2030 | 0.28 |
| 10/6/1993 | 2230 | 0.20 | 10/15/1994 | 1000 | 0.24 | 10/5/1993 | 1200 | 0.28 |
| 10/6/1993 | 1300 | 0.20 | 8/20/1995 | 2200 | 0.71 | 8/29/1993 | 500 | 0.24 |
| 8/28/1993 | 1730 | 0.20 | 9/28/1995 | 500 | 0.63 | 8/29/1993 | 300 | 0.24 |
| 1/7/1993 | 2300 | 0.20 | 9/28/1995 | 430 | 0.43 | 1/7/1993 | 1330 | 0.24 |
| 10/15/1994 | 930 | 0.20 | 8/14/1995 | 2030 | 0.31 | 10/5/1993 | 1230 | 0.2 |
| 8/20/1995 | 2000 | 1.34 | 9/28/1995 | 300 | 0.28 | 3/26/1993 | 2230 | 0.2 |
| 8/11/1995 | 2230 | 0.79 | 8/29/1995 | 1600 | 0.2 | 3/26/1993 | 2100 | 0.2 |
| 9/28/1995 | 300 | 0.59 | 2/15/1995 | 1200 | 0.2 | 1/18/1993 | 1500 | 0.2 |
| 8/20/1995 | 2300 | 0.47 | 8/29/1996 | 2130 | 0.35 | 1/10/1993 | 2230 | 0.2 |
| 11/1/1995 | 2030 | 0.39 | 8/18/1996 | 2200 | 0.35 | 8/19/1994 | 1430 | 0.51 |
| 9/28/1995 | 900 | 0.35 | 8/26/1997 | 1100 | 0.59 | 10/15/1994 | 800 | 0.31 |
| 2/15/1995 | 1830 | 0.31 | 8/26/1997 | 1030 | 0.31 | 12/6/1994 | 30 | 0.28 |
| 8/11/1995 | 2330 | 0.24 | 11/11/1997 | 1300 | 0.28 | 9/2/1994 | 2030 | 0.28 |
| 8/11/1995 | 2300 | 0.24 | 9/15/1997 | 1830 | 0.2 | 12/23/1994 | 1330 | 0.24 |
| 8/23/1995 | 230 | 0.20 | 9/11/1997 | 1300 | 0.2 | 10/15/1994 | 830 | 0.24 |

| Cave Creek | | | Asher Hills | | | Cline, Anthem, Anthem2, Saguaro | | |
|---|---|---|---|---|---|---|---|---|
| Gauge ID: 21000 | | | Gauge ID: 75500 | | | Gauge ID: 62300 | | |
| Date | Time | I30 (inches/30min) | Date | Time | I30 (inches/30min) | Date | Time | I30 (inches/30min) |
| 8/20/1995 | 2230 | 0.20 | 9/8/1997 | 1930 | 0.2 | 12/23/1994 | 1330 | 0.24 |
| 9/1/1996 | 2400 | 0.91 | 9/2/1997 | 1900 | 0.2 | 10/15/1994 | 830 | 0.24 |
| 9/2/1996 | 30 | 0.59 | 8/26/1997 | 1130 | 0.2 | 12/25/1994 | 1800 | 0.2 |
| 7/14/1996 | 2130 | 0.35 | 1/13/1997 | 2330 | 0.2 | 11/12/1994 | 200 | 0.2 |
| 7/25/1996 | 2030 | 0.28 | 10/26/1998 | 600 | 0.43 | 5/11/1994 | 1530 | 0.2 |
| 9/11/1996 | 600 | 0.24 | 3/26/1998 | 2030 | 0.28 | 8/11/1995 | 2330 | 0.51 |
| 9/11/1996 | 230 | 0.20 | 11/9/1998 | 100 | 0.24 | 9/28/1995 | 30 | 0.39 |
| 9/1/1996 | 2330 | 0.20 | 10/26/1998 | 700 | 0.24 | 9/27/1995 | 2400 | 0.31 |
| 8/14/1996 | 1830 | 0.20 | 10/26/1998 | 630 | 0.2 | 1/26/1995 | 630 | 0.31 |
| 7/14/1996 | 2100 | 0.20 | 10/26/1998 | 330 | 0.2 | 8/11/1995 | 2400 | 0.28 |
| 9/2/1997 | 1930 | 0.28 | 2/15/1998 | 300 | 0.2 | 1/5/1995 | 800 | 0.28 |
| 7/31/1997 | 30 | 0.20 | 2/15/1998 | 230 | 0.2 | 1/4/1995 | 1930 | 0.28 |
| 2/27/1997 | 2200 | 0.20 | 8/27/1999 | 1700 | 0.79 | 11/6/1995 | 800 | 0.2 |
| 1/13/1997 | 430 | 0.20 | 7/23/1999 | 1730 | 0.47 | 9/28/1995 | 330 | 0.2 |
| 8/15/1998 | 1900 | 0.51 | 7/15/1999 | 630 | 0.39 | 8/20/1995 | 2400 | 0.2 |
| 8/15/1998 | 1930 | 0.35 | 9/19/1999 | 2100 | 0.24 | 3/6/1995 | 230 | 0.2 |
| 3/26/1998 | 2000 | 0.35 | 9/19/1999 | 2130 | 0.2 | 1/25/1995 | 2300 | 0.2 |
| 10/26/1998 | 800 | 0.24 | 8/27/1999 | 1730 | 0.2 | 1/25/1995 | 1930 | 0.2 |
| 4/1/1998 | 1300 | 0.24 | 10/27/2000 | 1600 | 0.55 | 9/6/1995 | 2200 | 0.24 |
| 3/26/1998 | 530 | 0.20 | 8/30/2000 | 1530 | 0.43 | 8/14/1996 | 1830 | 0.67 |
| 2/24/1998 | 1100 | 0.20 | 10/22/2000 | 730 | 0.28 | 9/2/1996 | 230 | 0.31 |
| 2/24/1998 | 300 | 0.20 | 2/21/2000 | 1830 | 0.24 | 9/9/1996 | 2300 | 0.24 |
| 7/14/1999 | 1630 | 0.31 | 10/11/2000 | 230 | 0.2 | 7/25/1996 | 2100 | 0.24 |
| 7/5/1999 | 1630 | 0.31 | 10/10/2000 | 600 | 0.2 | 7/25/1996 | 2030 | 0.2 |
| 4/2/1999 | 1230 | 0.31 | 6/23/2000 | 2400 | 0.2 | 7/16/1996 | 1530 | 0.2 |
| 8/28/1999 | 2230 | 0.28 | 4/6/2001 | 200 | 0.2 | 9/11/1997 | 1130 | 0.55 |
| 7/15/1999 | 600 | 0.28 | 3/7/2001 | 1030 | 0.2 | 8/8/1997 | 1930 | 0.35 |
| 9/19/1999 | 2230 | 0.24 | 7/23/2002 | 2000 | 0.28 | 1/13/1997 | 2300 | 0.28 |
| 7/14/1999 | 1600 | 0.24 | 8/14/2003 | 2000 | 0.51 | 9/11/1997 | 1330 | 0.2 |
| 9/22/1999 | 2200 | 0.20 | 2/13/2003 | 1530 | 0.39 | 8/8/1997 | 2000 | 0.2 |
| 7/15/1999 | 630 | 0.20 | 3/16/2003 | 1430 | 0.35 | 7/7/1998 | 1530 | 0.59 |
| 7/13/1999 | 1600 | 0.20 | 11/12/2003 | 1400 | 0.28 | 7/7/1998 | 1500 | 0.59 |
| 7/10/1999 | 1800 | 0.20 | 3/16/2003 | 2100 | 0.2 | 3/26/1998 | 930 | 0.28 |
| 7/5/1999 | 1600 | 0.20 | 2/13/2003 | 2400 | 0.2 | 9/4/1998 | 1300 | 0.2 |
| 8/28/2000 | 1230 | 0.51 | 3/5/2004 | 500 | 0.28 | 8/27/1999 | 1700 | 0.43 |
| 6/24/2000 | 100 | 0.43 | 3/5/2004 | 130 | 0.24 | 7/15/1999 | 300 | 0.43 |
| 10/27/2000 | 1600 | 0.31 | 12/29/2004 | 500 | 0.2 | 9/23/1999 | 1430 | 0.39 |
| 10/22/2000 | 330 | 0.31 | 3/5/2004 | 200 | 0.2 | 9/23/1999 | 1300 | 0.24 |
| 6/24/2000 | 130 | 0.31 | 8/23/2005 | 100 | 0.67 | 7/6/1999 | 1700 | 0.24 |
| 10/22/2000 | 930 | 0.20 | 8/9/2005 | 1630 | 0.51 | 8/27/1999 | 1630 | 0.2 |
| 10/22/2000 | 600 | 0.20 | 8/8/2005 | 930 | 0.35 | 7/15/1999 | 530 | 0.2 |
| 2/21/2000 | 1800 | 0.20 | 4/23/2005 | 2200 | 0.35 | 8/17/2000 | 1930 | 0.67 |
| 8/9/2001 | 30 | 0.28 | 1/4/2005 | 330 | 0.35 | 8/17/2000 | 1900 | 0.67 |
| 7/29/2001 | 2230 | 0.24 | 2/11/2005 | 730 | 0.28 | 6/29/2000 | 1930 | 0.39 |
| 7/25/2001 | 1500 | 0.24 | 8/9/2005 | 1700 | 0.24 | 10/22/2000 | 500 | 0.35 |
| 7/29/2001 | 2200 | 0.20 | 8/5/2005 | 1800 | 0.24 | 10/22/2000 | 100 | 0.31 |
| 1/9/2001 | 230 | 0.20 | 2/11/2005 | 2300 | 0.24 | 10/21/2000 | 2230 | 0.31 |
| 7/24/2002 | 700 | 0.20 | 2/11/2005 | 2330 | 0.2 | 8/17/2000 | 1830 | 0.31 |
| 7/14/2002 | 2030 | 0.20 | 9/4/2006 | 1830 | 0.67 | 10/22/2000 | 700 | 0.28 |
| 8/14/2003 | 2000 | 0.63 | 8/10/2006 | 1600 | 0.51 | 10/30/2000 | 1400 | 0.24 |
| 8/19/2003 | 1030 | 0.28 | 9/9/2006 | 1030 | 0.43 | 6/24/2000 | 30 | 0.24 |
| 2/13/2003 | 2400 | 0.24 | 6/30/2006 | 2030 | 0.35 | 8/29/2000 | 730 | 0.2 |
| 10/10/2003 | 1000 | 0.20 | 7/30/2006 | 100 | 0.31 | 7/29/2001 | 2300 | 0.35 |
| 3/16/2003 | 2030 | 0.20 | 7/21/2006 | 1600 | 0.31 | 7/29/2001 | 2330 | 0.31 |
| 2/25/2003 | 1900 | 0.20 | 5/16/2006 | 1600 | 0.28 | 8/11/2001 | 330 | 0.28 |
| 2/13/2003 | 1800 | 0.20 | 10/8/2006 | 1530 | 0.2 | 9/7/2002 | 1800 | 0.43 |
| 2/13/2003 | 1530 | 0.20 | 7/30/2006 | 30 | 0.2 | 12/23/2002 | 1200 | 0.31 |

| Cave Creek | | | Asher Hills | | | Cline, Anthem, Anthem2, Saguaro | | |
|---|---|---|---|---|---|---|---|---|
| Gauge ID: 21000 | | | Gauge ID: 75500 | | | Gauge ID: 62300 | | |
| Date | Time | I30 (inches/30min) | Date | Time | I30 (inches/30min) | Date | Time | I30 (inches/30min) |
| 2/13/2003 | 1130 | 0.20 | 7/27/2006 | 630 | 0.2 | 12/23/2002 | 1400 | 0.24 |
| 7/30/2006 | 30 | 0.59 | 7/31/2007 | 1830 | 1.22 | 12/21/2002 | 1430 | 0.24 |
| 6/30/2006 | 2000 | 0.63 | 7/31/2007 | 1900 | 0.47 | 10/10/2003 | 430 | 0.51 |
| 9/9/2006 | 930 | 0.63 | 12/8/2007 | 300 | 0.24 | 8/14/2003 | 2030 | 0.47 |
| 8/8/2006 | 1600 | 0.98 | 8/29/2007 | 1830 | 0.24 | 10/10/2003 | 500 | 0.39 |
| 11/30/2007 | 1800 | 0.47 | 7/30/2007 | 1600 | 0.24 | 8/14/2003 | 2000 | 0.28 |
| 9/16/2007 | 1800 | 0.43 | 11/30/2007 | 2400 | 0.2 | 2/13/2003 | 2130 | 0.28 |
| 7/31/2007 | 1930 | 0.43 | 11/30/2007 | 1530 | 0.2 | 2/13/2003 | 2200 | 0.24 |
| 7/31/2007 | 1830 | 0.71 | 3/22/2007 | 1600 | 0.2 | 11/12/2003 | 2200 | 0.2 |
| 7/31/2007 | 1900 | 1.22 | 7/25/2009 | 1830 | 0.55 | 9/19/2004 | 1300 | 0.83 |
| 1/7/2008 | 1130 | 0.43 | | | | 9/19/2004 | 1400 | 0.28 |
| 7/4/2008 | 1930 | 0.91 | | | | 9/4/2004 | 800 | 0.28 |
| | | | | | | 3/5/2004 | 400 | 0.28 |
| | | | | | | 7/26/2004 | 30 | 0.24 |
| | | | | | | 8/11/2004 | 1800 | 0.2 |
| | | | | | | 7/26/2004 | 130 | 0.2 |
| | | | | | | 3/5/2004 | 300 | 0.2 |
| | | | | | | 8/24/2006 | 1030 | 0.47 |
| | | | | | | 9/9/2006 | 900 | 0.98 |
| | | | | | | 4/11/2009 | 700 | 0.51 |

# APPENDIX F

# COMPARISON OF SSY DATA FOR WARM DESERT (BWH KÖPPEN-GIGER) SITES

| ID | Continent | Country | River/Catchment Name | Measuring location | Lat (°) | Lon (°) | A (km²) | SSY (t/km²/y) | SSY mark | Rainfall (mm) | MP | MP length (y) | Land Use | Type | References |
|---|---|---|---|---|---|---|---|---|---|---|---|---|---|---|---|
| 1 | Am | United States | Cigar | | 33.685117 | -112.534267 | 2.60 | 89.20 | | 218 | 1990-2004 | 15 | GT | R | This study |
| 2 | Am | United States | Cigar | | 33.685117 | -112.534267 | 2.60 | 102.40 | | 178 | 2005-2009 | 5 | GT | R | This study |
| 3 | Am | United States | Saguaro | | 33.800925 | -112.204050 | 1.40 | 48.70 | | 200 | 1990-2004 | 15 | GT | R | This study |
| 4 | Am | United States | Saguaro | | 33.800925 | -112.204050 | 1.40 | 143.20 | | 198 | 2005-2009 | 5 | I | R | This study |
| 5 | Am | United States | Cline | | 33.853465 | -112.149325 | 1.50 | 52.00 | | 326 | 1989-1995 | 7 | GT | R | This study |
| 6 | Am | United States | Cline | | 33.853465 | -112.149325 | 1.50 | 103.70 | | 192 | 1996-2003 | 8 | B | R | This study |
| 7 | Am | United States | Cline | | 33.853465 | -112.149325 | 1.50 | 174.70 | | 282 | 2003-2004 | 2 | B | R | This study |
| 8 | Am | United States | Anthem | | 33.862595 | -112.123726 | 0.88 | 136.70 | | 305 | 1989-1992 | 4 | GT | R | This study |
| 9 | Am | United States | Anthem | | 33.862595 | -112.123726 | 0.88 | 334.00 | | 269 | 1993-1997 | 5 | F1 | R | This study |
| 10 | Am | United States | Anthem 2 | | 33.850572 | -112.101617 | 0.58 | 77.50 | | 305 | 1989-1992 | 4 | GT | R | This study |
| 11 | Am | United States | Anthem 2 | | 33.850572 | -112.101617 | 0.58 | 276.70 | | 355 | 1993-1995 | 3 | F1 | R | This study |
| 12 | Am | United States | Anthem 2 | | 33.850572 | -112.101617 | 0.58 | 330.90 | | 190 | 1996-1998 | 3 | F2 | R | This study |
| 13 | Am | United States | Anthem 2 | | 33.850572 | -112.101617 | 0.58 | 156.20 | | 178 | 1999-2002 | 4 | F2 | R | This study |
| 14 | Am | United States | Anthem 2 | | 33.850572 | -112.101617 | 0.58 | 255.70 | | 63 | 2002 | 1 | B | R | This study |
| 15 | Am | United States | Pepe | | 33.786100 | -112.159939 | 0.99 | 38.40 | | 206 | 1989-2008 | 20 | B | R | This study |
| 16 | Am | United States | Bronco | | 33.774765 | -112.117174 | 0.45 | 43.70 | | 231 | 1989-1998 | 10 | GT | R | This study |

(Continues)

| ID | Continent | Country | River/Catchment Name | Measuring location | Lat (°) | Lon (°) | A (km²) | SSY (t/km²/y) | SSY mark | Rainfall (mm) | MP | MP length (y) | Land Use | Type | References |
|---|---|---|---|---|---|---|---|---|---|---|---|---|---|---|---|
| 17 | Am | United States | Bronco | | 33.774765 | -112.117174 | 0.45 | 137.40 | | 158 | 1999-2003 | 5 | I | R | This study |
| 18 | Am | United States | Circle | | 33.767891 | -112.069517 | 0.60 | 51.00 | | 203 | 1990-2010 | 21 | GT | R | This study |
| 19 | Am | United States | Circle | | 33.767891 | -112.069517 | 0.60 | 128.50 | | 168 | 2010-2013 | 4 | I | R | This study |
| 20 | Am | United States | Charlie | | 33.773722 | -111.949346 | 0.91 | 264.30 | | 213 | 1989-2004 | 16 | B | R | This study |
| 21 | Am | United States | Rock | | 33.758838 | -111.877228 | 0.54 | 53.60 | | 388 | 1989-1992 | 4 | GT | R | This study |
| 22 | Am | United States | Rock | | 33.758838 | -111.877228 | 0.54 | 224.00 | | 374 | 1992-1997 | 6 | F1 | R | This study |
| 23 | Am | United States | Rock | | 33.758838 | -111.877228 | 0.54 | 175.70 | | 254 | 1998-2003 | 6 | F2 | R | This study |
| 24 | Am | United States | Rock | | 33.758838 | -111.877228 | 0.54 | 90.90 | | 304 | 2004-2009 | 6 | F2 | R | This study |
| 25 | Am | United States | Cave Creek | | 33.821477 | -111.860042 | 0.19 | 102.20 | | 320 | 1989-1992 | 4 | GT | R | This study |
| 26 | Am | United States | Cave Creek | | 33.821477 | -111.860042 | 0.19 | 258.50 | | 325 | 1992-1999 | 8 | F1 | R | This study |
| 27 | Am | United States | Cave Creek | | 33.821477 | -111.860042 | 0.19 | 128.80 | | 228 | 2000-2003 | 4 | B | R | This study |
| 28 | Am | United States | Buckhorn | | 33.771593 | -111.726559 | 4.40 | 106.20 | | 362 | 1989-1999 | 11 | GT | R | This study |
| 29 | Am | United States | Buckhorn | | 33.771593 | -111.726559 | 4.40 | 133.40 | | 190 | 2000-2002 | 3 | B | R | This study |
| 30 | Am | United States | The Rocks | | 33.735184 | -111.843395 | 2.36 | 227.60 | | 380 | 1989-1996 | 8 | B | R | This study |
| 31 | Am | United States | 128th St | | 33.719610 | -111.805910 | 0.85 | 110.30 | | 399 | 1989-1994 | 6 | GT | R | This study |
| 32 | Am | United States | 128th St | | 33.719610 | -111.805910 | 0.85 | 342.00 | | 271 | 1995-2000 | 6 | F1 | R | This study |

(Continues)

| ID | Continent | Country | River/Catchment Name | Measuring location | Lat (°) | Lon (°) | A (km²) | SSY (t/km²/y) | SSY mark | Rainfall (mm) | MP | MP length (y) | Land Use | Type | References |
|---|---|---|---|---|---|---|---|---|---|---|---|---|---|---|---|
| 33 | Am | United States | 128th St | | 33.719610 | -111.805910 | 0.85 | 159.90 | | 295 | 2001-2008 | 8 | I | R | This study |
| 34 | Am | United States | 128th St 2 | | 33.716550 | -111.791170 | 0.31 | 109.50 | | 399 | 1989-1994 | 6 | GT | R | This study |
| 35 | Am | United States | 128th St 2 | | 33.716550 | -111.791170 | 0.31 | 278.70 | | 271 | 1995-2000 | 6 | FI | R | This study |
| 36 | Am | United States | 128th St 2 | | 33.716550 | -111.791170 | 0.31 | 149.10 | | 295 | 2001-2008 | 8 | I | R | This study |
| 37 | Am | United States | AsherHills | | 33.731003 | -111.703998 | 2.10 | 140.50 | | 264 | 1989-2001 | 13 | GT | R | This study |
| 38 | Am | United States | AsherHills | | 33.731003 | -111.703998 | 2.10 | 199.10 | | 217 | 2002-2007 | 6 | B | R | This study |
| 39 | Am | United States | Gold Cyn | | 33.367485 | -111.515636 | 5.10 | 57.30 | | 243 | 1989-2009 | 21 | B | R | This study |
| 40 | Am | United States | Peralta | | 33.334978 | -111.429506 | 0.78 | 52.20 | | 252 | 1989-2000 | 12 | GT | R | This study |
| 41 | Am | United States | Peralta | | 33.334978 | -111.429506 | 0.78 | 77.40 | | 234 | 2001-2005 | 5 | B | R | This study |
| 42 | Am | United States | Peralta | | 33.334978 | -111.429506 | 0.78 | 8.70 | | 229 | 2006-2009 | 4 | B | R | This study |
| 43 | Am | United States | Casandro Wash | | Nearest town | AZ | 3.21 | 221.48 | | N.A. | | | G | R | CH2M-Hill. 1994a |
| 44 | Am | United States | Rawhide Wash | | Nearest town | AZ | 35.33 | 278.64 | | N.A. | | | G | R | CH2M-Hill. 1994b |
| 45 | Am | United States | Phoenix Mount Preserve (Tatum Wash) | | Nearest town | AZ | 4.97 | 1357.46 | | N.A. | | | G | | JE Fuller Hydrology & Geomorphology, INC. (JEF). 1997 |
| 46 | Am | United States | Shea Boulevard (Tatum Wash) | | Nearest town | AZ | 5.62 | 1500.35 | | N.A. | | | G | | JE Fuller Hydrology & Geomorphology, INC. (JEF). 1997 |
| 47 | Am | United States | Rillito Creek Recharge Dam | | Nearest town | AZ | N.A. | 71.45 | | N.A. | | | G | | JE Fuller Hydrology & Geomorphology, INC. (JEF). 1997 |
| 48 | Am | United States | Bunkerville Detention Basin | | Nearest town | AZ | N.A. | 643.01 | | N.A. | | | G | | JE Fuller Hydrology & Geomorphology, INC. (JEF). 1997 |

(Continues)

| ID | Continent | Country | River/Catchment Name | Measuring location | Lat (°) | Lon (°) | A (km²) | SSY (t/km²/y) | SSY mark | Rainfall (mm) | MP | MP length (y) | Land Use | Type | References |
|---|---|---|---|---|---|---|---|---|---|---|---|---|---|---|---|
| 49 | Am | United States | Town Wash detention Basin | | Nearest town | AZ | N.A. | 643.01 | | N.A. | | | G | | JE Fuller Hydrology & Geomorphology, INC. (JEF). 1997 |
| 50 | Am | United States | Western Tributary (Cherokee Wash) | | Nearest town | AZ | 0.36 | 1543.21 | | N.A. | | | G | | WEST Consulting. 1997 |
| 51 | Am | United States | Desert Park Tributary (Cherokee Wash) | | Nearest town | AZ | 0.78 | 1414.61 | | N.A. | | | G | | WEST Consulting. 1997 |
| 52 | Am | United States | Desert Greenbelt Project | | Nearest town | AZ | 22.22 | 71.45 | | N.A. | | | G | | Hjalmarson, 1996 |
| 53 | Am | United States | Cave Creek | | Nearest town | AZ | 313.39 | 221.48 | | N.A. | | | G | | Hjalmarson, 1996 |
| 54 | Am | United States | Spookhill Dam | | Nearest town | AZ | 42.48 | 107.17 | | N.A. | | | G | | Hjalmarson, 1996 |
| 55 | Am | United States | Shaddle back Dam | | Nearest town | AZ | 77.70 | 57.16 | | N.A. | | | G | | Hjalmarson, 1996 |
| 56 | Am | United States | Davis Tank | | Nearest town | AZ | 0.54 | 685.87 | | N.A. | | | G | R | Peterson, 1962 |
| 57 | Am | United States | Kennedy Tank | | Nearest town | AZ | 2.51 | 192.90 | | N.A. | | | G | R | Peterson, 1962 |
| 58 | Am | United States | Juniper Wash | | Nearest town | AZ | 5.18 | 207.19 | | N.A. | | | G | R | Peterson, 1962 |
| 59 | Am | United States | Alhambra Tank | | Nearest town | AZ | 17.12 | 21.43 | | N.A. | | | G | R | Peterson, 1962 |
| 60 | Am | United States | Black Hills Tank | | Nearest town | AZ | 2.95 | 485.83 | | N.A. | | | G | R | Peterson, 1962 |
| 61 | Am | United States | Black Hills tank | | Nearest town | AZ | 4.04 | 414.38 | | N.A. | | | G | R | Langbein et al. 1951 |
| 62 | Am | United States | Mesquite Tank | | Nearest town | AZ | 23.31 | 21.43 | | N.A. | | | G | R | Peterson, 1962 |
| 63 | Am | United States | Tank 76 | | Nearest town | AZ | 3.03 | 150.03 | | N.A. | | | G | R | Peterson, 1962 |
| 64 | Am | United States | Spook Hill Apache Junction FRS | | Nearest town | AZ | 15.02 | 50.01 | | 217 | N.A. | 14 | G | | Henze, 2000 |

(Continues)

| ID | Continent | Country | River/Catchment Name | Measuring location | Lat (°) | Lon (°) | A (km²) | SSY (t/km²/y) | SSY mark | Rainfall (mm) | MP | MP length (y) | Land Use | Type | References |
|---|---|---|---|---|---|---|---|---|---|---|---|---|---|---|---|
| 65 | Am | United States | Spook Hill Signal Butte FRS | | Nearest town | AZ | 27.56 | 78.59 | | 217 | N.A. | 14 | G | | Henze, 2000 |
| 66 | Am | United States | Spook Hill Spook Hill FRS | | Nearest town | AZ | 35.43 | 100.02 | | 217 | N.A. | 14 | G | | Henze, 2000 |
| 67 | Am | United States | Spook Hill Spook Hill Floodway | | Nearest town | AZ | 7.49 | 114.31 | | 217 | N.A. | 14 | G | | Henze, 2000 |
| 68 | Am | United States | Tributary of Gila River | Half moon reservoir | Nearest town | Florence, AZ | 0.52 | 590.74 | | N.A. | 1941-1960 | 19 | G | R | Dendy et al. 1978 |
| 69 | Am | United States | Tributary of Gila River | Homestead | Nearest town | Florence, AZ | 2.33 | 651.18 | | N.A. | 1954-1960 | 6 | G | R | Dendy et al. 1978 |
| 70 | Am | United States | Magma Wash | Magma No.1 | Nearest town | Florence, AZ | 4.61 | 111.08 | | | 1948-1959 | 11 | G | R | Dendy et al. 1978 |
| 71 | Am | United States | Magma Wash | Magma No.2 | Nearest town | Florence, AZ | 0.98 | 118.32 | | | 1954-1959 | 5.4 | G | R | Dendy et al. 1978 |
| 72 | Am | United States | Magma Wash | Magma No.3 | Nearest town | Florence, AZ | 18.13 | 20.85 | | | 1949-1959 | 10 | G | R | Dendy et al. 1978 |
| 73 | Am | United States | Tributary of Gila River | Whitlow Old Tank | Nearest town | Florence, AZ | 1.92 | 181.31 | | | 1950-1960 | 10 | G | R | Dendy et al. 1978 |
| 74 | Am | United States | Tributary of Queen Creek | Willams-Chandler Pd. #1 | Nearest town | Florence Junction, AZ | 2.82 | 18.30 | | | 1931-1961 | 30 | G | R | Dendy et al. 1978 |
| 75 | Am | United States | Tributary of Queen Creek | Willams-Chandler Pd. #2 | Nearest town | Florence Junction, AZ | 1.68 | 74.06 | | | 1944-1961 | 17 | G | R | Dendy et al. 1978 |
| 76 | Am | United States | Tributary of Centennial Wash | Big Horn Mt. Tank #1 | Nearest town | Tonopah, AZ | 1.32 | 48.52 | | | 1960-1964 | 4.3 | G | R | Dendy et al. 1978 |

(Continues)

| ID | Continent | Country | River/Catchment Name | Measuring location | Lat (°) | Lon (°) | A (km²) | SSY (t/km²/y) | SSY mark | Rainfall (mm) | MP | MP length (y) | Land Use | Type | References |
|---|---|---|---|---|---|---|---|---|---|---|---|---|---|---|---|
| 77 | Am | United States | Tributary of Centennial Wash | Big Horn Mt. Tank #2 | Nearest town | Tonopah, AZ | 1.14 | 51.07 | | | 1960-1964 | 4.3 | G | R | Dendy et al. 1978 |
| 78 | Am | United States | Tributary of Centennial Wash | Centennial Wash Tank | Nearest town | Tonopah, AZ | 1.55 | 76.61 | | | 1954-1965 | 11 | G | R | Dendy et al. 1978 |
| 79 | Am | United States | Tributary of Centennial Wash | New Tank | Nearest town | Tonopah, AZ | 4.87 | 67.25 | | | 1945-1965 | 20 | G | R | Dendy et al. 1978 |
| 80 | Am | United States | Tributary of Centennial Wash | West Tank | Nearest town | Salome, AZ | 0.75 | 63.42 | | | 1960-1964 | 4.3 | G | R | Dendy et al. 1978 |
| 81 | Am | United States | Tiger Wash | Upper Twin Tank | Nearest town | Aguila, AZ | 4.74 | 6.38 | | | 1944-1964 | 20 | G | R | Dendy et al. 1978 |
| 82 | Am | United States | Tributary of Brown's Canyon | Harquahala Mt. Tank #1 | Nearest town | Aguila, AZ | 0.28 | 83.42 | | | 1958-1964 | 6.3 | G | R | Dendy et al. 1978 |
| 83 | Am | United States | Tributary of Verde River | Keller Tank | | Scottsdale, AZ | 0.16 | 168.61 | * | | 1941-1970 | 29.2 | G | R | Dendy et al. 1978 |
| 84 | Am | United States | Walker River | Weber | | Shurz, NV | 6319.57 | 14.29 | * | | 1935-1939 | 4 | G | R | Dendy et al. 1978 |
| 85 | Am | Chile | Rio Lluta | | -13.600000 | -69.900000 | 2550 | 6.61 | | 20 | 1988-2002 | 15 | G | GS | Kober et al. 2007 |
| 86 | Am | Chile | Rio Lluta | | -13.600000 | -69.900000 | 2500 | 13.93 | | 250 | 1994/2001 El Nino | 2 | G | GS | Kober et al. 2007 |
| 87 | Au | Australia | Murray-Darling Basin | | -20.911554 | 116.309280 | 0.01 | 156.00 | | N.A. | N.A. | N.A. | G | E | Wasson 1994 |
| 88 | Au | Australia | Murray-Darling Basin | | -20.911554 | 116.309280 | 1068 | 89.00 | | N.A. | N.A. | N.A. | G | R | Wasson 1994 |
| 89 | Au | Australia | Murray-Darling Basin | | N.A. | N.A. | 1060 | 15.90 | | N.A. | Pre-European settlement | N.A. | U | N.A. | Wasson et al. 1996 |

(Continues)

| ID | Continent | Country | River/Catchment Name | Measuring location | Lat (°) | Lon (°) | A (km²) | SSY (t/km²/y) | SSY mark | Rainfall (mm) | MP | MP length (y) | Land Use | Type | References |
|---|---|---|---|---|---|---|---|---|---|---|---|---|---|---|---|
| 90 | Au | Australia | Murray-Darling Basin | | N.A. | N.A. | 1060 | 28.00 | | N.A. | Post-Erupocan settlement | N.A. | G | N.A. | Wasson et al. 1996 |
| 91 | ME | West Bank | Qumeran | Dead Sea highway | 31° 42' N | 35° 25' E | 47 | 62.00 | | N.A. | N.A. | N.A. | G | M | Moshe et al. 2008 |
| 92 | ME | West Bank | Qidron | Dead Sea highway | 31° 41' N | 35° 20' E | 123 | 35.00 | | N.A. | N.A. | N.A. | G | M | Moshe et al. 2008 |
| 93 | ME | West Bank | Darga | Dead Sea highway | 31° 37' N | 35°18' E | 237 | 90.00 | | N.A. | N.A. | N.A. | G | M | Moshe et al. 2008 |
| 94 | ME | West Bank | Qedem | Dead Sea highway | 31° 31' N | 35° 24' E | 12 | 152.00 | | N.A. | N.A. | N.A. | G | M | Moshe et al. 2008 |
| 95 | ME | West Bank | Ishai | Dead Sea highway | 31° 29' N | 35° 24' E | 2 | 4.50 | | N.A. | N.A. | N.A. | G | M | Moshe et al. 2008 |
| 96 | ME | West Bank | Hever | Dead Sea highway | 31° 26' N | 35° 15' E | 175 | 50.00 | | N.A. | N.A. | N.A. | G | M | Moshe et al. 2008 |
| 97 | ME | West Bank | Zeelim | Dead Sea highway | 31° 20' N | 35° 15' E | 253 | 39.00 | | N.A. | N.A. | N.A. | G | M | Moshe et al. 2008 |
| 98 | ME | West Bank | Neqarot | | N.A. | N.A. | 984 | 72.00 | | 70 | N.A. | N.A. | G | R | Laronne and Wilhelm, 2001 |
| 99 | ME | West Bank | Hiyyon | | N.A. | N.A. | 1118 | 43.00 | | 40 | N.A. | N.A. | G | R | Laronne and Wilhelm, 2001 |
| 100 | ME | Israel | Nahal Eshtemoa | | 31.300000 | 34.966667 | 119 | 472.00 | | 185 | 1992-1995 | 4 | G | GS | Powell et al., 1996 |
| 101 | ME | Israel | Nahal Yael | | 29.587910 | 34.942364 | 0.60 | 400.00 | | 31 | 1967-1976 | 10 | G | R | Schick and Lekach, 1993 |
| 102 | ME | Israel | Nahal Yael | | 29.587910 | 34.942364 | 0.60 | 170.00 | | 31 | 1981-1990 | 10 | G | R | Schick and Lekach, 1993 |
| 103 | ME | Israel | Nahal Yael | | 29.587910 | 34.942364 | 0.60 | 138.00 | | 39 | 1967-2000 | >33 | G | R | Clapp et al., 2000 |
| 104 | ME | Israel | Giv'at Hayil | Backhoe trench | 30.994170 | 34.680835 | 0.17 | 1230.00 | | 100 | 1986-1988 | 3 | G | T | Schwartz and Greenbaum, 2008 |
| 105 | ME | Israel | Be'er Sheva Leeman South | | 31.240000 | 34.840000 | 0.23 | 377.00 | | 210 | N.A. | N.A. | G | R | Laronne 1990 |
| 106 | ME | Israel | Be'er Sheva Leeman North | | 31.240000 | 34.840000 | 2.90 | 259.00 | | 220 | N.A. | N.A. | G | R | Laronne 1990 |
| 107 | ME | Israel | Boker | | 30.920000 | 34.780000 | 35 | 46.00 | | 95 | N.A. | N.A. | G | R | Shanan 2000 |

(Continues)

| ID | Continent | Country | River/Catchment Name | Measuring location | Lat (°) | Lon (°) | A (km²) | SSY (t/km²/y) | SSY mark | Rainfall (mm) | MP | MP length (y) | Land Use | Type | References |
|---|---|---|---|---|---|---|---|---|---|---|---|---|---|---|---|
| 108 | ME | Israel | Haroeh | | 30.900000 | 34.830000 | 43 | 70.00 | | 95 | N.A. | N.A. | G | R | Shanan 2000 |
| 109 | ME | Israel | Heimar | | 31.150000 | 35.240000 | 360 | 164.00 | | 80 | N.A. | N.A. | G | GS | Powell et al., 1996 |
| 110 | Af | Egypt | Nile | High Aswan | 23.894400 | 32.866700 | 2960000 | 41.10 | | | N.A. | N.A. | A | R | Shahin 1993 |
| 111 | Af | Sudan | Nile | Wadi Halfa | 21.792000 | 31.370900 | 2600000 | 38.00 | | | N.A. | N.A. | A | GS | Dedkov and Mozzherin, 1984 |
| 112 | Af | Sudan | Blue Nile | Khartoum | 15.571353 | 32.593300 | 324859 | 708.00 | | | 1964 - 1990 | 27 | A | GS | Billi and el Badri Ali, 2010 |
| 113 | Af | Sudan | Atbara | Khashm el Girba | 14.872100 | 35.896800 | 20000 | 3422.00 | | | 1964 - 1976 | 13 | A | R | FAO, 2008 |
| 114 | Af | Sudan | Gash | Kassala | 15.439782 | 36.391811 | 24642 | 365.20 | | | N.A. | 2 | A | GS | Nyssen et al., 2004 |
| 115 | Af | Sudan | Atbara | outlet | 17.667577 | 34.024200 | 68800 | 203.50 | | | N.A. | N.A. | A | GS | Nyssen et al., 2004 |
| 116 | Af | Sudan | Blue Nile | Sennar | 13.541714 | 33.638293 | 277286 | 339.00 | | | 1993 - 1996 | 4 | A | GS | Billi and el Badri Ali, 2010 |
| 117 | Af | Niger | Sirba | Garbe Kourou | 13.731594 | 1.604889 | 38704 | 24.80 | | | HY 2006/2007 - HY 2007/2008 | 2 | G | GS | Amogu, 2009 |
| 118 | Af | Niger | Gorouol | Alcongui | 14.748588 | 0.597706 | 44540 | 17.70 | | | HY 2006/2007 - HY 2007/2008 | 2 | A | GS | Amogu, 2009 |
| 119 | Af | Niger | Niger | Farié-Haossa | 13.783635 | 1.649525 | 650380 | 19.60 | | | HY 2007/2008 | 1 | A | GS | Amogu, 2009 |
| 120 | Af | Niger | Niger | Latakabiey | 13.758310 | 1.679255 | 689130 | 19.60 | | | HY 2007/2008 | 1 | A | GS | Amogu, 2009 |
| 121 | Af | Niger | Gorouol | Dolbel | 14.616700 | 0.283300 | 7500 | 22.10 | | | HY 1976/1977 - HY 1982 - 1983 | 7 | A | GS | Amogu, 2009; Gallaire, 1986 |
| 122 | Af | Niger | Niger | Niamey | 13.503032 | 2.107030 | 700000 | 12.60 | | | HY 1984/1985 - HY 1985/1986; HY 2006/2007 - HY 2007/2008 | 4 | A | GS | Amogu, 2009; Gallaire, 1986 |

(Continues)

| ID | Continent | Country | River/Catchment Name | Measuring location | Lat (°) | Lon (°) | A (km²) | SSY (t/km²/y) | SSY mark | Rainfall (mm) | MP | MP length (y) | Land Use | Type | References |
|---|---|---|---|---|---|---|---|---|---|---|---|---|---|---|---|
| 123 | Af | Niger | Niger | Kandadji | 14.614552 | 0.965856 | 628830 | 4.80 | | | HY 1976/1977 - HY 1982/1983; HY 2007/2008 | 8 | A | GS | Amogu, 2009; Gallaire, 1986 |
| 124 | Af | Senegal | Sénégal | Dagana | 16.522000 | -15.512900 | 270000 | 10.60 | | | 1981 - 1983 | 3 | A | GS | Liénou et al., 2005 |
| 125 | Af | Senegal | Sénégal | near outlet | 16.126200 | -16.486400 | 270000 | 11.10 | | | N.A. | N.A. | G | GS | Milliman and Fansworth, 2011 |
| 126 | Af | Morocco | Draa | near outlet | 28.698880 | -11.164700 | 114000 | 122.80 | | | N.A. | N.A. | G | GS | Milliman and Fansworth, 2011 |
| 127 | Af | Morocco | Draa | Mansour Eddahbi | 30.923100 | -6.789500 | 15000 | 410 | | | 1972 - 1986 | 15 | A | R | FAO, 2008 |
| 128 | Af | Morocco | Massa | Youssef b Tachfine | 29.802800 | -9.466400 | 3784 | 378.00 | | | 1973 - 1986 | 14 | G | R | FAO, 2008 |
| 129 | Af | Ethiopia | Wabi Shebelle | Gode | 5.925545 | 43.547301 | 127300 | 118.00 | | | N.A. | N.A. | A | GS | Nyssen et al., 2004 |
| 130 | Af | Algeria | | Djorf Torba | 31.529500 | -2.760900 | 22000 | 160.40 | | | 1969 - 1985 | 17 | G | R | Lahlou, 1996; Bengueddach and Chabouni, 1997 |
| 131 | Af | Algeria | El Abiod | Mchouneche | 34.942900 | 5.997400 | 1050 | 401.00 | | | 1972 - 1979 | 8 | A | GS | FAO, 2008 |
| 132 | Af | Algeria | Isser | El Izdibar | 34.851900 | 5.738400 | 1140 | 117.00 | | | 1989 - 1998 | 10 | G | GS | Terfous et al., 2003 |
| 133 | Af | South Africa | Oranje | Prieska | -29.660800 | 22.756600 | 820000 | 85.00 | | | N.A. | 18 | A | GS | Dedkov and Mozzherin, 1984 |
| 134 | Af | South Africa | Van Wyksvlei | Van Wyksvlei | -30.380749 | 21.810750 | 1339 | 26.00 | | | 1884 - 1979 | 95 | A | R | Rooseboom et al., 1992 |
| 135 | Af | South Africa | Ongers | Smartt | -30.625800 | 23.295400 | 13114 | 4.00 | | | 1912 - 1980 | 68 | A | R | Rooseboom et al., 1992 |
| 136 | In-Ar | India | Nagaur District | | 24° 31' N - 26° 00' N | 73° 05' N - 75° 22' E | N.A. | 2145.00 | * | 384 | 1977-1980 | 4 | G | R | Sharma and Chatterji, 1982 |

Table legend

| Column | Explanation |
|---|---|
| ID | Entry identifier |
| Continent | Continent in which the SSY observation was made. 'Am' indicates America. 'Au' indicates Australia. 'ME' indicates Middle East. 'Af' indicates Africa. 'In-Ar' indicates Indo-Arabia. |
| Country | Country in which the SSY observation was made |
| River/Catchment Name | Name of the river/catchment (if available) |
| Measuring location | Description of the measuring location |
| Lat (°) | Estimated latitude of the measuring location |
| Lon (°) | Estimated longitude of the measuring location |
| A (km²) | Catchment area (km²) |
| SSY (t/km²/y) | Area-specific catchment sediment yield. For the majority of the observations, this value corresponds with the SSY-value reported in the indicated data source. |
| SSY Mark | In some cases, the sediment volume-value was reported instead SSY-value. We calculated SSY-value based on the assumption of bulk density as 1.5 t/km3 in that cases. |
| Rainfall (mm) | Mean annual precipitation (mm) |
| MP | Description of the measuring period. 'HY' stands for 'Hydrological Year' (the start and end date of such a year depends on the study considered). 'N.A.' means not available. |
| MP length (y) | Duration of the measuring period in year. 'N.A.' means not available. |
| Land Use | Dominant land use during the period of SSY measurement. 'GT' indicates grazing from this study 'G' indicates grazing from literature. 'U' indicates undisturbed land. 'O' indicates off-road vehicle use. 'I' indicates infrastructure (pipeline/road) construction. 'B' indicates building. 'F1' indicates immediately after wildfire.' F2' indicates more than 3 years after fire. 'A' indicates agricultural use. |
| Type | Method used to obtain the SSY value. 'R' indicates that the SSY value was obtained from bathymetric surveys in reservoirs. 'GS' indicates that the value was obtained from measurements at a gauging station. 'E' indicates that the value was obtained from erosion plot. 'M' indicates that the value was obtained from model-derived sediment flux. 'T' indicates that the value was obtained from sediment trap. |
| Reference | Original references for the indicated entry. Full references are available online at: https://onlinelibrary.wiley.com/doi/10.1002/ldr.3207 |

# APPENDIX G

# COMPARISON OF SSV DATA FOR WARM DESERT (BWH KÖPPEN-GIGER) SITES

| ID | Continent | Country | River/Catchment Name | Measuring location | Lat (°) | Lon (°) | A (mi²) | A (km²) | SSV (ac-ft/mi²/yr) | SSV (m³/km²/yr) | Rainfall (mm) | MP | MP length (yr) | Land Use | Type | References |
|---|---|---|---|---|---|---|---|---|---|---|---|---|---|---|---|---|
| **1. Representative of conditions to be expected in Maricopa county** | | | | | | | | | | | | | | | | |
| 1 | Am | U.S.A. | Cave Creek Dam | AZ | | | 121.00 | 313.39 | 0.24 | 114.30 | | N.A. | N.A. | G | R | USACE, 1974 |
| 2 | Am | U.S.A. | Spookhill FRS | AZ | | | 16.40 | 42.48 | 0.15 | 71.44 | | N.A. | N.A. | ? | R | USDA, Natural Resources Conservation Service file data |
| 3 | Am | U.S.A. | Saddleback FRS | AZ | | | 30.00 | 77.70 | 0.08 | 38.10 | | N.A. | N.A. | ? | R | USDA, Natural Resources Conservation Service file data |
| 4 | Am | U.S.A. | Davis Tank | AZ | 5S | 30E | 0.21 | 0.54 | 0.96 | 457.20 | | 1945-1950 | 6 | G | R | Peterson, 1962 |
| 5 | Am | U.S.A. | Kennedy Tank | AZ | 8S | 30E | 0.97 | 2.51 | 0.27 | 128.59 | | 1945-1950 | 6 | G | R | Peterson, 1962 |
| 6 | Am | U.S.A. | Juniper Tank | AZ | 1S | 22E | 2.00 | 5.18 | 0.29 | 138.11 | | 1945-1950 | 6 | G | R | Peterson, 1962 |
| 7 | Am | U.S.A. | Alhambra Tank | AZ | 17S | 8E | 6.61 | 17.12 | 0.03 | 14.29 | | 1942-1950 | 9 | G | R | Peterson, 1962 |
| 8 | Am | U.S.A. | Black Hills Tank | AZ | 5N | 5E | 1.14 | 2.95 | 0.68 | 323.85 | | 1945-1949 | 5 | G | R | Peterson, 1962 |
| 9 | Am | U.S.A. | Black Hills Tank | AZ | 5N | 5E | 1.56 | 4.04 | 0.58 | 276.22 | | N.A. | N.A. | G | R | Peterson, 1962 |
| 10 | Am | U.S.A. | Mesquite Tank | AZ | 3N | 10W | 9.00 | 23.31 | 0.03 | 14.29 | | N.A. | N.A. | G | R | Langbein et al., 1951 |
| 11 | Am | U.S.A. | Tank 76 | AZ | 16S | 6E | 1.17 | 3.03 | 0.21 | 100.01 | | 1947-1948 | 1 | G | R | Peterson, 1962 |
| 12 | Am | U.S.A. | Camp Marston | CA | | | 1.59 | 4.12 | 0.14 | 66.67 | | N.A. | N.A. | G | R | Peterson, 1962 |
| 13 | Am | U.S.A. | Embudo Arroyo | NM | | | 20.68 | 53.56 | 0.07 | 33.34 | | 1980-1992 | 13 | ? | R | USDA, Natural Resources Conservation Service file data |
| 14 | Am | U.S.A. | La Cueva | NM | | | 8.00 | 20.72 | 0.05 | 23.81 | | 1980-1992 | 13 | ? | R | Mussetter et al., 1994 |
| 15 | Am | U.S.A. | Baca Arroyo | NM | | | 11.55 | 29.91 | 0.34 | 161.92 | | 1980-1992 | 13 | ? | R | Mussetter et al., 1994 |
| 16 | Am | U.S.A. | North Pino Arroyo | NM | | | 2.82 | 7.30 | 0.22 | 104.77 | | 1980-1992 | 13 | ? | R | Mussetter et al., 1994 |
| 17 | Am | U.S.A. | South Pino Arroyo | NM | | | 9.33 | 24.16 | 0.13 | 61.91 | | 1980-1992 | 13 | ? | R | Mussetter et al., 1994 |
| 18 | Am | U.S.A. | Bear Arroyo | NM | | | 15.50 | 40.14 | 0.12 | 57.15 | | 1980-1992 | 13 | ? | R | Mussetter et al., 1994 |
| 19 | Am | U.S.A. | Vinyard Arroyo | NM | | | 0.98 | 2.54 | 0.28 | 133.35 | | 1980-1992 | 13 | ? | R | Mussetter et al., 1994 |
| 20 | Am | U.S.A. | Hahn Arroyo | NM | | | 5.80 | 15.02 | 0.01 | 4.76 | | 1980-1992 | 13 | ? | R | Mussetter et al., 1994 |
| 21 | Am | U.S.A. | N. Diversion Channel | NM | | | 101.01 | 261.61 | 0.21 | 100.01 | | 1980-1992 | 13 | ? | R | Mussetter et al., 1994 |

(Continues)

| ID | Continent | Country | River/Catchment Name | Measuring location | Lat (°) | Lon (°) | A (mi²) | A (km²) | SSV (ac-ft/mi²/yr) | SSV (m³/km²/yr) | Rainfall (mm) | MP | MP length (yr) | Land Use | Type | References |
|---|---|---|---|---|---|---|---|---|---|---|---|---|---|---|---|---|
| **2. Jeong and Dorn (2019)** | | | | | | | | | | | | | | | | |
| 22 | Am | U.S.A. | Cigar | | 33.685117 | -112.534267 | 1.00 | 2.60 | 0.14 | 66.54 | 218 | 1990-2004 | 15 | U | R | Jeong and Dorn, 2019 |
| 23 | Am | U.S.A. | Cigar | | 33.685117 | -112.534267 | 1.00 | 2.60 | 0.16 | 75.82 | 178 | 2005-2009 | 5 | U | R | Jeong and Dorn, 2019 |
| 24 | Am | U.S.A. | Saguaro | | 33.800925 | -112.204050 | 0.54 | 1.40 | 0.07 | 34.98 | 200 | 1990-2004 | 15 | G | R | Jeong and Dorn, 2019 |
| 25 | Am | U.S.A. | Saguaro | | 33.800925 | -112.204050 | 0.54 | 1.40 | 0.20 | 95.29 | 198 | 2005-2009 | 5 | U | R | Jeong and Dorn, 2019 |
| 26 | Am | U.S.A. | Cline | | 33.853465 | -112.149325 | 0.58 | 1.50 | 0.07 | 33.68 | 326 | 1989-1995 | 7 | U | R | Jeong and Dorn, 2019 |
| 27 | Am | U.S.A. | Cline | | 33.853465 | -112.149325 | 0.58 | 1.50 | 0.16 | 75.91 | 192 | 1996-2003 | 8 | U | R | Jeong and Dorn, 2019 |
| 28 | Am | U.S.A. | Cline | | 33.853465 | -112.149325 | 0.58 | 1.50 | 0.22 | 102.74 | 282 | 2003-2004 | 2 | U | R | Jeong and Dorn, 2019 |
| 29 | Am | U.S.A. | Anthem | | 33.862595 | -112.123726 | 0.34 | 0.88 | 0.18 | 84.19 | 305 | 1989-1992 | 4 | G | R | Jeong and Dorn, 2019 |
| 30 | Am | U.S.A. | Anthem | | 33.862595 | -112.123726 | 0.34 | 0.88 | 0.43 | 203.64 | 269 | 1993-1997 | 5 | F1 | R | Jeong and Dorn, 2019 |
| 31 | Am | U.S.A. | Anthem 2 | | 33.850572 | -112.101617 | 0.22 | 0.58 | 0.13 | 59.61 | 305 | 1989-1992 | 4 | G | R | Jeong and Dorn, 2019 |
| 32 | Am | U.S.A. | Anthem 2 | | 33.850572 | -112.101617 | 0.22 | 0.58 | 0.39 | 184.48 | 355 | 1993-1995 | 3 | F1 | R | Jeong and Dorn, 2019 |
| 33 | Am | U.S.A. | Anthem 2 | | 33.850572 | -112.101617 | 0.22 | 0.58 | 0.42 | 197.76 | 190 | 1996-1998 | 3 | F2 | R | Jeong and Dorn, 2019 |
| 34 | Am | U.S.A. | Anthem 2 | | 33.850572 | -112.101617 | 0.22 | 0.58 | 0.19 | 91.16 | 178 | 1999-2002 | 4 | F2 | R | Jeong and Dorn, 2019 |
| 35 | Am | U.S.A. | Anthem 2 | | 33.850572 | -112.101617 | 0.22 | 0.58 | 0.36 | 172.76 | 63 | 2002 | 1 | U | R | Jeong and Dorn, 2019 |
| 36 | Am | U.S.A. | Pepe | | 33.786100 | -112.159939 | 0.38 | 0.99 | 0.07 | 34.00 | 206 | 1989-2008 | 20 | G | R | Jeong and Dorn, 2019 |
| 37 | Am | U.S.A. | Bronco | | 33.774765 | -112.117174 | 0.17 | 0.45 | 0.08 | 37.86 | 231 | 1989-1998 | 10 | G | R | Jeong and Dorn, 2019 |
| 38 | Am | U.S.A. | Bronco | | 33.774765 | -112.117174 | 0.17 | 0.45 | 0.25 | 117.43 | 158 | 1999-2003 | 5 | U | R | Jeong and Dorn, 2019 |
| 39 | Am | U.S.A. | Circle | | 33.767891 | -112.069517 | 0.23 | 0.60 | 0.10 | 46.76 | 203 | 1990-2010 | 21 | G | R | Jeong and Dorn, 2019 |
| 40 | Am | U.S.A. | Circle | | 33.767891 | -112.069517 | 0.23 | 0.60 | 0.17 | 82.72 | 168 | 2010-2013 | 4 | U | R | Jeong and Dorn, 2019 |
| 41 | Am | U.S.A. | Charlie | | 33.773722 | -111.949346 | 0.35 | 0.91 | 0.35 | 164.52 | 213 | 1989-2004 | 16 | U | R | Jeong and Dorn, 2019 |
| 42 | Am | U.S.A. | Rock | | 33.758838 | -111.877228 | 0.21 | 0.54 | 0.10 | 45.27 | 388 | 1989-1992 | 4 | G | R | Jeong and Dorn, 2019 |
| 43 | Am | U.S.A. | Rock | | 33.758838 | -111.877228 | 0.21 | 0.54 | 0.36 | 169.70 | 374 | 1992-1997 | 6 | F1 | R | Jeong and Dorn, 2019 |
| 44 | Am | U.S.A. | Rock | | 33.758838 | -111.877228 | 0.21 | 0.54 | 0.22 | 102.94 | 254 | 1998-2003 | 6 | F2 | R | Jeong and Dorn, 2019 |
| 45 | Am | U.S.A. | Rock | | 33.758838 | -111.877228 | 0.21 | 0.54 | 0.12 | 56.56 | 304 | 2004-2009 | 6 | F2 | R | Jeong and Dorn, 2019 |
| 46 | Am | U.S.A. | Cave Creek | | 33.821477 | -111.860042 | 0.07 | 0.19 | 0.15 | 72.98 | 320 | 1989-1992 | 4 | G | R | Jeong and Dorn, 2019 |
| 47 | Am | U.S.A. | Cave Creek | | 33.821477 | -111.860042 | 0.07 | 0.19 | 0.32 | 151.75 | 325 | 1992-1999 | 8 | F1 | R | Jeong and Dorn, 2019 |
| 48 | Am | U.S.A. | Cave Creek | | 33.821477 | -111.860042 | 0.07 | 0.19 | 0.19 | 91.75 | 228 | 2000-2003 | 4 | U | R | Jeong and Dorn, 2019 |
| 49 | Am | U.S.A. | Buckhorn | | 33.771593 | -111.726559 | 1.70 | 4.40 | 0.16 | 76.06 | 362 | 1989-1999 | 11 | U | R | Jeong and Dorn, 2019 |

(Continues)

| ID | Continent | Country | River/Catchment Name | Measuring location | Lat (°) | Lon (°) | A ($mi^2$) | A ($km^2$) | SSV (ac-ft/$mi^2$/yr) | SSV ($m^3/km^2/yr$) | Rainfall (mm) | MP | MP length (yr) | Land Use | Type | References |
|---|---|---|---|---|---|---|---|---|---|---|---|---|---|---|---|---|
| **3. Henze's MS work** | | | | | | | | | | | | | | | | |
| 64 | Am | U.S.A. | Casandro Wash | | Nearest town | AZ | 1.24 | 3.21 | 0.31 | 147.64 | N.A. | N.A. | N.A. | G | R | CH2M-Hill. 1994a |
| 65 | Am | U.S.A. | Rawhide Wash | | Nearest town | AZ | 13.64 | 35.33 | 0.39 | 185.74 | N.A. | N.A. | N.A. | G | R | CH2M-Hill. 1994b |
| 66 | Am | U.S.A. | Phoenix Mount Preserve (Tatum Wash) | | Nearest town | AZ | 1.92 | 4.97 | 1.90 | 904.87 | N.A. | N.A. | N.A. | G | | JE Fuller Hydrology & Geomorphology, INC. (JEF). 1997 |
| 67 | Am | U.S.A. | Shea Boulevard (Tatum Wash) | | Nearest town | AZ | 2.17 | 5.62 | 2.10 | 1000.12 | N.A. | N.A. | N.A. | G | | JE Fuller Hydrology & Geomorphology, INC. (JEF). 1997 |
| 68 | Am | U.S.A. | Western Tributary (Cherokee Wash) | | Nearest town | AZ | 0.14 | 0.36 | 2.16 | 1028.70 | N.A. | N.A. | N.A. | G | | WEST Consulting. 1997 |
| 69 | Am | U.S.A. | Desert Park Tributary (Cherokee Wash) | | Nearest town | AZ | 0.3 | 0.78 | 1.98 | 942.97 | N.A. | N.A. | N.A. | G | | WEST Consulting. 1997 |
| 70 | Am | U.S.A. | Desert Greenbelt Project | | Nearest town | AZ | 8.58 | 22.22 | 0.10 | 47.62 | N.A. | N.A. | N.A. | G | | Hjalmarson, 1996 |
| 71 | Am | U.S.A. | Cave Creek | | Nearest town | AZ | 121 | 313.39 | 0.31 | 147.64 | N.A. | N.A. | N.A. | G | | Hjalmarson, 1996 |
| 72 | Am | U.S.A. | Spookhill Dam | | Nearest town | AZ | 16.4 | 42.48 | 0.15 | 71.44 | N.A. | N.A. | N.A. | G | | Hjalmarson, 1996 |
| 73 | Am | U.S.A. | Shaddle back Dam | | Nearest town | AZ | 30 | 77.70 | 0.08 | 38.10 | N.A. | N.A. | N.A. | G | | Hjalmarson, 1996 |
| 74 | Am | U.S.A. | Black Hills tank | | Nearest town | AZ | 1.56 | 4.04 | 0.58 | 276.22 | N.A. | N.A. | N.A. | G | R | Langbein et al. 1951 |
| 75 | Am | U.S.A. | Spook Hill Apache Junction FRS | | Nearest town | AZ | 5.8 | 15.02 | 0.07 | 33.34 | 217 | N.A. | N.A. | G | R | Henze, 2000 |
| 76 | Am | U.S.A. | Spook Hill Signal Butte FRS | | Nearest town | AZ | 10.64 | 27.56 | 0.11 | 52.39 | 217 | N.A. | N.A. | G | R | Henze, 2000 |
| 77 | Am | U.S.A. | Spook Hill Spook Hill FRS | | Nearest town | AZ | 13.68 | 35.43 | 0.14 | 66.67 | 217 | N.A. | N.A. | G | R | Henze, 2000 |
| 78 | Am | U.S.A. | Spook Hill Spook Hill Floodway | | Nearest town | AZ | 2.89 | 7.49 | 0.16 | 76.20 | 217 | N.A. | N.A. | G | R | Henze, 2000 |



(Continues)

| ID | Continent | Country | River/Catchment Name | Measuring location | Lat (°) | Lon (°) | A (mi²) | A (km²) | SSV (ac-ft/mi²/yr) | SSV ($m^3/km^2/yr$) | Rainfall (mm) | MP | MP length (yr) | Land Use | Type | References |
|---|---|---|---|---|---|---|---|---|---|---|---|---|---|---|---|---|
| **4. Gilla River Basin (Below Hoover Dam)** | | | | | | | | | | | | | | | | |
| 79 | Am | U.S.A. | Agua Fria River | Lake Pleasant | Nearest town | Phoenix, AZ | 1444.00 | 3739.94 | 0.43 | 205.74 | | 1941-1954 | 13 | G | R | Dendy et al. 1978 |
| 80 | Am | U.S.A. | Tributrary of Gila River | Halfmoon | Nearest town | Florence, AZ | 0.20 | 0.52 | 3.75 | 1785.93 | | 1960-1979 | 19 | G | R | Dendy et al. 1978 |
| 81 | Am | U.S.A. | Tributrary of Gila River | Homestead | Nearest town | Florence, AZ | 0.90 | 2.33 | 0.87 | 412.75 | | 1960-1966 | 6 | G | R | Dendy et al. 1978 |
| 82 | Am | U.S.A. | Foote Wash | Lower Foote Wash | Nearest town | Safford, AZ | 0.63 | 1.63 | 0.21 | 98.27 | | 1958-1980 | 22 | G | R | Dendy et al. 1978 |
| 83 | Am | U.S.A. | Magma Wash | Magma No.1 | Nearest town | Florence, AZ | 1.78 | 4.61 | 0.08 | 40.13 | | 1959-1970 | 11 | G | R | Dendy et al. 1978 |
| 84 | Am | U.S.A. | Magma Wash | Magma No.2 | Nearest town | Florence, AZ | 0.38 | 0.98 | 0.39 | 187.99 | | 1959-1965 | 5 | G | R | Dendy et al. 1978 |
| 85 | Am | U.S.A. | Magma Wash | Magma No.3 | Nearest town | Florence, AZ | 7.00 | 18.13 | 0.00 | 2.04 | | 1959-1969 | 10 | G | R | Dendy et al. 1978 |
| 86 | Am | U.S.A. | Tributary of Gila River | Whitlow Old Tank | Nearest town | Florence, AZ | 0.74 | 1.92 | 0.31 | 148.02 | | 1960-1970 | 10 | G | R | Dendy et al. 1978 |
| 87 | Am | U.S.A. | Tributary of Queen Creek | Willams-Chandler Pd. #1 | Nearest town | Florence, AZ | 1.09 | 2.82 | 0.03 | 14.42 | | 1961-1991 | 30 | G | R | Dendy et al. 1978 |
| 88 | Am | U.S.A. | Tributary of Queen Creek | Willams-Chandler Pd. #2 | Nearest town | Florence, AZ | 0.65 | 1.68 | 0.20 | 95.25 | | 1961-1978 | 17 | G | R | Dendy et al. 1978 |
| 89 | Am | U.S.A. | Tributary of Queen Creek | Willams-Chandler Pd. #2 | Nearest town | Florence, AZ | 0.65 | 1.68 | 0.09 | 43.96 | | 1974-1987 | 13 | G | R | Dendy et al. 1978 |
| 90 | Am | U.S.A. | Tributary of Centennial Wash | Big Horn Mt. Tank #1 | Nearest town | Tonopah, AZ | 0.51 | 1.32 | 0.22 | 102.72 | | 1964-1969 | 4 | G | R | Dendy et al. 1978 |
| 91 | Am | U.S.A. | Tributary of Centennial Wash | Big Horn Mt. Tank #2 | Nearest town | Tonopah, AZ | 0.44 | 1.14 | 0.25 | 119.06 | | 1964-1969 | 4 | G | R | Dendy et al. 1978 |
| 92 | Am | U.S.A. | Tributary of Centennial Wash | Centennial Wash Tank | Nearest town | Tonopah, AZ | 0.60 | 1.55 | 0.15 | 71.44 | | 1965-1976 | 11 | G | R | Dendy et al. 1978 |
| 93 | Am | U.S.A. | Tributary of Centennial Wash | New Tank | Nearest town | Tonopah, AZ | 1.88 | 4.87 | 0.05 | 23.81 | | 1965-1985 | 20 | G | R | Dendy et al. 1978 |
| 94 | Am | U.S.A. | Tributary of Centennial Wash | West Tank | Nearest town | Salome, AZ | 0.29 | 0.75 | 0.45 | 213.49 | | 1964-1969 | 4 | G | R | Dendy et al. 1978 |
| 95 | Am | U.S.A. | Tiger Wash | Upper Twin Tank | Nearest town | Aguila, AZ | 1.83 | 4.74 | 0.01 | 3.90 | | 1964-1984 | 20 | G | R | Dendy et al. 1978 |
| 96 | Am | U.S.A. | Tributary of Browns' Canyon wash | Harquahala Mt. Tank #1 | Nearest town | Aguila, AZ | 0.11 | 0.28 | 1.64 | 779.32 | | 1964-1971 | 6 | G | R | Dendy et al. 1978 |
| 97 | Am | U.S.A. | Judia Wash | Judia Wash Retarding Dam | Nearest town | Solomone, AZ | 4.57 | 11.84 | 0.03 | 14.59 | | 1964-1971 | 7 | G | R | Dendy et al. 1978 |

(Continues)

| ID | Continent | Country | River/Catchment Name | Measuring location | Lat (°) | Lon (°) | A (mi²) | A (km²) | SSV (ac-ft/mi²/yr) | SSV (m³/km²/yr) | Rainfall (mm) | MP | MP length (yr) | Land Use | Type | References |
|---|---|---|---|---|---|---|---|---|---|---|---|---|---|---|---|---|
| **6. Other BWh catchments** | | | | | | | | | | | | | | | | |
| 103 | Am | Chile | Rio Lluta | | -13.600000 | -69.900000 | 984.56 | 2550 | 0.01 | 4.41 | 20 | 1988-2002 | 15 | G | GS | Kober et al. 2007 |
| 104 | Am | Chile | Rio Lluta | | -13.600000 | -69.900000 | 965.26 | 2500 | 0.02 | 9.29 | 250 | 1994/2001 El Nino | 2 | G | GS | Kober et al. 2007 |
| 105 | Au | Australia | Murray-Darling Basin | | -20.911554 | 116.309280 | 0.00 | 0.01 | 0.22 | 104.00 | N.A. | N.A. | N.A. | G | E | Wasson 1994 |
| 106 | Au | Australia | Murray-Darling Basin | | -20.911554 | 116.309280 | 412.36 | 1068 | 0.12 | 59.33 | N.A. | N.A. | N.A. | G | R | Wasson 1994 |
| 107 | Au | Australia | Murray-Darling Basin | | N.A. | N.A. | 409.27 | 1060 | 0.02 | 10.60 | N.A. | Pre-European settlement | N.A. | P | N.A. | Wasson et al. 1996 |
| 108 | Au | Australia | Murray-Darling Basin | | N.A. | N.A. | 409.27 | 1060 | 0.04 | 18.67 | N.A. | Post-Erupoean settlement | N.A. | G | N.A. | Wasson et al. 1996 |
| 109 | ME | West Bank | Qumeran | Dead Sea highway | 31° 42' N | 35° 25' E | 18.15 | 47 | 0.09 | 41.33 | N.A. | N.A. | N.A. | G | M | Moshe et al. 2008 |
| 110 | ME | West Bank | Qidron | Dead Sea highway | 31° 41' N | 35° 20' E | 47.49 | 123 | 0.05 | 23.33 | N.A. | N.A. | N.A. | G | M | Moshe et al. 2008 |
| 111 | ME | West Bank | Darga | Dead Sea highway | 31° 37' N | 35°18' E | 91.51 | 237 | 0.13 | 60.00 | N.A. | N.A. | N.A. | G | M | Moshe et al. 2008 |
| 112 | ME | West Bank | Qedem | Dead Sea highway | 31° 31' N | 35° 24' E | 4.63 | 12 | 0.21 | 101.33 | N.A. | N.A. | N.A. | G | M | Moshe et al. 2008 |
| 113 | ME | West Bank | Ishai | Dead Sea highway | 31° 29' N | 35° 24' E | 0.77 | 2 | 0.01 | 3.00 | N.A. | N.A. | N.A. | G | M | Moshe et al. 2008 |
| 114 | ME | West Bank | Hever | Dead Sea highway | 31° 26' N | 35° 15' E | 67.57 | 175 | 0.07 | 33.33 | N.A. | N.A. | N.A. | G | M | Moshe et al. 2008 |
| 115 | ME | West Bank | Zeelim | Dead Sea highway | 31° 20' N | 35° 15' E | 97.68 | 253 | 0.05 | 26.00 | N.A. | N.A. | N.A. | G | M | Moshe et al. 2008 |
| 116 | ME | West Bank | Neqarot | | N.A. | N.A. | 379.92 | 984 | 0.10 | 48.00 | 70 | N.A. | N.A. | G | R | Laronne and Wilhelm, 2001 |
| 117 | ME | West Bank | Hiyyon | | N.A. | N.A. | 431.66 | 1118 | 0.06 | 28.67 | 40 | N.A. | N.A. | G | R | Laronne and Wilhelm, 2001 |
| 118 | ME | Israel | Nahal Eshtemoa | | 31.300000 | 34.966667 | 45.95 | 119 | 0.66 | 314.67 | 185 | 1992-1995 | 4 | G | GS | Powell et al., 1996 |
| 119 | ME | Israel | Nahal Yael | | 29.587910 | 34.942364 | 0.23 | 0.60 | 0.56 | 266.67 | 31 | 1967-1976 | 10 | G | R | Schick and Lekach, 1993 |
| 120 | ME | Israel | Nahal Yael | | 29.587910 | 34.942364 | 0.23 | 0.60 | 0.24 | 113.33 | 31 | 1981-1990 | 10 | G | R | Schick and Lekach, 1993 |
| 121 | ME | Israel | Nahal Yael | | 29.587910 | 34.942364 | 0.23 | 0.60 | 0.19 | 92.00 | 39 | 1967-2000 | >33 | G | R | Clapp et al., 2000 |
| 122 | ME | Israel | Giv'at Hayil | Backhoe trench | 30.994170 | 34.680835 | 0.07 | 0.17 | 1.72 | 820.00 | 100 | 1986-1988 | 3 | G | T | Schwartz and Greenbaum, 2008 |
| 123 | ME | Israel | Be'er Sheva Leeman South | | 31.240000 | 34.840000 | 0.09 | 0.23 | 0.53 | 251.33 | 210 | N.A. | N.A. | U | R | Laronne 1990 |
| 124 | ME | Israel | Be'er Sheva Leeman North | | 31.240000 | 34.840000 | 1.12 | 2.90 | 0.36 | 172.67 | 220 | N.A. | N.A. | U | R | Laronne 1990 |
| 125 | ME | Israel | Boker | | 30.920000 | 34.780000 | 13.51 | 35 | 0.06 | 30.67 | 95 | N.A. | N.A. | G | R | Shanan 2000 |
| 126 | ME | Israel | Haroeh | | 30.900000 | 34.830000 | 16.60 | 43 | 0.10 | 46.67 | 95 | N.A. | N.A. | G | R | Shanan 2000 |
| 127 | ME | Israel | Heimar | | 31.150000 | 35.240000 | 139.00 | 360 | 0.23 | 109.33 | 80 | N.A. | N.A. | G | GS | Powell et al., 1996 |

(Continues)

| ID | Continent | Country | River/Catchment Name | Measuring location | Lat (°) | Lon (°) | A (mi²) | A (km²) | SSV (ac-ft/mi²/yr) | SSV (m³/km²/yr) | Rainfall (mm) | MP | MP length (yr) | Land Use | Type | References |
|---|---|---|---|---|---|---|---|---|---|---|---|---|---|---|---|---|
| **6. Other BWh catchments** | | | | | | | | | | | | | | | | |
| 134 | Af | Sudan | Blue Nile | Sennar | 13.541714 | 33.638293 | 107060.73 | 277286 | 0.47 | 226.00 | | 1993 - 1996 | 4 | U | GS | Billi and el Badri Ali, 2010 |
| 135 | Af | Niger | Sirba | Garbe Kourou | 13.731594 | 1.604889 | 14943.69 | 38704 | 0.03 | 16.53 | | HY 2006/2007 - HY 2007/2008 | 2 | G | GS | Amogu, 2009 |
| 136 | Af | Niger | Gorouol | Alcongui | 14.748588 | 0.597706 | 17196.98 | 44540 | 0.02 | 11.80 | | HY 2006/2007 - HY 2007/2008 | 2 | A | GS | Amogu, 2009 |
| 137 | Af | Niger | Niger | Farié-Haossa | 13.783635 | 1.649525 | 251113.02 | 650380 | 0.03 | 13.07 | | HY 2007/2008 | 1 | A | GS | Amogu, 2009 |
| 138 | Af | Niger | Niger | Latakabiey | 13.758310 | 1.679255 | 266074.47 | 689130 | 0.03 | 13.07 | | HY 2007/2008 | 1 | A | GS | Amogu, 2009 |
| 139 | Af | Niger | Gorouol | Dolbel | 14.616700 | 0.283300 | 2895.77 | 7500 | 0.03 | 14.73 | | HY 1976/1977 - HY 1982 - 1983 | 7 | A | GS | Amogu, 2009; Gallaire, 1986 |
| 140 | Af | Niger | Niger | Niamey | 13.503032 | 2.107030 | 270271.40 | 700000 | 0.02 | 8.40 | | HY 1984/1985 - HY 1985/1986; HY 2006/2007 - HY 2007/2008 | 4 | U | GS | Amogu, 2009; Gallaire, 1986 |
| 141 | Af | Niger | Niger | Kandadji | 14.614552 | 0.965856 | 242792.52 | 628830 | 0.01 | 3.20 | | HY 1976/1977 - HY 1982/1983; HY 2007/2008 | 8 | A | GS | Amogu, 2009; Gallaire, 1986 |
| 142 | Af | Senegal | Sénégal | Dagana | 16.522000 | -15.512900 | 104247.54 | 270000 | 0.01 | 7.07 | | 1981 - 1983 | 3 | A | GS | Liénou et al., 2005 |
| 143 | Af | Senegal | Sénégal | near outlet | 16.126200 | -16.486400 | 104247.54 | 270000 | 0.02 | 7.40 | | N.A. | N.A. | G | GS | Milliman and Fansworth, 2011 |
| 144 | Af | Morocco | Draa | near outlet | 28.698880 | -11.164700 | 44015.63 | 114000 | 0.17 | 81.87 | | N.A. | N.A. | G | GS | Milliman and Fansworth, 2011 |
| 145 | Af | Morocco | Draa | Mansour Eddahbi | 30.923100 | -6.789500 | 5791.53 | 15000 | 0.57 | 273.33 | | 1972 - 1986 | 15 | A | R | FAO, 2008 |
| 146 | Af | Morocco | Massa | Youssef b Tachfine | 29.802800 | -9.466400 | 1461.01 | 3784 | 0.53 | 252.00 | | 1973 - 1986 | 14 | G | R | FAO, 2008 |
| 147 | Af | Ethiopia | Wabi Shebelle | Gode | 5.925545 | 43.547301 | 49150.78 | 127300 | 0.17 | 78.67 | | N.A. | N.A. | U | GS | Nyssen et al., 2004 |
| 148 | Af | Algeria | | Djorf Torba | 31.529500 | -2.760900 | 8494.24 | 22000 | 0.22 | 106.93 | | 1969 - 1985 | 17 | G | R | Lahlou, 1996; Benguedach and Chabouni, 1997 |
| 149 | Af | Algeria | El Abiod | Mchouneche | 34.942900 | 5.997400 | 405.41 | 1050 | 0.56 | 267.33 | | 1972 - 1979 | 8 | U | GS | FAO, 2008 |
| 150 | Af | Algeria | Isser | El Izdibar | 34.851900 | 5.738400 | 440.16 | 1140 | 0.16 | 78.00 | | 1989 - 1998 | 10 | U | GS | Terfous et al., 2003 |

Table legend

| Column | Explanation |
|---|---|
| ID | Entry identifier |
| Continent | Continent in which the SSY observation was made. 'Am' indicates America. 'Au' indicates Australia. 'ME' indicates Middle East. 'Af' indicates Africa. 'In-Ar' indicates Indo-Arabia. |
| Country | Country in which the SSY observation was made |
| River/Catchment Name | Name of the river/catchment (if available) |
| Measuring location | Description of the measuring location |
| Lat (°) | Estimated latitude of the measuring location |
| Lon (°) | Estimated longitude of the measuring location |
| A (mile²) | Catchment area (mile²) |
| A (km²) | Catchment area (km²) |
| SSV (acre-feet/mile²/yr) | Area-specific catchment sedimentation volume. For the majority of the observations, this value corresponds with the SSV-value reported in the indicated data source. |
| SSV ($m^3/km^2/yr$) | Area-specific catchment sedimentation volume. For the majority of the observations, this value corresponds with the SSV-value reported in the indicated data source. |
| Rainfall (mm) | Mean annual precipitation (mm) |
| MP | Description of the measuring period. 'HY' stands for 'Hydrological Year' (the start and end date of such a year depends on the study). 'N.A.' means not available. |
| MP length (yr) | Duration of the measuring period in year. 'N.A.' means not available. |
| Land Use | Dominant land use during the period of SSY measurement. 'G' indicates grazing. 'P' indicates undisturbed land. 'O' indicates off-road vehicle use. 'U' indicates urban land use. 'F1' indicates immediately after wildfire.' F2' indicates more than 3 years after fire. 'A' indicates agricultural use. |
| Type | Method used to obtain the SSY value. 'R' indicates that the SSY value was obtained from bathymetric surveys in reservoirs. 'GS' indicates that the value was obtained from measurements at a gauging station. 'E' indicates that the value was obtained from erosion plot. 'M' indicates that the value was obtained from model-derived sediment flux. 'T' indicates that the value was obtained from sediment trap. |
| References | Original references for the indicated entry. Full references are available online at: https://onlinelibrary.wiley.com/doi/10.1002/ldr.3207 |

# APPENDIX H

## DIFFERENT APPROACHES TO REPORTING SEDIMENT YIELD

**1. Different approaches to represent the amount of sediment that has been moved from its original sites**

| Agency | Reported term | Unit | Reference |
|---|---|---|---|
| Food and Agriculture Organization of the United Nations | annual sediment yield | [M $L^{-2}$ $T^{-1}$] (t $km^{-2}$ $yr^{-1}$) | FAO (2008) |
| U.S. Department of the Interior, Bureau of Reclamation | Sediment yield | [M $T^{-1}$], [$L^3$ $T^{-1}$] ($tons^{-1}$ $yr^{-1}$), ($m^3$ $yr^{-1}$) | U.S. Department of the Interior Bureau of Reclamation (2009) |
| U.S. Department of the Interior, Bureau of Reclamation | Sediment yield rate | [M $L^{-2}$ $T^{-1}$], [$L^3$ $L^{-2}$ $T^{-1}$] ($m^3$ $km^{-2}$ $yr^{-1}$) (ac ft $mi^{-2}$ $yr^{-1}$) | U. S. Department of the Interior Bureau of Reclamation (2009), Strand and Pemberton (1982) |
| U.S. Department of Agriculture Natural Resources Conservation Service (USDA-NRCS) | Sediment yield | [M $T^{-1}$] (tons $yr^{-1}$) | USDA-NRCS (1983) |
| EUROPEAN SOIL DATA CENTRE (ESDAC) | Sediment yield | [M $T^{-1}$] (Pg $yr^{-1}$) | Borrelli et al. (2018) |
| EUROPEAN SOIL DATA | Area-specific sediment yield | [M $L^{-2}$ $T^{-1}$], | Borrelli et al. (2018) |

| | | | |
|---|---|---|---|
| CENTRE (ESDAC) | | (Mg $ha^{-1}$ $yr^{-1}$) | |

**2. Soil erosion and sediment yield models**

| Model Name | Reported term | Unit | Reference |
|---|---|---|---|
| Universal Soil Loss Equation (USLE), Revised Universal Soil Loss Equation (RUSLE) | Average annual soil loss | [M $L^{-2}$ $T^{-1}$], (tons $acre^{-1}$ $yr^{-1}$) | Wischmeier and Smith (1965, 1978) |
| Soil and Water Assessment Tool (SWAT) | Sediment yield | [M $L^{-2}$], (t $ha^{-1}$), | Arnold et al. (1998) |
| AGricultural Non-Point Source Pollution Model (AGNPS) | Eroded sediments<br>Sediment yield for catchment | [M $L^{-2}$], (tons $acre^{-1}$)<br>[M], (tons) | Young et al. (1989) |
| Water Erosion Prediction Project (WEPP) | Average annual soil loss<br>Average annual sediment yield | [M $L^{-2}$ $T^{-1}$], (ton $acre^{-1}$ $yr^{-1}$) | Laflen et al. (1991)<br>USDA-ARS |

**3. CWDR scholarship compared CWDR-derived background rate (time scale: $10^3$-$10^5$) to modern rate (time scale: $10^0$-$10^2$)**

| Approach | Background rate | Modern rate | Unit | References |
|---|---|---|---|---|
| 1. Convert modern-area specific sediment yield (SSY) to erosion rate using bedrock | Catchment-wide denudation rate (CWDR) | Erosion rate (Area-specific sediment yield / Bedrock density (2.6-2.7 g $cm^{-3}$)) | [L $T^{-1}$], (m $Myr^{-1}$) | Schaller et al. (2001)<br>Bierman et al. (2005) |

| | | | | |
|---|---|---|---|---|
| density (2.6-2.7 g $cm^{-3}$) | | | | |
| 2. Convert CWDR to SSY using bedrock density (2.6-2.7 g $cm^{-3}$) | Area-specific sediment yield (CWDR * bedrock density (2.6-2.7 g $cm^{-3}$)) | Area-specific sediment yield calculated using sediment density (1.x g $cm^{-3}$) | [M $L^{-2}$ $T^{-1}$], (Mg $km^{-2}$ $yr^{-1}$) (kg $m^{-2}$ $yr^{-1}$) | Hewawasam et al. (2003)* Clapp et al. (2001)** Gellis et al. (2004)*** This study |

# APPENDIX I

# THE CHANGE OF LAND-USE, PRECIPITATION VARIABLES, AND EROSION RATES OF 18 STOCK POND CATCHMENTS

The purpose of the appendix I is to show the change of land-use, precipitation variables, and erosion rates of 18 stock pond catchments during the monitoring period: **a,** ID01 Cigar. **b,** ID02 Saguaro. **c,** ID03 Cline. **d,** ID04 Anthem. **e,** ID05 Anthem 2. **f,** ID06 Pepe. **g,** ID07 Bronco. **h,** ID08 Circle. **i,** ID09 Charlie. **j,** ID10 Rock. **k,** ID11 Cave Creek. **l,** ID12 Buckhorn. **m,** ID13 The Rocks. **n,** ID14 128th St. **o,** ID15 128th St 2. **p,** ID16 AsherHills. **q,** ID17 Gold Cyn. **r,** ID18 Peralta.

Each figure shows individual examples of stock pond watersheds experiencing urban sprawl in metropolitan Phoenix. Each stock pond is named and is provided a number that corresponds with Table 5.3 and 5.4.

Each stock pond figure plots precipitation variables (mean annual precipitation and rainfall intensity) from the nearest rain gauge (Maricopa County Flood Control District, n.d) (http://alert.fcd.maricopa.gov/showrpts_mc.html) and land use/land cover variables on the graph to illustrate how the variables influence stock pond catchment erosion rate. The acceleration of erosion from urbanization in this Bwh climate was likely dampened due to the climatic conditions that occurred during the study period from 1989 to 2013. The first decade, dominated by grazing in the study sites, was wetter than the second decade more dominated by urbanization land-use land-cover change. Yet, despite less annual rainfall and less cumulative time of intense rainfall, sudden and aerially extensive exposure of bare ground from urbanization processes significantly increased soil erosion and sediment yield.

**a** ID01: Cigar (1990-2009)

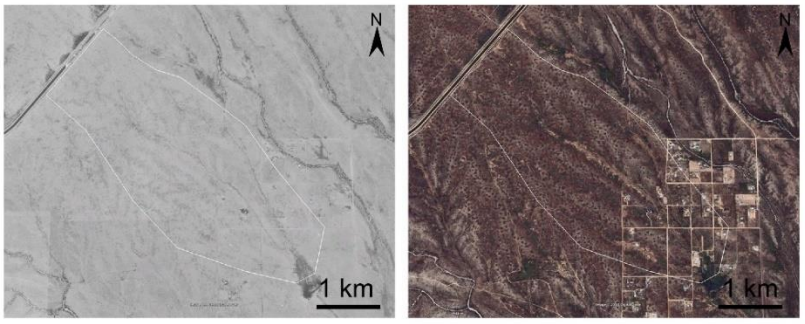


1997: Cattle grazing  2005: Grazing and off-road vehicle

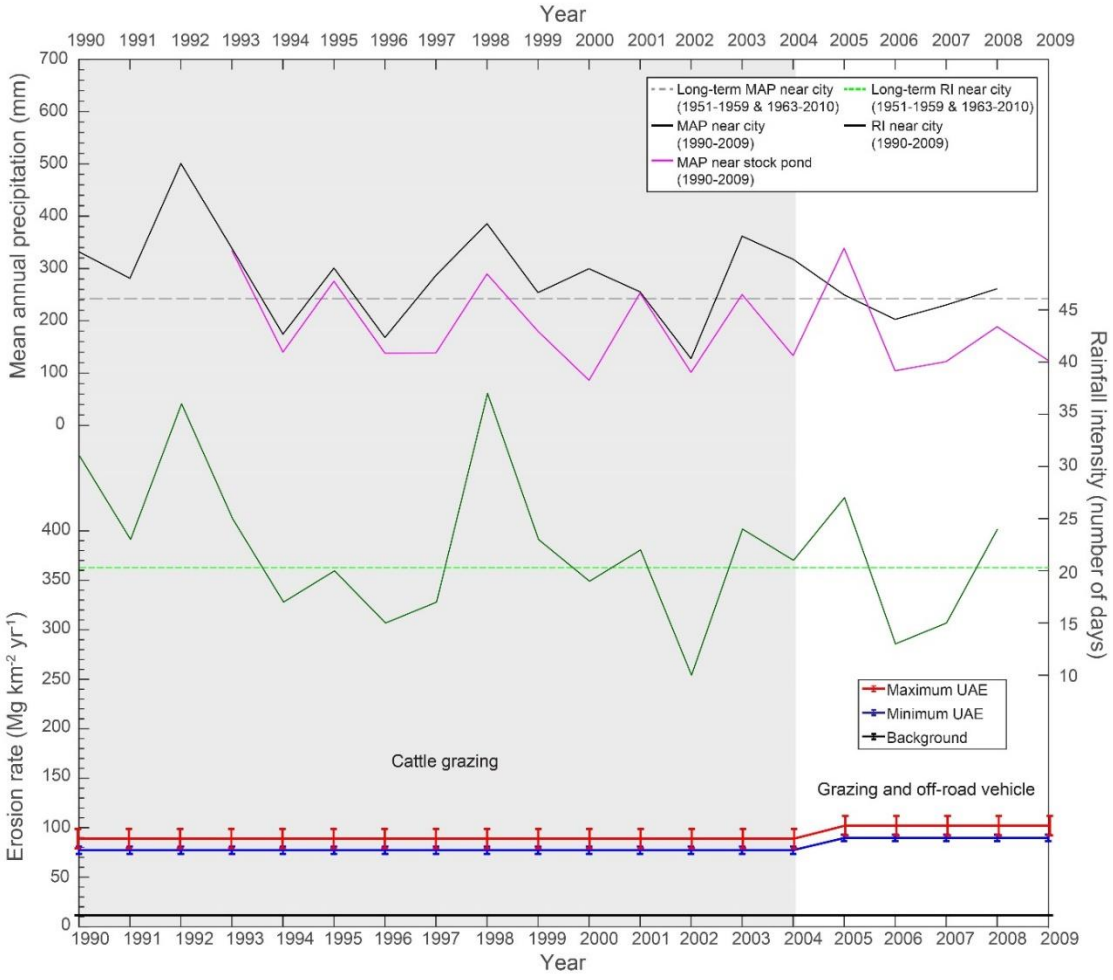

**b** ID02: Saguaro (1990-2009)

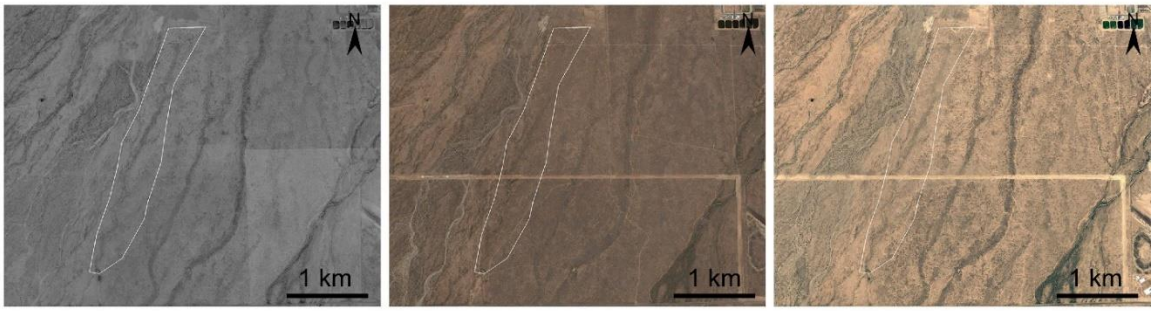


1997: Cattle grazing | 2006: Pipeline construction | 2007: Pipeline construction

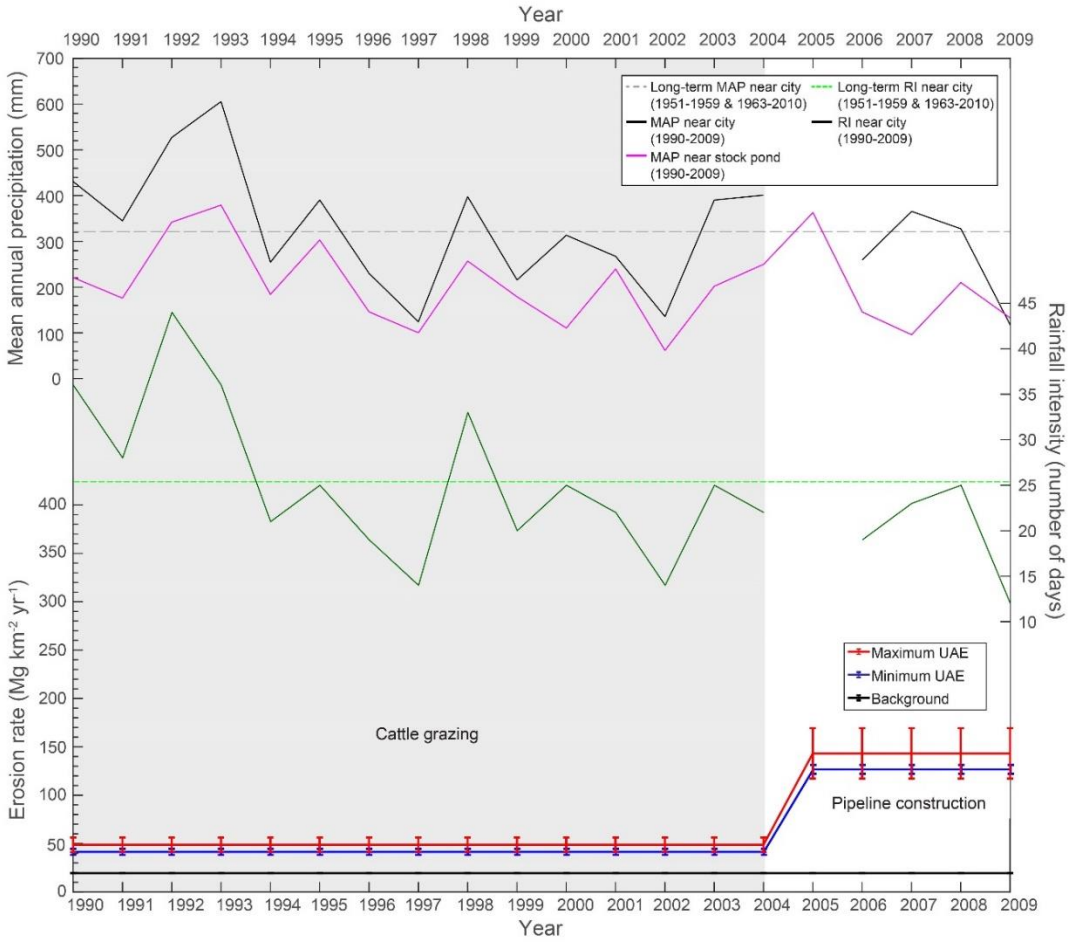

## **c** ID03: Cline (1989-2004)

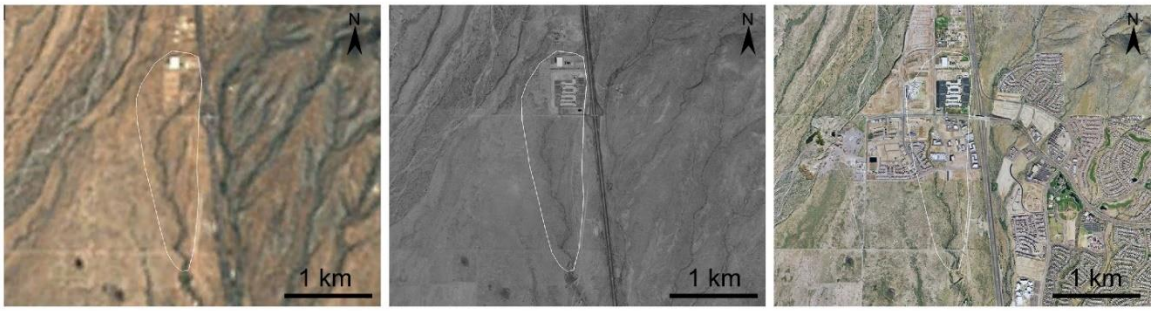


1991: Cattle grazing  1997: Construction (commercial)  2004: Constrcution (subdivision)

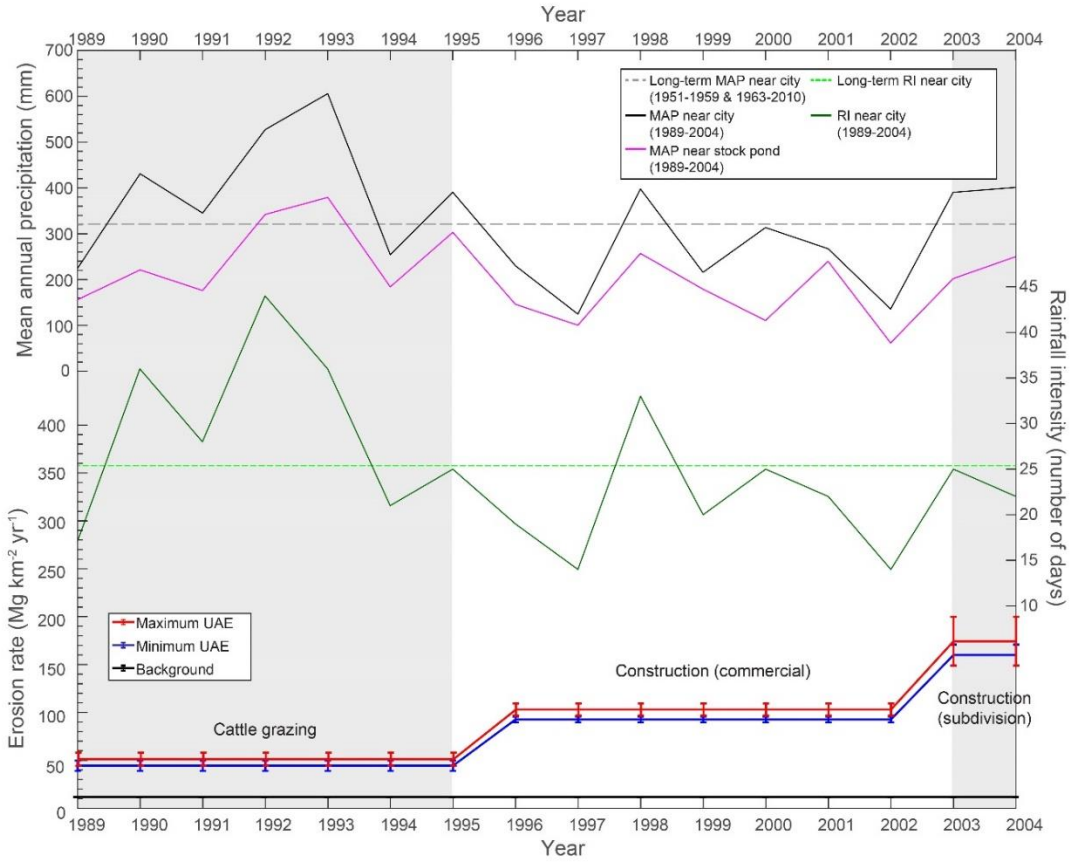

**d** ID04: Anthem (1989-1997)

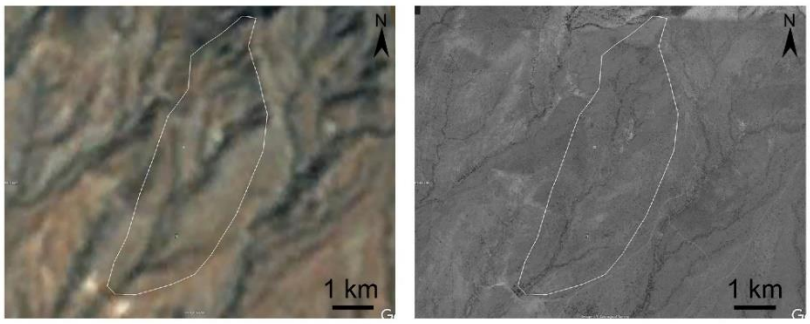


1992: Cattle grazing 1997: wildfire

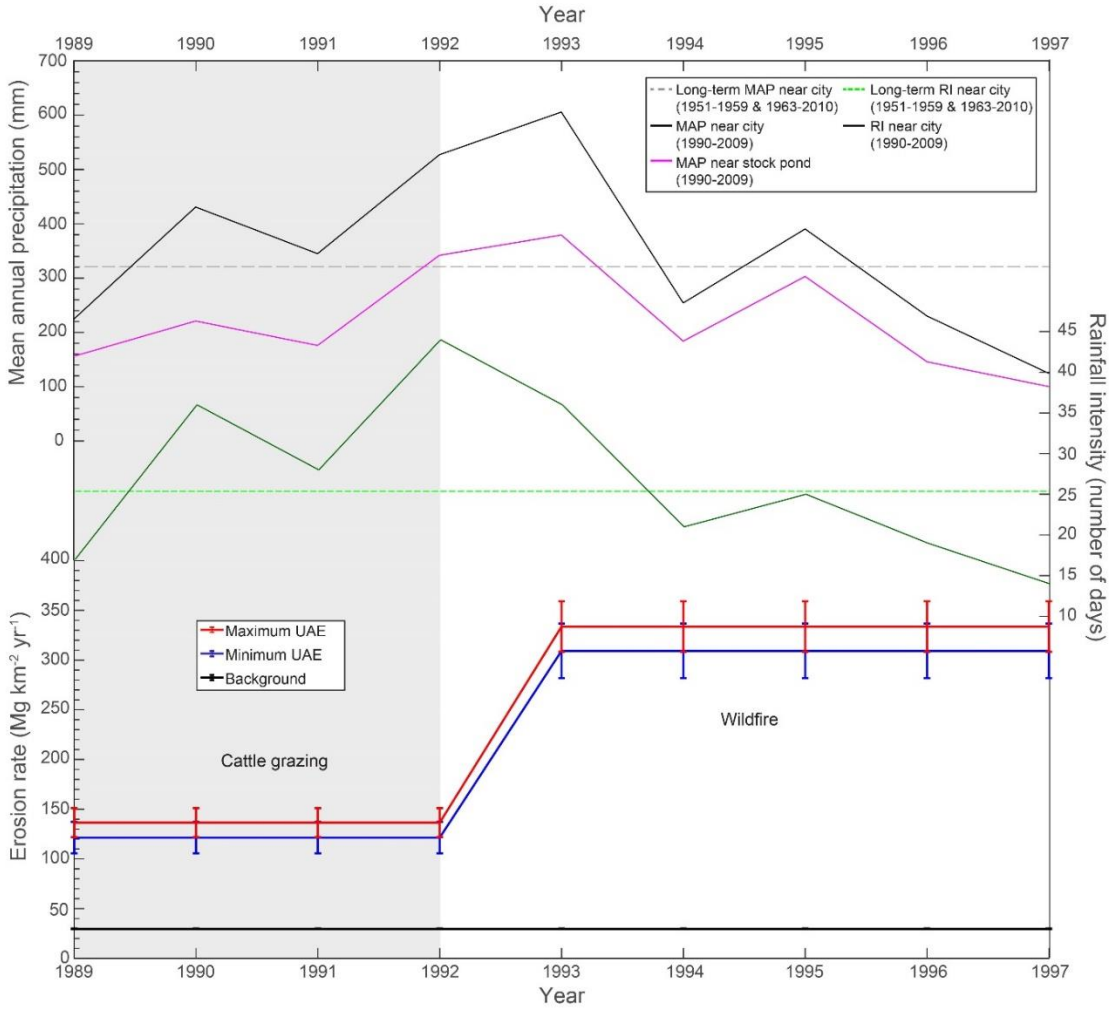

**e** ID05: Anthem 2 (1989-2002)

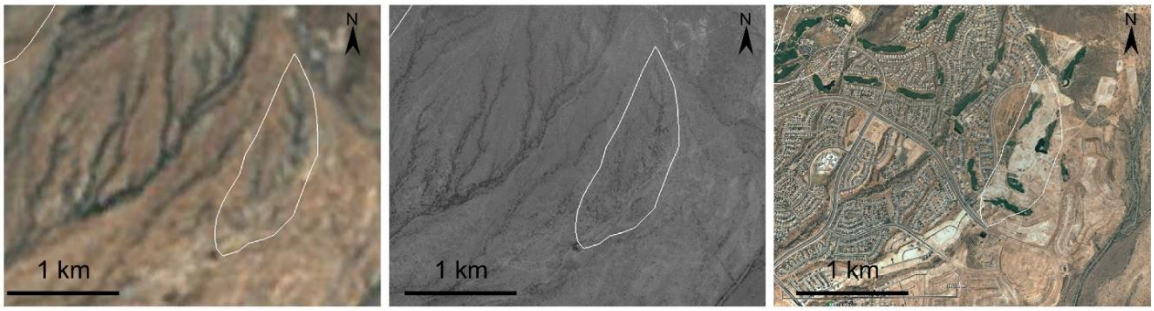


1991: Cattle grazing | 1997: Wildfire II | 2003: Housing

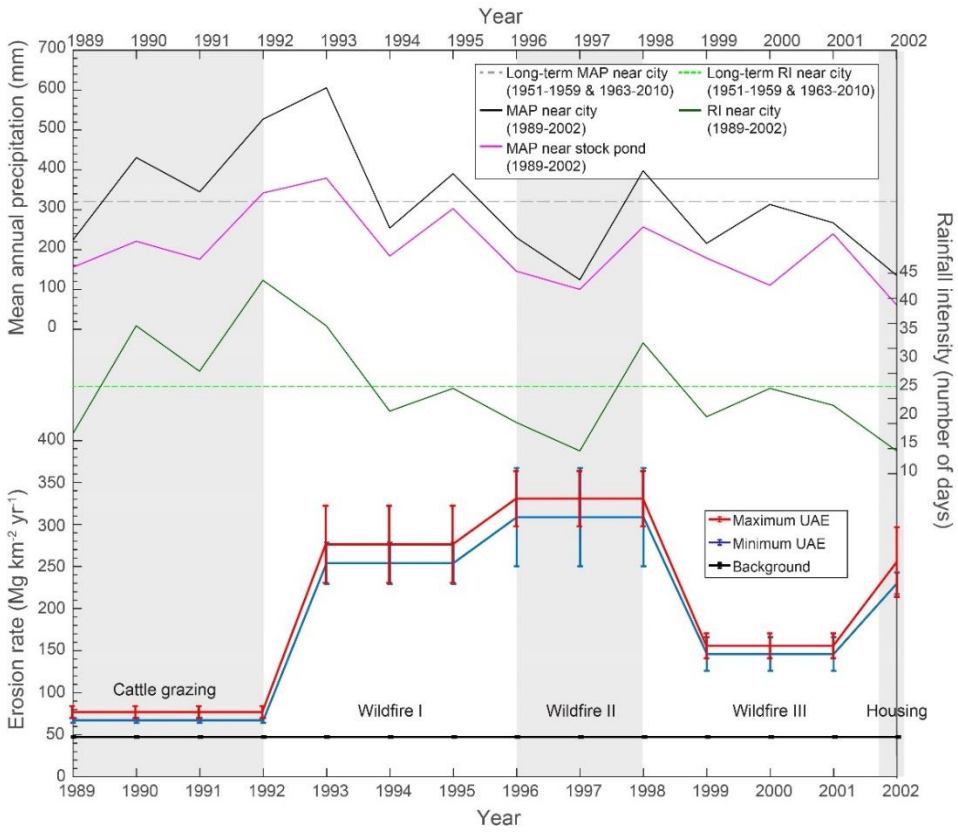

# f ID06: Pepe (1989-2008)


1989: Cattle grazing & house construction & road construction

2003: Cattle grazing & house construction & road construction

2007: Cattle grazing & house construction & road construction

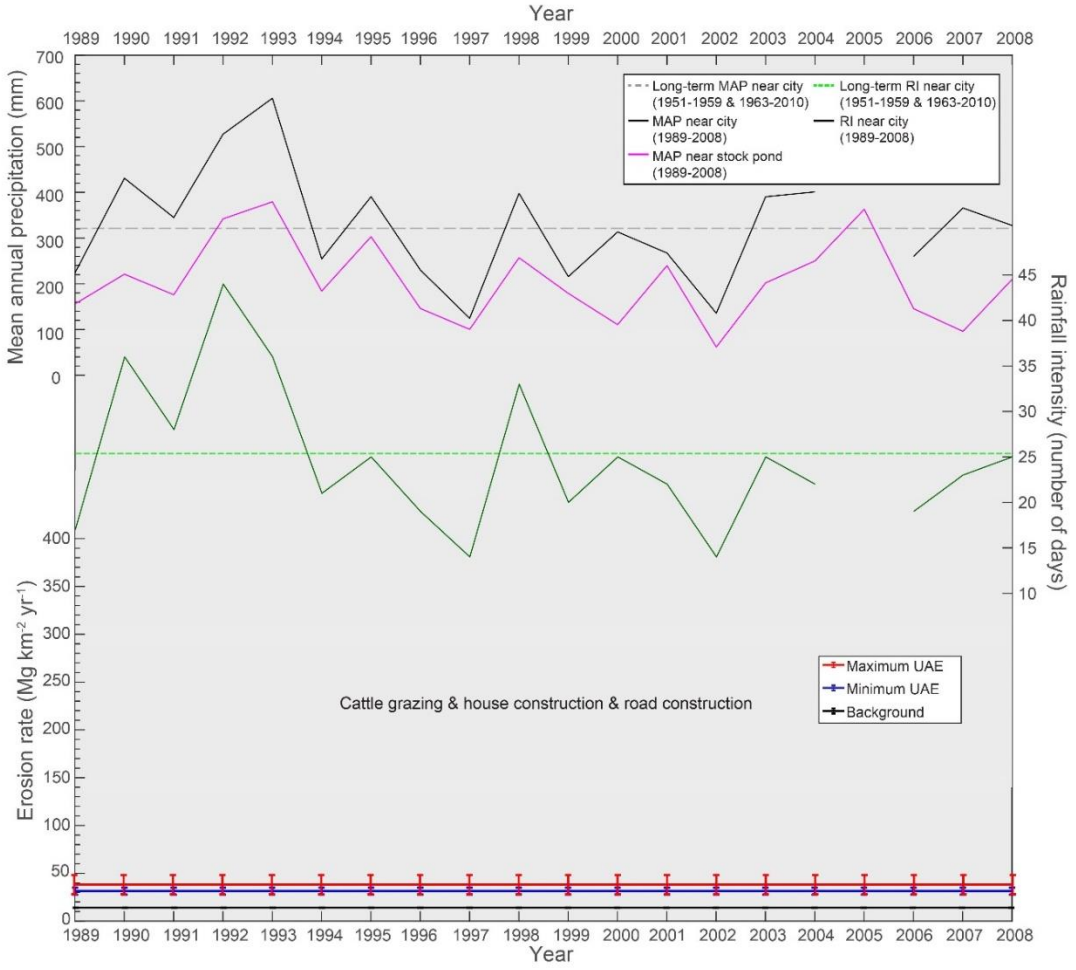

## **g** ID07: Bronco (1990-2003)

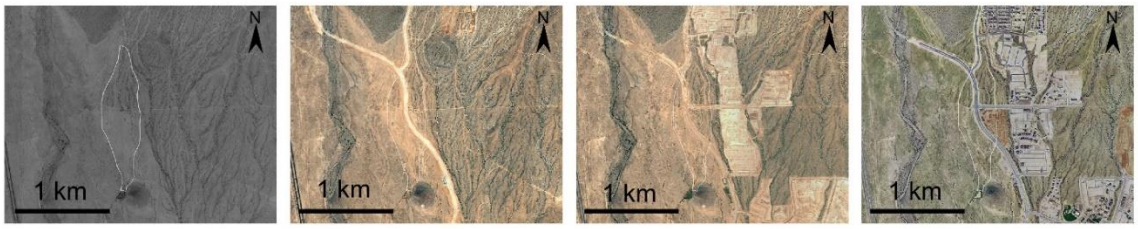


1997: Cattle grazing  2002: Road constructon  2003: Road construction  2004: Road construction

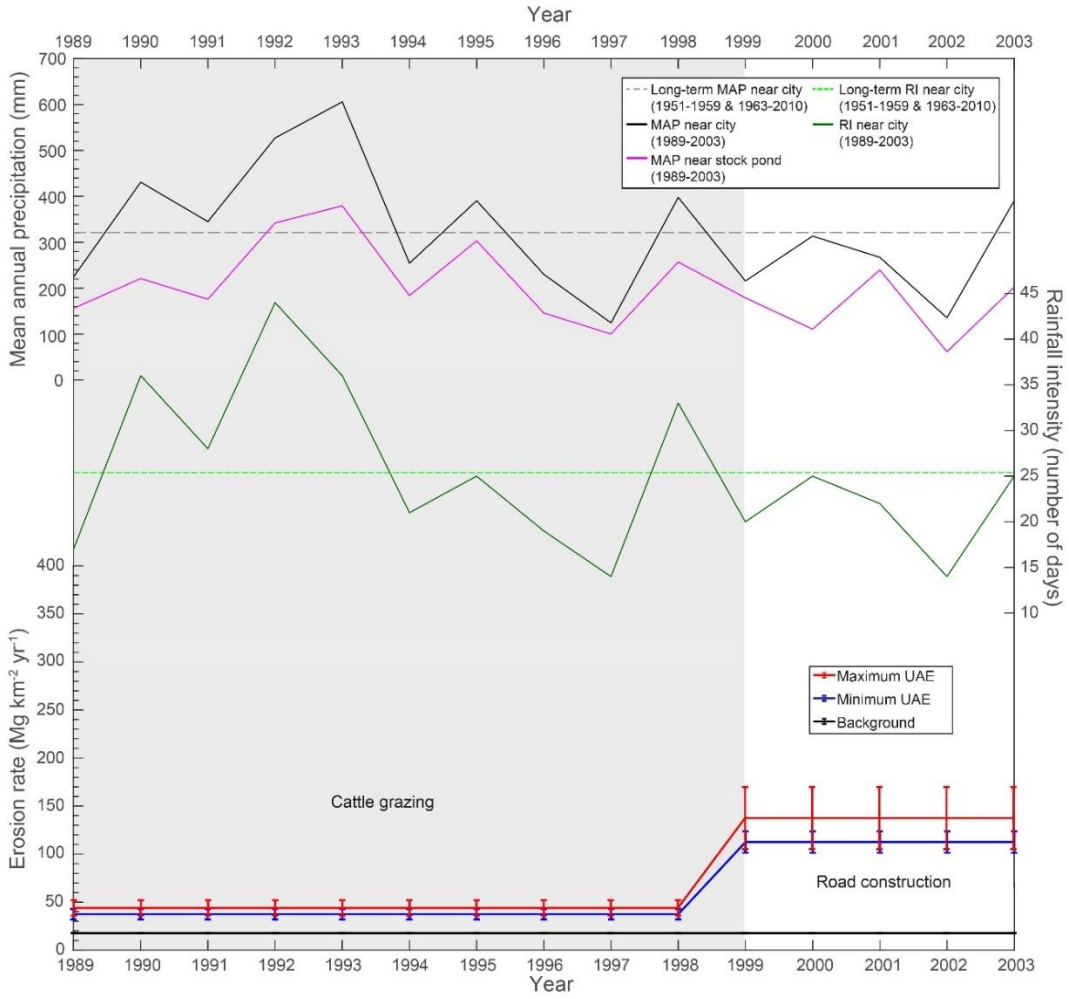

## **h** ID08: Circle (1990-2013)

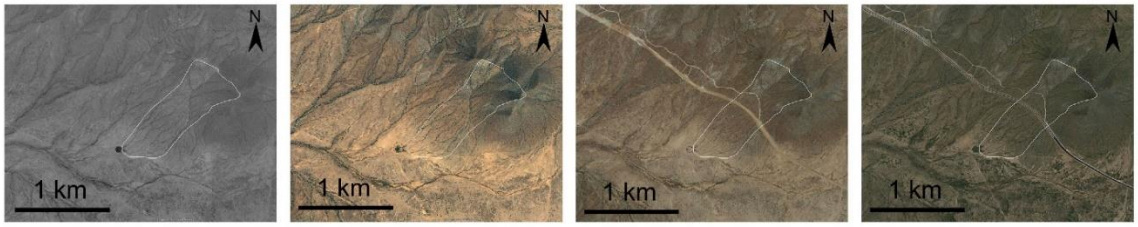


1997: Cattle grazing | 2003: Cattle grazing | 2012: Road construction | 2013: Road construction

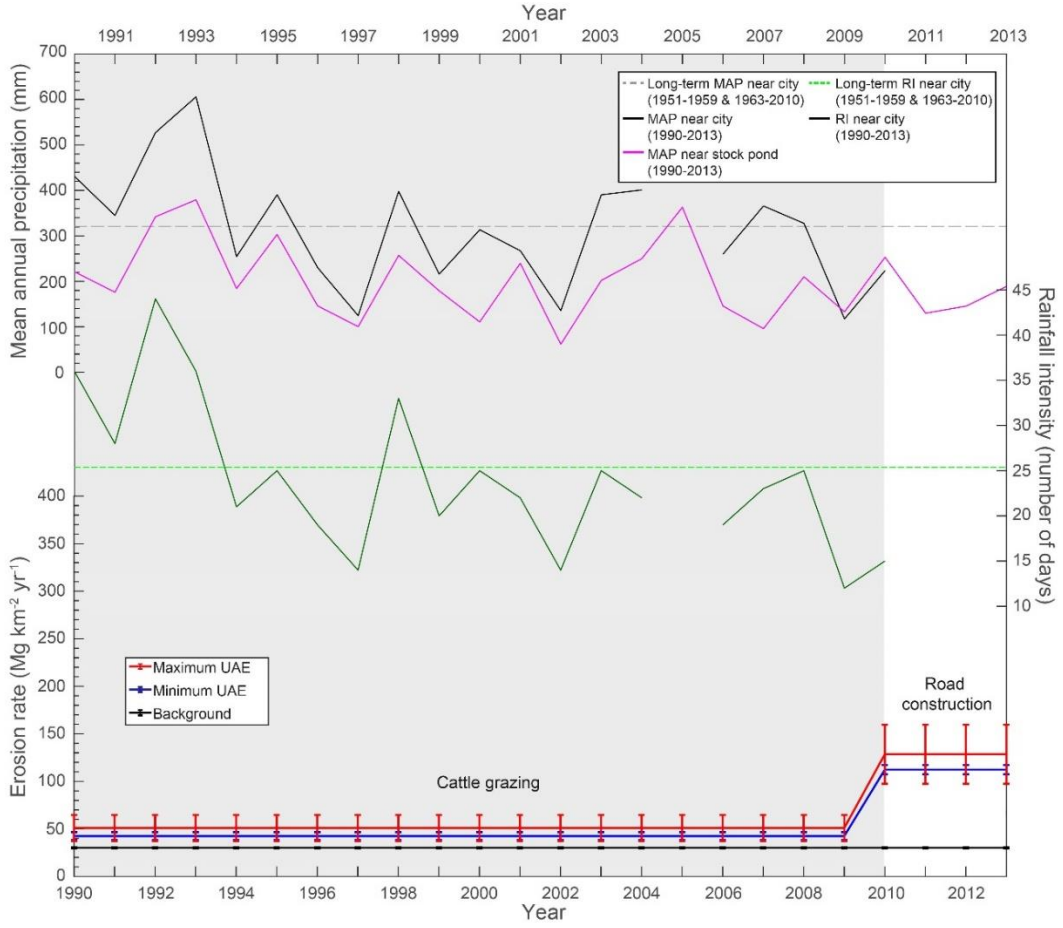

# i ID09: Charlie (1989-2004)


1992: House construtions 2002: House construction 2004: House construction

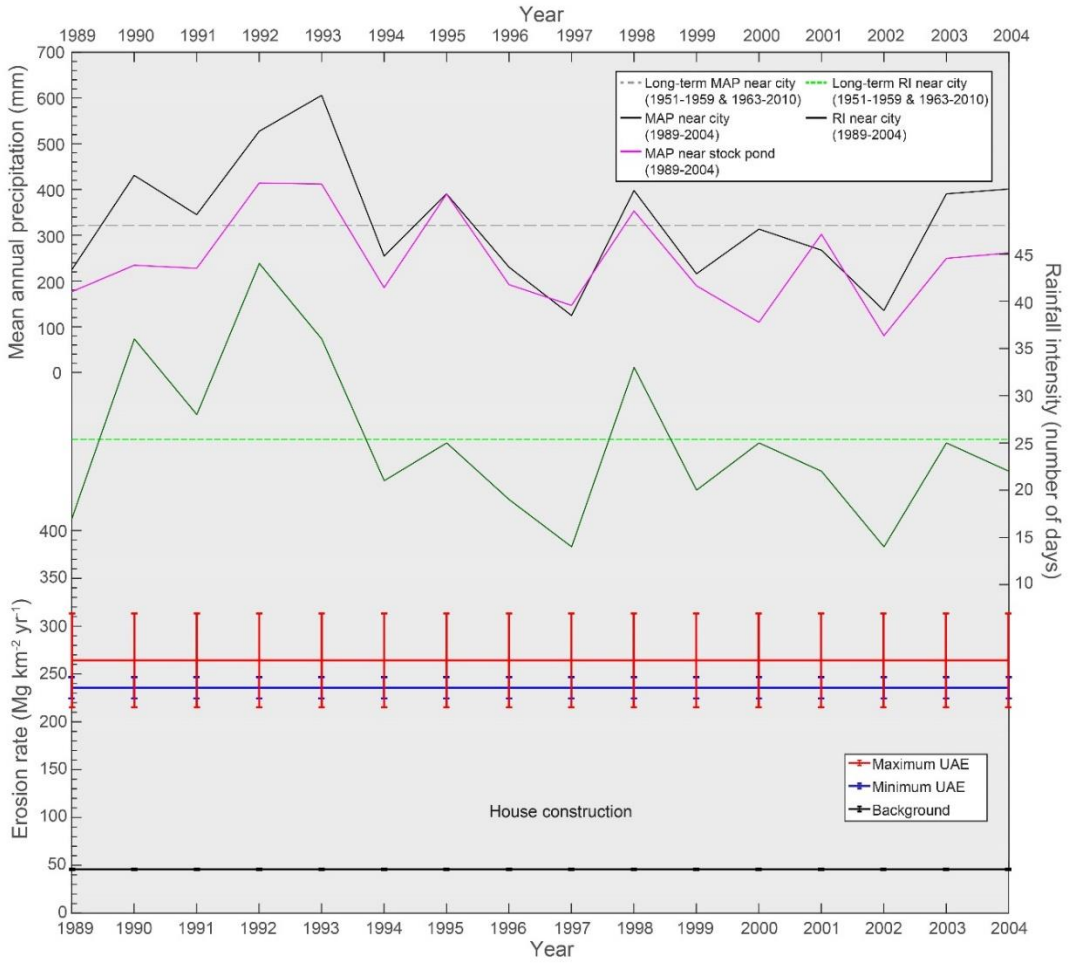

# **j** ID10: Rock (1989-2009)


1992: Cattle grazing | 2002: Wildfire II | 2007: Wildfire III

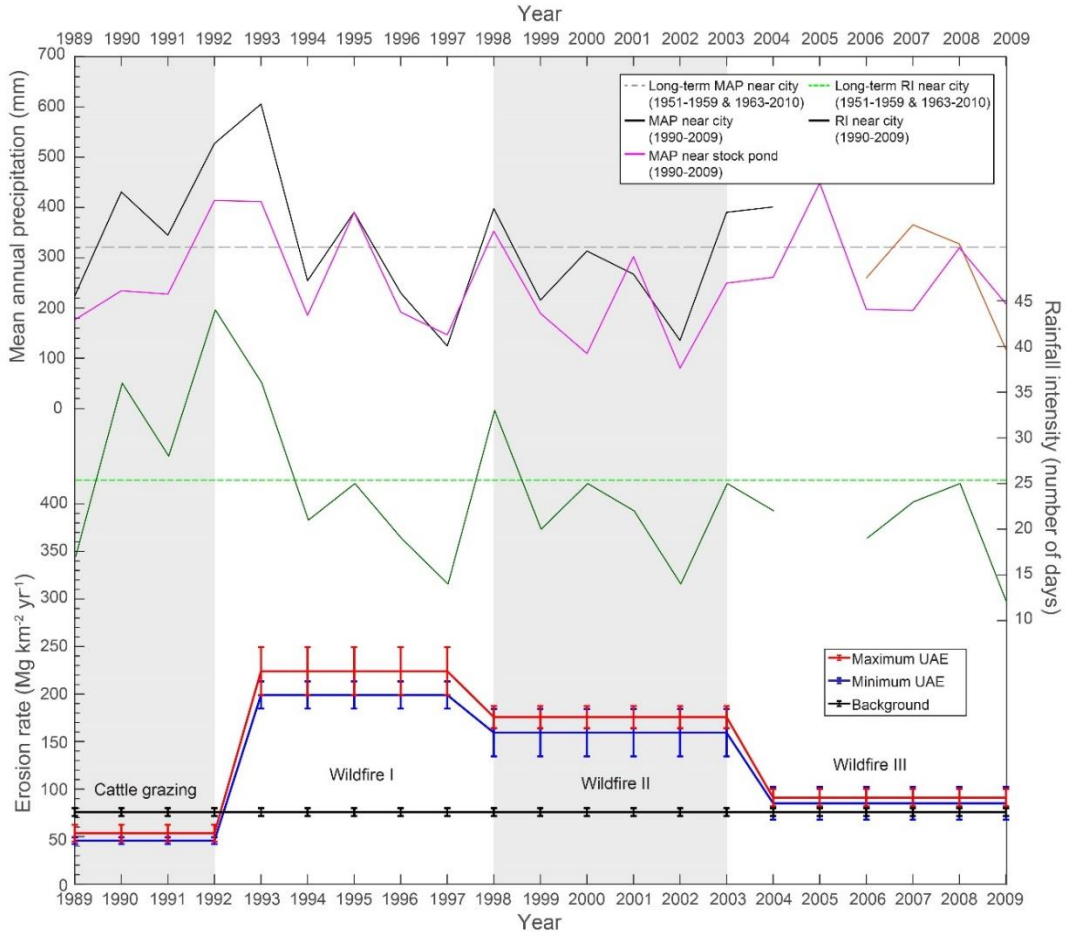

## **k** ID11: Cave Creek (1989-2003)

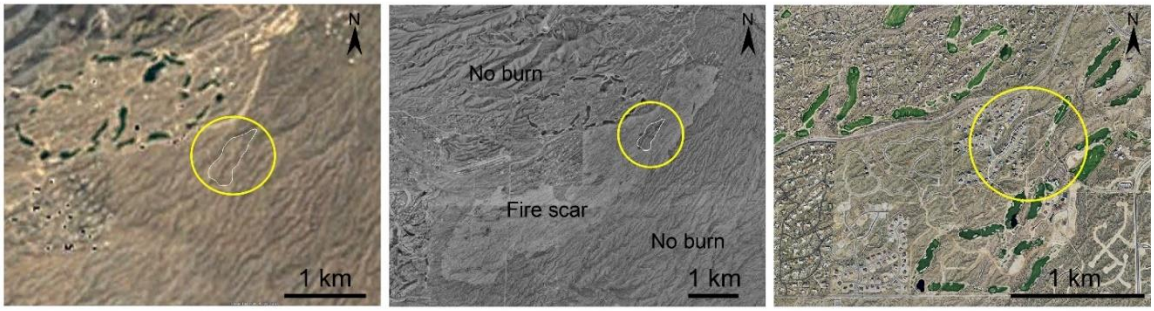


1990: Cattle grazing | 1992: Wildfire | 2004: House construction

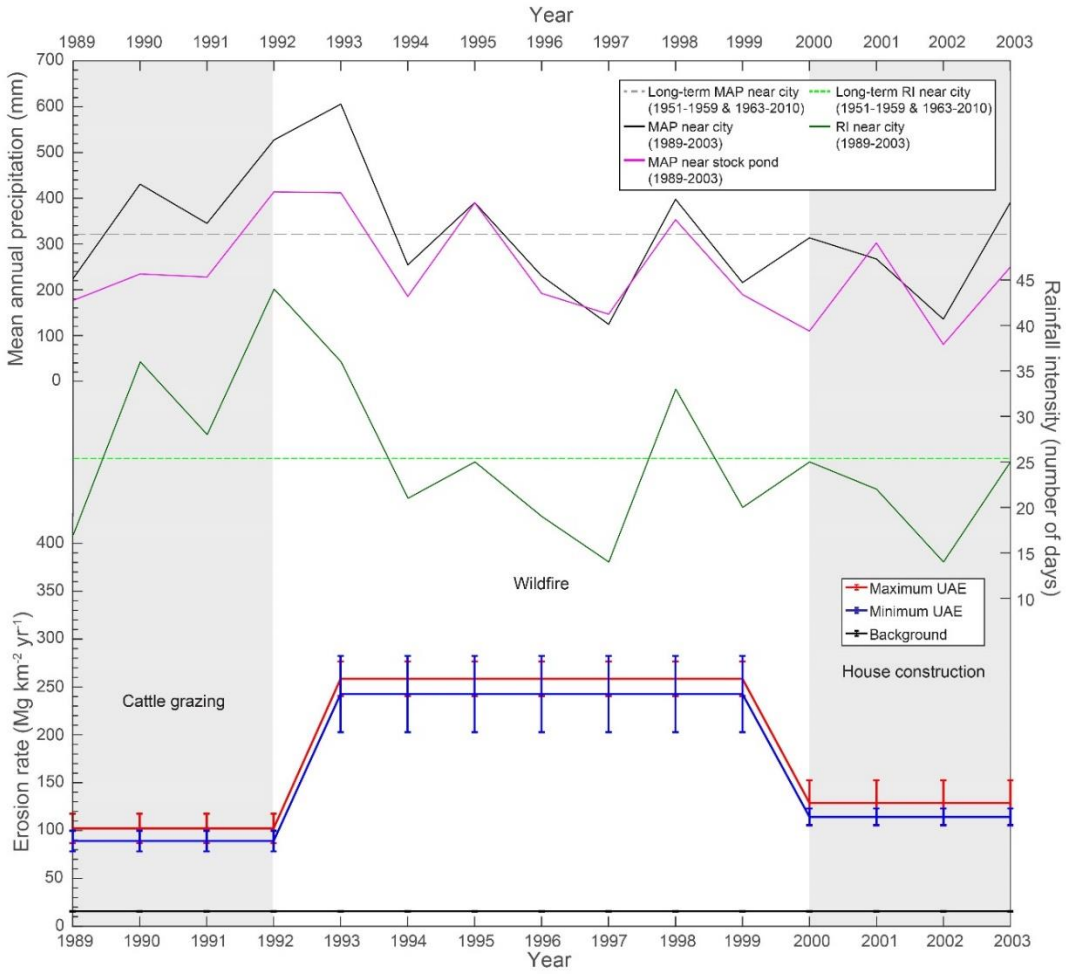

# ID12: Buckhorn (1989-2002)

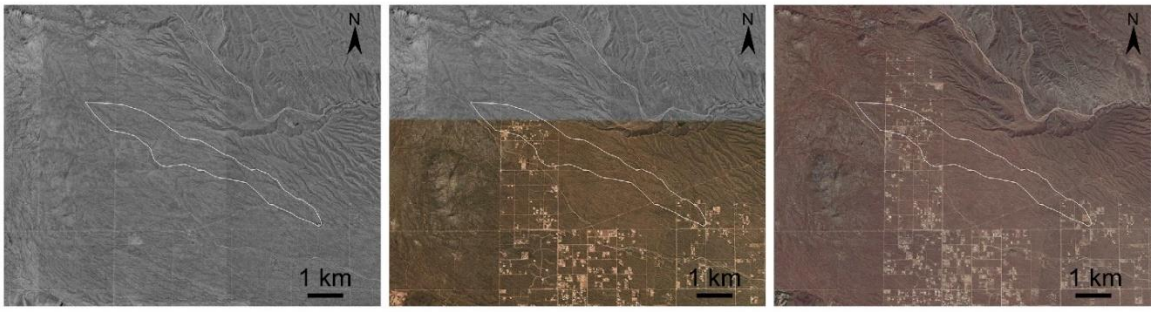


1992: Cattle grazing | 2003: House construction | 2005: House construction

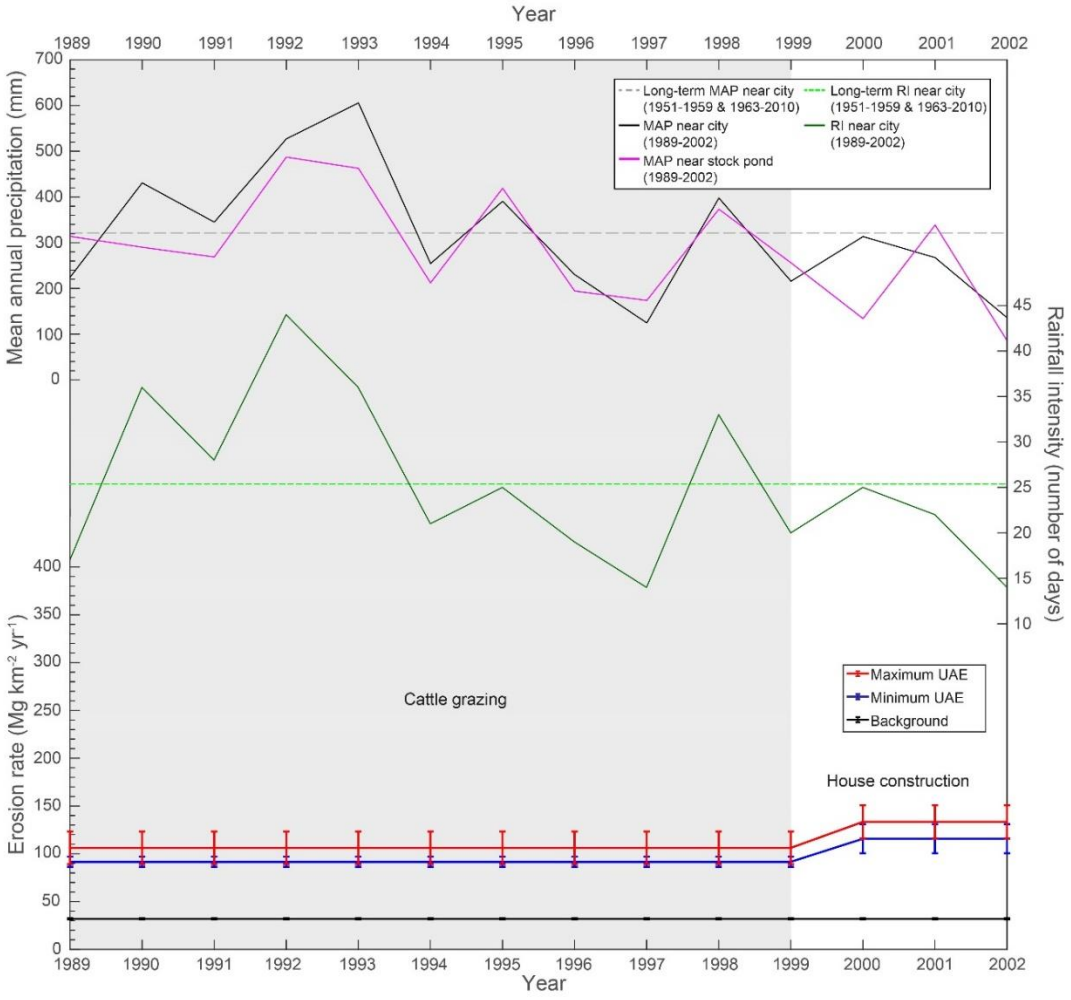

## m ID13: The Rocks

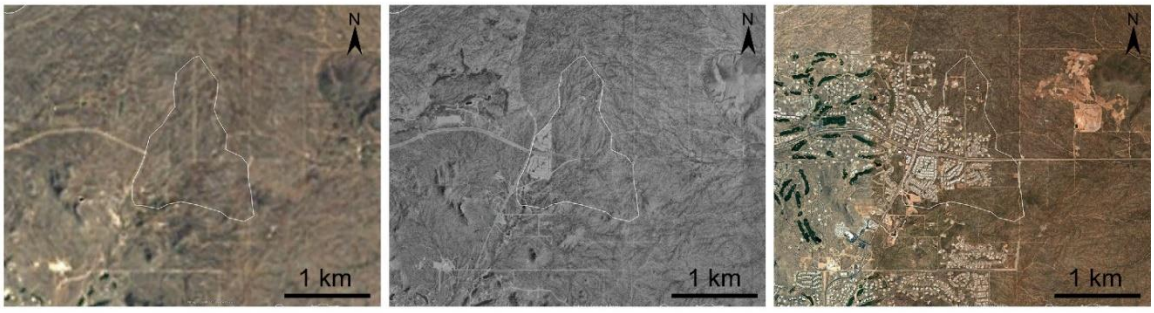


1989: House construtions 1992: House construction 2003: House construction

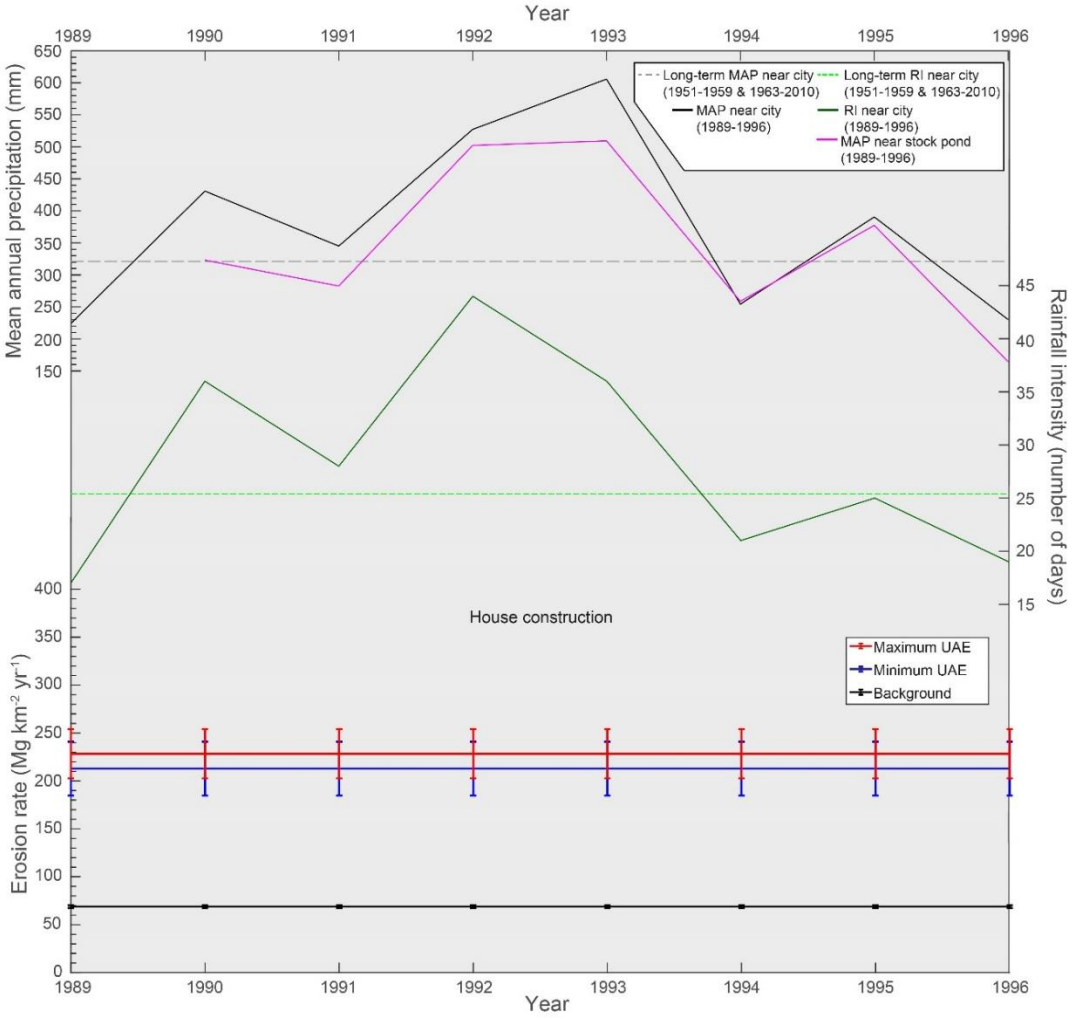

## **n** ID14: 128th St. (1989-2008)


1992: Cattle grazing 1996: Wildfire 2003: Road construction

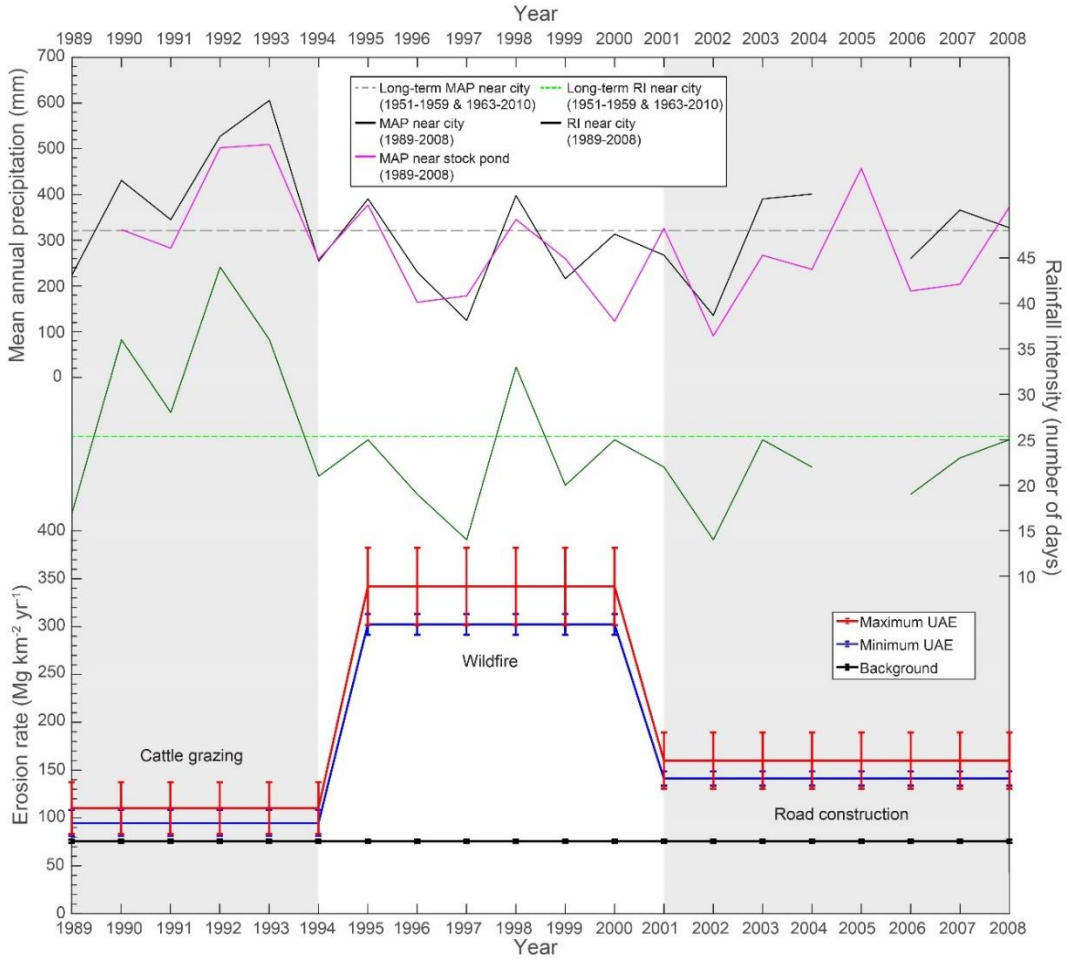

## o ID15: 128th St. 2


1992: Cattle grazing | 1996: Wildfire | 2003: Roadconstruction

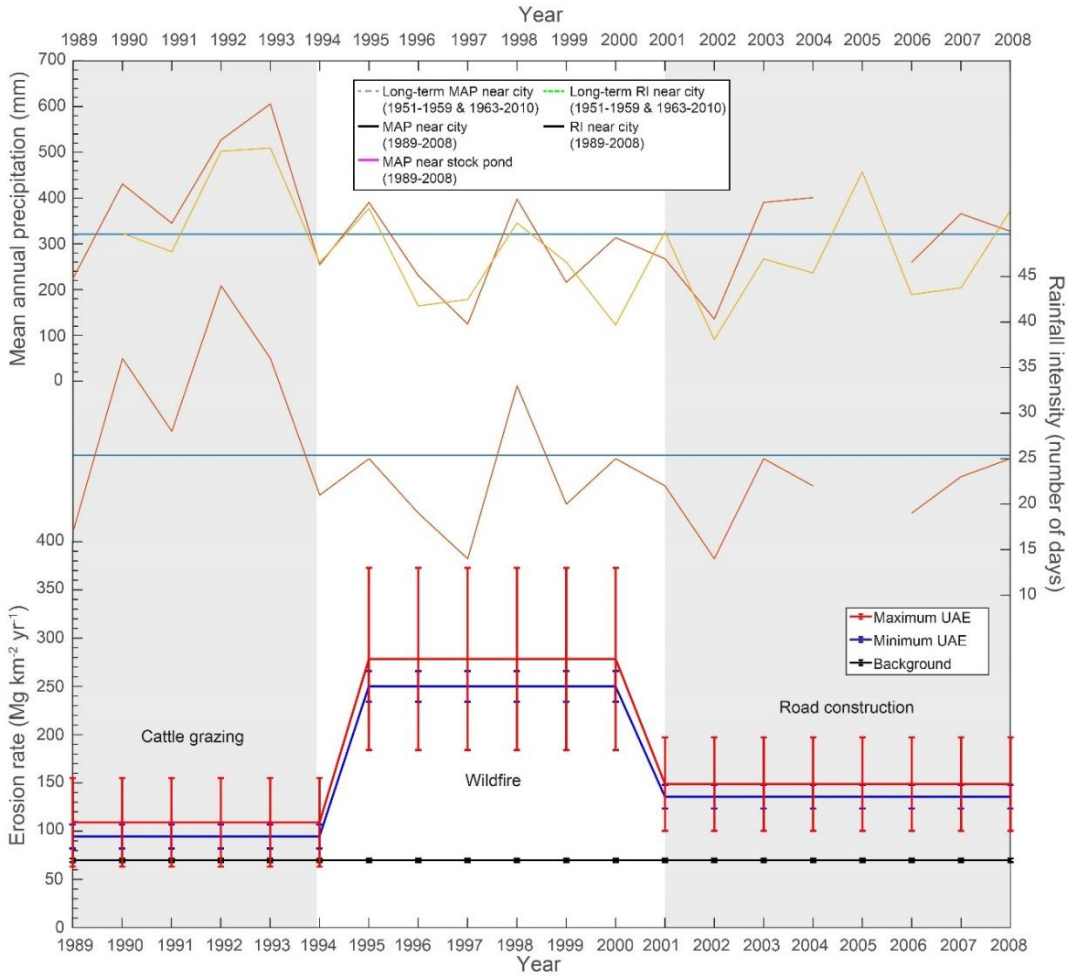

# **p** ID16: Asher Hills (1989-2007)


1992: Cattle grazing | 2003: House construction | 2007: House construction

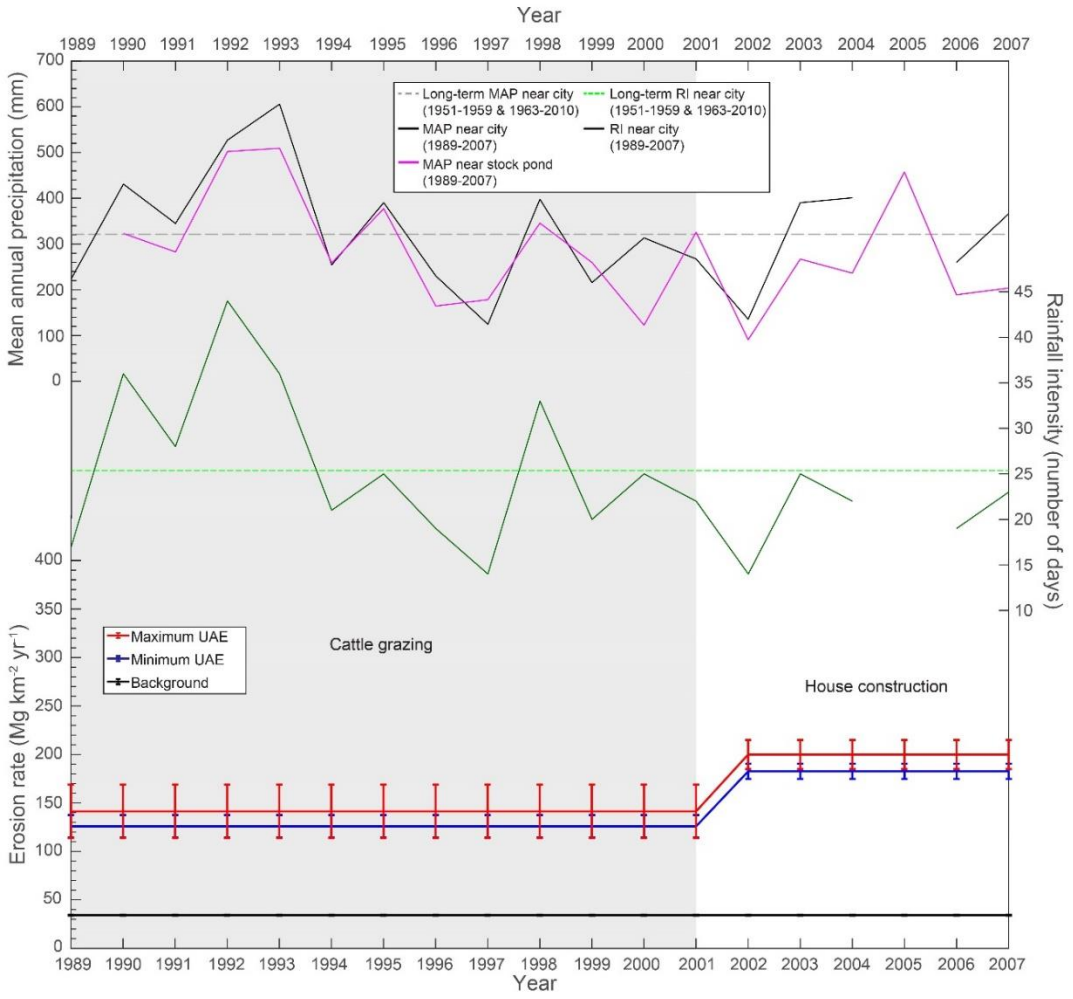

# **q** ID17: Gold Canyon (1989-2009)


1989: House constrution | 1992: House construction | 2003: House construction

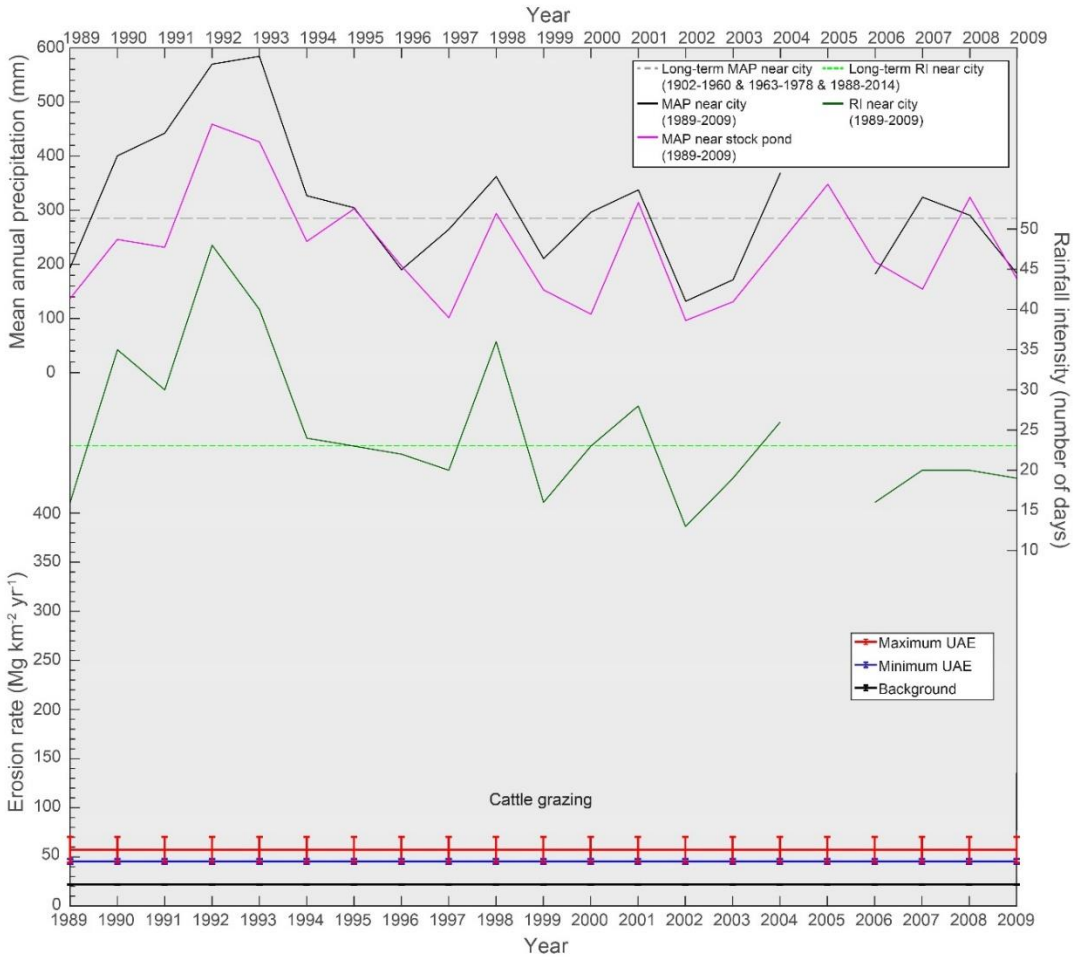

# APPENDIX J

## PHOENIX METROPOLITAN REGION EROSION MODELLING MAPS

The purpose of the appendix J is to show the phoenix metropolitan region erosion modelling maps: **a,** Background erosion on hillshade map. **b,** UAE on hillshade map. **c,** UAE on satellite map. **d,** UAEN on hillshade map. **e,** UAEN on satellite map.

**a,** Background erosion on hillshade map

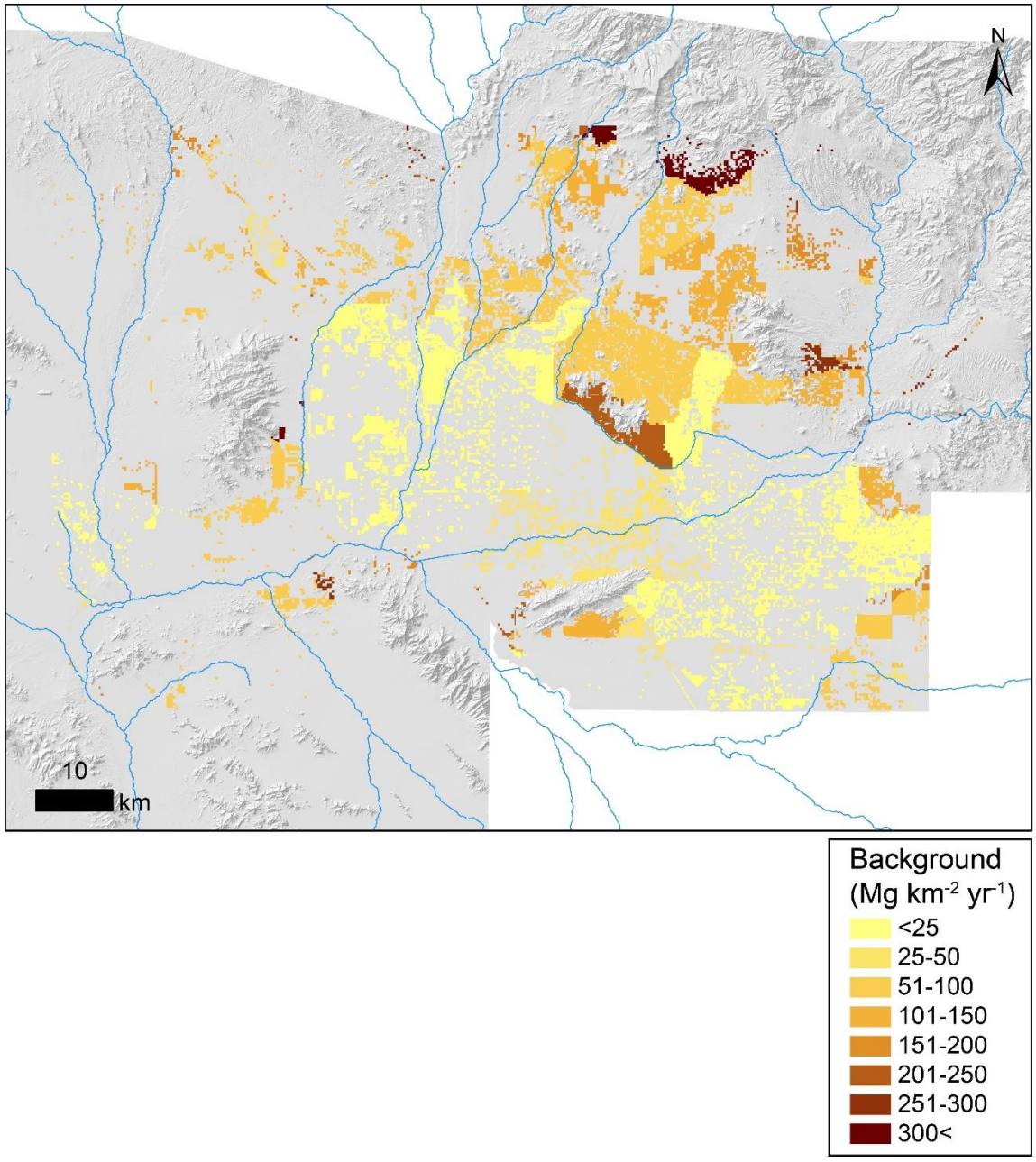

**b,** UAE on hillshade map

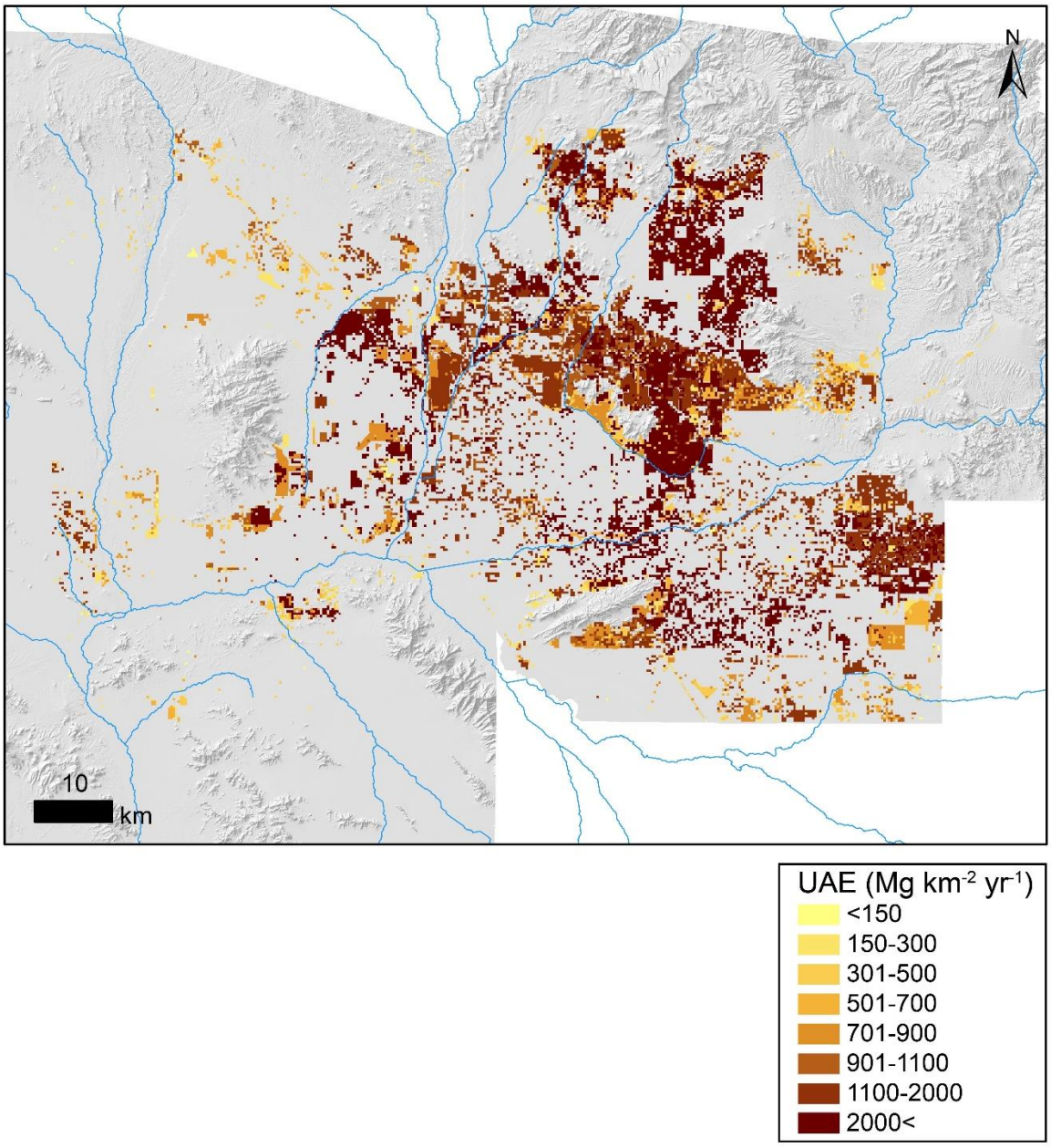

**c,** UAE on satellite map

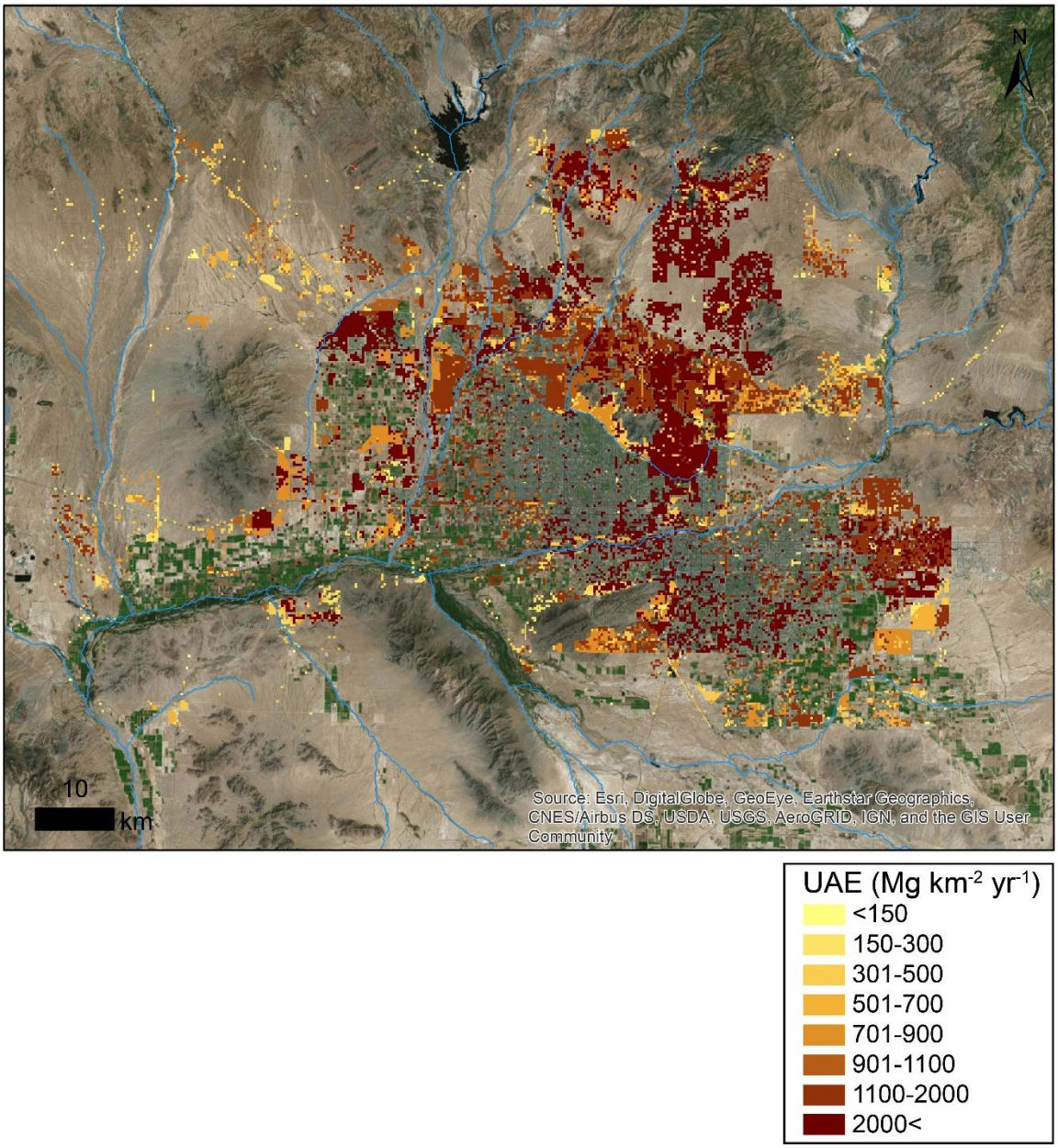

**d,** UAEN on hillshade map

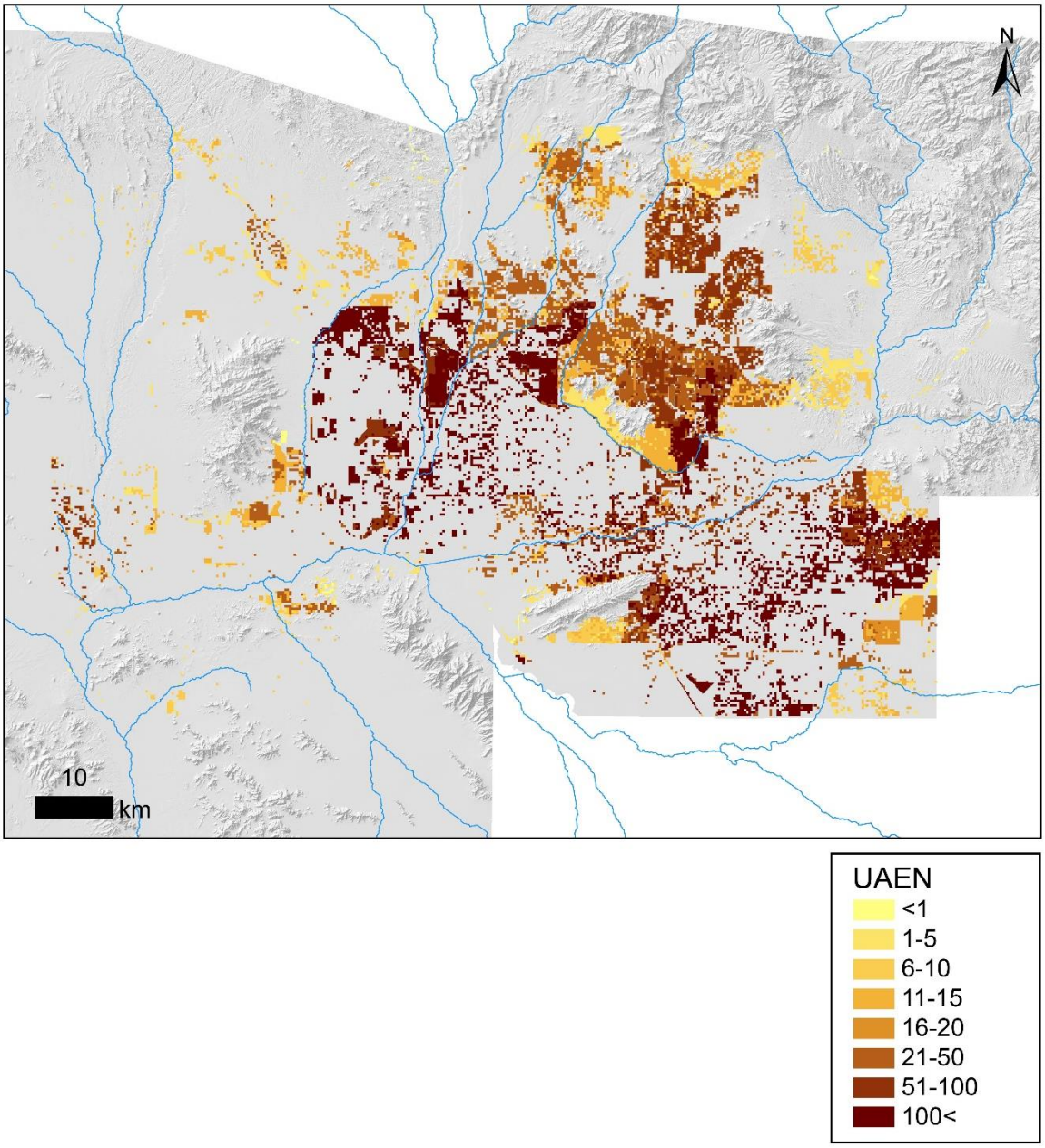

**e,** UAEN on satellite map

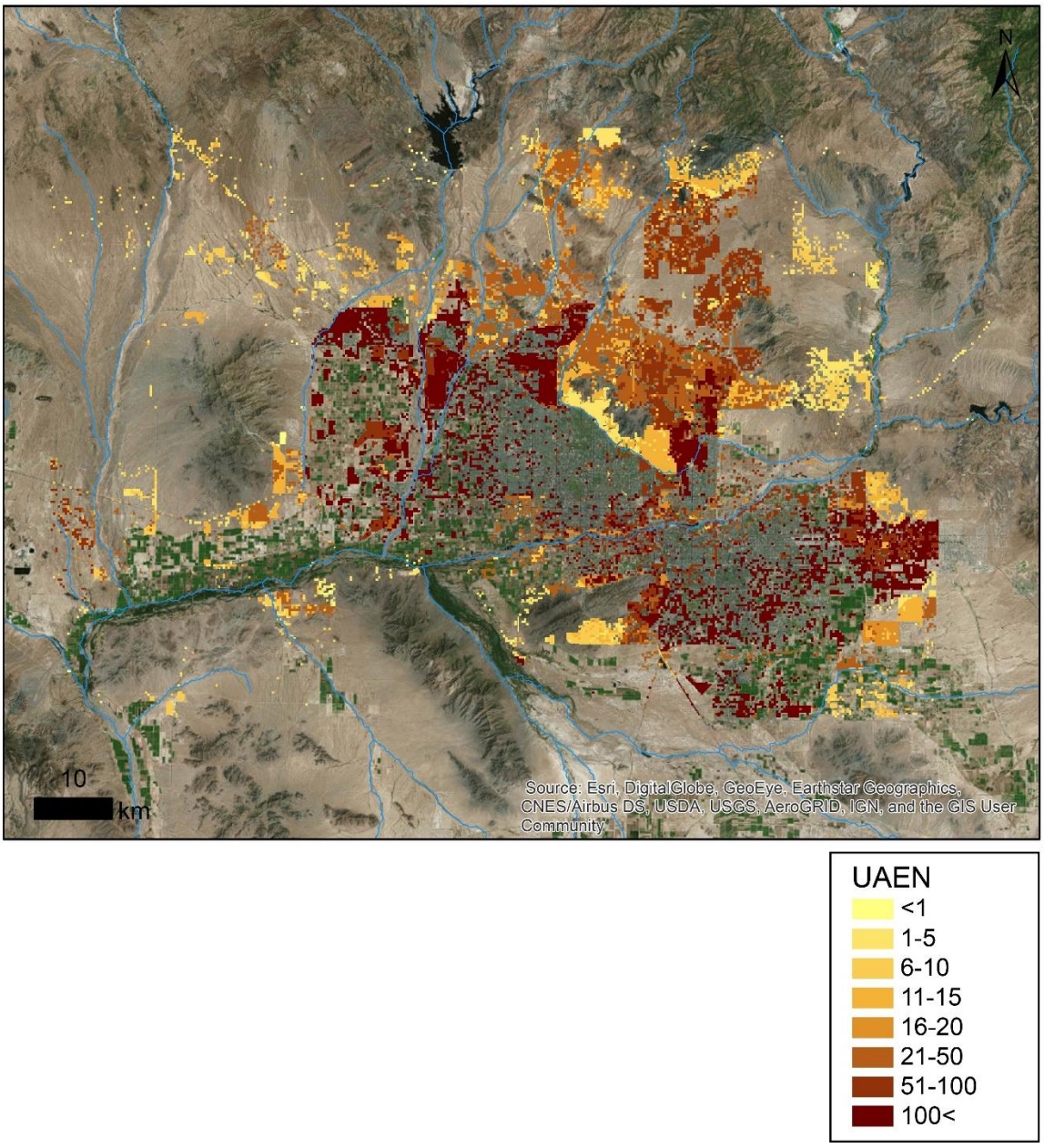

# APPENDIX K

# MEASURED SEDIMENT YIELDS FROM URBANIZING WATERSEHDS AND ESTIMATED BACKGROUND

Sediment yield data was compiled by Russell et al. (2017). Background erosion was estimated by CWDR from Phoenix case study.

| ID | Country | Location | Climate zone | Watershed condition | Drainage area (km2) | Slope | Median UAE (Mg km$^{-2}$ yr$^{-1}$) | References | Median Background (Mg km$^{-2}$ yr$^{-1}$) | References |
|---|---|---|---|---|---|---|---|---|---|---|
| **1** | USA | Patuxent River Basin, Maryland | Cold | Range - basins with active construction | Unknown | Unknown | 236 | (Fox, 1976) in (Russell et al., 2017) | 90 | (This study) |
| **2** | USA | Phoenix | Arid | Construction areas only (computed) | Entire Phoenix | mean slope: $4^0$ | 244 | (This study) | 90 | (This study) |
| **3** | USA | Rock Creek and Anacostia River Basins, Maryland | Cold | Construction (2-14% construction) | 1.2-25.2 | Unknown | 470 | (Yorke and Herb, 1978) | 90 | (This study) |
| **4** | USA | Maryland & D.C. | Cold | Urbanizing (includes urban area as well as area undergoing development) | 11-189 | Unknown | 604 | (Wark and Keller, 1963) in (Wolman and Schick, 1967) | 90 | (This study) |
| **5** | Malaysia | Sg. Jinjang, Sg. Kelang | Tropical | Light-moderate construction | 10.3-29 | Unknown | 1372 | (Balamurugan, 1991) | 90 | (This study) |
| **6** | USA | Rock Creek and Anacostia River Basins, Maryland | Cold | Construction areas only (computed) | 0.05-0.61 | 4-7% | 4750 | (Yorke and Herb, 1978) | 90 | (This study) |
| **7** | Japan | Suburbs of Tokyo | Temperate | Construction: 100% disturbed | 0.31-1.42 | 80-100 m relief | 8340 | (Kinosita and Yamazaki, 1974) | 90 | (This study) |

| | | | | | | | | | | |
|---|---|---|---|---|---|---|---|---|---|---|
| **8** | USA | Baltimore, Maryland | Cold | Construction sites and subdivisions with active construction | 0.0065-0.60 | 1-10% | 27000 | (Wolman and Schick, 1967) | 90 | (This study) |